Durham E-Theses

Parton-parton scattering at two-loops

Yeomans, Maria Elena Tejeda

Parton-Parton Scattering at Two-Loops

a Ph.D. thesis by

Maria Elena Tejeda Yeomans

July 2001

Abstract

We present an algorithm for the calculation of scalar and tensor one- and two-loop integrals that contribute to the virtual corrections of $2 \to 2$ partonic scattering. First, the tensor integrals are related to scalar integrals that contain an irreducible propagator-like structure in the numerator. Then, we use Integration by Parts and Lorentz Invariance recurrence relations to build a general system of equations that enables the reduction of any scalar integral (with and without structure in the numerator) to a basis set of master integrals. Their expansions in $\epsilon = 2 - D/2$ have already been calculated and we present a summary of the techniques that have been used to this end, as well as a compilation of the expansions we need in the different physical regions.

We then apply this algorithm to the direct evaluation of the Feynman diagrams contributing to the $\mathcal{O}(\alpha_s^4)$ one- and two-loop matrix-elements for massless like and unlike quark-quark, quark-gluon and gluon-gluon scattering. The analytic expressions we provide are regularised in Convensional Dimensional Regularisation and renormalised in the $\overline{MS}$ scheme. Finally, we show that the structure of the infrared divergences agrees with that predicted by the application of Catani's formalism to the analysis of each partonic scattering process.

The results presented in this thesis provide the complete calculation of the one- and two-loop matrix-elements for $2 \to 2$ processes needed for the next-to-next-to-leading order contribution to inclusive jet production at hadron colliders.

Parton-Parton Scattering at Two-Loops

A thesis presented to the University of Durham

for the

Degree of Doctor of Philosophy

by

Maria Elena Tejeda Yeomans

Physics Department

University of Durham
2001

Contents

List of Figures

List of Tables

Declaration

The work described in this thesis was undertaken between October 1998 and August 2001 whilst the author was a research student under the supervision of Dr. E.W.N. Glover in the Department of Physics at the University of Durham. This has not been submitted for any other degree at this or any other University.

Aspects of Chapters 3-6 are based on the research carried out in collaboration with C. Anastasiou, E. W. N. Glover, C. Oleari and J. B. Tausk, and presented in the following publications

- C. Anastasiou, J. B. Tausk and M. E. Tejeda-Yeomans, *The on-shell massless planar double box diagram with an irreducible numerator*, Nucl. Phys. Proc. Suppl. **89**, 262 (2000), [hep-ph/0005328].

- E. W. N. Glover and M. E. Tejeda-Yeomans, *Progress towards 2 to 2 scattering at two-loops*, Nucl. Phys. Proc. Suppl. **89**, 196 (2000), [hep-ph/0010031].

- C. Anastasiou, E. W. N. Glover, C. Oleari and M. E. Tejeda-Yeomans, *Two-loop QCD corrections to the scattering of massless distinct quarks*, Nucl. Phys. **B601**, 318 (2001), [hep-ph/0010212].

- C. Anastasiou, E. W. N. Glover, C. Oleari and M. E. Tejeda-Yeomans, *Two-loop QCD corrections to massless identical quark scattering*, Nucl. Phys. **B601**, 341 (2001), [hep-ph/0011094].

- C. Anastasiou, E. W. N. Glover, C. Oleari and M. E. Tejeda-Yeomans, *One-loop QCD corrections to quark scattering at NNLO*, Phys. Lett. **B506**, 59 (2001), [hep-ph/0012007].

- C. Anastasiou, E. W. N. Glover, C. Oleari and M. E. Tejeda-Yeomans, *Two-loop QCD corrections to massless quark-gluon scattering*, Nucl. Phys. **B605**, 486 (2001), [hep-ph/0101304].

- E. W. N. Glover, C. Oleari and M. E. Tejeda-Yeomans, *Two-loop QCD corrections to gluon-gluon scattering*, Nucl. Phys. **B605**, 467 (2001), [hep-ph/0102201].

- E. W. N. Glover and M. E. Tejeda-Yeomans, *One-loop QCD corrections to gluon-gluon scattering at NNLO*, JHEP **0105**, 010 (2001), [hep-ph/0104178].

Acknowledgements

I want to thank my supervisor Nigel Glover for giving me the opportunity to work with him. He incorporated me to his research work in a way that allowed me to learn by doing, to explore and implement ideas and sometimes (most of the times, rather) provide highly inefficient solutions to our problems. Nevertheless, he always motivated me by following my progress with continuous interest and support.

Also, many thanks go to Babis (C. Anastasiou). For all those valuable physics discussions that helped me clarify problems and solutions and to put ideas into practice. And obviously, for being such a good friend.

To the other members of the *Two-Loop People*, Lee Garland and Thanos Koukoutsakis I thank them for their willingness to share ideas, adventures and CPU time, even in times of scarceness.

To Martin Kimber, the *Spelling Adviser to the Stars*. Undoubtedly the friendliest and kindest of them all. I cherish our friendship and I am sure this is not the last I see of you and Catherine.

To Marco Zimmer, Jafar Sadeghi, Autakit Chattaraputi, Camel Benhadou, Joanna Kiryluk and all the people of the Physics building, I thank them for providing a friendly and warm working atmosphere.

I am grateful to Jeppe Andersen and Steve Burby, for always lending a hand to the computationally challenged.

A special mention goes to Jean and Cathryn who have always been there to give their love, at times of happiness as well as times of terrible desperation.

Este trabajo lo dedico

a mi Carlos y por mi Carlos.

a mis papas y a mis hermanos.

a la familia y a la universitaria.

Hay quienes luchan un dia y son buenos.

Hay quienes luchan un año y son mejores.

Pero hay quienes luchan toda su vida.

Esos son los imprescindibles.

Bertold Brecht

Preface

Parton-Parton Scattering at Two-Loops

The aim of this thesis is to provide an insight into the workings of Quantum Chromo-dynamics (QCD) as a quantum field theory. More precisely, to use perturbation theory at high orders and calculate matrix elements for partonic scattering processes.

Before presenting our main results in Chapter 6, the structure of this thesis aims at providing the tools needed to perform a higher order matrix element calculation as well as describing the general context on which it stands. This enables the reader to find out what (s)he needs to undertake such a calculation and which are the next steps to be taken in order to move forward in the description of QCD phenomena within perturbative calculations at high orders.

In the first two Chapters we review some of the basic concepts of QCD starting with a description of the dynamics of the theory in terms of its Lagrangian. We continue with concepts inherent to the nature of QCD, such as *asymptotic freedom* and finish the introductory discussion with an exploration into the type of phenomena we can use this description for, namely highly energetic *jets*.

Chapters 3, 4 and 5 encompass a discussion centered around the main techniques and algorithms for explicit loop integration, loop integral reduction in terms of simpler integrals and isolation of their divergent behaviour. We present the complete calculation of one- and two-loop matrix elements for $2 \rightarrow 2$ scattering, needed for the improvement in the theoretical description of jet production at hadron colliders, in Chapter 6.

In the last Chapter, we provide a summary of our main results and a brief account of recent work within the fields that complement matrix element calculations (such as analytic cancellation of singularities and distribution functions), which are needed for a complete estimate of a jet cross section. We finish with an outlook on future calculations and lines of work that could build on the methods currently used.

Chapter 1

Basics of Quantum Chromodynamics

In this Chapter we discuss briefly the basic aspects of Quantum Chromodynamics as a gauge theory and as a tool for perturbative calculations. By no means do we intend to present an exhaustive exploration of these topics, but we do provide a guide that can be followed with the aid of several text books*.

We begin with an introduction to the quark model that leads us to the dynamics of partons presented in section 1.2 through the QCD Lagrangian. There we look at its different pieces and make a small exploration into their nature. In section 1.3 we give the Feynman rules that allow a diagrammatic study of the strong interactions in the perturbative limit. This is followed by two very important topics in QCD: regularisation and renormalisation in sections 1.4 and 1.5.

In these last two sections we provide qualitative and quantitative arguments on the nature of the divergent behaviour of the perturbative analysis we use in QCD and on the implication it has on our description of strong interactions. We finish by looking into the concept of *asymptotic freedom* and on the *running* of the strong coupling.

1.1 The Quark Model

Particle Physics is concerned with the fundamental constituents of matter and their interactions. In particular, the field theory that allows us to study the phenomena arising from strong interactions, is Quantum Chromodynamics (QCD).

All the particles that interact strongly such as *baryons* and *mesons*, are called *hadrons*. The large number of observed hadrons led to the supposition that they were not elementary but that they had a more basic structure. As it is today, our theoretical understanding of strong interactions started with the identification of these elementary particles

---

*For a more formal and detailed discussion of QCD and Quantum Field Theory the references [1, 2, 3, 4, 5, 6, 7, 8] and references therein, are recommended.

called *fermions*.

The quark model establishes a structure for hadrons. Mesons are a bound state of a quark-antiquark pair $q\bar{q}$, while baryons are bound states of three quarks qqq. At present, there have been observed 6 species (flavours) of quarks all carrying spin 1/2. The electric charge of the up(u), charm(c) and top(t) is $+2/3$, while that of the down(d), strange(s) and bottom(b) is $-1/3$. When correctly assembled, the quark quantum numbers reproduce the quantum number belonging to the composite mesons and baryons.

Nevertheless, this quark scheme forces us to combine three quarks with the same spin in order to reproduce experimental results for some baryonic states, such as the $\Delta^{++} = uuu$ baryon, thereby violating Fermi statistics. To avoid this problem an additional quantum number is introduced for quarks, the so called *colour* charge. This helps to distinguish between identical quarks and since the hadrons contain at most three quarks, we need three different values or colour charges, i.e. *red*, *green* and *blue*.

The fact that experimentally no single quark or colour-full bound state had been observed reinforced the idea of hadrons being *confined* to colour-less states, e.g. $(blue, anti-blue)$ or $(red, green, blue)$. The confinement of the quarks is an additional theoretical hypothesis that has yet to be understood fully and that is likely to be a direct consequence of the dynamical properties of the quarks.

As we mentioned before, the dynamical interactions of all elementary particles in hadrons are described using QCD. In this theory, quarks are considered to be point-like entities carrying colour charge and interacting via the exchange of spin 1 bosons called *gluons* (in analogy to the photon for electro-magnetic interactions).

Furthermore, the theory postulates invariance of the physical description for the interacting quarks inside hadrons to redefine their colour labels at any point in space-time. To compensate for this local phase invariance there are 8 gluons that carry colour charge and also self-interact.

More formally, the theory postulates invariance under local $SU(3)_c$ transformations. In particular, quarks transform in the fundamental representation and gluons in the adjoint representation, giving a symmetric colour singlet for mesons $q_i\bar{q}_i$ and a totally antisymmetric one for baryons $\epsilon_{ijk}q_iq_jq_k$.

In this thesis we are interested in the short-distance (or high energy) limit of QCD, where the strong interactions inside hadrons become weak. Here, the quarks and gluons are *asymptotically free* and we are able to use a sensible diagrammatic perturbation theory study of these interactions.

1.2   The gauge principle in QCD

In this thesis we are interested in using the perturbative SU(3) model of QCD and the Feynman rules derived from it in the analysis of physical processes. In this section we give a brief discussion of QCD as a gauge theory and touch upon the topics related to it that comprise the tools needed for our work.

1.2.1   Quarks and gluons

The Lagrangian density that describes the quark content of the theory of QCD is

$$\mathcal{L}_{\text{quark}} = \sum_f \bar{\psi}_f (\underbrace{i\not{D}}_{\substack{kinetic \\ term}} - \underbrace{m_f \mathbb{1}}_{\substack{mass \\ term}})\psi_f, \tag{1.1}$$

where the quark fields ψ_f carry a flavour index f. We use a shorthand notation for the contraction of an arbitrary vector with the gamma matrices γ^μ,

$$v_\mu \gamma^\mu = \not{v}$$

which themselves must fulfill the Clifford algebra anticommutation relation

$$\{\gamma^\mu, \gamma^\nu\} = 2\,g^{\mu\nu}. \tag{1.2}$$

In eq.(1.1), every quark field flavour is actually formed by a triplet of fields in colour space (usually referred to as *red*, *green* and *blue*)

$$\psi_f(x) = \begin{pmatrix} \psi_f^r(x) \\ \psi_f^g(x) \\ \psi_f^b(x) \end{pmatrix}.$$

These internal degrees of freedom do not manifest in an actual physical measurement. The fact that any physical observable is independent of them is a consequence of the freedom we have to rotate any of these fields into one another. This can be enforced upon the quark field arbitrarily at any point in space-time to introduce a *local* SU(3) *symmetry*.

Formally, this means that the Lagrangian density must be invariant under any local SU(3) transformation $U(x)$ which can be parametrized as

$$U(x) = \exp\left(i\,T\cdot\theta(x)\right), \tag{1.3}$$

where $T \cdot \theta = T^a \theta_a$ and T^a are the generators of SU(3) in the fundamental representation and the matrix $U(x)$ is unitary so the generators T^a are traceless and satisfy the following commutation relation

$$\left[T^a, T^b \right] = i \underbrace{f^{abc}}_{\substack{structure \\ constant}} T^c. \tag{1.4}$$

The quark field transforms as

$$\psi_f \to U(x)\psi_f,$$

under the SU(3) rotation, so unitarity ensures that the quark mass term in eq.(1.1) is invariant as well. On the other hand, the kinetic term of the Lagrangian requires a more thorough analysis. We must ensure that the *covariant derivative* (which is contracted with the γ matrices) has a structure that balances with the rotation of the quark fields accompanying it.

The covariant derivative term transforms as

$$D_\mu(x)\psi_f(x) \to U(x) \ D_\mu(x) \ \psi_f(x),$$

so in order to have a term that cancels out the rotation of the quark fields, we must add a new vector *gauge* field A_μ^a to the definition of the covariant derivative. This field represents the degrees of freedom corresponding to the gluons, and carries colour indices $a = 1, ..., 8$. Then the definition of the covariant derivative is

$$D_\mu \equiv \partial_\mu \mathbf{1} + igT^a A_\mu^a, \tag{1.5}$$

where the coupling strength between the quarks and gluons is g. We must also have a term in the Lagrangian that comprises the dynamics of the gauge particles. The kinetic energy term of the gluon fields is built in terms of the commutator between two covariant derivatives,

$$[D_\mu, D_\nu] \psi_f(x) = igT \cdot F_{\mu\nu}\psi_f(x), \tag{1.6}$$

where

$$F_{\mu\nu}^a = \underbrace{\partial_\mu A_\nu^a - \partial_\nu A_\mu^a}_{Abelian} - \underbrace{gf^{abc} A_\mu^b A_\nu^c}_{Non-Abelian}. \tag{1.7}$$

The Non-Abelian (not present in QED) term in this equation is the one representing the interactions amongst gluons. In the Lagrangian density, the term associated with the presence of gluons, will contain the normalized trace of the field-strength as

$$\mathcal{L}_{\text{gluon}} = -\frac{1}{4}F_a^{\mu\nu} F_{\mu\nu}^a, \tag{1.8}$$

which is a gauge invariant kinetic term.

So the classical Lagrangian of QCD is given by

$$
\begin{aligned}
\mathcal{L}_{\text{classical}} &= \mathcal{L}_{\text{quark}} + \mathcal{L}_{\text{gluon}} \\
&= \sum_f \bar{\psi}_f(i\slashed{D} - m_f \mathbf{1})\psi_f - \frac{1}{4}F_a^{\mu\nu}F_{\mu\nu}^a,
\end{aligned}
\tag{1.9}
$$

which is built under the basic principle of gauge invariance, where the fields transform as

$$
\begin{aligned}
\psi_f &\rightarrow U(x)\psi_f, \\
T^a A_\mu^a &\rightarrow U(x)\left(T^a A_\mu^a - \frac{i}{g}U^{-1}(x)\partial_\mu U(x)\right)U(x)^{-1}.
\end{aligned}
$$

This part of the QCD lagrangian describes the dynamics of the quarks as particles with spin 1/2 that carry colour charge and interact with the gluons, which are bosons with spin 1, also carrying colour.

1.2.2 Gauges and ghosts

The next step towards a consistent quantum theory of gauge fields is the quantization itself. Inevitably this will lead to inconsistencies that must be fixed in order to have a sensibly defined theory.

In the canonical quantization method, we use the fields of the theory as operators and calculate canonical commutation relations for them. If we apply this method to the gluon fields, the time-like component of the conjugate momentum vanishes. This contradicts the non-vanishing commutation relation that is calculated for the time-like components of the gluon field and its conjugate canonical momentum.

The fact that we rely on a gauge invariant Lagrangian where the field A_μ^a has the freedom of gauge transformations (it changes by a total derivative and leaves the Lagrangian invariant), will always lead to this difficulty.

We can eliminate the freedom of the gauge transformation by adding constraints to the gluon field. For example, we may choose the Lorentz condition

$$
\partial^\mu A_\mu^a = 0,
$$

which is effectively a *gauge fixing condition*. This is not the only choice we can make to fix the gauge. We can otherwise use the Coulomb gauge ($\partial_i A_i^a = 0$), axial gauge ($n \cdot A^a = 0$ with $n^2 = 1$) or temporal gauge ($A_0^a = 0$). We want to quantize the theory in a covariant way, so we use the Lorentz gauge. In this manner, the gauge fixing term we add to the

Lagrangian is the following

$$\mathcal{L}_{\text{gauge-fixing}} = -\frac{1}{2\xi} \left(\partial^\mu A_\mu^a \right)^2 , \qquad (1.10)$$

where the parameter ξ is called the *gauge parameter*.

Due to this term, the QCD lagrangian is not gauge invariant any more, but any physical prediction that arises from it, will be gauge invariant and independent of the gauge parameter ξ [†]. Since the value of ξ is not relevant, we can choose a value for it, for example

$$\underbrace{\xi = 0}_{\substack{Landau \\ gauge}} , \qquad \underbrace{\xi = 1}_{\substack{Feynman \\ gauge}} , \qquad \underbrace{\xi \to \infty}_{\substack{Unitary \\ gauge}} .$$

In the rest of this thesis we will work within the Feynman gauge, i.e. $\xi = 1$.

The same choice of gauge has to be made at some point if one uses, for example, the Feynman path-integral formalism. This occurs because the functional integral over the exponential of the action diverges (as the region of integration is infinite) when we consider the infinite number of gauge transformations the gluon field can sustain, without changing the action.

There are still unphysical degrees of freedom that we must take care of. We must restrict the gluon fields to have only two physical polarisations. We introduce the Fadeev-Popov *ghost* field that enables us to cancel the contribution of those unphysical polarisations. These are scalar fields with a fermionic property: they are anticommuting scalar fields. The ghost term contributing to the QCD lagrangian is then

$$\begin{aligned}
\mathcal{L}_{\text{ghost}} &= \left(\partial_\mu \eta^{a*} \right) D_{ab}^\mu \eta^b \\
&= \left(\partial_\mu \eta^{a*} \right) \left(\partial^\mu \delta_{ab} + g f_{abc} A_c^\mu \right) \eta^b .
\end{aligned} \qquad (1.11)$$

The contribution of the Fadeev-Popov ghost should be added to every loop diagram, in order to obtain the correct result. On the other hand, we can work in the axial gauge and this would restrict the gluon polarisations to be only two at the level of the gauge-fixing term, thus avoiding the use of ghost fields.

[†]In fact this constitutes an important and reliable test in big calculations. If one decides to keep an arbitrary value for ξ, the result associated to a physical observable, must be independent of this parameter.

1.2.3 The QCD lagrangian

As a summary, we collect the terms given by eqs.(1.9), (1.10) and (1.11) and present the full Lagrangian density for the gauge theory of QCD,

$$
\begin{aligned}
\mathcal{L}_{\mathrm{QCD}} &= \mathcal{L}_{\mathrm{clasical}} + \mathcal{L}_{\mathrm{gauge-fixing}} + \mathcal{L}_{\mathrm{ghost}} \\
&= \sum_f \bar{\psi}_f (i\slashed{D} - m_f 1)\psi_f - \frac{1}{4} F_a^{\mu\nu} F_{\mu\nu}^a - \frac{1}{2\xi}\left(\partial^\mu A_\mu^a\right)^2 + (\partial_\mu \eta^{a*}) D_{ab}^\mu \eta^b \quad (1.12)
\end{aligned}
$$

The QCD lagrangian is the platform on which the theoretical calculation of physical observables are resting. This theoretical description should match that coming from the experimental observations which, in a broad sense, consist of setting up a well characterised initial state of particles, having them interact in a "controlled" manner and measuring the production rates of particles in the final state.

A way to proceed in the theoretical calculation of any physical observable, is to divide the Lagrangian into a free field piece $\mathcal{L}_0$ and an interacting one $\mathcal{L}_I$ (proportional to the coupling g),

$$
\begin{aligned}
\mathcal{L}_{\mathrm{QCD}} &= \mathcal{L}_0 + \mathcal{L}_I \\
&= \mathcal{L}_0 - \Bigg\{ g\bar{\psi}T^a \slashed{A}^a \psi \\
&\quad + \frac{1}{2}g f_{abc}\left(\partial_\mu A_\nu^a\right) A^{b\mu} A^{c\nu} \\
&\quad - \frac{1}{2}g f_{abc}\left(\partial_\nu A_\mu^a\right) A^{b\mu} A^{c\nu} \\
&\quad - \frac{1}{4}g^2 \left(f_{eab} A_\mu^a A_\nu^b\right)\left(f_{ecd} A^{c\mu} A^{d\nu}\right) \\
&\quad - g f_{abc}\left(\partial_\mu \eta^{a*}\right) \eta^b A^{c\mu} \Bigg\}.
\end{aligned} \quad (1.13)
$$

The free field part of the Lagrangian, contains only dynamical terms for the propagation of the fields involved in the theory: quarks, gluons and ghosts. In the interaction part of the Lagrangian, the first of the three non-linear terms gives the fermion-gauge boson vertex interaction, the second and third terms lead to a triple gauge boson vertex interaction and the fourth term to a quartic gauge boson vertex interaction. These last two interactions are coming directly from the non-Abelian terms of the field strength tensor and are not present in QED, since photons do not self-interact. The last term represents the ghost-gluon vertex interaction.

If we consider the action defined as

$$
\mathcal{S} = \int \mathcal{L}_{\mathrm{QCD}} \, d^4 x,
$$

then the interacting theory can be solved perturbatively as an expansion in the strong coupling. This approximation will be valid if the coupling of the strong interactions is small and we will see that this is so at high energies.

The perturbative expansion involves the calculation of transition probabilities from initial to final states and taking into account all possible interaction configurations of the transition process between these states. More precisely, the description of the dynamical evolution between these two states is done in terms of the $S-$ matrix (or scattering matrix). The fact that we evaluate this matrix perturbatively is inherent to its highly complex nature.

A convenient way of describing pictorially each of the interaction terms involved in the perturbative calculation is by using *Feynman diagrams*, regulated by *Feynman rules*. These are nothing more than a book-keeping mechanism that allows us to represent the elements and topology of an interaction in a condensed manner. Each diagram, contributes to a particular order in the perturbation series and we only need to consider those which contribute to the order of the approximation that interests us.

In this way, the terms arising from the free field action $\mathcal{S}_0$ lead to propagators of the fields in momentum space (lines in a Feynman diagram), while $\mathcal{S}_I$ leads to quark-gluon and gluon-gluon interactions in momentum-conserving vertices.

1.3   The Feynman rules

In this section we present the Feynman rules for QCD. Quarks are depicted as solid lines, gluons as curly lines and ghosts as dashed lines. For the external legs we have,

incoming lines: outgoing lines:

$u(p)$ $\bar{u}(p)$

$\bar{v}(p)$ $v(p)$

$\epsilon^{\mu}(p)$ $\epsilon^{\mu *}(p)$
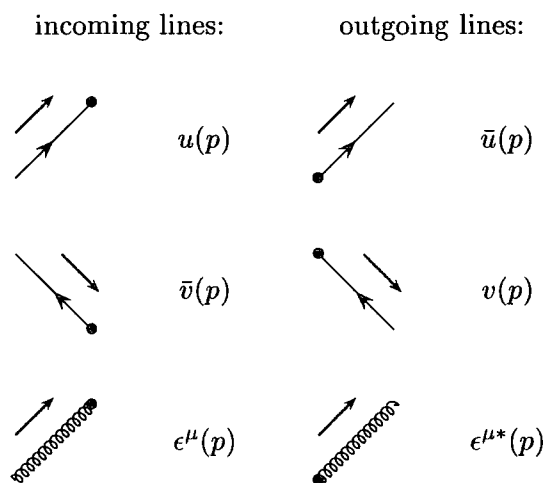
where the momentum flow along a lines is p in the direction indicated by the arrow alongside it. For fermion lines, the arrow on the line itself indicates the momentum flow.

The quark, gluon and ghost propagators are,

$$\frac{i(\not{p}+m)}{p^2-m^2+i\varepsilon}\delta_{ij}$$

$$\frac{-i}{p^2+i\varepsilon}\left[g^{\mu\nu}-(1-\xi)\frac{p^\mu p^\nu}{p^2}\right]\delta^{ab}$$

$$\frac{-i}{p^2+i\varepsilon}\delta^{ab}$$

The Lorentz indices are denoted with $\{\mu,\nu,...\}$. For the colour indices of gluons and ghosts we use $\{a,b,...\}$ and for the quarks i,j. Spinor and flavour indices for the quarks are implicit. The quark-gluon, ghost-gluon and gluon-gluon interaction vertices are,

$$-ig\gamma^\mu\,(T^a)_{ij}$$

$$gf^{abc}p^\mu$$

$$-gf^{abc}[\ \ (p_1-p_2)^\rho g^{\mu\nu}$$
$$+(p_2-p_3)^\mu g^{\nu\rho}$$
$$+(p_3-p_1)^\nu g^{\mu\rho}\ \ ]$$

$$-ig^2 f^{abe}f^{cde}\,(g^{\nu\sigma}g^{\mu\rho}-g^{\mu\sigma}g^{\nu\rho})$$
$$-ig^2 f^{ace}f^{bde}\,(g^{\rho\sigma}g^{\mu\nu}-g^{\mu\sigma}g^{\nu\rho})$$
$$-ig^2 f^{ade}f^{cbe}\,(g^{\nu\sigma}g^{\mu\rho}-g^{\rho\sigma}g^{\mu\nu})$$

Note that the gluon propagator is given in a covariant gauge specified by the parameter ξ. Also, we use the Feynman prescription and assign a positive imaginary part to the

denominator of the propagators, to ensure that the propagation is from earlier to later times. In the triple gluon vertex all particles are outgoing and momentum is conserved $(p_1^\mu + p_2^\mu + p_3^\mu = 0)$.

Together with the previous set of rules, we must also

1. integrate over loop momentum k for every closed loop, with a measure

$$\int \frac{d^4k}{(2\pi)^4},$$

2. multiply by a factor of (-1) for every quark or ghost loop,

3. multiply by a symmetry factor that normalises for permutations of the fields in a diagram. For example, multiply by a factor of $1/(n!)$ for a loop with n identical gluons.

In principle, we are able to write an expression for any physical amplitude $i\mathcal{M}$ at any order in perturbation theory, provided we follow these rules and sum over all relevant diagrams. For the squared of the amplitude (or matrix elements), the following sums will also be needed

$$\sum_{spins} \bar{u}(p)u(p) = \not{p} + m, \tag{1.14}$$

$$\sum_{spins} \bar{v}(p)v(p) = \not{p} - m, \tag{1.15}$$

and in the Feynman gauge the sum over gluon polarisations is

$$\sum_{pols.} (\epsilon^\mu)^* \epsilon^\nu = -g^{\mu\nu}. \tag{1.16}$$

It can be easily inferred that the squared matrix elements will always be proportional to an even power of the coupling g, therefore it is usual to have the perturbative expansion in powers of α_S, where

$$\alpha_S = \frac{g^2}{4\pi} \tag{1.17}$$

Once we have summed over the spins and polarisations, we can simplify the gamma matrices using identities that are easily derived from the Clifford algebra expression (1.2). Things can be further simplified if we neglect the masses of the quarks. This turns out to be a good assumption if the physical observations we are comparing our results with, are done at high energies. Throughout this thesis, this will be assumed.

1.4   Regularisation

The Feynman rules given in the previous section, allow us to calculate easily Feynman diagrams at tree-level (or without loops). But, as soon as we calculate diagrams with loops (which are associated with higher order terms in the perturbative calculation of any physical observable), we will discover that these generate divergent integrals due to the behavior of the integrand at high and low virtual momenta.

For example, consider the following one-loop integral, associated with the diagram shown,

$$I = \int \frac{d^4\ell \; f(\ell^2)}{\ell^2 (\ell+p)^2 (\ell+p_2)^2}.$$

The divergences of the integrand associated with high virtual momenta,

$$\ell \to \infty \quad \Longrightarrow \quad I \to \infty \quad (logarithmically),$$

are called *ultraviolet* (UV) *divergences*. Furthermore, there are divergences appearing when one of the propagators in the loop becomes zero for a specific value of loop momenta, i.e. when for example

$$\ell \to 0, -p_2 \quad \Longrightarrow \quad I \to \infty,$$

where we consider $p_1^2 = p_2^2 = 0$. These are the so-called *infrared* (IR) *divergences*. If the propagators are massive, e.g. $(\ell+p)^2 - m^2$, the mass plays the role of regulator. In QCD, the presence of massless gluons and the assumption of light quarks, give rise to this IR divergent behavior.

At first sight, the presence of these divergences would render all the perturbation procedure, meaningless. Fortunately, QCD is a renormalisable quantum field theory. In practice, this means we have a well defined set of rules which allow us to calculate matrix elements that are free from UV divergences order by order in the interaction coupling constant of the perturbative series (see section 1.5). On the other hand, we will see in Chapter 2, that IR divergences cancel for a particular kind of physical observables and that we are now able to largely predict their structure even for one- and two-loop amplitudes.

To be able to manipulate these integrals in a safe manner, we must first regularise them, i.e. provide a well defined meaning to their divergent behavior and be able to isolate it. The regularisation prescription we use, must preserve the gauge invariance of the theory, otherwise the renormalisability of the theory cannot be guaranteed [‡]

Let us look at the different methods we have to regulate Feynman integrals by means of a simple example. We will see in Chapter 3 that to be able to integrate out the loop-momenta from these integrals, we will need to calculate the following (Minkowski space) integral

$$I \sim \int_{-\infty}^{+\infty} d^4\ell \frac{1}{(\ell^2 - \Delta + i\varepsilon)^m}, \tag{1.18}$$

where m is a positive integer and the $i\varepsilon$ term is the Feynman prescription for the propagators to keep the integral convergent for all values of Δ. If we do not have this imaginary piece, there is a value of Δ for which the denominator of this integral vanishes, producing a singularity that cannot be regularised.

The contents of the parameter Δ are linear combinations of invariant masses (Mandelstam variables) and masses of the fields. The fact that singularities can arise when a scale acquires a value that makes it cross a discontinuity in the kinematic phase space is precisely what we want to avoid.

This always happens when we want to calculate a loop integral in what would otherwise be an inaccessible region of the kinematic phase space. So the $i\varepsilon$ piece provides appropriate analytic continuations that prescribe the imaginary part gained by the integral after a scale (or scales) shifts its value to a value below its physical threshold. A complete discussion about the analytic properties of Feynman integrals, can be found in ref.[9] and a recent example of analytical continuation of a Feynman integral, in ref. [10].

Now, let us go back to the description of the integral in eq. (1.18). Its denominator is,

$$den \equiv (\ell_0)^2 - \underline{\ell}^2 - \Delta + i\varepsilon \tag{1.19}$$

and has poles in the complex ℓ_0 plane at $(-\sqrt{\underline{\ell}^2 + \Delta} + i\varepsilon', \sqrt{\underline{\ell}^2 + \Delta} - i\varepsilon')$. So it would be best to rotate the integration contour, to be able to integrate along the complex direction, i.e. we want to Wick rotate (WR) the integration space. This means

$$\text{Minkowski space} \quad \mapsto \quad \text{Euclidean space}$$

[‡]Gauge invariance of the theory must be preserved otherwise the Slavnov-Taylor identities (which are needed to prove the renormalisability of the theory) are not longer valid. Invariance under local gauge transformations imply extensive relations among Green's functions. In non-abelian theories these relations are the so called Slavnov-Taylor identities. In QED, they are the Ward-Takahashi identities [1, 3, 4].

$$\ell_0 \quad \mapsto \quad i\ell_0^E \tag{1.20}$$

$$d^4\ell \quad \mapsto \quad id^4\ell^E \tag{1.21}$$

so that eq.(1.19), becomes

$$den = -(\ell_0^E)^2 - \underline{\ell}^2 - \Delta, \tag{1.22}$$

where the Feynman prescription is implicit. With this decision, we have made the denominator of the integral, to be dependent only on the length of the momentum vector. Therefore it is more natural to work in polar coordinates, so eq.(1.21) becomes

$$d^4\ell^E = \underbrace{d\Omega_4}_{\substack{\text{surface of a} \\ 4 - \text{dim sphere}}} \times (\ell^E)^3 \ d\ell^E = 2\pi^2 \ (\ell^E)^3 \ d\ell^E \tag{1.23}$$

and the integral in eq.(1.18) is now

$$I = \int_{-\infty}^{+\infty} d^4\ell \frac{1}{(\ell^2 - \Delta + i\varepsilon)^m} \xrightarrow{WR} i(-1)^m \int d\Omega_4 \int_0^{+\infty} \frac{(\ell^E)^3}{[(\ell^E)^2 + \Delta]^m} d\ell^E. \tag{1.24}$$

We have not dealt with the divergences yet. We can see that our integral is still divergent when ℓ^E grows and in fact if we apply the change of variables $x = (\ell^E)^2$, to this integral in Euclidean space, we get

$$I = \frac{1}{2} \int_0^{+\infty} \frac{x}{(x + \Delta)^m} dx = \frac{1}{2(m - 1)(m - 2)\Delta^{m-2}}, \tag{1.25}$$

which is singular for a particular choice in the power m. This would still happen even if we had extra powers of loop momenta in the numerator.

We now want to regulate these integrals, so we briefly look into the three most important regularisation procedures

1. *Cut-off regularisation* Instead of integrating up to infinity, introduce a large, but finite, momentum cut-off. For example, in eq.(1.25), for $m = 2$ the integral is clearly divergent, but with the cut-off Λ we have

$$\int_0^{+\Lambda} \frac{x}{(x + \Delta)^2} dx = \ln\left(\frac{\Lambda + \Delta}{\Delta}\right) - \frac{\Lambda}{\Lambda + \Delta},$$

which is now a regulated integral. This is all fine, except for the fact that by introducing the momentum cut-off we are automatically spoiling Lorentz invariance.

2. *Pauli-Villars regularisation* Introduce massive auxiliary fields called *regulators* in order to eliminate the singularities from propagators, so for each one we would have

$$\frac{1}{\ell^2} \rightarrow \frac{1}{\ell^2} - \frac{1}{\ell^2 - \Lambda^2},$$

for a large mass of the new particle Λ^2. When $\ell^2 \gg \Lambda^2$, propagators partially cancel. Our previous example would now look like

$$\int_0^{+\infty} \left[\frac{1}{(x+\Delta)^2} - \frac{1}{(x+\Delta_\Lambda)^2} \right] x\,dx = \ln\left(\frac{\Delta_\Lambda}{\Delta}\right),$$

where $\Delta_\Lambda = \Delta + \alpha\Lambda^2$. Again, this is a regulated integral, but when applying this procedure we spoil gauge invariance, since we would need to introduce a mass for the gluon.

3. *Dimensional regularisation* Make a continuation of the integral in the number of dimensions by assuming that they are analytic functions of the number of dimensions $D = 4 - 2\epsilon$, where ϵ is a small parameter. The divergent integrals are now well behaved and the divergent pieces are explicit poles in the dimensional continuation parameter ($1/\epsilon^n$, $n = 1, 2, 3, \ldots$). Dimensional regularisation allows a consistent gauge invariant treatment of divergent Feynman integrals to all orders in perturbation theory. For the reminder of this section we will concentrate on this method, since it is the one we choose to apply in our calculations.

The integral we have been using as our example is based on that of eq. (1.24), but now, using dimensional regularisation (DR), it will be written as

$$I = i(-1)^m \int d\Omega_4 \int_0^{+\infty} d\ell^E \frac{(\ell^E)^3}{[(\ell^E)^2 + \Delta]^m} \xrightarrow{DR} i(-1)^m \int d\Omega_D \int_0^{+\infty} d\ell^E \frac{(\ell^E)^{D-1}}{[(\ell^E)^2 + \Delta]^m} \tag{1.26}$$

The integral for the area of a D-dimensional sphere (or integral over the solid angle), can be done knowing that

$$\pi^{1/2} = \int_{-\infty}^{\infty} dx\, e^{-x^2},$$

then

$$\pi^{D/2} = \prod_i^D \int_{-\infty}^{\infty} dx_i\, e^{-x_i^2} = \int_{-\infty}^{\infty} d^D x\, \exp\left(-\sum_i^D x_i^2\right),$$

but, the r.h.s. can also be written in polar coordinates as

$$\pi^{D/2} = \int d\Omega_D \int_0^{\infty} dr\, r^{D-1}\, e^{-r^2}.$$

Finally, we can change variables to $y = p^2$ and use the definition of the Gamma function[§]

[§]The integral form of the Gamma function for an arbitrary complex number (with positive real part) is

$$\Gamma(z) = \int_0^{+\infty} dt\, t^{z-1} e^{-t}$$

to have

$$\pi^{D/2} \quad = \quad \int d\Omega_D \times \frac{1}{2} \int_0^\infty dy \; y^{\frac{D-2}{2}} \; e^{-y} = \int d\Omega_D \times \frac{1}{2}\Gamma\left(\frac{D}{2}\right).$$

So for the integration over the solid angle we have

$$\int d\Omega_D = \frac{2\pi^{\frac{D}{2}}}{\Gamma\left(\frac{D}{2}\right)}. \tag{1.27}$$

To complete the integrations in eq. (1.26), we need to calculate the integral over the loop momenta. If we consider the change of variables

$$x = \frac{\Delta}{(\ell^E)^2 + \Delta},$$

and use the definition of the Beta function[¶], we obtain

$$i(-1)^m \int_0^{+\infty} d\ell^E \frac{(\ell^E)^{D-1}}{[(\ell^E)^2 + \Delta]^m} \quad = \quad \frac{i(-1)^m}{2}\Delta^{D/2-m} \int_0^1 dx \; x^{m-1-D/2} \; (1-x)^{D/2-1}$$

$$= \quad \frac{i(-1)^m}{2}\Delta^{D/2-m}\frac{\Gamma\left(m-\frac{D}{2}\right)\Gamma\left(\frac{D}{2}\right)}{\Gamma(m)}. \tag{1.28}$$

Finally, the integration in DR (Euclidean space) can be obtained after substitution of eqs. (1.27) and (1.28) in eq. (1.26), as

$$i(-1)^m \int d\Omega_D \int_0^{+\infty} d\ell^E \frac{(\ell^E)^{D-1}}{[(\ell^E)^2 + \Delta + i\varepsilon]^m} = i(-1)^m \pi^{\frac{D}{2}}\frac{\Gamma\left(m-\frac{D}{2}\right)}{\Gamma(m)}\Delta^{D/2-m}. \tag{1.29}$$

The same procedure can be applied to an integral that has an arbitrary power of squared loop momentum in the numerator. So a general integral in Minkowski space that is dimensionally regulated,

$$I_{\alpha\beta} \equiv \int_{-\infty}^{+\infty} d^D\ell \frac{(\ell^2)^\alpha}{(\ell^2 - \Delta + i\varepsilon)^\beta},$$

will be in Euclidean space,

$$I_{\alpha\beta} \equiv \underbrace{i(-1)^{\alpha+\beta}}_{WR} \int_{-\infty}^{+\infty} d^D\ell^E \frac{(\ell^E)^{2\alpha}}{[(\ell^E)^2 + \Delta]^\beta} = i(-1)^{\alpha+\beta} \int d\Omega_D \int_0^{+\infty} d\ell^E \frac{(\ell^E)^{2\alpha+D-1}}{[(\ell^E)^2 + \Delta]^\beta}.$$

Applying the same substitutions and changes of variable as before, we get

$$I_{\alpha\beta} = i(-1)^{\alpha+\beta}\frac{\pi^{\frac{D}{2}}}{\Gamma\left(\frac{D}{2}\right)}\frac{\Gamma\left(\alpha+\frac{D}{2}\right)\Gamma\left(\beta-\alpha-\frac{D}{2}\right)}{\Gamma(\beta)\Delta^{\beta-\alpha-\frac{D}{2}}}. \tag{1.30}$$

[¶]The Beta function is defined as follows

$$\beta(a,b) = \int_0^1 dt \; t^{a-1} \; (1-t)^{b-1} = \frac{\Gamma(a)\Gamma(b)}{\Gamma(a+b)}$$

It must be noted that to arrive to this result we are implicitly assuming that the dimension is a positive integer and that it must satisfy $\frac{D}{2} < \beta - \alpha$, (or $\frac{D}{2} < m$, in the previous examples) otherwise, the integrals would not be convergent.

So far, we have looked at how DR affects the way we perform loop integrals. But, this is not the only aspect of a perturbative calculation that changes. To have a consistent result we must have in mind the following modifications

- the loop integral measure given in the Feynman rules, changes (as already seen)

$$\int \frac{d^4\ell}{(2\pi)^4} \to \int \frac{d^D\ell}{(2\pi)^D}$$

- the Clifford algebra of eq. (1.2) will be affected in the sense that we now have D gamma matrices spanning this space. So when summing over μ and ν, we will have extra terms proportional to D, i.e. $g_{\mu\nu}g^{\mu\nu} = D$, $\gamma_\mu\gamma_\nu\gamma^\mu = (2 - D)\gamma_\nu$, etc.

- the integration of a physical observable over the external momenta phase space, will also change,

$$\int \frac{d^3p}{2E\,(2\pi)^3} \cdots (2\pi)^4 \delta^4(p_i - p_f) \to \int \frac{d^{D-1}p}{2E\,(2\pi)^{D-1}} \cdots (2\pi)^D \delta^D(p_i - p_f)$$

- the action

$$\mathcal{S} = \int d^D x \, \mathcal{L}$$

is a dimensionless quantity, so the QCD lagrangian has to be modified to have a consistent number of dimensions. From the kinetic energy terms of the quarks and gluons of this Lagrangian, we can see that the mass dimension of their fields are

$$\text{from} \quad m\bar{\psi}_f\psi_f \quad \implies \quad [\psi_f] = \frac{D-1}{2}$$

$$\text{from} \quad \partial_\mu A_\nu^a \partial_\nu A_\mu^a \quad \implies \quad [A_\mu^a] = \frac{D}{2} - 1$$

Then the interaction term $g\bar{\psi}_f \slashed{A}\psi_f$ is actually telling us that $[\bar{\psi}_f \slashed{A}\psi_f] = 3D/2 - 2$ (when in fact it should be D). This automatically imposes a dimension for the coupling g such that at $D = 4$ the coupling has no dimension. We introduce an arbitrary mass scale μ to replace the coupling as

$$g \to \mu^\epsilon g, \qquad \epsilon = 2 - \frac{D}{2}. \tag{1.31}$$

We have one more scale in our theory because we use the dimension as a regulator.

We have seen how DR impacts the structure of loop integration and forces us to introduce a new scale to regulate the dimension of the action. Still, we have some freedom to choose the number of polarisations of internal and external gluon and quark fields, which defines different DR schemes. In our calculations and throughout this thesis, we use the Conventional Dimensional Regularisation (CDR) scheme. This implies that we make no distinction between real and virtual partons (radiated partons and partons in loops, respectively). Furthermore, we consider quarks to have two helicity states and gluons to have $D - 2$. A thorough discussion of the different DR schemes can be found in ref.[11] and references therein. For an introduction to the technique of DR and some applications see ref.[12] and references therein.

1.5   Renormalisation

In section 1.4 we saw how the Feynman integrals, arising from a perturbative calculation in QCD, are singular in the high (UV singularities) and low (IR singularities) momentum limit. Then, we isolated this divergent behaviour using a regularisation scheme (CDR). We have hinted to the fact that IR singularities will cancel and this will be discussed further on. In this section, we will discuss how renormalisation provides a theory free from UV divergences.

Current experimental set-ups can only probe with energies ~ 1 TeV, which imposes boundaries on the phenomena we are able to describe and on the way the description itself is done. There is a limit on the resolution of our measurement and this must be reflected by the theoretical calculations we do.

The fact that UV divergences stem from a high loop momentum limit of an integral rendering it infinite, has repercussions on any perturbative calculation that involves such terms. The mere existence of UV divergences (before renormalisation) means that in any physical process there are contributions from quantum fluctuations on every time (distance) scale [4]. However, there is a way to describe physical observables perturbatively that is consistent with our experimental (*finite*) results.

Let us explain what we mean using the diagram in fig.(1.1). We can insert a perturbative correction to the propagators and vertices of a generic Feynman diagram. The loop integrals in these kind of Feynman graphs will have big contributions from momenta much larger than, say, $\sqrt{s}$ (the scale of the process). This means that our perturbative calculation for a physical observable, e.g. a cross section, will have big contributions from

$$\Delta t \sim \frac{1}{\sqrt{s}}$$
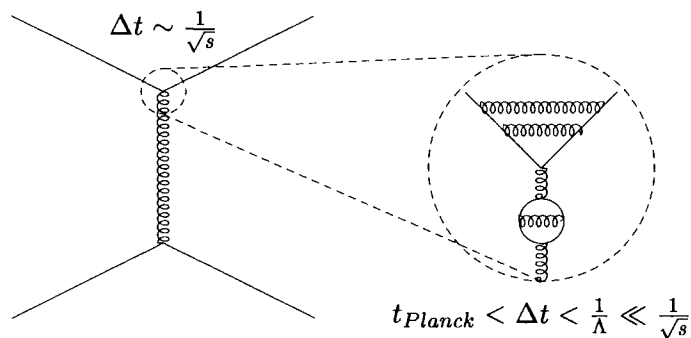
$$t_{Planck} < \Delta t < \frac{1}{\Lambda} \ll \frac{1}{\sqrt{s}}$$

Figure 1.1: Physics at different time scales

interactions that occur on time scales much smaller than $1/\sqrt{s}$.

Furthermore, consider loop corrections on short time scales (and before gravity takes over),

$$t_{Planck} < \Delta t < 1/\Lambda,$$

where Λ is a UV cut off scale much larger than the characteristic scale $\sqrt{s}$. Then these contributions can be absorbed into changes in the definition of the couplings, masses and normalisation of fields of the theory if we are willing to neglect contributions to the cross section of $\mathcal{O}(\frac{\sqrt{s}}{\Lambda})$ (or smaller than the cross section itself) [13, 4].

The process of consistently absorbing short-time physics into a *finite* number of parameters (associated with the masses, couplings and fields of the theory) and performing it to *all orders* of the perturbative expansion, is called renormalisation.

In practice, this means we take the fields and coupling from the QCD Lagrangian of eq.(1.12), and redefine them with a multiplicative factor

$$\psi_f^i \quad \rightarrow \quad Z^{1/2}\psi_{f,R}^i, \tag{1.32}$$

$$A_\mu^a \quad \rightarrow \quad Z_A^{1/2}A_{\mu,R}^a, \tag{1.33}$$

$$\eta^a \quad \rightarrow \quad Z_\eta^{1/2}\eta_R^a, \tag{1.34}$$

$$g \quad \rightarrow \quad Z_g g_R, \tag{1.35}$$

$$m \quad \rightarrow \quad Z_m m_R, \tag{1.36}$$

$$\xi \quad \rightarrow \quad Z_A \xi_R, \tag{1.37}$$

where we have used the R subscript to denote the renormalised quantities. The renormalisation constant for the gauge parameter ξ is the same as the one for the gluon fields, so that the gauge fixing term in the Lagrangian, remains with the same structure as before.

Since we have only redefined the fields and couplings, we expect that the integration over the exponential of the action (or generating functional from which the Green's functions are derived) does not change. Therefore everything that we have extracted from it, such as the structure of the S-matrix and Feynman rules, is still valid for the renormalised quantities.

The idea is that the Green's functions for the unrenormalised fields carrying the UV divergences, are proportional to the Green's functions for the renormalised fields with the renormalisation constant as the constant of proportionality. If we can absorb the UV divergences from the Green's functions of the original fields into the renormalisation constant, and leave the new ones as quantities free from UV singularities, then our theory has been renormalised.

In this way the renormalised fields are interpreted as the ones that have a physical meaning and the renormalised couplings as the ones we (indirectly) measure.

As we mentioned in section 1.4, QCD is a renormalisable theory and it has been proven that the renormalisation procedure works at all orders by adjusting the renormalisation constants at each order. The proof is rather involved and uses the symmetries of the Lagrangian, such as gauge invariance, to obtain relations amongst the renormalisation constants. These are the so called Slavnov-Taylor identities, which are equivalent to the Ward-Takahashi identities found in QED.

Apart from absorbing the UV divergences in the Z factors, we may want to absorb an extra finite quantity and this should just be a matter of choice. In fact, there is a degree of arbitrariness on the amount of information we can add to the multiplicative factors after absorbing the singular piece. The choice we make defines the renormalisation *scheme* with which we decide to renormalise the theory and present our results.

In this thesis we use the $\overline{\text{MS}}$ (Modified Minimal subtraction) scheme, where we only remove the UV singularity as poles of the following structure

$$\frac{1}{\bar{\epsilon}} = (4\pi)^{\epsilon} \exp(-\epsilon\gamma) \frac{1}{\epsilon} \tag{1.38}$$

where, $\gamma = 0.5772\ldots$ is Euler's constant.

The choice of renormalisation scheme goes hand in hand with the fact that we have introduced a parameter that is not intrinsic to the theory. Since we regularised with CDR, we had to use a mass scale μ (renormalisation scale) that keeps the action dimensionless.

The dependence on this renormalisation scale μ is present on the renormalised fields and couplings. Depending on the value we chose for μ (and on the renormalisation scheme

we work in), we will have a different value for the same physical observable. But, this does not mean that our results are inconsistent. On the contrary, the description we make of an observable in a particular scheme should be equivalent to any other. This automatically restricts the behaviour of renormalised quantities when we change from one scheme to another and take different values for the renormalisation scale.

Mathematically, the behaviour of a physical observable under these changes of scheme and scale are compiled in differential equations called *renormalisation group equations*. These equations are based on the ultimate independence on μ for all physical observables (since μ is not a parameter natural to the theory).

There is a nice but approximate way of thinking of μ, that follows on the argumentation we gave at the beginning of this section. When we choose a particular value of $\mu = \hat{\mu}$, we are effectively removing the physics of time scales $\Delta t \ll 1/\hat{\mu}$, from the perturbative calculation of a physical observable. Then, these effects are accounted for by the dependence on μ of the value of the strong coupling in eq.(1.17), i.e. $\alpha_S \to \alpha_S(\hat{\mu})$.

1.5.1 The running of α_S

From eqs. (1.17), (1.31) and (1.35), we can write the renormalised strong coupling constant as

$$\alpha_0 = Z_g^2 \ (\mu^2)^\epsilon \ \alpha_R, \tag{1.39}$$

where we have used the subscripts 0 and R for the unrenormalised ("bare") and renormalised coupling, respectively.

Here, the value of Z_g can be calculated perturbatively for a general SU(N) gauge theory (see for example [1, 6]) to give

$$\alpha_0 S_\epsilon = (\mu^2)^\epsilon \alpha_R \left[1 - \frac{\beta_0}{\epsilon} \left(\frac{\alpha_R}{2\pi} \right) + \left(\frac{\beta_0^2}{\epsilon^2} - \frac{\beta_1}{2\epsilon} \right) \left(\frac{\alpha_R}{2\pi} \right)^2 + \mathcal{O}(\alpha_R^3) \right], \tag{1.40}$$

where

$$S_\epsilon = \exp(-\epsilon\gamma) \ (4\pi)^\epsilon, \tag{1.41}$$

and

$$\beta_0 = \frac{1}{6} \left(11 C_A - 4 T_R N_F \right) \tag{1.42}$$

$$\beta_1 = \frac{1}{6} \left(17 C_A^2 - 10 C_A T_R N_F - 6 C_F T_R N_F \right). \tag{1.43}$$

In these equations, we have used the usual notation

$$C_F = \frac{N^2 - 1}{2N}, \quad C_A = N \quad \text{and} \quad T_R = \frac{1}{2} \tag{1.44}$$

and N_F is the number of quark flavours.

The parameters β_0 and β_1 are actually the first two coefficients in a perturbative expansion of the β function (renormalisation group equation) which provides the μ dependence of the strong coupling and is given by

$$\beta(\alpha_S(\mu^2)) \equiv \mu^2 \frac{\partial \alpha_S}{\partial \mu^2} = -\beta_0 \alpha_S(\mu^2)^2 - \beta_1 \alpha_s(\mu^2)^3 - \cdots, \qquad (1.45)$$

where we now refer to the renormalised coupling, simply as α_S.

Eq.(1.45) can be verified by taking eq.(1.39) and calculating the differential form of the beta function. Using the expression for Z_g used in eq.(1.40), one is able to check order by order the expansion on the r.h.s. of eq.(1.45).

The renormalisation group equation tells us how to account for the short time scale physics in the value of the renormalised coupling, given that we know its value for a particular mass scale μ_0. This is what was represented in fig. (1.1) as the scale cut-off Λ.

The scale μ_0 represents the boundary condition for the differential equation of (1.45) which can also be expressed as

$$\int_{\alpha_S(\mu_0^2)}^{\alpha_S(\mu^2)} \frac{d\alpha_S}{\beta(\alpha_S)} = \log\left(\frac{\mu^2}{\mu_0^2}\right), \qquad (1.46)$$

with solution

$$\frac{1}{\alpha_S(\mu^2)} - \frac{1}{\alpha_S(\mu_0^2)} = \beta_0 \log\left(\frac{\mu^2}{\mu_0^2}\right) - \frac{\beta_1}{\beta_0} \log\left(\frac{\alpha_S(\mu^2)}{\alpha_S(\mu_0^2)}\right), \qquad (1.47)$$

when we keep the first two terms of the beta function. Or for simplicity

$$\alpha_S(\mu^2) = \frac{\alpha_S(\mu_0^2)}{1 + \alpha_S\, \beta_0 \log\left(\frac{\mu^2}{\mu_0^2}\right)}, \qquad (1.48)$$

when we keep only the first one. Note that the value of α_S decreases as μ increases. This means QCD enjoys the property of *asymptotic freedom*[||]. In other words, QCD acts like a weakly interacting theory on short time scales (or high energies).

The same conclusion can be drawn from the fact that any physical observable must not depend on the renormalisation scale, when we consider all orders of its perturbative expansion in the strong coupling. In fact, a dimensionless physical observable (for example a decay rate Γ) can only depend on the dimensionless ratio s/μ^2, where s is the energy of the system.

We can then write the renormalisation group equation for the rate as

$$\frac{d\Gamma}{d\mu^2} \equiv \left[-\frac{\partial}{\partial t} + \beta(\alpha_S)\frac{\partial}{\partial \alpha_S} \right] \Gamma(\alpha_S(\mu^2), \exp(t)) = 0, \qquad (1.49)$$

[||]Together with β_0 having a positive value for $N_F \leq 16$. This is crucial since β_0 with the opposite sign would make the coupling increase at large μ^2.

where $t = \log(s/\mu^2)$. The fact that $\Gamma(\alpha_S(s), 1)$ is a solution to this equation[**], proves that we are allowed to have a perturbative expansion to describe the rate (in terms of the strong coupling and at high energies) as

$$\Gamma = \Gamma(\alpha_S(s), 1) = a\,\alpha_S(s) + b\,\alpha_S s^2 + c\,\alpha_S(s)^3 + \cdots \tag{1.50}$$

1.5.2 α_S from experiment

Consider the result of solving the renormalisation group equation with all the coefficients β_i beyond β_0 set to zero, then we have (see eq.(1.48))

$$
\begin{aligned}
\alpha_S(\mu) &= \alpha_S(Q) - \left(\frac{\beta_0}{\pi}\right)\ln\left(\frac{\mu^2}{Q^2}\right)\alpha_S^2(Q) + \left(\frac{\beta_0}{\pi}\right)^2\ln^2\left(\frac{\mu^2}{Q^2}\right)\alpha_S^3(Q) + \cdots \\
\alpha_S(\mu) &= \frac{\alpha_S(Q)}{1 + \left(\frac{\beta_0}{\pi}\right)\ln\left(\frac{\mu^2}{Q^2}\right)\alpha_S(Q)}.
\end{aligned}
\tag{1.51}
$$

We can see that a series in powers of $\alpha_S(Q)$, i.e. the strong coupling at a large scale (GUT scale), is summed into a simple function of μ. Then the renormalisation group equation is summing the effects of short-time physics. Here $\alpha_S(Q)$ appears as a parameter for the solution, the boundary value for the differential equation.

In theory, we can have solutions to this equation for different boundary values, given a description for different versions of QCD. Thus the parameter $\alpha_S(Q)$, tells us which version of QCD we have. It should be possible then to extract the value of this parameter by making a number of experimental observations at different energy scales Q. The results can be compared with the theoretical prediction given by eq.(1.45), to confirm that the coupling behaves as we expected.

Instead of eq.(1.51) and since we know that the coupling diverges as we reduce the energy scale, a more convenient way to write the solution for the running coupling is

$$\alpha_S(\mu) = \frac{1}{\beta_0 \ln\left(\frac{\mu^2}{\Lambda^2}\right)}, \tag{1.52}$$

where we introduced a parameter Λ, a scale near which perturbation theory becomes unreliable. These two forms of description of the running coupling are completely equivalent. Nevertheless, Λ has been disfavored (since its definition changes order-by-order in

---

[**]Just by changing the derivatives on the first term of eq.(1.49) we can see that

$$\frac{\partial\Gamma(\alpha_S(s), 1)}{\partial t} = \frac{\partial\alpha_S}{\partial t}\frac{\partial\Gamma(\alpha_S(s), 1)}{\partial\alpha_S} \to \beta(\alpha_S)\frac{\partial\Gamma(\alpha_S(s), 1)}{\partial\alpha_S},$$

which cancels the second term of the same equation.

perturbation theory) and instead it has become more common to use $Q = M_Z$ the mass of the Z boson, so

$$\alpha_S(\mu) \;=\; \frac{\alpha_S(M_Z)}{1 + \left(\frac{\beta_0}{\pi}\right) \ln\left(\frac{\mu^2}{M_Z^2}\right)\, \alpha_S(M_Z)}. \tag{1.53}$$

This last choice, moves the description to the asymptotic region where perturbation theory works best. Moreover, the experimental measurements on the Z-pole are of high precision (LEP) due to high statistics.

The most recent data analysis, compiles measurements of the strong coupling from a wide rage of experiments and scales. The values are consistent with the theory and at NNLO is [14]

$$\alpha_S(M_Z) = 0.1172 \pm 0.0045. \tag{1.54}$$

1.5.3   Scale choice and uncertainty

In eq.(2.31) of section 2.1.4 we will calculate the rate for the (next-to-leading order to the leading-order) cross section in e^+e^- annihilation to hadrons via virtual photon as

$$\Gamma = 1 + \frac{\alpha_S(\mu)}{\pi}.$$

In fact more than the next-to-leading correction is known [15] and we can write it in the following form

$$\begin{aligned}
\Gamma \;=\; & 1 + \frac{\alpha_S(\mu)}{\pi} + \left[1.4092 + 1.9167 \ln\left(\frac{\mu^2}{s}\right)\right]\left(\frac{\alpha_S(\mu)}{\pi}\right)^2 \\
& + \left[-12.805 + 7.8186 \ln\left(\frac{\mu^2}{s}\right) + 3.674 \ln^2\left(\frac{\mu^2}{s}\right)\right]\left(\frac{\alpha_S(\mu)}{\pi}\right)^3 \\
& + \cdots
\end{aligned} \tag{1.55}$$

Since we have higher order terms, we have to use for $\alpha_S(\mu)$, the solution of the renormalisation group equation with at least two terms included (see eq.(1.47)).

We discussed in the previous section how we define the running of the strong coupling by a particular choice of μ. In the r.h.s. of eq.(1.55), both α_S and the perturbative coefficients depend on μ. On the l.h.s. the rate does not depend on μ, so we still have

$$\frac{d}{d\ln\mu^2}\Gamma = 0. \tag{1.56}$$

Nevertheless, if in eq.(1.55) we truncate the series and use only the first correction to the rate, we spoil its μ independence. Let us demonstrate what we mean by writing the rate

as a general series

$$\Gamma \sim \sum_{i=1}^{\infty} c_n(\mu)\alpha_S^n(\mu). \tag{1.57}$$

Then, let us truncate this series to take only N terms. If we differentiate this truncated series we get, from eq.(1.56),

$$\frac{d}{d\ln\mu^2} \sum_{i=1}^{N} c_n(\mu)\alpha_S^n(\mu) = -\frac{d}{d\ln\mu^2} \sum_{i=N+1}^{\infty} c_n(\mu)\alpha_S^n(\mu),$$

this reminder is of order α_S^{N+1} as $\alpha_S \to 0$, i.e.

$$\frac{d}{d\ln\mu^2} \sum_{i=1}^{N} c_n(\mu)\alpha_S^n(\mu) = \mathcal{O}\left(\alpha_S^{N+1}(\mu)\right). \tag{1.58}$$

This obviously means that the more higher order terms we calculate, the less the rate depends on the renormalisation scale. If we truncate the series, we do not allow for the cancellation of the scale dependence between different orders and we have a residual dependence on μ of one order higher than the truncation order.

We can ultimately assess the uncertainty in a perturbative calculation, if we allow the renormalisation scale to vary in an interval proportional to the physical scale Q, usually $Q/2 \leq \mu \leq 2Q$. This uncertainty (theoretical error) will then dominate all determinations of our measurements. Thus, as more orders of the perturbation theory are included, the determination becomes more accurate and the uncertainty is reduced. In section 2.4.1 we will see an example of this behaviour.

For the moment let us turn to a more practical discussion in terms of electron-positron annihilation. We will show the infrared singular behaviour of some terms in a higher order calculation and how we can deal with them. This will lead to the discussion of the hard scattering cross section which is directly related to the partonic matrix element calculation we shall present in the last Chapter.

Chapter 2

Partons, Hadrons and Jets

Electron-positron annihilation into hadrons at high energies provides an example that helps to illustrate the basic ideas and properties of perturbative QCD. Experimentally, it represents one of the cleanest and therefore most precise environments in which to make QCD studies.

In section 2.1, we calculate the *total cross section* for $e^+e^- \to hadrons$ at leading order (LO), and see how the IR singularities arise and cancel at next-to-leading order (NLO).

This serves as a didactic introduction into section 2.2 where the concept of an infrared observable is discussed giving particular attention to *jets*. A jet is a highly collimated spray of hadrons and perturbative QCD confirms the intricate jet structure observed in high energy experiments for electron-positron annihilation. To be able to describe this phenomena, we need to explore the jet definition together with the discussion of $e^+e^- \to hadrons$, already mentioned.

Moving closer to our final goal, which is the calculation of partonic matrix elements, in section 2.3 we establish the link between these and the total hadronic cross section using factorisation. We also provide a summary of the parts needed for such a partonic matrix element calculation and isolate the ones that need to be calculated.

In the last section of this Chapter, we explore the different areas upon which a NNLO calculation has an impact. In section 2.2 we discuss briefly the improvements on the jet description and in section 2.4.1, we show how the dependence on the renormalisation scale is reduced, using a concrete example. The Chapter ends with a discussion of a possible new physics signature at the TeV scale in the single jet inclusive cross section.

2.1 Electron-positron annihilation

For simplicity we consider the cross section for e^+e^- annihilation into two *massless* partons (a quark-antiquark pair), via a virtual photon*.

Furthermore, we will leave the fermion current out of our calculation, since it will contribute with the same overall factor to all orders. Effectively, we look at the "decay" $\gamma^* \to q\bar{q}$ at LO and NLO.

2.1.1 LO cross section: no emissions

At lowest order, the Feynman diagram we must analyse is the one shown in fig.(2.1), where p_i^μ are the momenta for the outgoing quarks and $Q^2 = s$. Applying the Feynman
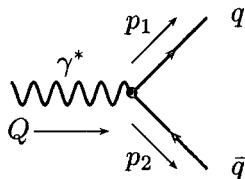
Figure 2.1: Leading order Feynman diagram for $\gamma^* \to q\bar{q}$

rules of section 1.3 we get the following LO scattering amplitude

$$i\mathcal{M}_0 = \bar{u}(p_2)(-i\ q_q\ \gamma^\mu)\ \varepsilon_\mu(Q)u(p_1), \tag{2.1}$$

where q_q is the quark charge and Q is the virtuality of the photon. We take the sum over spins and colours, so that the matrix element squared is

$$\sum_{spin,col.} |\mathcal{M}_0|^2 = -N \sum_q q_q^2\ \mathrm{tr}\left(\slashed{p}_2\gamma^\mu\ \slashed{p}_1\gamma_\mu\right), \tag{2.2}$$

where N is the number of colours. Using the Clifford algebra in CDR (see section 1.4) will give

$$\sum_{spin,col.} |\mathcal{M}_0|^2 = 2(D-2)\ N \sum_q q_q^2\ s, \tag{2.3}$$

where we have also used the invariant mass scale (or Mandelstam variable) s for massless partons, defined as

$$s = (p_1 + p_2)^2 = 2\ p_1 \cdot p_2. \tag{2.4}$$

---

*The Z^0 boson also contributes since it can couple to electrons and quarks, but we shall only look at the γ channel.

Schematically, the LO differential cross section for 2 partons in the final state is

$$\int d\sigma_{LO} = \frac{1}{F} \sum_{spin,col.} |\mathcal{M}_0|^2 \int d\Phi_2,$$ (2.5)

where $d\Phi_2$ is the differential phase space for 2 partons (in D dimensions) and F is the incident flux [†].

To obtain the cross section we need to integrate over the available phase space for this reaction. In Appendix A, we provide this result in eq.(A.6). Substituting this result and eq.(2.3) in eq.(2.5), gives the LO cross section as

$$\sigma_{LO} = \frac{1}{F} \frac{s^{\frac{D-2}{2}}}{2^{2D-5}\pi^{\frac{D-3}{2}}} \frac{(D-2)}{\Gamma\left(\frac{D-1}{2}\right)} N \sum_q q_q^2,$$ (2.6)

or, doing $D = 4 - 2\epsilon$,

$$\sigma_{LO} = \frac{1}{F} \frac{s^{1-\epsilon}}{2^{2-4\epsilon}\pi^{\frac{1}{2}-\epsilon}} \frac{(1-\epsilon)}{\Gamma\left(\frac{3}{2}-\epsilon\right)} N \sum_q q_q^2.$$ (2.7)

This is better presented as a rate, i.e.

$$\frac{\sigma(e^+e^- \to q\bar{q})}{\sigma(e^+e^- \to \mu^+\mu^-)} = N \sum_{q=1}^{N_F} q_q^2,$$ (2.8)

at lowest order.

2.1.2 NLO cross section: real emissions

For the NLO real contribution to the cross section, we have to consider the Feynman diagrams shown in fig.2.2. In this diagram, again we have $\sqrt{s}$ as the total energy in the
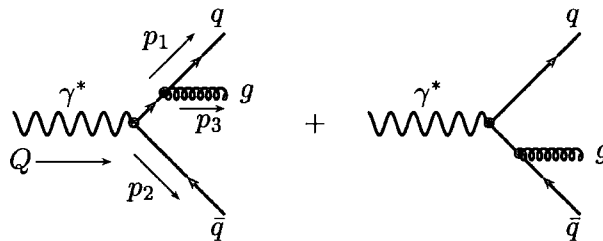
Figure 2.2: Next-to-leading order Feynman diagrams for the real emission in $\gamma^* \to q\bar{q}$

[†]For a general collision between particles 1 and 2, $F = 4[(p_1 \cdot p_2)^2 - m_1^2 m_2^2]^{1/2}$. Note also that the dimensions for the cross section are $[\sigma] = 1/F$ and that the matrix element squared is dimensionless. Recall we have an implicit overall factor from the electron current.

c.m. rest frame, i.e. $Q^2 = s$. Also, the p_i^μ are the momenta of the outgoing partons, so that $p_i^0 = E_i$.

It is convenient to define *energy fractions* x_i, as

$$x_i = \frac{2\,E_i}{\sqrt{s}} = \frac{2\,p_i \cdot Q}{s}, \qquad x_i > 0. \tag{2.9}$$

In this notation, energy conservation provides the following constraint on the energy fractions

$$\sum_i x_i = \frac{2\,(\sum_i p_i) \cdot Q}{s} = 2, \tag{2.10}$$

therefore, only two of the energy fractions x_i are independent.

We can also have a description of the kinematics of this system if we use the angle θ_{ij} between the momenta for partons i and j. The energy fractions and the angles are related as follows (given conservation of momenta)

$$(Q - p_3)^2 = (p_1 + p_2)^2$$
$$\Rightarrow s - 2\,Q \cdot p_3 = s(1 - x_3) = 2\,E_1 E_2\,(1 - \cos\theta_{12}). \tag{2.11}$$

Rearranging this expression, we can see that we have three relations for the angles and the energy fractions

$$2(1 - x_1) = x_2 x_3 (1 - \cos\theta_{23}), \tag{2.12}$$

$$2(1 - x_2) = x_3 x_1 (1 - \cos\theta_{31}), \tag{2.13}$$

$$2(1 - x_3) = x_1 x_2 (1 - \cos\theta_{12}). \tag{2.14}$$

We can see that the energy fractions must also be $x_i < 1$. To further our analysis, we can construct the allowed x_i space and relate the boundary values within this region, to parton physical configurations.

More precisely, we can take the limits $x_i \to 0$, $x_i \to 1$ and construct diagrams like the ones shown in fig.(2.3). There we have three possible soft configurations when $x_i \to 0$ and three collinear configurations when

$$x_1 \to 1 \iff \theta_{23} \to 0,$$
$$x_2 \to 1 \iff \theta_{31} \to 0, \tag{2.15}$$
$$x_3 \to 1 \iff \theta_{12} \to 0.$$

The diagram on the l.h.s of this figure shows the allowed region in the (x_1, x_2) space as a triangle, which is built using the constraint relations for the energy fractions, i.e.

$0 \leq x_i \leq 1$ and $x_3 = 2 - x_2 - x_3$. From the diagram of the r.h.s, we can see that the edges of the allowed region $(x_i = 1)$ correspond to two partons being collinear and the corners $(x_i = 0)$ to one parton momentum being soft.
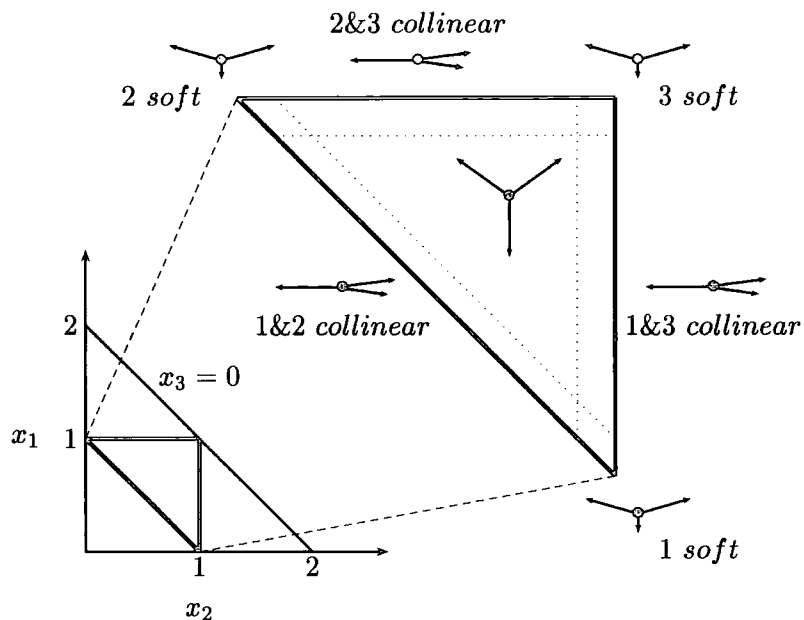
Figure 2.3: The diagram on the left presents the allowed region for the energy fractions (x_1, x_2). On the right we show the physical configuration of the partons for limiting behaviour within the allowed triangle.

The real emission cross section can be calculated using energy fractions and CDR, as we did for the LO cross section. Since this cross section has contributions from both diagrams shown in fig.(2.2), the expression is somewhat large. We will omit a few algebraic (Clifford and Dirac trace algebra) steps and present the matrix element squared

$$\sum_{spin,col.} |\mathcal{M}_1^R|^2 = C_F \, 2(D-2) \, q_e^2 \, (\mu^\epsilon g)^2 \, N \sum_q q_q^2$$

$$\times \left\{ (D-2) \left(\frac{1-x_1}{1-x_2} + \frac{1-x_2}{1-x_1} \right) + 4\frac{(x_1 + x_2 - 1)}{(1-x_1)(1-x_2)} + 2(D-4) \right\},$$

$$(2.16)$$

where we use the colour factor $C_F = 4/3$ (which is $C_F = (N^2 - 1)/(2N)$ for SU(N)).

Similar to the LO case, the real cross section can be written as

$$\int \sigma_{NLO}^R = \frac{1}{F} \int \sum_{spin,col.} |\mathcal{M}_1^R|^2 \, d\Phi_3.$$ (2.17)

Here, the flux factor is the same as before. The matrix element is given by eq.(2.16) and the integration over phase space has been provided in eq.(A.21) of Appendix A.

This provides the following expression for the real cross section

$$\sigma_{NLO}^R = \sigma_{LO} \, C_F \, g^2 \, \left(\frac{\mu^2}{s}\right) \, \frac{\pi^{2-\epsilon} 2^{3-2\epsilon}}{\Gamma(1-\epsilon)}$$

$$\times \int \int dx_1 dx_2 \, \frac{x_1^2 + x_2^2 - \epsilon(x_1 + x_2 - 2)^2}{(1-x_1)^{1+\epsilon}(1-x_2)^{1+\epsilon}(x_1 + x_2 - 1)^\epsilon}$$ (2.18)

where we have used eq.(2.7) and applied $D = 4 - 2\epsilon$ and the integration region is $0 \le x_1, x_2 \le 1$, $x_1 + x_2 \ge 1$.

If we had not applied CDR to this calculation, the integral in eq.(2.18) would have singularities for certain values of the integration variables. From this equation, we can look at the divergent behaviour of the differential cross section in 4-dimensions,

$$\frac{1}{\sigma_{LO}} \frac{d\sigma_{NLO}^R}{dx_1 dx_2} \propto \frac{x_1^2 + x_2^2}{(1-x_1)(1-x_2)}.$$ (2.19)

The cross section has *collinear* singularities (see fig.(2.3))

$$\text{for} \quad x_1 \to 1 \quad \implies \quad (1-x_1) \to 0, \quad \text{(partons 2 and 3 collinear)}$$

$$\text{for} \quad x_2 \to 1 \quad \implies \quad (1-x_2) \to 0, \quad \text{(partons 1 and 3 collinear)}.$$ (2.20)

Also, there is a *soft* singularity. This occurs when $x_3 \to 0$, which in terms of x_1 and x_2, is

$$x_1, \, x_2 \to 1 \quad \implies \quad (1-x_1), \, (1-x_2) \to 0.$$ (2.21)

These singularities are manifest as poles in $\epsilon = 0$ when we regulate with CDR. Indeed, if we calculate the integrals over the phase space in eq.(2.18), we obtain

$$\sigma_{NLO}^R = \sigma_{LO} \, C_F \, \frac{\alpha_S}{2\pi} \, \left(\frac{4\pi \, \mu^2}{s}\right)^\epsilon \left\{\frac{2}{\epsilon^2} + (3 - 2\gamma)\frac{1}{\epsilon}\right.$$

$$\left. + \left(\frac{19}{2} + (\gamma - 3)\gamma - 7\zeta(2)\right) + \mathcal{O}(\epsilon)\right\},$$ (2.22)

which can be renormalised in the $\overline{\text{MS}}$ scheme to be

$$\sigma_{NLO}^R = \sigma_{LO} \, C_F \, \frac{\alpha_S}{2\pi} \, \left(\frac{\mu^2}{s}\right)^\epsilon \frac{e^{\epsilon\gamma} \, \Gamma(1-\epsilon)^2}{\Gamma(1-3\epsilon)} \left\{\frac{2}{\epsilon^2} + \frac{3}{\epsilon} + \frac{19}{2} + \mathcal{O}(\epsilon)\right\}.$$ (2.23)

2.1.3   NLO cross section: virtual emissions

The virtual contribution to the NLO cross section takes into account the interference of the Feynman diagram shown in fig.(2.4), with the LO diagram. Effectively, one has to calculate the real part of the momentum integral arising from the bubble diagram shown in the same figure.
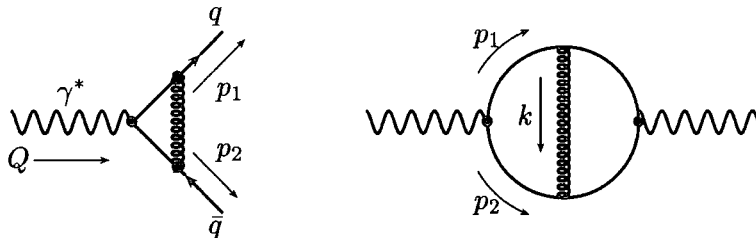
Figure 2.4: Next-to-leading order Feynman diagrams for the virtual emission in $\gamma^* \to q\bar{q}$

The necessary tools for this calculation, are to be discussed further on in this thesis. However, for the sake of completion, we present here the basic steps, as we did for the previous contributions.

The matrix element squared is

$$\sum_{spin,col.} |\mathcal{M}_1^V|^2 = -i\, C_F\, (\mu^\epsilon g)^2\, N \sum_q q_q^2$$

$$\times \int \frac{d^D k}{(2\pi)^D} \frac{\mathrm{tr}\,(\gamma^\mu \slashed{p}_1 \gamma^\alpha (\slashed{p}_1 - \slashed{k})\gamma_\mu(\slashed{p}_2 + \slashed{k})\gamma_\alpha \slashed{p}_2)}{k^2(p_1 - k)^2(p_2 + k)^2}. \qquad (2.24)$$

We can see that this integral becomes divergent when one of the factors of the denominator in the integrand vanishes. The *soft* infrared singularities occur for small values of the loop momentum (in contrast with ultraviolet singularities). Note that the *collinear* infrared singularities would not be present if we had massive quarks. In this case the divergent behaviour is said to be regulated by the mass and instead of poles in ϵ, we would have mass dependent logarithms.

After some Dirac-matrix algebra and using *Feynman parameters* (see Chapter 3), we can integrate out the loop momentum and be left with integrals over the Feynman parameters (y, z) as

$$\sum_{spin,col.} |\mathcal{M}_1^V|^2 = (-1)^\epsilon\, C_F\, (\mu^\epsilon g)^2\, N \sum_q q_q^2 \frac{s^{1-\epsilon}}{2^{1-2\epsilon}\pi^{2-\epsilon}}(1-\epsilon)$$

$$\times \left\{ \Gamma(1+\epsilon) \int_0^1 dz \int_0^{1-z} dy \frac{(\epsilon-1)yz + y + z - 1}{(yz)^{1+\epsilon}} \right.$$

$$+ (1-\epsilon)^2 \Gamma(\epsilon) \int_0^1 dz \int_0^{1-z} dy(yz)^{-\epsilon} \Big\}, \tag{2.25}$$

which after integration, becomes

$$\sum_{spin,col.} |\mathcal{M}_1^V|^2 = (-1)^\epsilon C_F (\mu^\epsilon g)^2 N \sum_q q_q^2 \frac{s^{1-\epsilon}}{2^{1-2\epsilon}\pi^{2-\epsilon}} \frac{(1-\epsilon)}{(1-2\epsilon)}$$
$$\times \frac{\Gamma(1+\epsilon)\Gamma^2(1-\epsilon)}{\Gamma(1-2\epsilon)} \left(-\frac{1}{\epsilon^2} + \frac{1}{2\epsilon} - 1 \right). \tag{2.26}$$

Now, we can proceed with the virtual contribution to the NLO cross section and write it schematically as

$$\int \sigma_{NLO}^V = 2 \operatorname{Re} \left\{ \frac{1}{F} \sum_{spin,col.} |\mathcal{M}_1^V|^2 \int d\Phi_2 \right\}. \tag{2.27}$$

In terms on the LO contribution and using eq.(A.6) in the Appendix, we have

$$\sigma_{NLO}^V = \sigma_{LO} C_F \frac{\alpha_S}{2\pi} \left(\frac{4\pi \mu^2}{s} \right)^\epsilon \left\{ -\frac{2}{\epsilon^2} + (-3+2\gamma)\frac{1}{\epsilon} \right.$$
$$\left. + (-4 - (\gamma-3)\gamma + 7\zeta(2)) + \mathcal{O}(\epsilon) \right\}, \tag{2.28}$$

which can be renormalised in the $\overline{\text{MS}}$ scheme to be

$$\sigma_{NLO}^V = \sigma_{LO} C_F \frac{\alpha_S}{2\pi} \left(\frac{\mu^2}{s} \right)^\epsilon \frac{e^{\epsilon\gamma} \Gamma(1-\epsilon)^2}{\Gamma(1-3\epsilon)} \left\{ -\frac{2}{\epsilon^2} - \frac{3}{\epsilon} - 4 + \mathcal{O}(\epsilon) \right\}. \tag{2.29}$$

2.1.4 Cancellation and nature of IR singularities

We can calculate the rate for the NLO cross section normalised to the LO cross section as

$$\Gamma \equiv \lim_{\epsilon \to 0} \frac{\sigma_{NLO}}{\sigma_{LO}} = \lim_{\epsilon \to 0} \left(1 + \frac{\sigma_{NLO}^R}{\sigma_{LO}} + \frac{\sigma_{NLO}^V}{\sigma_{LO}} \right). \tag{2.30}$$

We insert in this expression, the real and virtual contributions from eq.(2.23) and eq.(2.29). Immediately we can see that the poles cancel so we can take the limit safely, to arrive at

$$\Gamma = 1 + \frac{\alpha_S}{\pi}. \tag{2.31}$$

Note that the correction to the rate is independent of the exchanged boson. Therefore, the same correction applies to the Z^* decay into a massless quark-antiquark pair.

So far we have only given a summary of the NLO calculation and we have shown that the singularities indeed cancel. But we have not discussed the nature of these singularities nor the concept underlying their, almost *miraculous*, cancellation.

The singularity structure arising from Feynman diagrams in a perturbative calculation such as the cross section, implies that there are large contributions from particular parton configurations. These can be either partons moving in fast collinear bunches or soft momentum partons that probe large distances but with no preferential direction.

In terms of the example we adopted in this section, we can give a qualitative argument about the final state of the process $e^+e^- \to hadrons$. According to perturbative QCD, the final state should have *jets* (reflected in the detector as a highly collimated spray of hadrons) of almost collinear particles and soft particles that move with no preferential direction. However, if we want quantitative predictions we must be prepared to find observables we can measure and that are insensitive to interactions that occur much later than the (hard) partonic interaction. We discuss this in the next section.

2.2   IR-safe observables and jets

The total cross section to produce hadrons in e^+e^- annihilation is an example of a measurement that is not sensitive to long-time physics. In this case, the cancellation of divergences associated with the inter-emission of a virtual gluon against the divergences associated with the radiation of a soft/collinear gluon, implies that these final states are indistinguishable long after the partons are created.

More formally, the cancellation of soft and collinear singularities between real and virtual diagrams in our example is by no means *miraculous*. There are theorems [‡] which guarantee that any transition rate will be free of singularities in the massless limit, if we take into account all degenerate states. If we perform a calculation of a physical observable (at some fixed order in perturbative QCD) where we sum over all radiative configurations which degenerate into the same final-state (i.e. have the same behaviour in the soft/collinear limit), then the result is guaranteed to be finite. The total hadronic cross section in electron-positron annihilation is an example of such quantities, whereas the production of a quark-antiquark pair plus a gluon (σ_{NLO}^R) is not.

There are other quantities that are not sensitive to infrared effects (long-time physics). They are all called *infrared safe* quantities and are insensitive to, for example,

- a mother particle that divides into two collinear daughter particles sharing its momentum,

---

[‡]Kinoshita-Lee-Nauenberg [16, 17] and Bloch-Nordsieck [18] theorems. For a thorough discussion see for example [2].

   ○ a mother particle that decays into a daughter particle carrying most of its momen-
      tum and a soft daughter particle carrying almost no momentum,

   etc.

In other words, for an infrared safe quantity a physical event with jets in the final
state, should give (approximately) the same measurement as a parton event, with each
jet replaced by a parton. Following our intuition, we can say now that a jet is a spray
of fast particles all going in approximately the same direction. But, this definition is not
enough if we want to make precise calculations at high energies, where we can have more
than three jets.

There are several algorithms that exploit different properties of these highly collimated
particles, to define a jet. The simplest one starts with a list of momenta $\{p_1^\mu, p_2^\mu, ..., p_N^\mu\}$
for each of the partons in the final state and uses a parameter y_{cut}. Then

1. finds the pair (i, j) such that the test variable d_{ij} (e.g. the invariant mass $d_{ij} =
   (p_i + p_j)^2$ or $d_{ij} = 2 \min(E_i^2, E_j^2)(1 - \cos\theta_{ij})$ for the k_T algorithm) between them is
   the smallest.

2. If $(p_i + p_j)^2 > y_{cut}\, s$, exits. Otherwise,

3. it replaces the two momenta p_i and p_j in the list by their sum $p_i^\mu + p_j^\mu = p_k^\mu$ (two
   daughter particles → mother particle).

4. Returns to 1.

At the end we have a list of momenta for the jets, instead of the partons. The other
algorithms are variations of this simple one and they can have different specifications on
the test variable (step 1), the resolution condition (step 2) or the combination prescription
(step 3) [19].

Apart from the $e^+e^- \rightarrow hadrons$ cross section, there are other infrared safe observables
which we can study and that we have not mentioned, such as the thrust distribution and
the energy-energy correlation. Their study is not directly relevant to this work, but a
thorough discussion can be found in ref.[5].

2.3   The hard scattering cross section and factorisation

The study of processes with quarks and gluons in the initial state has a great impact on
the description of hard scattering processes at the LHC and the Tevatron.

The cross section for a hard scattering process is illustrated in fig.(2.5) and has the following factorised structure

$$\sigma(P_1, P_2) = \sum_{ij} \int dx_1 \; dx_2 \; f_{i/1}(x_1, \mu_F^2) \; f_{j/2}(x_2, \mu_F^2) \; \hat{\sigma}_{ij}(p_1, p_2, \alpha_S(\mu^2), s/\mu^2, s/\mu_F^2).$$

$$(2.32)$$

The partons participating in the hard scattering have a fraction of the momenta of the incoming hadrons P_i, i.e. $p_i = x_i \; P_i$. As usual, we used the physical scale to be $s = (P_1 + P_2)^2$, the characteristic scale for the hard scattering.
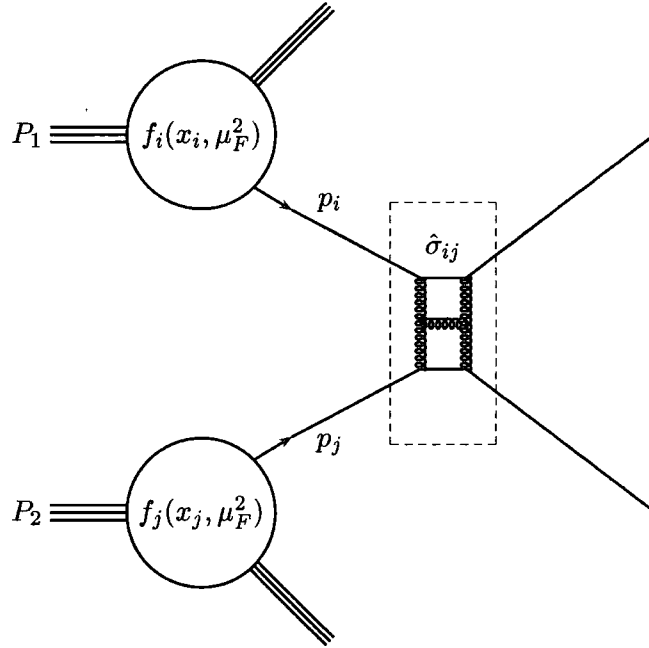
Figure 2.5: Schematic representation for the cross section factorisation of a hard scattering process

The first two terms in the r.h.s. of eq.(2.32), the functions $f_{a/h}(x, \mu_F^2)$, are the so called *parton distribution functions* (pdf's). The quantity $dx \; f_{a/h}(x, \mu_F^2)$ gives the probability to find a parton with flavour a in hadron h, carrying a momentum fraction between x and $x + dx$. Effectively, these functions describe the initial state hadrons in terms of their constituents and comprise non-perturbative effects. Nevertheless, they can be determined indirectly from experiments such as deeply inelastic scattering.

The last factor in eq.(2.32), $\hat{\sigma}_{ij}(p_k, \alpha_S(\mu^2), s/\mu^2, s/\mu_F^2)$ is the hard scattering matrix that involves the interaction of partons (i, j) arising from hadrons $(1, 2)$, respectively. This hard scattering matrix can be calculated perturbatively.

The property of factorisation for the hard scattering cross section presented in eq.(2.32) is well established [20]. This is done by showing that the perturbative expansion can be

rearranged so that the contributions from long time scales appear in the pdf's, while the ones from short time scales are left as part of the hard scattering $\hat{\sigma}$. For example, a high transverse momentum gluon emitted from a parton inside one hadron can probe the second hadron, therefore its effects should be taken into account when calculating $\hat{\sigma}$. On the other hand, a small transverse momentum gluon cannot resolve the second hadron and must be included in the pdf's.

This separation of short and long time physics (hard and soft radiation), requires the introduction of a *factorisation scale* μ_F. An important consequence of this break up is that both the pdf's and the hard scattering matrix depend on μ_F.

Thus, the structure suggested for the factorised cross section will have functions depending on both the renormalisation and factorisation scale. But, as with μ, the cross section does not depend on μ_F. In theoretical calculations, one often sets $\mu_F = \mu$.

Again, there is an equation

$$\frac{d\sigma}{d\mu_F} = 0,$$

that is satisfied within the accuracy of the perturbative expansion used. Clearly, the more higher order terms we include, the less the dependence on μ_F.

2.3.1 Matrix elements for the partonic cross section

The calculation of the total hadronic cross section involves several steps. First, one must obtain the matrix elements for all possible partonic processes involved in the hadronic scattering, which is what concerns this thesis. Second, these matrix elements are integrated over their corresponding phase space which depends on the number of particles in the final state. The study and cancellation of infrared divergences (see section 2.1.4) also has to occur at this stage.

Finally, and before integrating over the energy fractions in eq.(2.32), one must obtain the pdf's and their evolution at an accuracy that matches that of the matrix element calculation. In a NNLO calculation this requires the knowledge of the three-loop splitting functions. At this order, the even moments of the splitting functions are known for the flavour singlet and non-singlet structure functions F_2 and F_L up to $N = 12$ while the odd moments up to $N = 13$ are known for F_3 [21, 22, 23]. The numerically small N_F^2 non-singlet contribution is also known [24] and Van Neerven and Vogt have provided accurate parametrisations of the splitting functions in $x-$space [25, 26, 27] which are now starting to be implemented in global analyses [28].

So far, the calculation of a total hadronic cross section has been achieved for NLO accuracy and this required a great amount of work (see for example [29, 30, 31, 32, 33] and references therein).

At NNLO, the partonic cross section for 2-particle production can be written as follows

$$\hat{\sigma}_{2\ \text{jet}} \sim \int \left[|\langle \mathcal{M}^{(0)}|\mathcal{M}^{(0)}\rangle|^2 \right]_4 d\Phi_4$$

$$+ \int \left[\langle \mathcal{M}^{(0)}|\mathcal{M}^{(1)}\rangle + \langle \mathcal{M}^{(1)}|\mathcal{M}^{(0)}\rangle \right]_3 d\Phi_3$$

$$+ \int \left[\langle \mathcal{M}^{(1)}|\mathcal{M}^{(1)}\rangle + \langle \mathcal{M}^{(0)}|\mathcal{M}^{(2)}\rangle + \langle \mathcal{M}^{(2)}|\mathcal{M}^{(0)}\rangle \right]_2 d\Phi_2 \qquad (2.33)$$

where $[\ ]_n$ indicates the number of particles in the final state with $d\Phi_n$ the corresponding phase space and $\mathcal{M}^{(i)}$ is the i-th order scattering amplitude.

We can see that we need three sets amplitudes

1. 4-particle production amplitudes at tree-level,

2. 3-particle production amplitudes at tree-level and one-loop,

3. 2-particle production amplitudes at tree-level, one-loop and two-loops

and in table 2.1 we present what has already been calculated.

In terms of matrix elements, the integrand of the last row in eq.(2.33) (or equivalently, the contents of the bottom-right square on table 2.1) needs to be calculated for all $2 \rightarrow 2$ partonic scattering. We have accomplished these calculations and they shall be presented in Chapter 6 of this thesis.

2.4 Beyond NLO

In the previous section we showed that there is a missing piece in the matrix elements needed for the NNLO partonic cross section. So far, the only motivation to perform this highly non trivial calculation is that if we have a higher order term in our perturbative calculation, then the cross section dependence on μ and μ_F can be reduced.

If the dependence on these scales is reduced, we can have a more accurate determination of QCD parameters, in particular α_s. This is an important achievement in itself but, it is better if we can give an estimate on how it would change the already existing description of, say the jet inclusive cross section.

We summarise some of the areas in which a NNLO calculation has an impact in the following sections.

n	Processes	Tree-Level	One-Loop	Two-Loop
4	$gg \to gggg$ $q\bar{q} \to gggg$ $q\bar{q} \to q'\bar{q}'gg$ $q\bar{q} \to q'\bar{q}'q''\bar{q}''$	see ref.[34, 35, 36, 37]	not required	not required
3	$gg \to ggg$ $q\bar{q} \to ggg$ $q\bar{q} \to q'\bar{q}'g$	see ref.[32, 31, 38]	see ref.[32, 31, 38]	not required
2	$gg \to gg$ $q\bar{q} \to gg$ $q\bar{q} \to q'\bar{q}'$ $q\bar{q} \to q\bar{q}$	see ref.[39]	see ref.[39]	**in this Thesis** refs.[40, 41, 42, 43, 44, 45]

Table 2.1: Summary of 3,4-particle production (helicity) amplitudes for parton scattering. In the case of 2-particle production, the matrix elements for the tree self-interference and its interference with the one-loop amplitude have also been calculated.

2.4.1 Scale dependence at NNLO order

As we mentioned in section 1.5.3, the sensitivity on μ of the truncated perturbative expansion, decreases as we increase the number of calculated terms. Let us see how well this works taking on an example.

Consider, the single jet inclusive differential cross section at NNLO [§]

$$
\begin{aligned}
\frac{d\sigma}{dE_T} \;=\; & A\,\alpha_S^2(\mu) \\
& + \left[B + 2\beta_0 A\ln\left(\frac{\mu}{E_T}\right) \right] \alpha_S^3(\mu) \\
& + \left[C + 3\beta_0 B\ln\left(\frac{\mu}{E_T}\right) + A\left(3\beta_0^2\ln^2\left(\frac{\mu}{E_T}\right) + 2\beta_1\ln\left(\frac{\mu}{E_T}\right)\right) \right] \alpha_S^4(\mu),
\end{aligned}
$$

$$(2.34)$$

where the NNLO coefficient C is unknown.

[§]This can be easily obtained inserting the NNLO expansion for the running coupling in the NNLO perturbative expansion for the jet cross section

$$
\frac{d\sigma}{dE_T} = A\,\alpha_S^2 + B\,\alpha_S^3 + C\,\alpha_S^4
$$

Now, fig.(2.6) shows this prediction for the cross section. It has been calculated for jets with transverse energy of 100 GeV [46]. The renormalisation scale dependence is shown for the LO, NLO and NNLO predictions assuming that the (presently unknown) genuine contribution is zero, i.e. $C = 0$ in eq.(2.34). The factorisation scale and choice of parton density functions are kept fixed.
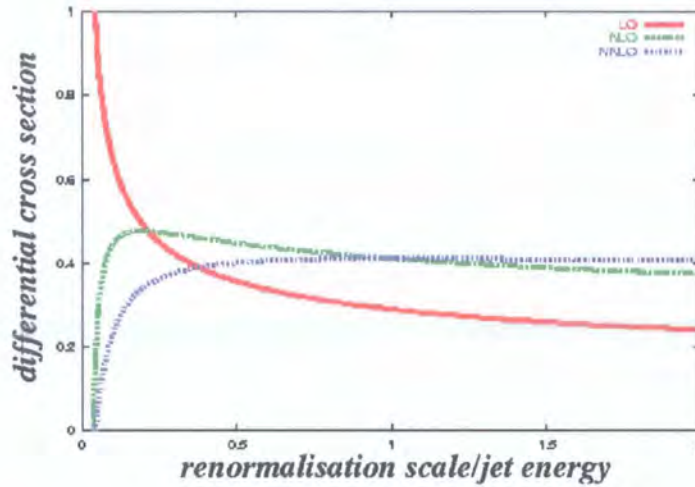
Figure 2.6: Renormalisation scale dependence for the single jet distribution at $E_T = 100 GeV$

We can see that for renormalisation scales with a value within a factor of two of the jet energy, the renormalisation scale uncertainty is reduced from 20% to 9% to 1%. Interestingly enough, the systematic error from CDF with Run 1 for this data point is about 10%, while the statistical experimental error is about 2%.

Currently, most of the theoretical predictions for physical observables in QCD are performed at the NLO accuracy and in general show a good agreement with the data, but our example shows that the dependence on the unphysical scale μ is still significant. Moreover, the forthcoming runs in the new generation accelerators such as LHC will provide high quality data with improved statistics leading to an experimental error smaller than the theoretical one. The theoretical prediction may be improved by including the NNLO contributions.

2.4.2 Improved jet description

The addition of NNLO effects also provides significant improvement on the jet description. When we consider higher order corrections we are automatically improving the matching

between the theoretically and experimentally defined jets.

As shown in in fig.(2.7), at leading order the jet will be represented by a single parton. But we can see that at NNLO there is a further improvement on the jet description, since the phase space available is extended and up to three partons can combine to form a jet.

LO   NLO   NNLO
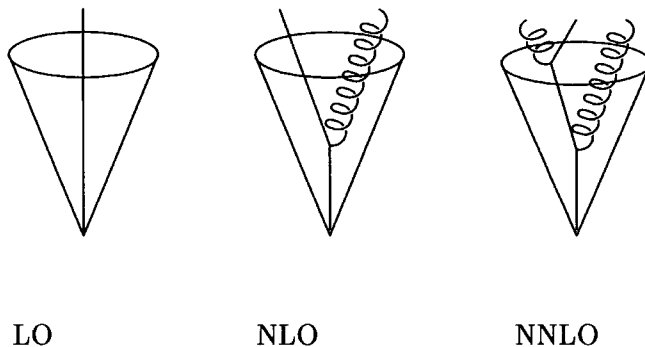
Figure 2.7: Partons contained in the jet cone at leading and higher order.

Together with this, higher order corrections involve more modelling of soft gluon radiation within the jet event so they provide a more accurate picture of the jet shape (fraction of the jet's energy within a cone of a given size, centred on the jet direction) and structure.

If we want to use jet algorithms to describe perturbative QCD phenomena (e.g. measure the inclusive jet cross section), it is important that the jet definition is IR-safe to all orders, not just the order at which the theoretical calculations are performed. In fact, when compared with the perturbative calculation, an unsafe algorithm can lead to a cross section that scales differently with energy [47, 48].

Recent studies [48] show that jet algorithms that are considered to be IR-safe at NLO, are found to be genuinely unsafe at NNLO. So a theoretical calculation at this order would help isolate the problems of infrared safeness, since it is based on the soft and collinear approximations. Moreover, it can also help identify the kinematic regions where the logarithms are large and enable a comparison with the numerical all orders resumed results from theory and from simulations.

2.4.3 New physics at the TeV scale

Unknown physics will obviously affect the couplings and masses of the Standard Model, but so far as we know these parameters have been well measured. Nevertheless, there may be another way in which unknown physics can tamper with current experiments [13].

Suppose there is a new particle that can be exchanged by quarks and has a heavy mass M of the order of a few TeV. It may well be that this new interaction introduces extra terms into the QCD Lagrangian that we may be able to probe with future experiments.

Taking into account the already existing terms of the Lagrangian, this new term will be typically proportional to $\hat{g}^2/M^2$. Since the mass of the new particle is quite big, the effects of these new terms are small. Therefore we need an experiment with good precision and that operates at high energies.

If we consider the experimental results for inclusive jet cross section in $p\bar{p}$ scattering (CDF and D0 at the Tevatron) and we compare with the theoretical prediction when the transverse energy of the jet is $E_T < M$, then on dimensional grounds we expect,

$$\frac{Data - Theory}{Theory} \propto \hat{g}^2 \, \frac{E_T^2}{M^2}. \tag{2.35}$$

This comparison is plotted in fig.(2.8) (taken from ref.[49]) for data from CDF and D0 [50, 51] and NLO theoretical results. The theory predicts correctly the experimental
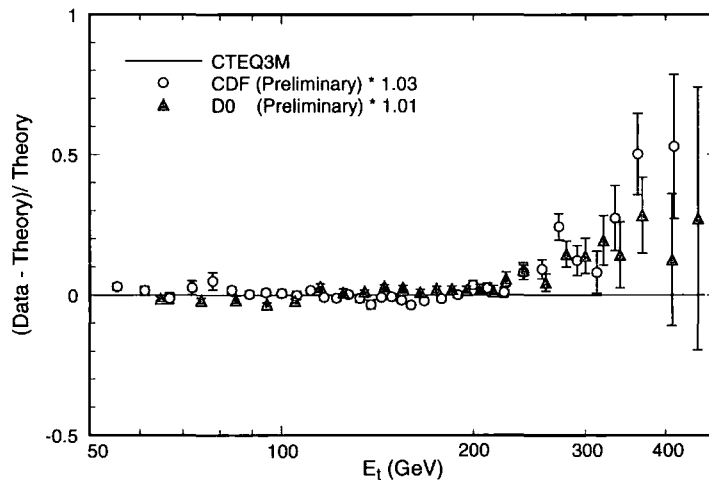
Figure 2.8: Inclusive jet cross sections from CDF and D0 compared to QCD theory.

results for $E_T < 200$ GeV, but for higher transverse energies there appears to be a deviation that could indicate non-Standard Model physics (or even quark substructure). Equation (2.35) offers a qualitative explanation to the nature of this excess.

On the other hand, the D0 measurements are in better agreement with the theory than the CDF measurements at high E_T, but the overlapping error bars prevent us from choosing one data set over the other. It has also been argued that this discrepancy between theory and data may be only a case of insufficient precision on the theoretical

uncertainties. [52]. In any case a next-to-next-to-leading order calculation will help clarify the picture.

Chapter 3 | *Loop Integrals*

Our final objective is to calculate two-loop matrix elements for $2 \rightarrow 2$ scattering of massless partons. This automatically imposes some conditions on the types of problems we have to solve in order to achieve this goal. One of the main problems we are faced with is the calculation of two-loop integrals.

The calculation of scalar loop integrals by itself is a complex task, but the fact that we want matrix elements adds an extra degree of complexity. There is now the need to calculate hundreds of two-loop integrals with a tensor structure.

In this Chapter we will explore the different ways of calculating loop integrals and the advantages (or disadvantages) a particular method may bring to the process. It is therefore important that we make a good description of the type of problem we want to solve, since this will be the discerning tool in the search for an adequate loop integration technique.

3.1   General structure of loop integrals

The analytic evaluation of two-loop parton matrix elements involves the calculation of up to a thousand Feynman diagrams, as shown in table 3.1.

Processes	One-Loop		Two-Loops	
	self-energy insertions	products and basic	self-energy insertions	products and basic
$gg \rightarrow gg$	27	54	739	1032
$q\bar{q} \rightarrow gg$	4	26	128	467
$q\bar{q} \rightarrow q\bar{q}$		18	26	290
$q_1\bar{q}_1 \rightarrow q_2\bar{q}_2$		10	13	176

Table 3.1: Basic classification of Feynman diagrams contributing to partonic processes.

These diagrams can come in various shapes and particle content. As a simple starting point on their description we can classify them as follows

- ○ basic graphs that represent a particular way of interconnecting the propagators, without resorting to insertions in propagators, i.e.
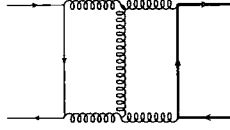
- ○ self energy insertions correspond to bubble insertions in the propagators of a basic graph, i.e.
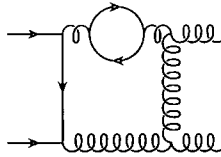
- ○ products of one-loop graphs, or graphs that arise from the elimination of propagators in a basic graph, i.e.
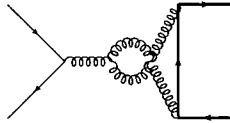
Each of these graphs carries information about the way the particles interact and about the particles themselves. Most of this is encoded in the tensor structure of the loop integral associated with each diagram.

Since we are dealing with particles that carry spin and interactions of up to two-loops, the types of integrals arising in matrix-element calculations such as
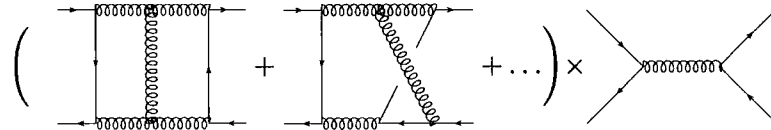
include integrals with scalar numerators

$$\int \frac{d^D k}{i\pi^{\frac{D}{2}}} \int \frac{d^D \ell}{i\pi^{\frac{D}{2}}} \frac{f(k_i \cdot k_j, k_i \cdot p_j, p_i \cdot p_j)}{A_1^{\nu_1} \dots A_n^{\nu_n}}, \tag{3.1}$$

where $k_i = k, \ell$ are the loop momenta, p_i are the external momenta and f is a scalar function. Here, the massless propagators A_i are typically

$$A_i \sim (k_i \pm v + i\varepsilon)^2, \tag{3.2}$$

where v can be any loop-momenta or external momenta. The term $+i\varepsilon$ gives the Feynman prescription for the analytical properties of the integral and its definition is crucial when
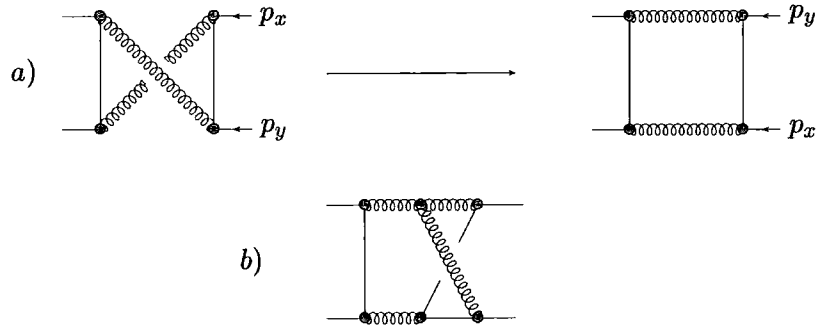
Figure 3.1: *a*) Deformation of what *seems* a non-planar graph to relate it to a planar one. *b*) Genuine non-planar topology (*two-loop crossed box*).

doing analytic continuations to other kinematically available regions (see section 1.4). In the rest of this thesis we will work within this prescription but we will not write it explicitly.

Also arising from these matrix elements calculations, are integrals with irreducible numerators (IN), which are generated through tensor integrals that carry information about the spin structure of the process

$$f_{\mu\nu\cdots}(p_i) \int \frac{d^D k}{i\pi^{\frac{D}{2}}} \int \frac{d^D \ell}{i\pi^{\frac{D}{2}}} \frac{f^{\mu\nu\cdots}(k,\ell)}{A_1^{\nu_1} \dots A_n^{\nu_n}}, \tag{3.3}$$

where now, the function $f_{\mu\nu\cdots}$ is a tensor that can depend on the momenta of the system and/or other tensors (such as the metric tensor $g_{\mu\nu}$).

In the examples we have shown so far all diagrams have been *planar* diagrams but, sometimes the structure of a graph can be more complicated than that. It will become clear that two-loop *non-planar* diagrams, have an intrinsically different description from that of the *planar* diagrams, although the structure of the nested divergences arising from both types of integrals is equally difficult to isolate.

The fact that a graph is non-planar will be reflected in the structure of its propagators. We will see that they have an extra propagator making up for a structure that cannot be mapped into the planar case, unless this extra propagator is cancelled by the appropriate numerator. These types of graphs have had a special rôle in the history of loop integration and the non-planar double box was one of the last issues to be resolved last year.

For example, figure 3.1 shows in (*a*) a very simple case of the equivalence between two graphs that seem to belong to different topologies and in (*b*) an authentic non-planar topology.

In order to describe the topology* of a graph (or to identify the properties of a graph that are unaffected by continuous distortion), one needs only to specify the set of propagators present in it (or equivalently the denominator of the actual integral).

Therefore, two graphs of the same topology must either have the same set of propagators or sets that are related by a linear mapping of the loop momenta and sometimes a permutation of the external momenta. Following the same line of argument, a sub-topology (or a *pinching*) can be a topology that contains a sub-set of the propagators of the original topology.

To summarise, we can say that the information in the numerator of an integral associated with a Feynman diagram provides information about the spinorial structure of the particles interacting in the loop. On the other hand, the denominator provides the momentum flow in the graph and gives a complete description of its skeleton or topology. The topology can be planar or non-planar and within these two categories we will identify sub-topologies or pinchings, depending on the absence of a particular sub-set of propagators.

In this way, we can identify *families* of integrals that can be treated in a similar way, enabling us to study groups of integrals and develop general procedures that apply to them without loss of generality.

3.1.1 Planar topologies

A way of encapsulating all information regarding the planar topologies is to create an object that can be a general representation of them. To this end we have created a (fictitious) general planar diagram, shown in figure 3.2. In it, each of the propagators
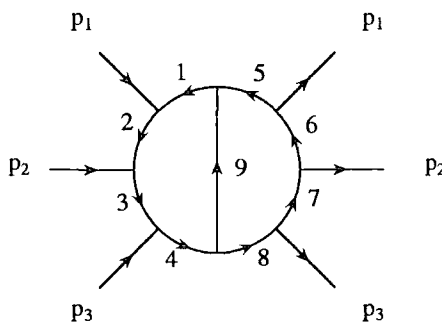
Figure 3.2: General planar diagram

---

*from the Greek, *topos* : $\tau o' \pi o \varsigma$, a place

is labelled by an integer and carries a specific momentum that fulfils conservation of momenta throughout. This can be verified with the following definition of the propagators

$$A_1 = k^2, \qquad\qquad\qquad A_5 = \ell^2,$$
$$A_2 = (k + p_1)^2, \qquad\qquad A_6 = (\ell + p_1)^2,$$
$$A_3 = (k + p_1 + p_2)^2, \qquad\qquad A_7 = (\ell + p_1 + p_2)^2,$$
$$A_4 = (k + p_1 + p_2 + p_3)^2, \qquad A_8 = (\ell + p_1 + p_2 + p_3)^2,$$
$$A_9 = (k - \ell)^2,$$

where we have a symmetric description of the k-loop and the ℓ-loop, mediated by the 9th propagator that participates in both. This is, *per se*, one of the first advantages of this particular description of the planar topologies. It allows us to interchange the k and ℓ loop without affecting the results.

A trivial remark, but worth mentioning, is that this general diagram does not represent a Feynman diagram arising from a $2 \to 2$ scattering process analysis. Nevertheless, all possible distributions of momenta in planar Feynman diagrams with different sets of propagators, can be obtained from this general diagram by pinching two or more propagators. This general representation is a good starting point to the description of all of them at once.

The graph in fig.(3.2) is associated with a general two-loop integral

$$\int \frac{d^D k}{i\pi^{\frac{D}{2}}} \int \frac{d^D \ell}{i\pi^{\frac{D}{2}}} \frac{1}{A_1^{\nu_1} A_2^{\nu_2} A_3^{\nu_3} A_4^{\nu_4} A_5^{\nu_5} A_6^{\nu_6} A_7^{\nu_7} A_8^{\nu_8} A_9^{\nu_9}}, \qquad (3.4)$$

where, the ν_i are arbitrary powers of the propagators. They can be positive (part of the topology description), negative (part of the numerator or tensor content) or zero for a pinched propagator.

We also need a compact way to present this information; a way that allows us to manipulate hundreds of integrals with the minimum amount of information and without compromising the accuracy of the description. So to refer to the general integral in eq.(3.4) we will use the powers of the propagators as entries in the following array

$$I^D[\nu_1, \nu_2, \nu_3, \nu_4, \nu_5, \nu_6, \nu_7, \nu_8, \nu_9, s_{12}, s_{23}], \qquad (3.5)$$

where the D indicates a two-loop integral in D-dimensional space. Using this array, we can represent any planar topology, by eliminating, increasing or decreasing the values of ν_i. The last two entries are for the characteristic scales of the graph.

So, for example, figure (3.3) shows two of the planar boxes that arise in the calculation of the scattering of two massless unlike quarks. Clearly, the graphs have the same topology,
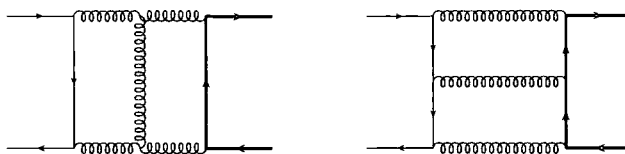
Figure 3.3: The planar box graphs for $q\bar{q} \to q'\bar{q}'$

but the distribution of momenta has been done in a different way. Their characteristic scales and propagators present will be different. Nevertheless, their treatment can be done with this general approach. The graph on the l.h.s of figure (3.3) will produce an integral like

$$\text{(box)}\ (s_{12}, s_{23}) \ = \ I^D[1,1,1,0,1,0,1,1,1,s_{12},s_{23}],$$

whereas the graph on the r.h.s will be related to

$$\text{(box)}\ (s_{23}, s_{12}) \ = \ I^D[1,1,0,1,0,1,1,1,1,s_{23},s_{12}].$$

In fact, we can get all possible orientations of the same topology, just by simultaneously inner-cycling the sections of the array that correspond to k and ℓ loop, i.e.

$$
\begin{aligned}
I^D[\nu_1,\nu_2,\nu_3,\nu_4,\nu_5,\nu_6,\nu_7,\nu_8,\nu_9,s_{12},s_{23}] \ &= \ I^D[\nu_2,\nu_3,\nu_4,\nu_1,\nu_6,\nu_7,\nu_8,\nu_5,\nu_9,s_{23},s_{12}] \\
&= \ I^D[\nu_3,\nu_4,\nu_1,\nu_2,\nu_7,\nu_8,\nu_5,\nu_6,\nu_9,s_{12},s_{23}] \\
&= \ I^D[\nu_4,\nu_1,\nu_2,\nu_3,\nu_8,\nu_5,\nu_6,\nu_7,\nu_9,s_{23},s_{12}]
\end{aligned}
$$

which reflects on the alternation of the scales. This, together with the fact that the integral is invariant to the interchange of loops,

$$I^D[\nu_1,\nu_2,\nu_3,\nu_4,\nu_5,\nu_6,\nu_7,\nu_8,\nu_9,s_{12},s_{23}] \ = \ I^D[\nu_5,\nu_6,\nu_7,\nu_8,\nu_1,\nu_2,\nu_3,\nu_4,\nu_9,s_{12},s_{23}]$$

is one of the advantages of this general description.

There are many different topologies that arise in a $2 \to 2$ matrix element calculation but the most complicated one is the double box. The propagators 4 and 6 do not appear in its description and the graphical representation is shown in fig. 3.4.

We can obtain some sub-topologies, by eliminating propagators from the two-loop box and in table 3.2 we see some examples that can clarify this.

In particular, we show a double box with one negative power on a propagator, this means it contains that particular propagator in the numerator. It is still a scalar integral, but contains tensorial structure embedded in its numerator.
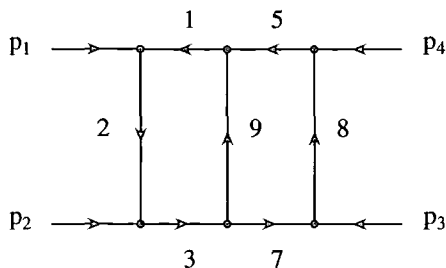
Figure 3.4: Structure of planar double box

Name	Diagram	Identification
PBOX1 (s_{12}, s_{23})		$I^D[1,1,1,0,1,0,1,1,1,s_{12},s_{23}]$
		$I^D[1,1,1,0,1,0,1,1,2,s_{12},s_{23}]$
PBOX2 (s_{12}, s_{23})		$I^D[1,1,1,-1,1,0,1,1,1,s_{12},s_{23}]$
ABOX (s_{12}, s_{23})		$I^D[1,1,1,0,0,0,0,1,1,s_{12},s_{23}]$
CBOX (s_{12}, s_{23})		$I^D[1,1,0,0,0,0,1,1,1,s_{12},s_{23}]$
TRI (s_{12}, s_{23})		$I^D[1,0,1,0,0,0,0,1,1,s_{12},s_{23}]$
GLASS (s_{12}, s_{23})		$I^D[1,0,1,0,1,0,1,0,0,s_{12},s_{23}]$
SUNC (s_{12}, s_{23})		$I^D[0,1,0,0,0,0,0,1,1,s_{12},s_{23}]$

Table 3.2: Some examples of planar diagrams with their identifications

3.1.2 Non-Planar topologies

Similar to the analysis we made on the planar topologies, we have a general diagram in fig.(3.5) that deals with all possible non-planar sub-topologies in a concise way.

Comparing fig.(3.5) with fig.(3.2), we note that the non-planar diagram involves a 10th propagator but not the 4th one. This makes the general diagram asymmetric on the k and l loops, but this does not exclude the possibility that a particular sub-topology may become symmetric when eliminating a sub-set of propagators.

This extra propagator also participates in both the k-loop and the ℓ-loop and is defined
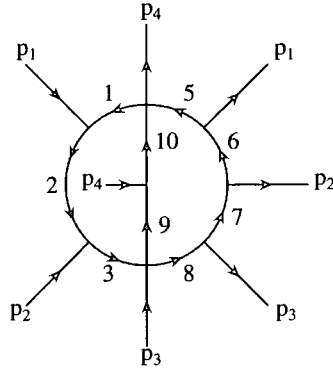
Figure 3.5: General non-planar diagram

as

$$A_{10} = (k - \ell - p_1 - p_2 - p_3)^2.$$

The rest of the propagators have the same definition as the one given in the previous section.

According to this description, we can assign the array

$$I^D[\nu_1, \nu_2, \nu_3, 0, \nu_5, \nu_6, \nu_7, \nu_8, \nu_9, \nu_{10}] \tag{3.6}$$

that represents all D-dimensional two-loop non-planar integrals, instead of using the integral itself

$$\int \frac{d^D k}{i\pi^{\frac{D}{2}}} \int \frac{d^D \ell}{i\pi^{\frac{D}{2}}} \frac{1}{A_1^{\nu_1} A_2^{\nu_2} A_3^{\nu_3} A_5^{\nu_5} A_6^{\nu_6} A_7^{\nu_7} A_8^{\nu_8} A_9^{\nu_9} A_{10}^{\nu_{10}}}. \tag{3.7}$$

Again, all powers of the propagators may be positive or negative and the pinched propagators are represented with 0.

Looking at the different topologies we can have in a $2 \rightarrow 2$ matrix element calculation, the crossed double box (shown in fig.(3.6)) is the most complicated non-planar topology. We can see that this topology does not have propagators 5 and 6 in its description (apart from the common absence of propagator 4 for all non-planar diagrams). Figure (3.7), presents the same crossed box, but the structure of the drawing allows us to examine it better. It is not so clear at the moment, but we may be able to see an internal symmetry in the loop formed by propagators $7 \rightarrow 10$ and between propagators 1 and 3. These observations can be used to shed some light in the design of a non-planar algorithm to treat these integrals.

We can obtain the rest of the sub-topologies, by eliminating propagators present in the crossed double box and in table 3.3 we see some examples that help to visualise this. Note the representation of the crossed box with propagator 5 having a negative power
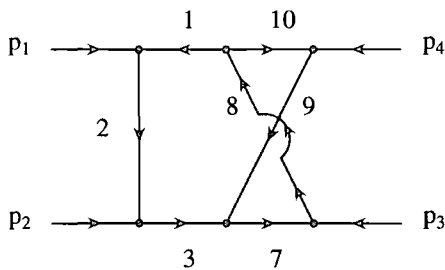
Figure 3.6: Structure of non-planar double box
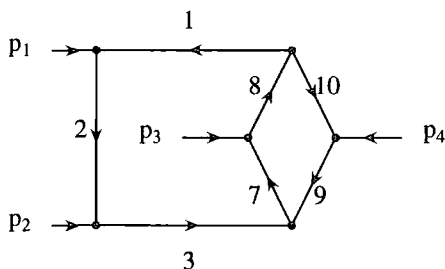
Figure 3.7: Another version of the structure of non-planar double box

Name	Diagram	Identification
XBOX1 (s_{12}, s_{23})		$I^D[1,1,1,0,0,0,1,1,1,1,s_{12},s_{23}]$
		$I^D[1,2,1,0,0,0,1,1,1,1,s_{12},s_{23}]$
XBOX2 (s_{12}, s_{23})		$I^D[1,1,1,0,-1,0,1,1,1,1,s_{12},s_{23}]$
XTRIA (s_{12}, s_{23})		$I^D[1,0,1,0,0,0,1,1,1,1,s_{12},s_{23}]$

Table 3.3: Some examples of non-planar diagrams with their identifications

which is of particular importance to us. It will be appearing in the rest of this work since it becomes part of a family of *master* integrals with a particular rôle in the matrix elements calculations. It is also worth mentioning that any extra pinchings on the crossed triangle sub-topology will produce a planar topology.

3.2 Explicit loop integration

So far we have seen that we can have different families of loop integrals, depending on their participating propagators, and they can either be scalar or tensor integrals. Also, we have found ways to collect all the information an integral carries in a compact way. But we still have not discussed how to calculate them.

The calculation of Feynman integrals is a very old matter. People have tried different approaches to the same problem: how to calculate multi-loop integrals of propagators with arbitrary powers and masses. In principle, our problem is not as general; we want to calculate two-loop integrals with massless propagators and say, up to 7 propagators and 5 tensors in the numerator. Nevertheless, this problem still requires a strategy that can help us undertake the loop integration for integrals with a rich propagator and tensor structure.

We can classify the loop integration strategies into two types

(a) Explicit evaluation of the loop integration which is the *brute force* approach. This may involve finding changes of variables, mappings to the complex plane and equivalent mathematical representations for a loop integral, in order to shrink the mathematical problem until a result is produced. So far these approaches have produced the strategically important results needed for the advancement of the more automated ways of tackling the same problem.

(b) Rewriting the integrals in terms of simpler known integrals. A system of equations relating several kinds of integrals, solved in a particular manner, can provide an automated reduction of integrals with large powers in the propagators in terms of simpler integrals; integrals that can easily be calculated using the explicit methods.

We will discuss the explicit calculation of loop-integrals in this section. Also, we will start the discussion on the methods using systems of equations in the last section of this Chapter, since Chapter 4 is entirely dedicated to precisely this topic.

3.2.1 Parametric forms of loop integrals and integration strategies

We start by looking at the Feynman and Schwinger prescriptions which have the same type of approach. They both express the propagators of a loop integral, in terms of integrations of real parameters over a particular range. The difference between these two prescriptions is in the types of relations these parameters have, and this is in turn

related to the kernel used in each representation (a δ-function in the Feynman form and the exponential function in the Schwinger form). In both of these approaches the loop momenta integration can be done easily and the remaining integrations over the parameters are doable for reasonably sized topologies.

Sometimes applying the Schwinger and Feynman parametric representations to a loop integral does not leave a parametric integral that can be solved easily. The solution of the integrals over the parameters already introduced can become cumbersome when the number of loops and external legs increases. Different techniques arose due to this situation.

The Mellin-Barnes (MB) [53, 54, 55] method is applied over a loop integral in a parametric form. It is based on the representation of a power of a sum as a contour integral over complex variables and the integration is performed over straight lines parallel to the imaginary axis. The result of the integration, after closing a contour, is a sum of all the enclosed residues that (most of the time) can be expressed as a hypergeometric series.

The Negative Dimensions (NDIM) [56, 57] technique takes the representation given by the Schwinger prescription and introduces a multinomial expansion of the sum of the variables of integration.

In this particular scheme, there are many conditions to be satisfied between the original parameters and the ones introduced by the multinomial expansion. This has immediate repercussions over the dimension D of the integration; D must be a negative integer number. One obtains solutions for different valid parameter regions and they all must be taken into account in the final result.

There are other strategies being explored by Binoth and Heinrich [58] whereby any Feynman integral associated to a particular graph is stripped of its infrared singularities analytically. The remaining integrations are too numerous and complicated to be done analytically, so a numerical result is obtained.

Let us begin with the discussion on the parametric forms and proceed afterwards with the different techniques developed to integrate over the parameters associated with each propagator.

The two parametric representations we already introduced are

1. *Feynman Parameters*   Based on Feynman's idea to express a set of propagators as integrals over parameters assigned to each propagator. The relation between these parameters is prescribed by a delta function so that the integration is over a unit

length, and normalised by a ratio of Γ functions. The prescription is as follows

$$\frac{1}{A_1^{\nu_1}...A_n^{\nu_n}} = \Gamma(N) \left[\prod_{i=1}^{n} \frac{1}{\Gamma(\nu_i)} \int_0^1 dx_i \; x_i^{\nu_i-1} \right] \delta \left(1 - \sum_{i=1}^{n} x_i \right) \left(\sum_{i=1}^{n} x_i A_i \right)^{-N} \quad (3.8)$$

with

$$N = \sum_{i=1}^{n} \nu_i. \quad (3.9)$$

2. *Schwinger Parameters*   Based on Schwinger's approach to use the exponential function, rather than the δ-function to express a propagator as an integral over some parameter. This time the integration is over an infinite interval and for a single propagator is as follows

$$\frac{1}{A_i^{\nu_i}} = \frac{(-1)^{\nu_i}}{\Gamma(\nu_i)} \int_0^{\infty} dx_i \; x_i^{\nu_i-1} \exp\left(x_i A_i\right), \quad (3.10)$$

then, for and arbitrary number of propagators we have

$$\frac{1}{A_1^{\nu_1}...A_n^{\nu_n}} = \left[\prod_{i=1}^{n} \frac{(-1)^{\nu_i}}{\Gamma(\nu_i)} \int_0^{\infty} dx_i \; x_i^{\nu_i-1} \right] \exp\left(\sum_{i=1}^{n} x_i A_i \right). \quad (3.11)$$

Both of the parametric forms allow the propagators in the denominator to be embedded into a polynomial that can be used to integrate out the loop momenta with a simple change of variables. The polynomial has the following structure

$$\sum_{i=1}^{n} x_i A_i = a k^2 + b\ell^2 + 2ck \cdot \ell + 2d \cdot k + 2e \cdot \ell + f, \quad (3.12)$$

where we have taken apart the actual inner structure of the propagators into the different contributions that may arise [†]. More precisely, a and b are sums of parameters associated with the propagators that contribute to the k and ℓ-loop, respectively. The tensors d^μ and e^μ pick up the tensorial contributions arising from terms like $p_j \cdot k_i$, where p_j can be any of the external momenta. In c, we collect information on the parameters that belong to propagators that participate in both the k and the ℓ loop. Last, the f term has all dependence on the external momenta squared. In all these terms we always have a linear dependence in the parameters x_i.

By now, we may have an idea of the structure of these terms since we already saw in section 3.1 how our general integral is described and how the propagators look like. More so, we may be able to read off the structure of the polynomial in eq.(3.12), from the actual graph associated with it.

Let us extract the structure of the polynomial associated with the general planar diagram shown in fig.(3.2), whose integral involves the following propagators

---

[†]In the one-loop case, taking the k-loop, we have to set : $b = c = e \equiv 0$

| | Terms contributing to : | | |
Propagator	a and b	c, d^μ and e^μ	f
$A_1 = \quad k^2$	k^2		
$A_2 = \quad (k+p_1)^2$	k^2	$+2k \cdot p_1$	
$A_3 = \quad (k+p_1+p_2)^2$	k^2	$+2k \cdot (p_1+p_2)$	$+2p_1 \cdot p_2$
$A_4 = \quad (k+p_1+p_2+p_3)^2$	k^2	$+2k \cdot (p_1+p_2+p_3)$	
$A_5 = \quad \ell^2$	ℓ^2		
$A_6 = \quad (\ell+p_1)^2$	ℓ^2	$+2\ell \cdot p_1$	
$A_7 = \quad (\ell+p_1+p_2)^2$	ℓ^2	$+2\ell \cdot (p_1+p_2)$	$+2p_1 \cdot p_2$
$A_8 = \quad (\ell+p_1+p_2+p_3)^2$	ℓ^2	$+2\ell \cdot (p_1+p_2+p_3)$	
$A_9 = \quad (k-\ell)^2$	$k^2+\ell^2$	$-2k \cdot \ell$	

where we have considered $p_i^2 = 0$ for all external momenta and we have made a clear separation of the terms contributing to each factor of the polynomial in eq.(3.12). Therefore we will have

$$
\begin{aligned}
a &= x_1 + x_2 + x_3 + x_4 + x_9, \\
b &= x_5 + x_6 + x_7 + x_8 + x_9, \\
c &= -x_9, \\
d^\mu &= x_2\, p_1^\mu + x_3\, (p_1+p_2)^\mu + x_4\, (p_1+p_2+p_3)^\mu, \\
e^\mu &= x_6\, p_1^\mu + x_7\, (p_1+p_2)^\mu + x_8\, (p_1+p_2+p_3)^\mu, \\
f &= 2\, (x_3 + x_7)\, p_1 \cdot p_2,
\end{aligned}
\tag{3.13}
$$

for the polynomial associated with the general planar integral of eq.(3.4).

With this in mind, we can apply either of the two parametrisations to an arbitrary two-loop integral

$$
I^D[\nu_1, ..., \nu_n] = \int \frac{d^D k}{i\pi^{\frac{D}{2}}} \int \frac{d^D \ell}{i\pi^{\frac{D}{2}}} \frac{1}{A_1^{\nu_1} \cdots A_n^{\nu_n}},
\tag{3.14}
$$

and use the structure of the polynomial we have analysed to solve the integration with respect to the loop momenta. We can do this easily with the following general change of variables,

$$
\begin{aligned}
k^\mu &\rightarrow K^\mu - \frac{c}{a}L^\mu + \frac{ce^\mu - bd^\mu}{ab - c^2}, \\
\ell^\mu &\rightarrow L^\mu + \frac{cd^\mu - ae^\mu}{ab - c^2}.
\end{aligned}
\tag{3.15}
$$

If we apply this change of variables to the l.h.s. of eq.(3.12), we are effectively diagonalising

the polynomial (completing the squares for the loop momenta) and have

$$
\begin{aligned}
\sum_{i=1}^{n} x_i A_i &= ak^2 + b\ell^2 + 2ck \cdot \ell + 2d \cdot k + 2e \cdot \ell + f \\
&= aK^2 + \frac{ab - c^2}{a} L^2 + \Delta \\
&= aK^2 + \frac{P}{a} L^2 + \Delta,
\end{aligned}
\tag{3.16}
$$

where,

$$
\Delta = \frac{-a\,e^2 - b\,d^2 + 2\,c\,d \cdot e + f(ab - c^2)}{ab - c^2} = \frac{Q}{P}
\tag{3.17}
$$

and

$$
P = ab - c^2.
\tag{3.18}
$$

Following on the example, the values of Q and P for the general planar topology are

$$
\begin{aligned}
Q &= \Big[x_5 x_7 \, (x_1 + x_2 + x_3 + x_4) + x_1 x_3 \, (x_5 + x_6 + x_7 + x_8) \\
&\quad + (x_1 + x_5)\,(x_3 + x_7)\,x_9 \Big] s_{12} \\
&\quad + \Big[x_6 x_8 \, (x_1 + x_2 + x_3 + x_4) + x_2 x_4 \, (x_5 + x_6 + x_7 + x_8) \\
&\quad + (x_2 + x_6)\,(x_4 + x_8)\,x_9 \Big] s_{23},
\end{aligned}
\tag{3.19}
$$

$$
\begin{aligned}
P &= (x_1 + x_2 + x_3 + x_4)\,(x_5 + x_6 + x_7 + x_8) \\
&\quad + (x_1 + x_2 + x_3 + x_4 + x_5 + x_6 + x_7 + x_8)\,x_9,
\end{aligned}
\tag{3.20}
$$

where $s_{ij} = 2\,p_i \cdot p_j$. The complex structure of these objects, makes the job of integrating over the parameters, a hard one.

In any case, according to what we have discussed so far, our arbitrary integral of eq.(3.14) can be written in two ways. If we use the Feynman prescription,

$$
\begin{aligned}
I^D[\nu_i, ..., \nu_n] &= \Gamma(N) \left[\prod_{i=1}^{n} \frac{1}{\Gamma(\nu_i)} \int_0^1 dx_i \, x_i^{\nu_i - 1} \right] \delta \left(1 - \sum_{i=1}^{n} x_i \right) \\
&\quad \times \int \frac{d^D K}{i\pi^{\frac{D}{2}}} \int \frac{d^D L}{i\pi^{\frac{D}{2}}} \left(aK^2 + \frac{P}{a} L^2 + \Delta \right)^{-N}
\end{aligned}
\tag{3.21}
$$

and if we use the Schwinger prescription,

$$
\begin{aligned}
I^D[\nu_i, ..., \nu_n] &= \left[\prod_{i=1}^{n} \frac{(-1)^{\nu_i}}{\Gamma(\nu_i)} \int_0^\infty dx_i \, x_i^{\nu_i - 1} \right] \\
&\quad \times \int \frac{d^D K}{i\pi^{\frac{D}{2}}} \int \frac{d^D L}{i\pi^{\frac{D}{2}}} \exp \left(aK^2 + \frac{P}{a} L^2 + \Delta \right).
\end{aligned}
\tag{3.22}
$$

Now, the dependence on the loop momenta is only through their magnitude, so we can integrate it out. We perform the Wick rotation in a similar way as we did in section 1.4 and integrate out the loop momentum.

We are left with the parametric integrations over the Q and P structures, which can be reconstructed directly from the graph (using a, b, c, d^μ, e^μ, f) to which the integral is associated. Therefore, the loop integration result is

$$I^D[\nu_1 \dots \nu_n] = \left(\prod_{i=1}^{n} \frac{(-1)^{\nu_i}}{\Gamma(\nu_i)} \int_0^1 dx_i x_i^{\nu_i-1}\right) \delta\left(1 - \sum_{i=1}^{n} x_i\right)$$
$$\times \Gamma(N - D) \ P^{N-\frac{3D}{2}} \ Q^{D-N}, \tag{3.23}$$

in the Feynman prescription, whereas in the Schwinger prescription, we have

$$I^D[\nu_1 \dots \nu_n] = \left(\prod_{i=1}^{n} \frac{(-1)^{\nu_i}}{\Gamma(\nu_i)} \int_0^\infty dx_i x_i^{\nu_i-1}\right) \times \frac{1}{P^{D/2}} \exp\left(\frac{Q}{P}\right). \tag{3.24}$$

3.2.1.1   Mellin-Barnes technique

Once we have an integral in the Feynman prescription we can integrate over the parameters using the Mellin-Barnes method which is based on the representation of a power of a sum as a contour integral. In the case of a sum of two terms with an arbitrary power,

$$\frac{1}{(A+B)^\nu} = \frac{1}{A^\nu \Gamma(\nu)} \int_{-i\infty}^{+i\infty} \frac{du}{2\pi i} \left(\frac{B}{A}\right)^u \Gamma(\nu + u)\Gamma(-u) \tag{3.25}$$

where we have introduced a complex variable u and the contour is separating the poles of the two Γ functions as it is shown in figure (3.8).
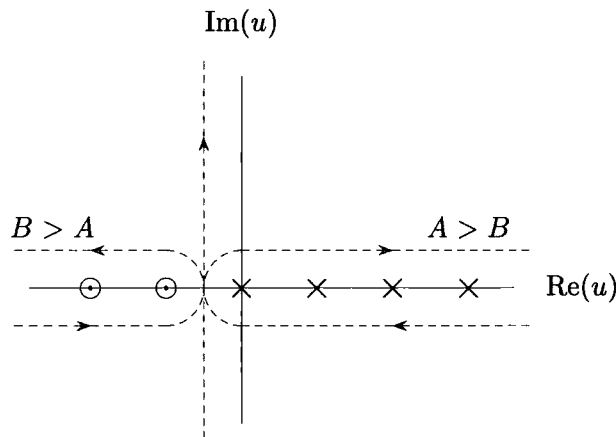
Figure 3.8: Region of integration with open and closed contour

This identity can be generalized to an arbitrary number of terms for the sum and

be applied to convert the term Q^{D-N} of the Feynman representation, into a product of integrations over complex variables.

Equation (3.25) can be easily verified. We can see that the integrand has poles for $u = n$ (positive branch) and for $u = -\nu - n$ (negative branch), with $n = 0, 1, 2, \ldots$. Depending on whether $B > A$ or not, we can close the contour to the left or to the right, respectively.

Taking $A > B$ to be the case, then we close the contour to the right (see fig.(3.8)) and pick up the residues corresponding to the poles at $u = n$, to apply Cauchy's residues theorem[‡] on the integral of eq.(3.25).

The residues of the integrand are

$$
\begin{aligned}
\text{Res}\,[\Gamma(-x)]_{x=n} &= \text{Res}\,[\Gamma(x)]_{x=-n} \\
&= \text{Res}\,[\Gamma(x' - n)]_{x'=0} \\
&= \text{Res}\,[(x' - n - 1)!]_{x'=0} \\
&= \text{Res}\left[\frac{\Gamma(x' + 1)}{x'(x' - 1)\cdots(x' - n)}\right]_{x'=0} \\
&= \frac{(-1)^n}{n!}
\end{aligned}
\tag{3.27}
$$

for $n = 0, 1, 2, \ldots$ With this, the integral in eq.(3.25) will become

$$
\begin{aligned}
\frac{1}{A^\nu \Gamma(\nu)} \int_{-i\infty}^{+i\infty} \frac{du}{2\pi i} \left(\frac{B}{A}\right)^u \Gamma(\nu + u)\Gamma(-u) &= \frac{1}{A^\nu \Gamma(\nu)} \sum_{n=0}^{\infty} \left(\frac{B}{A}\right)^n \Gamma(\nu + n)\frac{(-1)^n}{n!} \\
&= \frac{1}{A^\nu} \sum_{n=0}^{\infty} \left(-\frac{B}{A}\right)^n \frac{\Gamma(\nu + n)}{n!\,\Gamma(\nu)},
\end{aligned}
\tag{3.28}
$$

which is the Taylor expansion of $1/(A + B)^\nu$ for a very small B. A similar result can be obtained when closing the contour to the left.

In the literature, the MB method has been applied widely and successfully to one and two-loop integrals. For one-loop integrals, the method is fairly straightforward to apply. The two-loop integrals have proven to be a highly complex task and involve clever changes of variables and manipulations of the integrand.

3.2.1.2 Negative Dimensions technique

The Negative Dimensions method (NDIM) deals with the same kinds of sums that the MB deals with. It consists of writing a sum of terms that has an arbitrary power, as a

---

[‡]An integral over a closed contour of an analytic complex function is

$$
\oint \mathcal{F}(x)\, dx = 2\pi i \sum_i \text{Res}\,[\mathcal{F}(x_i)]
\tag{3.26}
$$

binomial expansion. However, an assumption that this power has to be a positive integer has repercussions on the dimension, forcing it to be negative.

To show this for a particular case, let us (temporarily) assume that $-\nu$ is a positive integer and make a binomial expansion,

$$\frac{1}{(A+B)^\nu} = \sum_{n_1,n_2=0}^{\infty} A^{n_1} B^{n_2} \frac{(n_1+n_2)!}{n_1!n_2!}, \tag{3.29}$$

which is subject to the constraint

$$n_1 + n_2 = -\nu. \tag{3.30}$$

To see that we can verify this expansion, we can look at the two solutions: either take n_1 as integer and $n_2 = -\nu - n_1$ or exchange the roles for n_1 and n_2.

Taking the case where $n_1 = n = 0, 1, 2, \ldots$ and $n_2 = -\nu - n$ then

$$\left[\sum_{n_1,n_2=0}^{\infty} A^{n_1} B^{n_2} \frac{(n_1+n_2)!}{n_1!n_2!} \right]_{n_1=n,n_2=-\nu-n} = \sum_{n=0}^{\infty} \frac{A^n B^{-\nu-n}}{n!} \frac{\Gamma(1-\nu)}{\Gamma(1-\nu-n)}$$

$$= B^{-\nu} \sum_{n=0}^{\infty} \frac{\Gamma(\nu+n)}{\Gamma(\nu)\,n!} \left(\frac{-A}{B} \right)^n,$$

which converges to $(1 + A/B)^{-\nu}$, provided that $A < B$. The other solution, corresponds to exchanging roles of A and B and converges when $B < A$.

Therefore, in the NDIM approach, it is necessary to explore all possible series solutions and collect the solutions that converge in the domains defined by the available kinematic regions of the particular system.

The name of the method arises due to the fact that when the generalised version of eq.(3.29) is applied to polynomial terms such as $P^{D/2}$ (from the parametrisation recipe), then several conditions such as the one in eq.(3.30) drive the dimension parameter D to be a negative integer. This is a valid assumption, since the loop integral is an analytic function of the number of dimensions D.

Multiple examples of loop integration using the MB and NDIM methods can be found in references [56, 57, 59] and references therein.

3.3 Loop integration through systems of equations

We have seen different ways of approaching the calculation of loop integrals. Some are more cumbersome than others and it is not yet straightforward how to implement these methods to be able to calculate integrals with arbitrary powers of propagators and with a fair load of tensorial structure.

However, there is another approach that produces an environment in which loop integrals can be treated in a general and automated way. Moreover, complex topologies with high powers on the propagators can be reduced down to integrals that can be solved with the methods described in the previous section and sometimes can be solved altogether. This reduction can be achieved using systems of equations stemming from Integration by Parts identities [60, 61, 62] and exploiting the Lorentz invariance of the Feynman integrals [63].

In this section we will study the basics of this method and will provide a simple example of its capabilities. This mechanism is the backbone of the algorithm with which we perform our calculations.

A detailed discussion of the automated reduction of loop integrals within the context of matrix elements calculations will be given in the next chapter.

3.3.1 Integration by Parts identities

Let us consider the arbitrary loop integral provided in eq.(3.14) and given by

$$I^D[\nu_1, ..., \nu_n] = \int \frac{d^D k}{i\pi^{\frac{D}{2}}} \int \frac{d^D \ell}{i\pi^{\frac{D}{2}}} \frac{1}{A_1^{\nu_1} \cdots A_n^{\nu_n}}.$$

The idea behind the integration by parts (IBP) method is to find relations between integrals generated through a total derivative with vanishing surface terms, expressed as the following identity

$$\int \frac{d^D k}{i\pi^{\frac{D}{2}}} \int \frac{d^D \ell}{i\pi^{\frac{D}{2}}} \frac{\partial}{\partial k_i^\mu} \left[\frac{\mathcal{V}^\mu}{A_1^{\nu_1} \cdots A_n^{\nu_n}} \right] \equiv 0, \tag{3.31}$$

where $k_i = k, \ell$ and $\mathcal{V}$ can be any internal or external momenta involved in the loop integration.

If we apply the derivative we will get two kinds of terms related to

1. the derivative of the numerator

$$\frac{1}{A_1^{\nu_1} \cdots A_n^{\nu_n}} \frac{\partial \mathcal{V}^\mu}{\partial k_i^\mu} = \begin{cases} \frac{D}{A_1^{\nu_1} \cdots A_n^{\nu_n}} & \text{if } \mathcal{V} \text{ depends on } k_i, \\ 0 & \text{otherwise,} \end{cases}$$

2. the derivative of the denominator

$$\frac{\mathcal{V}^\mu}{A_1^{\nu_1} \cdots A_n^{\nu_n}} \left[\frac{\partial}{\partial k_i^\mu} \frac{1}{A_i^{\nu_i}} \right] \begin{cases} \frac{-2\, \nu_i A_i \cdot \mathcal{V}}{A_1^{\nu_1} \cdots A_i^{\nu_i + 1} \cdots A_n^{\nu_n}} & \text{if } A_i \text{ depends on } k_i, \\ 0 & \text{otherwise.} \end{cases} \tag{3.32}$$

Note that we will generate a set of relations between integrals with dot products in the numerator, arising from terms like those in eq.(3.32). These dot products can be rewritten in terms of linear combinations of propagators as follows

$$2\, A_i \cdot \mathcal{V} \sim 2(k_i + g) \cdot (k_i + h) \quad = \quad (k_i + g)^2 + (k_i + h)^2 - (g - h)^2.$$

With this simple step we can rewrite all the contents of the numerator in terms of propagators that may or may not be part of the denominator. We then say that the numerator is *reducible* if we can cancel it through and *irreducible* otherwise. The former will make the integral less complex since it will diminish the power of a propagator (or eliminate it altogether if we are lucky), and the latter will make a more complex integral since it adds a tensorial structure to the numerator.

Even though we may not be able to have a relation between our original integral and simpler integrals (which would be the solution to our problem), we manage to construct an identity that relates different integrals on the same footing. We have found a way to *translate* the original integral into a sum of other integrals of different structure.

Now, in eq.(3.31) we can take all possible momenta of the system as the value of $\mathcal{V}$ and consider the derivative with respect to both the k and ℓ loop momenta, to have a system of identities with the characteristics mentioned. More precisely, for any two-loop integral we have two loop momenta and $\mathcal{V}$ can be any of the momenta of the graph k_i, p_i or combinations of them, e.g. $\{k_i, k_i + p_1, k_i + p_1 + p_2, k_i + p_1 + p_2 + p_3, k_i - k_j\}$. In this case we can have 10 IBP identities.

In general, for a graph with m loops and n independent external momenta, we have

$$N_{\text{IBP}} = m\,(m + n), \tag{3.33}$$

identities.

Having some irreducible numerators in the system of identities is not a very good thing but, there is always the possibility that we can manipulate it to build a new system of identities, free from irreducible numerators. We will discuss this possibility in the next chapter.

For now, let us turn our attention to a simple example where we can exercise what we have just learned.

3.3.1.1 An example using IBP

Consider the *Pentabox*, which is the name of the graph shown in fig.(3.9), with arbitrary powers in its propagators.
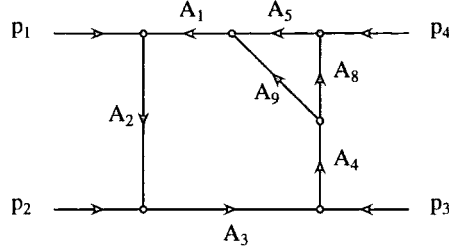
Figure 3.9: The *Pentabox* diagram

This diagram can be obtained by adding propagator 4 and eliminating propagator 7 in the double planar box shown in fig.(3.4), so it has the following propagators present

$$
\begin{array}{ll}
A_1 = k^2 & A_5 = \ell^2 \\
A_2 = (k + p_1)^2 & A_8 = (\ell + p_{123})^2 \\
A_3 = (k + p_{12})^2 & A_9 = (k - \ell)^2 \\
A_4 = (k + p_{123})^2 &
\end{array}
$$

where we have used the notation $p_{ijk} = p_i + p_j + p_k$.

We can apply the IBP identity of eq.(3.31) with any of these propagators in the numerator. For example, let us take $\mathcal{V}^\mu = (\ell + p_{123})^\mu$ and derivate with respect to ℓ^μ, to have

$$
0 \equiv \int \frac{d^D k}{i\pi^{\frac{D}{2}}} \int \frac{d^D \ell}{i\pi^{\frac{D}{2}}} \frac{\partial}{\partial \ell^\mu} \left[\frac{(\ell + p_{123})^\mu}{A_1^{\nu_1} A_2^{\nu_2} A_3^{\nu_3} A_4^{\nu_4} A_5^{\nu_5} A_8^{\nu_8} A_9^{\nu_9}} \right].
$$

Working on the r.h.s. of this expression and using the definitions for the propagators already provided, we find

$$
0 \equiv \int \frac{d^D k}{i\pi^{\frac{D}{2}}} \int \frac{d^D \ell}{i\pi^{\frac{D}{2}}} \left[\frac{1}{A_1^{\nu_1} A_2^{\nu_2} A_3^{\nu_3} A_4^{\nu_4} A_5^{\nu_5} A_8^{\nu_8} A_9^{\nu_9}} \right]
$$
$$
\times \left(D - \nu_5 \frac{2 \, (\ell + p_{123}) \cdot \ell}{A_5} - \nu_8 \frac{2 \, (\ell + p_{123}) \cdot (\ell + p_{123})}{A_8} \right.
$$
$$
\left. - \nu_9 \frac{2 \, (\ell + p_{123}) \cdot (\ell - k)}{A_9} \right).
$$

Following on, we can rewrite the dot products (recall eq.(3.33)) as

$$
2 \, (\ell + p_{123}) \cdot (\ell + p_{123}) = 2 A_8,
$$
$$
2 \, (\ell + p_{123}) \cdot \ell = A_5 + A_8,
$$
$$
2 \, (\ell + p_{123}) \cdot (\ell - k) = A_8 + A_9 - A_4.
$$

Introducing these expressions in the identity, gives

$$
0 \equiv \int \frac{d^D k}{i\pi^{\frac{D}{2}}} \int \frac{d^D \ell}{i\pi^{\frac{D}{2}}} \left[\frac{1}{A_1^{\nu_1} A_2^{\nu_2} A_3^{\nu_3} A_4^{\nu_4} A_5^{\nu_5} A_8^{\nu_8} A_9^{\nu_9}} \right]
$$

$$\times \left(D - \nu_5 - 2\,\nu_8 - \nu_9 - \nu_5 \frac{A_8}{A_5} - \nu_9 \frac{A_8}{A_9} + \nu_9 \frac{A_4}{A_9} \right).$$

We can see that, inside the integrand, we have produced some constant terms, but we have also produced ratios of propagators. A propagator in the numerator, will be absorbed in the denominator by reducing one power in the corresponding propagator and the terms in the denominator will do the opposite. This can be represented, using raising and lowering operators that act at the level of the integrand. More precisely, the equation above can be *symbolically* written as

$$0 \equiv \left(D - \nu_5 - 2\nu_8 - \nu_9 - \nu_5 \mathbf{5}^+ \mathbf{8}^- - \nu_9 \mathbf{9}^+ \mathbf{8}^- + \nu_9 \mathbf{9}^+ \mathbf{4}^- \right) I^{Pentabox}.$$

Perhaps it can be better appreciated if we write it as follows

$$I^{Pentabox} = \frac{1}{(D - \nu_5 - 2\nu_8 - \nu_9)} \left(\nu_5 \mathbf{5}^+ \mathbf{8}^- + \nu_9 \mathbf{9}^+ \mathbf{8}^- - \nu_9 \mathbf{9}^+ \mathbf{4}^- \right) I^{Pentabox}. \quad (3.34)$$

This relation allows us to determine the original *Pentabox* with arbitrary powers in the propagators, as a sum of three integrals, each of which have a unit reduction in one propagator and an increment in another. In practical terms, we could apply this relation recursively to *Pentabox* integrals that have large powers in propagators 4 and 8 until we eliminate completely these two propagators and obtain integrals of a smaller topology. This would bring us closer to an integral that we can calculate by other methods.

We can see how this would work if we take a *Pentabox* that has unit powers in all its propagators. In that case eq.(3.34) will be written as

$$I^{Pentabox} = \frac{1}{(D - 4)} \left(\mathbf{5}^+ \mathbf{8}^- - \mathbf{9}^+ \mathbf{8}^- + \mathbf{9}^+ \mathbf{4}^- \right) I^{Pentabox},$$

which can be best visualised with the aid of fig.(3.10). In this figure, each of the diagrams

Figure 3.10: Reduction of the *Penta box*.

on the r.h.s. are obtained by eliminating the corresponding propagator in the original *Pentabox* diagram of fig.(3.9). The black dots correspond to an extra power of the propagator on which they appear. We can find relations that act on the pinched integrals and reduce them further, until we arrive to a set of simpler integrals that can be easily calculated with MB or NDIM.

This example just shows how a particular identity for a specific topology can work. But, we can create many identities for each family of integrals and use the system as a tool to express any integral in terms of a handful of simpler integrals. The analysis has to be done on each topology since the types of terms that will produce irreducible numerators will change depending on such a topology. We will see some examples of this in Chapter 4.

3.3.2 Lorentz Invariance identities

In addition to the IBP identities, one can also exploit the fact that all integrals arising from the Feynman diagrams depend on scalar products of the external momenta. This means that any of these integrals must be invariant under a Lorentz transformation of the external momenta of the Feynman graph to which it is associated.

Specifically, any of these integrals fulfils

$$I(p_1', ..., p_n') = I(p_1, ..., p_n), \tag{3.35}$$

where we take the infinitesimal rotation to be

$$p_i'^\mu = \Lambda^\mu_\nu p_i^\nu \tag{3.36}$$

with $\Lambda^\mu_\nu = g_{\mu\nu} + \delta\epsilon_{\mu\nu}$ and $\epsilon_{\mu\nu} = -\epsilon_{\nu\mu}$.

We can Taylor expand the r.h.s. of eq.(3.35) to have

$$I(p_1', ..., p_n') = I(p_1, ..., p_n) + \delta\epsilon^\mu_\nu \, p_1^\nu \frac{\partial}{\partial p_1^\mu} I(p_1, ..., p_n) + \cdots + \delta\epsilon^\mu_\nu \, p_n^\nu \frac{\partial}{\partial p_n^\mu} I(p_1, ..., p_n).$$

Considering the initial requirement of eq.(3.35) we can see that the term on the l.h.s cancels against the first term on the r.h.s. of the equation above, therefore we get the following expression

$$\delta\epsilon^\mu_\nu \left(p_1^\nu \frac{\partial}{\partial p_1^\mu} + \cdots + p_n^\nu \frac{\partial}{\partial p_n^\mu} \right) I(p_1, ..., p_n) = 0.$$

Now, $\delta\epsilon^\mu_\nu$ has six independent components so, in principle we have six Lorentz Invariance (LI) identities. However, these identities are not always linearly independent. To maximise the number of linearly independent identities, we make use of the antisymmetry of $\delta\epsilon^\mu_\nu$, to get

$$\left(p_1^\nu \frac{\partial}{\partial p_1^\mu} - p_1^\mu \frac{\partial}{\partial p_1^\nu} + \cdots + p_n^\nu \frac{\partial}{\partial p_n^\mu} - p_n^\mu \frac{\partial}{\partial p_n^\nu} \right) I(p_1, ..., p_n) = 0. \tag{3.37}$$

This equation can now be used to generate identities between scalar integrals. We need only to contract it with all possible antisymmetric combinations of $p_i^\mu p_j^\nu$. For our

processes we will have diagrams with four legs and three independent external momenta, so we can choose the following three antisymmetric combinations

$$
\begin{aligned}
p_1^\mu p_2^\nu &- p_2^\mu p_1^\nu \\
p_1^\mu p_3^\nu &- p_3^\mu p_1^\nu \\
p_2^\mu p_3^\nu &- p_3^\mu p_2^\nu
\end{aligned}
\tag{3.38}
$$

providing 3 LI identities. In general we can have up to

$$
N_{\mathrm{LI}} = \frac{1}{2} n \times (n - 1)
\tag{3.39}
$$

identities for n independent external momenta.

The identities produced using this method, are similar to the ones produced using IBP. To achieve the reduction of two-loop planar integrals of arbitrary powers, the LI identities are not needed. However, for the non-planar topologies, they proved to be indispensable.

In Chapter 4, we will see the structure of these identities and briefly discuss their involvement in the reduction of the non-planar topologies. For now, let us see how we can tackle the problem of loop integrals with tensor structure.

3.4 Dealing with tensors in loop integration

So far, we have seen how we can calculate scalar loop integrals using different parametric representations and applying, for example, the MB and NDIM methods. Also, we discussed how we can have a system of equations that helps us write an integral in terms of integrals with different structure that may or may not be easier to deal with.

A system of equations like the ones we have discussed, have the potential to provide a complete reduction of an integral. But, they also can give us a partial answer that contains integrals with irreducible numerators. We must then find a way to deal with these.

We can work with either the isolated tensor structure (and calculate explicit tensor integrals), or the irreducible numerators themselves (and calculate scalar integrals). In this section we review the former approach and leave the discussion for the latter to the next chapter.

Consider an arbitrary integral with a tensor in the numerator, such as

$$
I^D[\nu_1, ..., \nu_n]\{\ell^\mu\} = \int \frac{d^D k}{i\pi^{\frac{D}{2}}} \int \frac{d^D \ell}{i\pi^{\frac{D}{2}}} \frac{\ell^\mu}{A_1^{\nu_1} \cdots A_n^{\nu_n}},
$$

and let us suppose that the tensor comes from a dot product in the numerator (such as $p_i \cdot \ell$) that cannot be written as a linear combination of the existing propagators, i.e. it comes from an irreducible numerator.

However, recall that to solve the integral using, say, the Schwinger parametrisation we shifted the loop momentum (see eq.(3.15)) as

$$
\begin{aligned}
\ell^\mu &\to L^\mu + \frac{cd^\mu - ae^\mu}{ab - c^2}, \\
&\to L^\mu + \frac{cd^\mu - ae^\mu}{P}.
\end{aligned}
$$

So if we apply this shift of momentum and perform the loop integration as was done in section 3.2.1 for the Schwinger parametrisation, we will have

$$
\begin{aligned}
I^D[\nu_1, ..., \nu_n]\{\ell^\mu\} &= \left(\prod_{i=1}^{n} \frac{(-1)^{\nu_i}}{\Gamma(\nu_i)} \int_0^\infty dx_i x_i^{\nu_i - 1} \right) \\
&\times \frac{1}{P^{D/2}} \exp\left(\frac{Q}{P}\right) \frac{cd^\mu - ae^\mu}{P},
\end{aligned} \tag{3.40}
$$

since the (odd) L^μ term does not contribute.

Let us look into the answer that integration provides. From eq.(3.13) we know that the terms a, b, c, d^μ and e^μ have a linear dependence on the Schwinger parameters x_i. Then, we can absorb the extra factors of x_i (coming from a, b, c, d^μ and e^μ) and P into the already present terms.

We will have two types of modifications in our integrand

1. extra powers in the Schwinger parameters

$$
\frac{x_i^{\nu_i - 1}}{\Gamma(\nu_i)} \underbrace{x_i}_{\text{from } \frac{cd^\mu - ae^\mu}{P}} \to \nu_i \frac{x_i^{\nu_i}}{\Gamma(\nu_i + 1)} \sim \nu_i \mathbf{i}^+
$$

2. and extra dimensions

$$
\frac{1}{P^{D/2}} \underbrace{\frac{1}{P}}_{\text{from } \frac{cd^\mu - ae^\mu}{P}} \to \frac{1}{P^{(D+2)/2}} \sim \mathbf{d}^{++}.
$$

Moreover, the term $cd^\mu - ae^\mu$ is quadratic in the x_i parameters, so the actual change of powers will occur in two propagators at a time. The integral of eq.(3.40) will be a sum of integrals with a similar structure, schematically

$$
I^D[\nu_1, ..., \nu_i, ..., \nu_j, ..., \nu_n]\{\ell^\mu\} \sim \sum \nu_i \, \nu_j \, I^{D+2}[\nu_1, ..., \nu_{i+1}, ..., \nu_{j+1}, ..., \nu_n]\{p_k^\mu\}. \tag{3.41}
$$

So we have written our tensor integral in terms of a sum of integrals that have extra powers in the propagators and extra dimensions.

This procedure can be applied to integrals with any number of tensors in the numerator, all that is needed is to apply the change of variables given in eq.(3.15). For example

$$\int \frac{d^D k}{i\pi^{\frac{D}{2}}} \int \frac{d^D \ell}{i\pi^{\frac{D}{2}}} \frac{k^\mu}{A_1^{\nu_1} \cdots A_n^{\nu_n}} = \int \mathcal{D}x \left(\frac{ce^\mu - bd^\mu}{P} \right),$$

$$\int \frac{d^D k}{i\pi^{\frac{D}{2}}} \int \frac{d^D \ell}{i\pi^{\frac{D}{2}}} \frac{\ell^\mu \ell^\nu}{A_1^{\nu_1} \cdots A_n^{\nu_n}} = \int \mathcal{D}x \left(\frac{(cd^\mu - ae^\mu)(cd^\nu - ae^\nu)}{P^2} - \frac{a}{2P}g^{\mu\nu} \right),$$

$$\int \frac{d^D k}{i\pi^{\frac{D}{2}}} \int \frac{d^D \ell}{i\pi^{\frac{D}{2}}} \frac{k^\mu \ell^\nu}{A_1^{\nu_1} \cdots A_n^{\nu_n}} = \int \mathcal{D}x \left(\frac{(ce^\mu - bd^\mu)(cd^\nu - ae^\nu)}{P^2} + \frac{c}{2P}g^{\mu\nu} \right),$$

$$\int \frac{d^D k}{i\pi^{\frac{D}{2}}} \int \frac{d^D \ell}{i\pi^{\frac{D}{2}}} \frac{k^\mu k^\nu}{A_1^{\nu_1} \cdots A_n^{\nu_n}} = \int \mathcal{D}x \left(\frac{(ce^\mu - bd^\mu)(ce^\nu - bd^\nu)}{P^2} - \frac{b}{2P}g^{\mu\nu} \right),$$

where

$$\int \mathcal{D}x = \left(\prod_{i=1}^{n} \frac{(-1)^{\nu_i}}{\Gamma(\nu_i)} \int_0^\infty dx_i x_i^{\nu_i - 1} \right) \frac{1}{P^{D/2}} \exp\left(\frac{Q}{P} \right). \tag{3.42}$$

In summary, we have replaced the problem of having a tensor integral with the problem of solving scalar integrals that have arbitrary powers in the propagators and arbitrary dimension.

For each loop momentum in the numerator, we would increase two propagators of the integral by a unit and increase the dimension of the integral by two. If we consider that we may need up to, say 4 tensors for the matrix element calculations, we can expect to have integrals with up to 4 extra powers in two different propagators and 8 extra dimensions. The reduction of such types of integral using IBP and LI identities, is an involved manipulation and turns out to be impractical.

In the next chapter we study an algorithm that helps us deal with tensor integrals without having to change the dimensions. Even more, this algorithm allows us to manipulate scalar integrals and integrals with irreducible numerators on the same footing and in an automated way.

Chapter 4

Reduction of Loop Integrals

In Chapter 3 we discussed how to calculate loop integrals using various techniques and we saw how the adequacy of a technique depends on the type of integral we are dealing with. The process of explicitly calculating a loop integral, involves choosing changes of variable, mappings to the complex plane and mathematical representations of a loop integral that can help disentangle the mathematical problem until a result is produced.

These methods have proven to be indispensable in the calculation of integrals that have a particular set of propagators, powers of propagators and dimension. Unfortunately, the results obtained for these particular cases do not cover all the possible integrals that can arise in a matrix element calculation. This does not mean that they are not useful. On the contrary, we can build an algorithm that can help us rewrite an arbitrary integral (planar or non-planar, scalar or tensorial) in terms of the ones we already calculated using MB, NDIM or any other method. This Chapter presents a discussion of precisely this idea.

We start by exploring a way of expressing the IBP and LI identities we have for the loop integrals in a symbolic and general manner. Then we can manipulate these expressions easily and find out how they can help in the task of loop integral reduction.

Afterwards, we build an algorithm to reduce the two-loop box integrals into a set of simpler integrals. This important set of integrals will be later refered to as Master Integrals (MI).

The symbolic algorithm is a powerful tool but it involves direct trial and error manipulation of the expressions. In section 4.2, we build and automatic algorithm that can reduce the integrals without resourcing to a manual (symbolic) manipulation. We also make particular choice of double box MI, due to the nature of this algorithm, that makes for a further improvement.

Finally, in section 4.4 we discuss the general algorithm we apply to perform matrix element calculations. Also, we describe briefly the ingredients, extra tools and practical

issues related to the algorithm.

4.1   Symbolic reduction of loop integrals

In the previous chapter, we saw how we could represent all planar two-loop topologies with the graph in fig.(3.2) and all non-planar ones with the one in fig.(3.5). We are looking for a general algorithm that can help us calculate these types of integrals. To that end, we devise a symbolic mechanism with which we can easily do a general manipulation of the two-loop integrals, using all the IBP and LI identities arising from a particular topology.

First, we will analyse what we can have in general and then we can apply it to a particular topology.

As usual, we will be considering lightlike vectors, i.e.

$$p_1^2 = p_2^2 = p_3^2 = p_4^2 = 0 \quad \text{with} \quad p_4 = -p_1 - p_2 - p_3. \tag{4.1}$$

To shorten the expressions, we use

$$
\begin{aligned}
p_i + p_j + p_k &\equiv p_{ijk}, \\
\nu_i + \nu_j + \nu_k + \nu_l &\equiv \nu_{ijkl}, \\
(p_i + p_j)^2 &= s_{ij}
\end{aligned}
$$

and to facilitate the manipulation of relations between integrals with different powers of propagators, we use a notation to represent the raising and lowering in the powers of the propagators (as we did on section 3.3.1.1), so that

$$
\begin{aligned}
\mathbf{i}^+ I^D[\nu_1, ..., \nu_i, ..., \nu_9] &= I^D[\nu_1, ..., \nu_i + 1, ..., \nu_9], \\
\mathbf{i}^- I^D[\nu_1, ..., \nu_i, ..., \nu_9] &= I^D[\nu_1, ..., \nu_i - 1, ..., \nu_9].
\end{aligned}
$$

4.1.1   Symbolic reduction for planar two-loop integrals

From the discussion on IBP in the previous chapter, we know that it led us to obtain a set of relations amongst integrals involving different powers of propagators. This was done by taking the total derivative with respect to either k^μ or ℓ^μ of the integrand that has been multiplied by any of the independent momenta of the system. This means taking

$$\int \frac{d^D k}{i\pi^{\frac{D}{2}}} \int \frac{d^D \ell}{i\pi^{\frac{D}{2}}} \frac{\partial}{\partial k_i^\mu} \left[\frac{(k_i + v)^\mu}{A_1^{\nu_1} A_2^{\nu_2} A_3^{\nu_3} A_4^{\nu_4} A_5^{\nu_5} A_6^{\nu_6} A_7^{\nu_7} A_8^{\nu_8} A_9^{\nu_9}} \right] \equiv 0. \tag{4.2}$$

where $k_i = k, \ell$ and the definitions of the propagators are those presented in section 3.1.1.

This will generate dot products in the numerator, but with the aid of eq.(3.33) we can write them as linear combinations of propagators so that we re-incorporate all the information to the integrand in terms of a change in the powers of the propagators. To clarify, let us fill in a couple of steps.

The derivation of the integrand will produce

$$\frac{\partial}{\partial k_i^\mu}\left[\frac{(k_i + v)^\mu}{A_1^{\nu_1}\cdots A_9^{\nu_9}}\right] = \frac{D}{A_1^{\nu_1}\cdots A_9^{\nu_9}} + (k_i + v)^\mu \frac{\partial}{\partial k_i^\mu}\left[\frac{1}{A_1^{\nu_1}\cdots A_9^{\nu_9}}\right]. \tag{4.3}$$

The loop derivative on the r.h.s of this equation will contain a sum of terms with the same structure

$$(k_i + v)^\mu \left(\frac{-2\nu_x A_x^\mu}{A_1^{\nu_1}\cdots A_x^{\nu_x+1}\cdots A_9^{\nu_9}}\right), \tag{4.4}$$

but since, in general

$$2(k_i + v)_\mu A_x^\mu = 2(k_i + v)\cdot(k_i + u) \;=\; (k_i + v)^2 + (k_i + u)^2 - (v - u)^2$$
$$= (k_i + v)^2 + A_x - (v - u)^2 \tag{4.5}$$

then

$$(k_i + v)^\mu \left(\frac{-2\nu_x A_x^\mu}{A_1^{\nu_1}\cdots A_x^{\nu_x+1}\cdots A_9^{\nu_9}}\right) \;=\; \frac{-\nu_x(k_i + v)^2 - \nu_x A_x + \nu_x(v - u)^2}{A_1^{\nu_1}\cdots A_x^{\nu_x+1}\cdots A_9^{\nu_9}}$$
$$= \left[-(k_i + v)^2\, \nu_x \mathbf{x}^+ - \nu_x \right.$$
$$\left. + (v - u)^2\, \nu_x \mathbf{x}^+ \right]\frac{1}{A_1^{\nu_1}\cdots A_x^{\nu_x}\cdots A_9^{\nu_9}}. \tag{4.6}$$

In this way, using the shorthand notation

$$I^D \equiv \int \frac{d^D k}{i\pi^{\frac{D}{2}}} \int \frac{d^D \ell}{i\pi^{\frac{D}{2}}} \left[\frac{1}{A_1^{\nu_1} A_2^{\nu_2} A_3^{\nu_3} A_4^{\nu_4} A_5^{\nu_5} A_6^{\nu_6} A_7^{\nu_7} A_8^{\nu_8} A_9^{\nu_9}}\right], \tag{4.7}$$

and taking the partial derivation to be with respect to $k_i^\mu = k^\mu, \ell^\mu$, we find the following two *general* expressions for the IBP symbolic reduction of planar two-loop integrals

$$(D - \nu_{1234} - \nu_9)I^D \;=\; \left[(k + v)^2 \mathbf{a}^+ - (\ell + v)^2 \nu_9 \mathbf{9}^+ \right.$$
$$- v^2 \nu_1 \mathbf{1}^+ - (v - p_1)^2 \nu_2 \mathbf{2}^+$$
$$\left. - (v - p_{12})^2 \nu_3 \mathbf{3}^+ - (v - p_{123})^2 \nu_4 \mathbf{4}^+ \right]I^D, \tag{4.8}$$

$$(D - \nu_{5678} - \nu_9)I^D \;=\; \left[(\ell + v)^2 \mathbf{b}^+ - (k + v)^2 \nu_9 \mathbf{9}^+ \right.$$
$$- v^2 \nu_5 \mathbf{5}^+ - (v - p_1)^2 \nu_6 \mathbf{6}^+$$
$$\left. - (v - p_{12})^2 \nu_7 \mathbf{7}^+ - (v - p_{123})^2 \nu_8 \mathbf{8}^+ \right]I^D. \tag{4.9}$$

All the propagators that belong to a particular loop, contribute to the derivative of the corresponding loop, so we introduced the following notation

$$\mathbf{a}^+ = \nu_1 1^+ + \nu_2 2^+ + \nu_3 3^+ + \nu_4 4^+ + \nu_9 9^+, \tag{4.10}$$

$$\mathbf{b}^+ = \nu_5 5^+ + \nu_6 6^+ + \nu_7 7^+ + \nu_8 8^+ + \nu_9 9^+, \tag{4.11}$$

$$\mathbf{c}^+ = -\nu_9 9^+, \tag{4.12}$$

since it groups the contribution coming from the propagators that belong to each loop and the contribution from the 9th propagator, which belongs to both.

If for loop i we choose v to be either 0, p_1, p_{12}, p_{123} or $-k_j$, we will generate a set of equations that will be a particular case of these previous ones.

For example, let us focus on eqs.(4.8) and (4.9) and take two cases on the values of v for both of them. We generate the following relations

- with $v = p_1$

$$(D - \nu_{1234} - \nu_9)I^D = \left[(k + p_1)^2 \mathbf{a}^+ - (\ell + p_1)^2 \nu_9 9^+ - s_{23} \, \nu_4 4^+ \right] I^D, \tag{4.13}$$

$$(D - \nu_{5678} - \nu_9)I^D = \left[(\ell + p_1)^2 \mathbf{b}^+ - (k + p_1)^2 \nu_9 9^+ - s_{23} \, \nu_8 8^+ \right] I^D. \tag{4.14}$$

- with $v = -\ell$

$$(D - \nu_{1234} - \nu_9)I^D = \left[(k - \ell)^2 \mathbf{a}^+ - \ell^2 \nu_1 1^+ - (\ell + p_1)^2 \nu_2 2^+ \right.$$
$$\left. - (\ell + p_{12})^2 \nu_3 3^+ - (\ell + p_{123})^2 \nu_4 4^+ \right] I^D, \tag{4.15}$$

$$(D - \nu_{5678} - \nu_9)I^D = -\left[(k - \ell)^2 \nu_9 9^+ + \ell^2 \nu_5 5^+ + (\ell + p_1)^2 \nu_6 6^+ \right.$$
$$\left. + (\ell + p_{12})^2 \nu_7 7^+ + (\ell + p_{123})^2 \nu_8 8^+ \right] I^D. \tag{4.16}$$

As it stands, this system of equations is potentially helpful. Depending on the propagators of the integral I^D we apply it upon, we may get relations that can help us reduce the integral. This is because we have written the system of equations is such a way that on the left hand side is the original integral multiplied by some constant $(D - \nu_{1234} - \nu_9,$ for example) and on the right hand side we have modifications on the same integral. These modifications can result in an easier integral, but they can also lead to irreducible numerators.

As we know, we have an IN when one of the momentum factors in the numerator does not cancel against one in the denominator. This can be addressed by taking linear combinations of the equations that contain these factors.

In the two particular cases taken above, if $(\ell + p_1)^2$ does not occur as a propagator in the denominator of integral I^D, then we have problems with eqs.(4.13 - 4.16), since they all contain this factor in some term. Having IN in all these equations makes them useless, in a sense, because we would be exchanging an integral with extra powers on the propagators (say) with an integral with IN. We would not be solving the problem. Finding a way to eliminate them and still have a useful identity, would be ideal.

Let us concentrate on equations (4.13) and (4.15). If we apply the rising operator $\nu_2 2^+$ on eq.(4.13) and the operator $\nu_9 9^+$ on eq.(4.15), we can eliminate the terms that contain $(\ell + p_1)^2$, by taking the difference of the modified equations.

The new relation arising from this operation, may now be of use for integrals that do not have $(\ell + p_1)^2$ in the denominator. This amounts to applying the integration by parts identities to the following integrand

$$\frac{\nu_2\,(k + p_1)^\mu}{A_1^{\nu_1} A_2^{\nu_2+1} A_3^{\nu_3} A_4^{\nu_4} A_5^{\nu_5} A_6^{\nu_6} A_7^{\nu_7} A_8^{\nu_8} A_9^{\nu_9}} - \frac{\nu_9\,(k - \ell)^\mu}{A_1^{\nu_1} A_2^{\nu_2} A_3^{\nu_3} A_4^{\nu_4} A_5^{\nu_5} A_6^{\nu_6} A_7^{\nu_7} A_8^{\nu_8} A_9^{\nu_9+1}}, \qquad (4.17)$$

which has the effect of producing identities that are linear combinations of the 10 identities we had before.

There's also another way of viewing this. It follows from the scaling of the external momenta in the loop integral. If we do $p \to \lambda p$ in an arbitrary integral, then

$$I^D(\lambda p) = \lambda^{2(D-N)} I^D(p), \qquad (4.18)$$

where N is the sum of the powers of the propagators involved in the integral. If we differentiate with respect to λ in both sides and then take $\lambda = 1$, we have

$$I^D(p) = \frac{1}{2(D-N)} \left[\frac{\partial}{\partial \lambda} I^D(\lambda p) \right]_{\lambda=1}.$$

What this expression means is that instead of having a term like

$$[k \cdot (k + p)]\, \nu_i i^+,$$

that would come from IBP (since we differentiate with respect to the loop momenta), it produces terms such as

$$[p \cdot (k + p)]\, \nu_i i^+,$$

since we differentiate with respect to λ that always brings out factors of external momenta. These terms can in turn be written as

$$\left[(k + p - k) \cdot (k + p) \right] \nu_i \mathbf{i}^+ = (k + p)^2 \nu_i \mathbf{i}^+ - k \cdot (k + p) \nu_i \mathbf{i}^+,$$

which is equivalent to a combination of two terms coming from IBP identities, just like in eq.(4.17). So we can see that the scaling saves us a bit of work when we are trying to get an expression free of irreducible numerators since it can produce a combination of IBP identities without us having to look for it. Still, this scheme depends on the cancellation of terms between numerator and denominator, and some relations are not IN free.

The way we generate expressions that contain irreducible numerators, depends on which propagators are present in the integral we use as the starting point. If the integral has propagators $\nu_1, ..., \nu_i$ missing, then the presence of the operators $\mathbf{1}^-, ..., \mathbf{i}^-$ in the IBP identities, indicates a reduction in the powers of precisely the missing propagators.

We then must find a way to combine the identities for a particular topology to assemble an algorithm that relates the integrals of this topology to integrals of simpler topology. If this is not possible, a relation to integrals of the same topology but with less powers on propagators and simpler integrals is also good.

This has already been done for all the MI we use in our algorithm [64, 10, 53, 54]. In fact, we already saw in section 3.3.1.1, how a *Pentabox* has a complete reduction in terms of triangles.

The derivation of these symbolic reduction formulae requires a lot of ingenuity and its disadvantage is that it is based on the direct inspection of the explicit form of the IBP identities for each topology. Nevertheless, it provides a useful insight into the symmetries and shortcuts we might have for different topologies, so let us look at an example of this symbolic manipulation [54, 53].

4.1.1.1   Symbolic IBP reduction of the Planar Double Box

The planar double box integral that arises from the general diagram of fig.(3.2) when pinching propagators 4 and 6 is the one shown in fig.(3.4). In terms of the integral that it represents, we have

$$I^D[\nu_1, \nu_2, \nu_3, 0, \nu_5, 0, \nu_7, \nu_8, \nu_9] = \int \frac{d^D k}{i\pi^{\frac{D}{2}}} \int \frac{d^D \ell}{i\pi^{\frac{D}{2}}} \frac{1}{A_1^{\nu_1} A_2^{\nu_2} A_3^{\nu_3} A_5^{\nu_5} A_7^{\nu_7} A_8^{\nu_8} A_9^{\nu_9}}, \qquad (4.19)$$

where the A_i's are the propagators as defined in section 3.1.1.

When we do integration by parts with all possible momenta in the numerator and with respect to both k and ℓ, we get 10 relations. Of these relations, the following are free of irreducible numerators:

$$s_{12}\,\nu_1 1^+ I^D = -(D - \nu_1 - \nu_2 - 2\nu_3 - \nu_9)I^D$$

$$+ \left[(\nu_1 1^+ + \nu_2 2^+)3^- + \nu_9 9^+(3^- - 7^-)\right]I^D, \qquad (4.20)$$

$$s_{12}\,\nu_3 3^+ I^D = -(D - 2\nu_1 - \nu_2 - \nu_3 - \nu_9)I^D$$

$$+ \left[(\nu_2 2^+ + \nu_3 3^+)1^- + \nu_9 9^+(1^- - 5^-)\right]I^D, \qquad (4.21)$$

$$s_{12}\,\nu_5 5^+ I^D = -(D - \nu_5 - 2\nu_7 - \nu_8 - \nu_9)I^D$$

$$+ \left[(\nu_5 5^+ + \nu_8 8^+)7^- + \nu_9 9^+(7^- - 3^-)\right]I^D, \qquad (4.22)$$

$$s_{12}\,\nu_7 7^+ I^D = -(D - 2\nu_5 - \nu_7 - \nu_8 - \nu_9)I^D$$

$$+ \left[(\nu_7 7^+ + \nu_8 8^+)5^- + \nu_9 9^+(5^- - 1^-)\right]I^D. \qquad (4.23)$$

Note also that these relations are symmetric in the propagators 1, 3, 5 and 7, which reflects the symmetry of the topology itself.

The remaining six relations that do contain irreducible numerators, are combined (in the same way as we did in the previous section) to get rid of these. We get two sets of symmetric relations (in propagators 2 and 8)

$$(D - 2 - \nu_1 - 2\nu_2 - \nu_3)\nu_2 2^+ I^D = (D - 2 - \nu_1 - \nu_3 - 2\nu_9)\nu_9 9^+ I^D$$

$$+ (\nu_2 - \nu_9)(\nu_1 1^+ + \nu_3 3^+)I^D$$

$$+ \left[\nu_1 1^+ \nu_9 9^+ 5^- + \nu_3 3^+ \nu_9 9^+ 7^-\right]I^D, \quad (4.24)$$

$$(D - 2 - \nu_5 - \nu_7 - 2\nu_8)\nu_8 8^+ I^D = (D - 2 - \nu_5 - \nu_7 - 2\nu_9)\nu_9 9^+ I^D$$

$$+ (\nu_8 - \nu_9)(\nu_5 5^+ + \nu_7 7^+)I^D$$

$$+ \left[\nu_5 5^+ \nu_9 9^+ 1^- + \nu_7 7^+ \nu_9 9^+ 3^-\right]I^D, \quad (4.25)$$

and

$$s_{23}\,\nu_8 8^+ \nu_9 9^+ I^D = -(D - 2 - \nu_5 - \nu_7 - \nu_8 - \nu_9)\nu_9 9^+ I^D$$

$$- (D - 1 - \nu_1 - \nu_2 - \nu_3 - \nu_9)(\nu_5 5^+ + \nu_7 7^+ + \nu_8 8^+ + \nu_9 9^+)I^D$$

$$+ (\mathbf{a}^+ \mathbf{b}^+ - \mathbf{c}^+ \mathbf{c}^+)2^- I^D, \qquad (4.26)$$

$$s_{23}\,\nu_2 2^+ \nu_9 9^+ I^D = -(D - 2 - \nu_1 - \nu_2 - \nu_3 - \nu_9)\nu_9 9^+ I^D$$

$$- (D - 1 - \nu_5 - \nu_7 - \nu_8 - \nu_9)(\nu_1 1^+ + \nu_2 2^+ + \nu_3 3^+ + \nu_9 9^+)I^D$$

$$+ (\mathbf{a}^+ \mathbf{b}^+ - \mathbf{c}^+ \mathbf{c}^+)8^- I^D, \qquad (4.27)$$

We can use eqs.(4.20 - 4.23) to reduce to unity the powers of propagators 1, 3, 5 and 7. Once this is done, we can use eqs.(4.24) and (4.25) to reduce to unity the powers of propagators 2 and 8.

So far all propagators but the 9th, can be manipulated to have unit powers. We can find a relation that can reduce the power of propagator 9 if we combine eqs.(4.25) and (4.26).

If we substitute the value of $\nu_8 8^+ I^D$ given by eq.(4.25) in the left and right hand side of eq.(4.26) we get

$$
\begin{aligned}
0 \;=\; & s_{23} \left[(D - 2 - \nu_5 - \nu_7 - 2\nu_9) + \nu_5 5^+ 1^- + \nu_7 7^+ 3^- \right] \nu_9 (\nu_9 + 1) 9^{++} I^D \\
& \left[s_{23} \, (\nu_8 - \nu_9)(5^+ + 7^+) \right. \\
& + (D - 1 - \nu_1 - \nu_2 - \nu_3 - \nu_9)(\nu_5 5^+ 1^- + \nu_7 7^+ 3^-) \\
& + (D - 2 - \nu_5 - \nu_7 - 2\nu_8)(D - 2 - \nu_5 - \nu_7 - \nu_8 - \nu_9) \\
& + (D - 2 - \nu_5 - \nu_7 - 2\nu_8)(D - 1 - \nu_1 - \nu_2 - \nu_3 - \nu_9) \\
& \left. + (D - 1 - \nu_1 - \nu_2 - \nu_3 - \nu_9)(D - 2 - \nu_5 - \nu_7 - 2\nu_9) \right] \nu_9 9^+ I^D \\
& + (D - 1 - \nu_1 - \nu_2 - \nu_3 - \nu_9)(D - 2 - \nu_5 - \nu_7 - \nu_8 - \nu_9)(5^+ + 7^+) I^D \\
& - (D - 2 - \nu_5 - \nu_7 - 2\nu_8)(\mathbf{a}^+ \mathbf{b}^+ - \mathbf{c}^+ \mathbf{c}^+) 2^- I^D .
\end{aligned}
\tag{4.28}
$$

Now, since this equation is going to be used when all but the 9th propagator have powers of one, we can shorten it. Furthermore, we can substitute the values of $\nu_5 5^+$ and $\nu_7 7^+$ given by eqs.(4.22) and (4.23), in the terms appearing as $(5^+ + 7^+)$, to have

$$
\begin{aligned}
0 \;=\; & s_{23} \left[(D - 4 - 2\nu_9) + 5^+ 1^- + 7^+ 3^- \right] \nu_9 (\nu_9 + 1) 9^{++} I^D \\
& \left[-\frac{s_{23}}{s_{12}} (1 - \nu_9)(2D - 8 - 2\nu_9) \right. \\
& + \frac{s_{23}}{s_{12}} (1 - \nu_9) \left((5^+ + 8^+)7^- + (7^+ + 8^+)5^- \right) \\
& + \frac{s_{23}}{s_{12}} (1 - \nu_9)(5^- + 7^- - 1^- - 3^-)\nu_9 9^+ \\
& + (D - 4 - \nu_9)(5^+ 1^- + 7^+ 3^-) \\
& + (D - 6)(D - 5 - \nu_9) \\
& + (D - 6)(D - 4 - \nu_9) \\
& \left. + (D - 4 - \nu_9)(D - 4 - 2\nu_9) \right] \nu_9 9^+ I^D \\
& - \frac{1}{s_{12}} (D - 4 - \nu_9)(D - 5 - \nu_9)(2D - 8 - 2\nu_9) I^D \\
& + \frac{1}{s_{12}} (D - 4 - \nu_9)(D - 5 - \nu_9) \left((5^+ + 8^+)7^- + (7^+ + 8^+)5^- \right) I^D
\end{aligned}
$$

$$+\frac{1}{s_{12}}\,(D-4-\nu_9)(D-5-\nu_9)(5^- + 7^- - 1^- - 3^-)9^+ I^D$$
$$-(D-6)(\mathbf{a}^+\mathbf{b}^+ - \mathbf{c}^+\mathbf{c}^+)2^- I^D. \tag{4.29}$$

But, we can also take advantage of the symmetry properties inherent to the integral. When the powers of the propagators are one, pinching with $\mathbf{1}^-$ is the same as pinching with $\mathbf{3}^-$ and the analogous happens with the symmetric side of the box (propagators 5 and 7). So in the end we can do $\mathbf{5}^+\mathbf{1}^- = \mathbf{7}^+\mathbf{3}^-$ in the equation above. Rearranging the terms we have
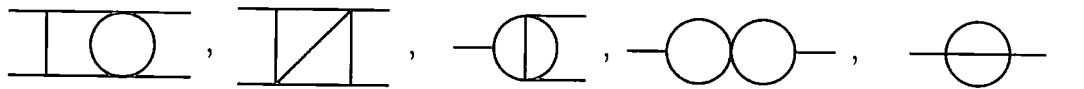
$$s_{23}\,\left[(D-4-2\nu_9) + 2\,\mathbf{5}^+\mathbf{1}^-\right]\nu_9(\nu_9+1)9^{++}I^D \;=$$
$$= \left[\frac{2s_{23}}{s_{12}}\,(1-\nu_9)(D-4-\nu_9) - \frac{2s_{23}}{s_{12}}\,(1-\nu_9)(5^+ + 8^+)7^-\right.$$
$$\left.-2(D-4-\nu_9)5^+1^- - (D-5-\nu_9)(3D-14-2\nu_9)\right]\nu_9 9^+ I^D$$
$$+\frac{2}{s_{12}}\,(D-4-\nu_9)^2(D-5-\nu_9)I^D$$
$$-\frac{1}{s_{12}}\,(D-4-\nu_9)(D-5-\nu_9)(5^+ + 8^+)7^- I^D$$
$$+(D-6)(\mathbf{a}^+\mathbf{b}^+ - \mathbf{c}^+\mathbf{c}^+)2^- I^D, \tag{4.30}$$

which is valid only when all powers of the propagators (except the 9th) are one. This identity provides a reduction of the power on propagator 9, but it can only reduce it to the values of 1 or 2 (depending of whether the initial integral has an odd or even value of ν_9). The two integrals at which we arrive are

$$\text{PBOX1} \equiv \quad \text{} \quad = \quad I^D[1,1,1,0,1,0,1,1,1] \tag{4.31}$$

$$\text{} \quad = \quad I^D[1,1,1,0,1,0,1,1,2]. \tag{4.32}$$

As can be seen by the pinching operators in eq.(4.30), the reduction not only produces these two box integrals, but also pinched integrals, such as

$$\text{} \tag{4.33}$$

which are described in table 3.2.

4.1.2 Symbolic reduction for non-planar two-loop integrals

The general symbolic reduction of non-planar two-loop integrals is highly non-trivial (in fact, it can only be achieved with the identities produced from both integration by parts

and Lorentz Invariance conditions). It was finally conceived and presented in ref.[10]. The way to obtain the IBP and LI identities is the same as that explained in the previous sections. The difference is that there is a more complicated way to combine these identities to be able to get a reduction algorithm.

In the end, the identities obtained provide a complete reduction of all topologies in terms of simpler topologies and integrals of the same topology. They found that the pattern is repeated; they also needed two crossed boxes as master integrals for the non-planar double box topology. We represent them as

$$\text{XBOX1} \equiv \qquad = \quad I^D[1,1,1,0,0,0,1,1,1,1] \qquad (4.34)$$

$$\qquad = \quad I^D[1,2,1,0,0,0,1,1,1,1]. \qquad (4.35)$$

Similar to the planar case, the reduction of the non-planar double box not only produces these two box integrals, but also pinched integrals, such as

$$\qquad (4.36)$$

and the planar pinchings shown in eq.(4.33), which are all described in tables (3.2) and (3.3).

4.2 Automatic reduction of loop integrals

So far we have dealt with IN in the past by expressing them in terms of a combination of tensors that are themselves related to integrals with very high powers on the propagators and also extra dimensions (see section 3.4). This generates the need to devise a mechanism to diminish the dimensions on top of the already existing need of reducing the powers of propagators.

This is because the basis of integrals which spans, through linear combinations, every possible integral (with and without IN) does not contain an integral with IN. So instead of having a reduction that encodes the information using IN, we have to encode the same information but using extra powers of propagators and extra dimensions.

This sole fact makes a huge difference in the amount of computing work before us when calculating integrals with up to 4 IN (or tensors). In fact it amounts to having integrals with up to 8 extra powers on the propagators and up to 4 shifts of the dimension. Since

we are contemplating the calculation of hundreds of integrals, having the IN as another form of encapsulating information on extra powers and dimensions, is rather appealing [63, 65].

Consider the following general structure of scalar two-loop integrals:

$$I(p_1, ..., p_n) = \int \frac{d^D k}{i\pi^{\frac{D}{2}}} \int \frac{d^D \ell}{i\pi^{\frac{D}{2}}} \frac{1}{A_1^{\nu_1} ... A_t^{\nu_t}},$$

where the A_i are massless scalar propagators that depend on the internal $k_i = k, \ell$ and external $p_1, ..., p_n$ momenta of the system. We choose to describe it using the following three positive parameters

$$r = \sum_i \nu_i \quad \forall \quad \nu_i \geq 1 \quad : \quad \text{dimension of denominator} \tag{4.37}$$

$$s = - \sum_i \nu_i \quad \forall \quad \nu_i \leq 0 \quad : \quad \text{dimension of numerator} \tag{4.38}$$

$$t \qquad \quad : \quad \text{number of propagators} \tag{4.39}$$

The topology of the integral is uniquely determined by the way the propagators and the external legs are interconnected and this is specified by the t parameter representing the set $\{A_1, ..., A_t\}$ of different propagators in the graph.

The specification of the integral is completed when we assign values to the positive and negative powers ν_i of the propagators, making them become part of the denominator and numerator, respectively. Therefore, integrals of a particular topology t with dimensions s of the numerator and r of the denominator, belong to a particular class of integrals $I_{r,s,t}$.

Now, as noted before, any of these integrals will depend on the external momenta and on the loop momenta. At two loops we can combine the loop momenta k and ℓ and the three external momenta, to form 9 different scalar products involving k or ℓ. Knowing that the propagators are linear combinations of scalar products, i.e.

$$A = (k + p)^2 = k^2 + 2\, k \cdot p + p^2, \tag{4.40}$$

only $9 - t$ different scalar products in the numerator of an integral with t propagators can give rise to irreducible numerators.

The number of different four-point integrals of a given topology t and a particular dimension of the numerator s and the denominator r, can be calculated with combinatorics. It is simple but is presented here for completion.

It is useful to recall from eq.(4.37) the definition of the parameter r. This has been done considering all powers of propagators bigger than 0. If we want to compute all the possible denominators of the integrals we can come upon when calculating matrix elements, we also have to consider the appearance of master integrals ($\nu_i = 1$). In that case, the sum of the powers of propagators will be

$$\sum_{i=1}^{t} \nu_i = r - t \quad \forall \quad \nu_i \geq 0 \tag{4.41}$$

Now, consider the number of combinations of n different objects, taken k at a time with their subsequent replacement. This is the same as the number of sets that can be made up of k objects chosen from the given n objects, each being used as often as desired,

$$C_k^n = \begin{pmatrix} n + k - 1 \\ k \end{pmatrix}. \tag{4.42}$$

Then the number of different $I_{r,s,t}$ is

$$
\mathcal{N}(I_{r,s,t}) = \boxed{\begin{array}{c} combinations \\ of\ different \\ numerators \end{array}} \times \boxed{\begin{array}{c} combinations \\ of\ different \\ denominators \end{array}}
$$

$$
= C_s^{9-t} \times C_{r-t}^{t}
$$

$$
= \begin{pmatrix} 8 - t + s \\ s \end{pmatrix} \times \begin{pmatrix} r - 1 \\ r - t \end{pmatrix} \tag{4.43}
$$

For a given topology, the number of integrals increases quickly as r and s become larger. We can see that for the case of the double box topology ($t = 7$), where we will have

$$\mathcal{N}(I_{r,s,t}) = \frac{1}{720} \frac{(1 + s)! \, (r - 1)!}{s! \, (r - 7)!}, \tag{4.44}$$

which, as can be seen in fig.(4.1) and table (4.1), reaches hundreds of integrals with only a few extra powers on propagators and irreducible numerators.

This is not so good, but, as we saw in the previous chapter, they are related among themselves by IBP and LI identities. For each value of r and s we can get 10 IBP and 3 LI identities. The identities applied to a *seed* integral $I_{r,s,t}$ will contain integrals of the type shown in fig.(4.2)

The loop integrals that arise in the calculation of $2 \rightarrow 2$ parton scattering are integrals of different topologies ($2 < t \leq 7$) that involve at the most 4 irreducible numerators ($s = 4$) and sometimes extra powers in the propagators ($r > t$).
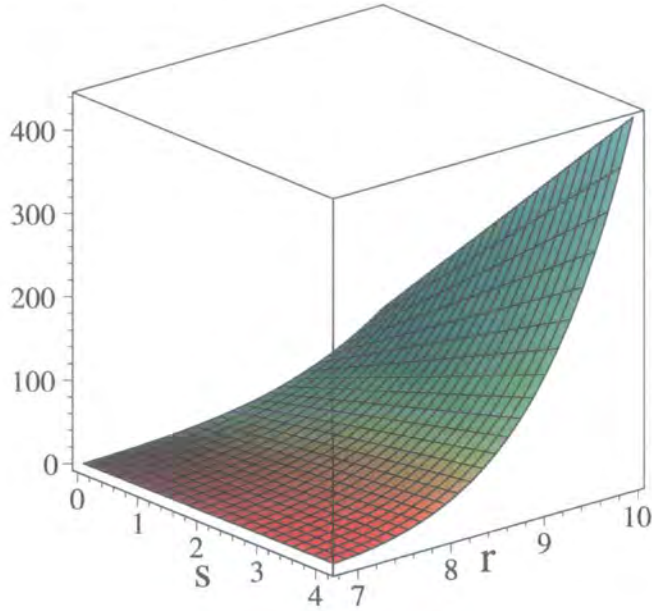
Figure 4.1: Growth of $\mathcal{N}(I_{r,s,t})$ for $t = 7$ and with increasing r and s

r \ s	0	1	2	3	4
7	1	1+1	3	4	5
8	1+6	14	21	28	35
9	28	56	84	112	140
10	84	168	252	336	420

Table 4.1: Number of different $I_{r,s,t}$
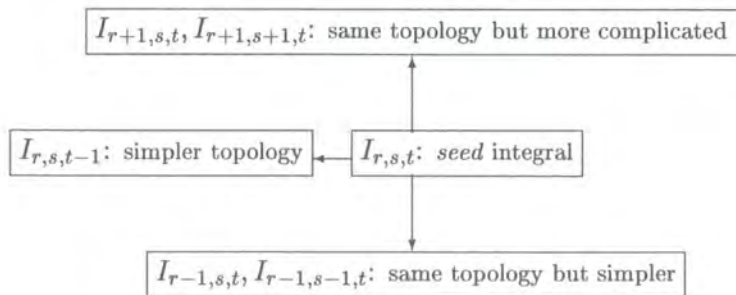
Figure 4.2: Integrals that result from the IBP and LI identities of a *seed* integral

It is therefore desirable to have an algorithm that can be used to solve IBP and LI identities for integrals of any topology but with fixed powers of propagators and irreducible numerators. So the idea is to have a collection of identities with the description given above and use them to obtain an algorithm for the reduction of complex integrals (i.e. $I_{r+1,s+1,t}$) in terms of the *seed* integral and simpler integrals (i.e. *pinchings* and known integrals).

In fig.(4.3) we have a schematic representation of the links between different integrals that belong to a system of identities generated by a particular *seed*. One of the *seed* integrals (labelled (r, s, t)) will be able to generate identities involving five types of integrals (shown in black dots). If we add to this group of identities, the system of identities generated by the next *seed* up (labelled $(r, s + 1, t)$), we will find more equations relating the same kinds of integrals (which are the dots in common between the two groups of *seed* links).
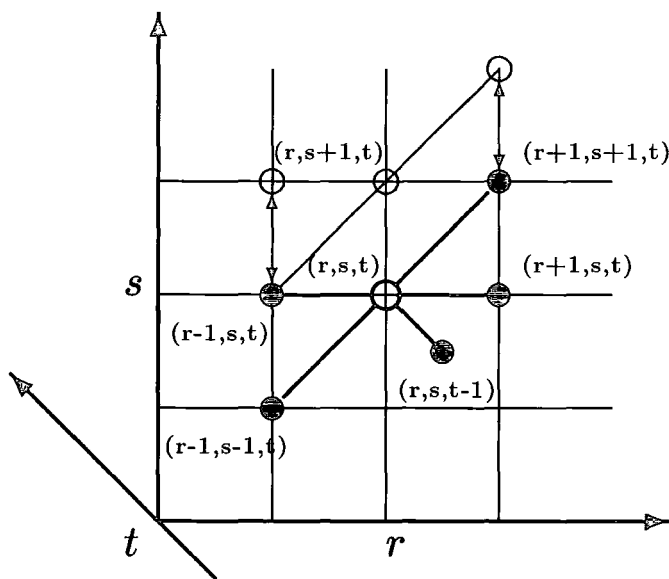
Figure 4.3: Links between systems of identities generated by different *seed* integrals

As a direct consequence of this, we can consider the set of all possible equations of a given topology t, generated by taking high enough values of r and s. We will have an over constrained system of equations that can be used for expressing the more complicated integrals, with greater values of r and s in terms of simpler ones.

We can find the values $\hat{r}$ and $\hat{s}$, for r and s, necessary to have a satisfactory reduction for our unknown integrals. Recall that the number of accumulated equations that will be

generated by using these values will be

$$(\mathcal{N}_{\text{IBP}} + \mathcal{N}_{\text{LI}}) \times \sum_{r=t}^{\hat{r}} \sum_{s=0}^{\hat{s}} \mathcal{N}_{r,s,t} = 13 \sum_{r=t}^{\hat{r}} \sum_{s=0}^{\hat{s}} \mathcal{N}_{r,s,t}. \tag{4.45}$$

To check if the number of equations is enough for the actual number of unknowns, we can compare it with the number of accumulated unknown integrals that are involved in the over constrained system, but removing the master integrals of the topology, which effectively means

$$\mathcal{N}(I_{r \leq \hat{r}+1, \ s \leq \hat{s}+1, \ t}) - I_{r=t,1,t} - I_{r=t,0,t}. \tag{4.46}$$

To clarify, we take on the following example. In table (4.2) we show the number of equations and unknowns for a topology with 7 propagators ($t = 7$). The squares given by $(\hat{r}, \hat{s}) = (7, 2), (8, 1)$ and $(9, 0)$ are the minimal values that can be used for a satisfactory reduction of the system.

r \ s	0	1	2	3
7	13	39	78	130
	22	45	76	115
8	104	312	624	1040
	106	213	354	535
9	468	1404	2808	4680
	358	717	1196	1795

Table 4.2: Accumulated equations (upper number) exceeding the number of accumulated unknowns (lower number) as r and s increase. Reduction of the system is achieved by choosing at least one of the couples $(\hat{r}, \hat{s}) = (7, 2), (8, 1)$ or $(9, 0)$

The fact that the system is over constrained can be helpful in some topologies, because it may lead to a complete reduction of the integrals under consideration, in terms of *pinched* and/or known integrals. What usually happens in topologies with $t > 4$ is that the system provides a reduction towards a small number (typically one or two) of integrals of the topology under consideration and integrals of simpler topology (*pinched* and known). The left over integrals are the master integrals (MI) of the particular topology and in principle we are free to choose them *a priori*, as long as they are independent from each other.

It is worth mentioning that the procedure described above is not the only way to attack the problem of reducing tensor integrals to doable scalar integrals. Nevertheless, by using a particular set of master integrals as a basis to generate all unknown integrals and combining with the automatic reduction, we were able to calculate all integrals needed for the parton processes we studied. This is no trivial task and in fact, we were able to customise our algorithm so as to have the possibility to calculate even higher numbers of irreducible numerators than the ones needed (the limitation always being computer power).

In the next section we will specify the nature of the actual algorithm we use and the extra software used to generate the Feynman diagrams contributing to the QCD parton processes. But before that, we must discuss how are we going to choose the MI of our algorithm, paying special attention to the double boxes.

4.2.1 A more natural set of master integrals

A particular choice of master integrals for a topology can make a great deal of difference in terms of the amount of work that will be done in the reduction of a system. In fact, our decision to choose

$$
\begin{aligned}
r = 7, s = 0, t = 7 \\
r = 7, s = 1, t = 7 \\
r = 7, s = 0, t = 7 \\
r = 7, s = 1, t = 7
\end{aligned}
\qquad (4.47)
$$

as master integrals for the double and crossed boxes topologies, arose from the idea of reducing integrals with high irreducible numerators in terms of a basis of integrals that contained irreducible numerators themselves.

This proved to be crucial in our algorithm, since we could have an easier system reduction without damping it with a further reduction of very high powers of propagators and extra dimensions.

The only problem is that the reduction for the double boxes (see section 4.1), leads to double boxes that have an extra power in one of the propagators, instead of an irreducible
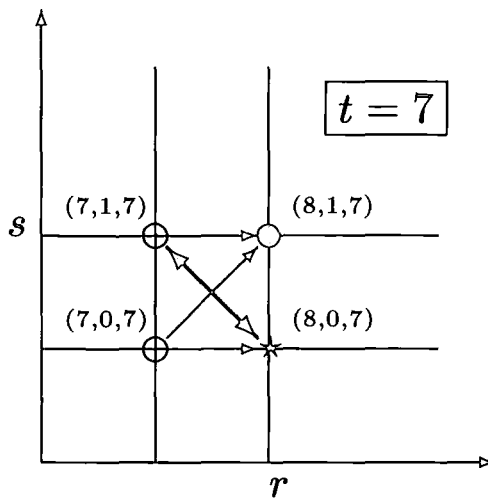
Figure 4.4: Links between the double box master integrals

numerator. So we must find a way to relate these two pairs, i.e.

$$
\text{(figure)} \longmapsto \text{(figure)} \quad \text{and} \quad \text{(figure)} \longmapsto \text{(figure)} . \tag{4.48}
$$

We can do this with the reduction algorithm we just studied in the last section. This is schematically represented in fig.(4.4). We apply our system of IBP and LI identities to two *seed* integrals (marked with $\oplus$) belonging to the topologies $(r, s, t) = (7, 0, 7), (7, 1, 7)$, which are precisely the two master integrals we want to use, as described in eq.(4.47).

The *seed* integral belonging to the $(7, 0, 7)$ family will produce an integral of the same topology $(t = 7)$, no numerator $(s = 0)$ and an extra power in a propagator $(r = 8)$ (shown in the figure with a $\star$) which is the integral we have arising from our general reduction.

Then, the links between the integrals of eq.(4.48) exist through the family of unknown integrals belonging to $(r, s, t) = (8, 1, 7)$ which are of no interest to us. Nevertheless, we can use this fact and eliminate these last uninteresting integrals, in favour of a relation (represented in the figure as $\searrow$) between the integral with irreducible numerator, the one with all unit powers and no irreducible numerator, and the one with an extra power in a propagator together with some pinched integrals.

For the planar double boxes, we obtain the following relation

$$
\text{(figure)}(s, t) \;=\; -\frac{1}{2}\frac{(3D - 14)s}{D - 4}\,\text{(figure)}(s, t) - \frac{1}{2}\frac{(D - 6)st}{(D - 4)(D - 5)}\,\text{(figure)}(s, t)
$$

$$-3\frac{(s+t)}{s^2 t}\left[\frac{(7D^2 - 68D + 164)s + (3D - 14)(3D - 16)t}{(D-5)(D-6)}\right]\ \square\!\!\!\diagdown\!\!\!\square\ (s,t)$$

$$+24\frac{(D-3)}{(D-6)t}\ \square\!\!\!\bigcirc\ (s,t) - 4\frac{(D-3)^2(2D-9)}{(D-4)^2(D-5)s^2}\ \bigcirc\!\!\!\bigcirc\ (s)$$

$$+\frac{3}{2}\frac{(D-3)(3D-10)}{(D-4)^2(D-5)^2(D-6)s^2 t}\Big[(-11D^3 + 158D^2 - 754D + 1196)t$$

$$+8(D-4)(D-5)^2 s\Big]\ \bigcirc\!\!\!\!\diagdown\ (s) + 3\frac{(D-3)(3D-8)(3D-10)}{(D-4)^3(D-5)^2(D-6)s^3 t}$$

$$\times\left[(D-5)(7D^2 - 68D + 164)s + (23D^3 - 337D^2 + 1640D - 2652)t\right]\ \bigcirc\!\!\!-\ (s)$$

$$+3\frac{(D-3)(3D-8)(3D-10)}{(D-4)^3(D-5)^2(D-6)s^2 t^2}\Big[(16D^3 - 229D^2 + 1088D - 1716)s$$

$$+(D-5)(3D-14)(3D-16)t\Big]\ \bigcirc\!\!\!-\ (t), \tag{4.49}$$

whereas for the non-planar boxes we get

$$\boxed{\otimes\!\!\!\diagup}(s,t)\ =\ \frac{1}{s+2t}\Bigg\{\frac{1}{2}\frac{(3D-14)s + 2(2D-9)t}{(2D-9)}\ \square\!\!\!\diagup\!\!\!\diagup(s,t)$$

$$+\frac{1}{2}\frac{st(s+t)(D-6)}{(2D-9)(D-5)}\ \square\!\!\!\diagup\!\!\!\diagup(s,t) + \frac{1}{2}\frac{s(D-4)}{(D-5)}\ \diagdown\!\!\!\!\diagup\!\!\!\diagup(s)$$

$$+\frac{3(D-3)(3D-14)[2(D-5)s + (3D-16)t]}{(s+t)(D-4)(D-5)(2D-9)}\ \square\!\!\!\bigcirc\ (s,-s-t)$$

$$+\frac{3(D-3)[(-D^2 + 6D - 6)s + (D^2 - 14D + 44)t]}{t(D-4)(D-5)(2D-9)}\ \square\!\!\!\bigcirc\ (s,t)$$

$$+\frac{3}{2}\frac{t(3D-14)[2(D-5)s + (3D-16)t]}{s(s+t)(D-5)(2D-9)}\ \square\!\!\!\diagdown\!\!\!\square\ (s,-s-t)$$

$$-\frac{3}{2}\frac{(s+t)[(-D^2 + 6D - 6)s + (D^2 - 14D + 44)t]}{st(D-5)(2D-9)}\ \square\!\!\!\diagdown\!\!\!\square\ (s,t)$$

$$-3\frac{s^2(D-4)(3D-14)}{(s+t)t(D-6)(2D-9)}\ \square\!\!\!\diagdown\!\!\!\square\ (t,-s-t)$$

$$+\frac{3}{2}\frac{(D-3)(3D-8)(3D-10)}{st^2(s+t)(D-4)^3(D-5)^2(D-6)(2D-9)}$$

$$\times\Big[(-16D^4 + 291D^3 - 1972D^2 + 5898D - 6564)s^2$$

$$+(-9D^4 + 154D^3 - 962D^2 + 2574D - 2444)st$$

$$+(D-5)(D-6)(D^2 - 14D + 44)t^2\Big]\ \bigcirc\!\!\!-\ (t)$$

$$+\frac{3}{2}\frac{(D-3)(3D-8)(3D-10)}{s^2 t(s+t)(D-4)^3(D-5)^2(2D-9)}$$

$$\times \left[-(D-5)(D^2 - 6D + 6)s^2 + (5D^3 - 82D^2 + 444D - 794)st \right.$$

$$\left. +(9D^3 - 140D^2 + 724D - 1244)t^2 \right] \!-\!\bigcirc\!- (s)$$

$$-\frac{3}{2} \frac{(D-3)(3D-8)(3D-10)(3D-14)}{st(s+t)^2(D-4)^3(D-5)^2(D-6)(2D-9)}$$

$$\times \left[-2(D-4)(D-5)^2 s^2 + (5D^3 - 72D^2 + 346D - 556)st \right.$$

$$\left. +(D-5)(D-6)(3D-16)t^2 \right] \!-\!\bigcirc\!- (-s-t)$$

$$+\frac{3}{2} \frac{(D-3)(3D-10)}{st(s+t)(D-4)^2(D-5)(2D-9)} \left[(-D^2 + 6D - 6)s^2 \right.$$

$$\left. +2(D-5)(4D-21)st + 12(D-5)^2 t^2 \right] \!-\!\square\!(s) \tag{4.50}$$

Equations (4.49) and (4.50) provide the "bridge" between the two types of choices of master integrals. If the irreducible numerators are going to be dismantled into tensors and translated to extra powers of propagators and dimensions, it is more adequate to use the integrals with extra powers, as MI. But if we want to manipulate the irreducible numerators keeping them as scalars and using them on the same footing as any other integral, the best choice is to have MI that have irreducible numerators. For the algorithm we use and described at the beginning of this section, this is best.

4.2.1.1 The new choice of master integrals

There is just one problem about this particular choice. Looking at eq.(4.49), we can see that the coefficients in front of the two planar boxes are of order $1/\epsilon$. This is due to the fact that in the reduction of integrals with one IN it is necessary to reduce the dimension from at least $D = 6 - 2\epsilon$, down to $D = 4 - 2\epsilon$. All this conspires together to leave a factor of $D - 4$ in the denominator of the two MI. This implies that in order to calculate the *new* MI up to order ϵ, one must know the expansions of the *old* MI (r.h.s. of eq.(4.49)) to one order higher in ϵ than they are given in refs.[54, 53].

To solve this problem, we calculated the planar double box with an IN [55], using the MB method and checked our results in two different ways; we verified that the result satisfies a system of differential equations and then, we used these differential equations to obtain the old set of MI in $D = 6$ dimensions and compare with the numerical result.

We use the reduction algorithm presented at the beginning of this section to obtain a

set of differential equations. As a result of doing

$$\frac{\partial}{\partial t}\text{PBOX1}(s,t) = \frac{\partial}{\partial t}\ \boxed{\Box\Box}\,(s,t),$$

$$\frac{\partial}{\partial t}\text{PBOX2}(s,t) = \frac{\partial}{\partial t}\ \boxed{\otimes\Box\Box}\,(s,t),$$

we will effectively be producing integrals with extra powers on the propagators. To these integrals, we can apply our reduction algorithm to write them again as a linear combination of MI. The result is the following,

$$\frac{\partial}{\partial t}\ \boxed{\Box\Box}\,(s,t) = \frac{[(D-5)s-t]}{(s+t)t}\ \boxed{\Box\Box}\,(s,t) + \frac{(D-4)}{(s+t)t}\ \boxed{\otimes\Box\Box}\,(s,t)$$

$$-6\frac{(D-4)}{st^2}\ \boxed{\boxtimes}\,(s,t) + 12\frac{(D-3)}{(s+t)t^2}\ \boxed{\boxdot}\,(s,t)$$

$$+4\frac{(D-3)^2}{(D-4)s^2t(s+t)}\ \text{—}\!\infty\!\text{—}\,(s)$$

$$+3\frac{(D-3)(3D-10)(2s+t)}{(D-4)s^2t^2(s+t)}\ \text{—}\!\boxdot\,(s)$$

$$+6\frac{(D-3)(3D-8)(3D-10)(s-t)}{(D-4)^2s^3t^2(s+t)}\ \text{—}\!\ominus\!\text{—}\,(s)$$

$$+6\frac{(D-3)(3D-8)(3D-10)}{(D-4)^2st^3(s+t)}\ \text{—}\!\ominus\!\text{—}\,(t), \qquad (4.51)$$

$$\frac{\partial}{\partial t}\ \boxed{\otimes\Box\Box}\,(s,t) = -\frac{1}{2}\frac{(D-4)s}{(s+t)t}\ \boxed{\otimes\Box\Box}\,(s,t) + \frac{1}{2}\frac{(D-4)s}{(s+t)}\ \boxed{\Box\Box}\,(s,t)$$

$$-9\frac{(D-4)}{st}\ \boxed{\boxtimes}\,(s,t) + 12\frac{(D-3)}{(s+t)t}\ \boxed{\boxdot}\,(s,t)$$

$$+2\frac{(D-3)^2(s+2t)}{(D-4)s^2t(s+t)}\ \text{—}\!\infty\!\text{—}\,(s)$$

$$+\frac{15}{2}\frac{(D-3)(3D-10)}{(D-4)st(s+t)}\ \text{—}\!\boxdot\,(s)$$

$$+6\frac{(D-3)(3D-8)(3D-10)}{(D-4)^2s^2t(s+t)}\ \text{—}\!\ominus\!\text{—}\,(s)$$

$$+9\frac{(D-3)(3D-8)(3D-10)}{(D-4)^2st^2(s+t)}\ \text{—}\!\ominus\!\text{—}\,(t). \qquad (4.52)$$

Expanding eqs.(4.51) and (4.52) in ϵ and inserting the expressions for the pinched integrals and the double boxes $\boxed{\Box\Box}$ and $\boxed{\Box{\mid}\Box}$, we find that they are satisfied, when we used the result

$$\boxed{\otimes\Box\Box}\,(s,t) = \frac{\Gamma(1+\epsilon)^2}{s^2(-s)^{2\epsilon}}\left\{\frac{9}{4\epsilon^4} - \frac{2}{\epsilon^3}X - \frac{7\pi^2}{3\epsilon^2}\right.$$

$$+\frac{1}{\epsilon}\left[\frac{4}{3}X^3 + \frac{14}{3}\pi^2 X - 4(X^2 + \pi^2)Y + 8\mathrm{Li}_3(-x) - 8X\mathrm{Li}_2(-x) - 16\zeta(3)\right]$$

$$-\frac{4}{3}X^4 - \frac{13}{3}\pi^2 X^2 + \left(\frac{16}{3}X^3 + \frac{26}{3}\pi^2 X\right)Y - 5\left(X^2 + \pi^2\right)Y^2$$

$$+\left(6X^2 - 20XY - \frac{4}{3}\pi^2\right)\mathrm{Li}_2(-x) + (8X + 20Y)\,\mathrm{Li}_3(-x)$$

$$20\mathrm{S}_{2,2}(-x) - 20X\mathrm{S}_{1,2}(-x) - 28\mathrm{Li}_4(-x) + (28X - 20Y)\,\zeta(3) - \frac{7\pi^4}{45}\Bigg\}$$

$$(4.53)$$

obtained by MB method integration directly in the region where $s,t < 0$ (see Appendix B) and where

$$x = \frac{t}{s}, \quad X = \log(x), \quad Y = \log(1 + x).$$

This calculation provides the last ingredient we need for our matrix element calculation. We have now all the master integrals required for the reduction of any generic integral arising from this calculation. In the next section we summarise the information we have for the master integrals themselves and discuss other work that has been done related to them.

4.3   Master integrals

Here we briefly summarise the master integrals we will need and provide the references where more information can be found about them.

1. The MI for the one-loop topologies are provided in table (4.3) and their expansions are in Appendix B. Actually, the one loop box in six dimensions is related to the

Name	Diagram	References
BUB(s)	⊸◯⊸	eq.(B.3) and ref.[1]
Box$^6(s,t)$	⊐6⊏	eqs.(B.1),(B.2) and ref.[64, 63]

Table 4.3: One-Loop Master Integrals

box in four dimensions and the bubble as follows

$$\boxed{6}(s,t) \quad = \quad \frac{st}{2(D-3)(s+t)}\;\square(s,t)$$

$$+ \frac{2}{(D-4)(s+t)} \left[-\bigcirc\!\!-\ (s) +\ -\bigcirc\!\!-\ (t) \right] \qquad (4.54)$$

2. The MI for the two-loop topologies are provided in table (4.4) and their expansions are also in Appendix B.

Name	Diagram	References
SUNC(s)		eqs.(B.4), (B.4) and ref.[64, 63]
TRI(s)		eqs.(B.5),(B.5) and ref.[64, 63]
GLASS(s)		eqs.(B.6),(B.6) and ref.[64, 63]
XTRI(s)		eqs.(B.7),(B.7) and ref.[66, 10]
CBOX(s, t)		eqs.(B.8),(B.8) and ref.[64]
ABOX(s, t)		eqs.(B.9),(B.9) and ref.[64]
PBOX1(s, t)		eqs.(B.10),(B.10) and ref.[54, 53]
PBOX2(s, t)		eqs.(B.11),(B.11) and ref.[55]
XBOX1(s, t)		eqs.(B.12),(B.12) and ref.[10]
XBOX2(s, t)		eqs.(B.13),(B.13)

Table 4.4: Two-Loop Master Integrals

All these integrals have been calculated (in the references mentioned) by means of parametrisation and MB or NDIM methods. But they have also been calculated in other ways. Binoth and Heinrich [58], have found a way to strip the singularities off the integrals, and calculated the divergence-free integral numerically.

Gehrmann and Remiddi [63, 67] derive differential equations in the internal propagator masses or in the external momenta for the master integrals and solve these for appropriate boundary conditions. This has turned out to be a good method and they have also managed to calculate the master integrals with one mass in one external leg (which are needed for i.e. $\gamma^* \to q\bar{q}g$) [68, 69].

These methods provide alternative ways to the calculation of MI. But, even without them, we have calculated the missing links, compiled the necessary results and turned the problem we are interested in to a manageable task. Tables 4.3 and 4.4, comprise

the basis set of MI that are required for a NNLO matrix element calculation for $2 \rightarrow 2$ massless scattering and their analytic expansions in ϵ has been calculated and presented in Appendix B.

4.4   General algorithm for matrix element calculations

Based on this new choice of master integrals we can undertake the calculation of the matrix elements themselves. We devise a mechanism to do it but it requires several parallel steps. In this section we give a brief account of this procedure and provide the most relevant practical issues that arose. After all, practical issues represent the challenging problems to overcome when faced with big calculations and their associated dilemmas of optimisation.

To start, we use QGRAF [70] to produce the two-loop Feynman diagrams to construct the one- and two-loop amplitudes. We then project by tree-level or one-loop amplitudes and perform the summation over colours and spins.

The trace over the Dirac matrices is carried out in D dimensions using conventional dimensional regularisation. It is then straightforward to identify the scalar and tensor integrals present in the calculation. We replace them with combinations of the basis set of master integrals using the symbolic reduction of two-loop integrals described in section 4.2, based on IBP and LI identities. The final result is a combination of master integrals in $D = 4 - 2\epsilon$ for which the expansions around $\epsilon = 0$ are presented in Appendix B.

Let us now draw on a few details and give the complete picture of the algorithm in a clearer way, with the aid of fig.(4.5).

4.4.1   Generation of Feynman diagrams with QGRAF

QGRAF is a computer program that generates symbolic descriptions of Feynman diagrams in quantum field theories. The generated output is a list of diagrams whose description depends on the style file that accompanies the compilation but it is based in the combinatorial design of the program (STEP 1 on fig.(4.5)). This means that together with the description of the topology, it assigns a symmetry factor and the sign that follows from anti-commutation rules.

The description of the field theory model is done by specifying the propagators and the interaction vertices in an input file. Similarly, there is another input file where one describes the style with which the output will be made.

Due to the fact that QGRAF starts distributing momenta in a non-fixed manner
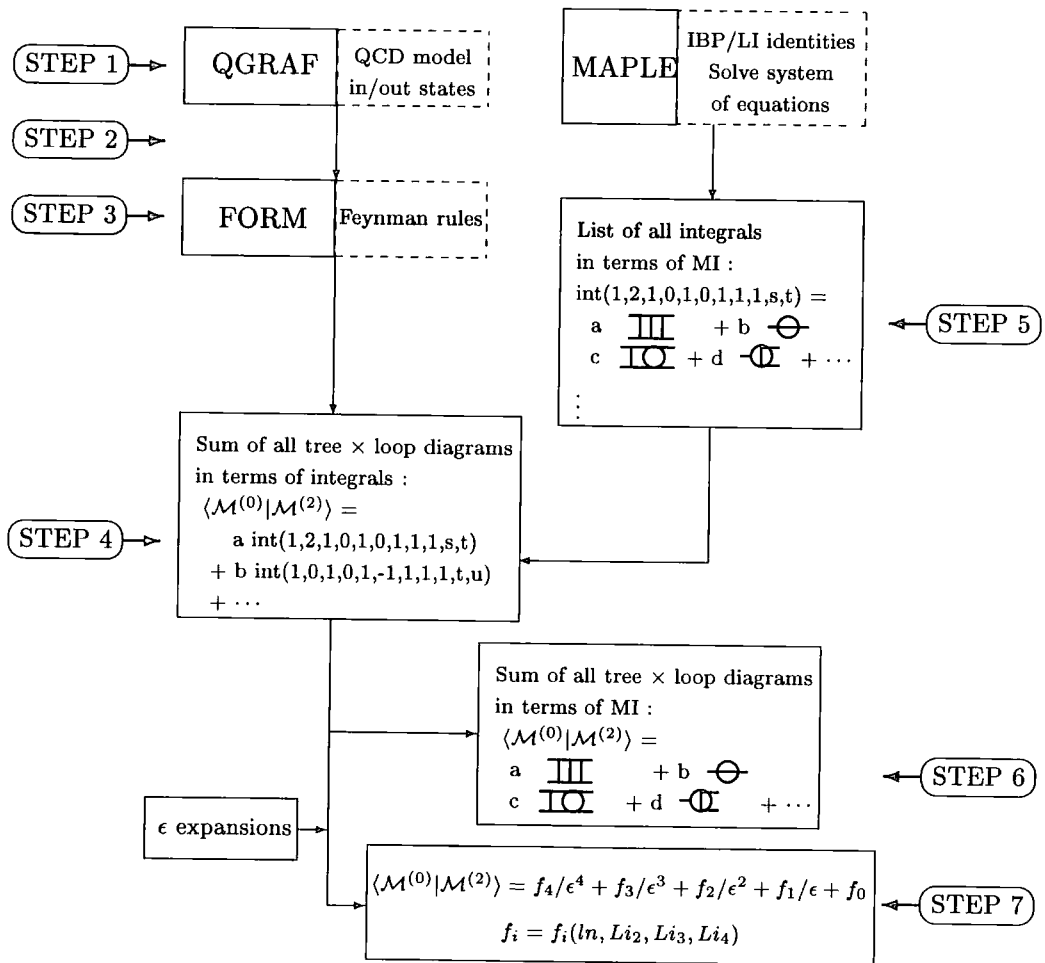
Figure 4.5: General algorithm to calculate matrix elements

(the s,t and u-channel version of the same graph, have different output descriptions), we needed to map all the information we have to a minimal set of topologies and carry any extra information as parameters of a minimal description. We designed a style for the description of the graphs that generated output we could use as input for MAPLE (STEP 2 on fig.(4.5)), where the mapping of the topologies was carried out.

Finally the specification for a particular process is done on yet another input file. Here one specifies the incoming and outgoing states of the process, the number of loops to be considered and extra options on the conditions of the external legs and tadpoles. Table 4.5 shows the number of Feynman diagrams that are generated by QGRAF in the processes that are of interest to us. Throughout, we have set the external legs to be free of self energy insertions and the graphs free of tadpoles.

QGRAF output				Actual Calculation	
Process	Tree	1-Loop	2-Loops	1-Loop × 1-Loop	2-Loops × Tree
$gg \to gg$	4	81	1771	6561	7084
$q\bar{q} \to gg$	3	30	595	900	1785
$q\bar{q} \to q\bar{q}$	2	18	316	324	632
$q_1\bar{q}_1 \to q_2\bar{q}_2$	1	10	189	100	189

Table 4.5: Number of Feynman diagrams generated by QGRAF. Also, number of terms involved in an the actual matrix element calculation

4.4.2 Performing the matrix element calculation with FORM

Once we have the set of diagrams for a particular process with a proper identification of the two-loop integral topology for each of them, we assemble the matrix element. This is done with a specifically designed FORM program (STEP 3 on fig.(4.5)).

In this program, each of the terms representing propagators and interaction vertices are assigned to their specific values, according to the Feynman rules. After performing the sums over colour and spin, we incorporate the information of extra (or less) powers of propagators into the basic integral and keep track of the additional information that may be generated after doing the trace over the Dirac matrices.

It should be noted that when summing over the gluon polarisations, we ensure that

the polarisations states are transversal (i.e. physical) by using an axial gauge

$$\sum_{\text{spins}} \epsilon_i^\mu \epsilon_i^{\nu *} = -g^{\mu\nu} + \frac{n_i^\mu p_i^\nu + n_i^\nu p_i^\mu}{n_i \cdot p_i} \tag{4.55}$$

where p_i is the momentum of gluon i and n_i is an arbitrary light-like 4-vector. For simplicity, we choose

$$\begin{aligned} n_1^\mu &= p_2^\mu, & n_2^\mu &= p_1^\mu \\ n_3^\mu &= p_4^\mu, & n_4^\mu &= p_3^\mu. \end{aligned}$$

At the end of this stage we have written the matrix elements in terms of hundreds of integrals of different topologies and with different amounts of powers in the propagators (STEP 4 on fig.(4.5)).

From the IBP reduction program that was described in section 4.1, we generated files for each topology, containing the expressions for all the integrals (within a range of powers of propagators and irreducible numerators) in terms of master integrals and simpler integrals (STEP 5 on fig.(4.5)). We feed this information to the result we have from FORM so far, and now we can express the matrix elements in terms of a linear combination of only a handful of master integrals (STEP 6 on fig.(4.5)).

The final input are the ϵ expansions for these master integrals. We finish the calculation with a result for the matrix elements that consists of a series in the parameter ϵ (STEP 7 on fig.(4.5)). The coefficients of this series are functions of the scales of the system and of the number of colours (for gluons) and flavours (for quarks). More precisely, they are sums of logarithms, polylogarithms and characteristic constants such as Riemann ζ function.

Chapter 5

Loop Amplitudes

In the last two chapters we have described how we constructed an algorithm that allows us to do a matrix element calculation for the virtual corrections to any $2 \to 2$ scattering of massless particles. The result of applying this algorithm to four partonic processes (and their crossed and time-reversed versions) shall be presented on Chapter 6.

This in itself is a tremendous amount of work and involves many different stages that can be checked within the calculation. Therefore it is desirable to have an independent way of verifying our results.

We will see that this is achieved at two levels. First, we can compare a subset of our results with the work presented by Bern, Dixon and Ghinculov in ref.[71]. Second, we can use the Catani formalism [72, 73] as a more general independent way of checking the singularity structure of our results.

In this Chapter we resume the discussion we had in Chapter 2 about the divergent behaviour of the matrix elements in a physical observable calculation. This time we want to touch upon these issues in a more general manner.

We want to discuss the possibility of isolating the divergent behaviour at the level of the loop amplitudes. We will briefly discuss the factorisation of collinear and soft singularities of an amplitude and how this allows their cancellation.

Then we will describe the Catani formalism and show how it can help us extract these singularities using (implicitly) the factorisation properties we just described. We finish by providing a concrete example to give an idea on how the last chapter will be presented and to illustrate the importance and limitations of this formalism.

5.1   Colour structure of QCD amplitudes

In previous chapters we have seen how we can expose and cancel the divergent behaviour in the calculation of infrared safe quantities. Now, we will discuss a procedure that makes the singularities easier to isolate, the decomposition of the matrix elements in terms of its colour factors.

In order to accomplish this, we need to separate each diagram involved in a QCD

amplitude into a term that contains the colour structure and another that is colour-less and contains all the kinematics. This allows us to regroup all the diagrams that contain the same colour structure into colour-less structures which we call *subamplitudes*. Each of these subamplitudes are gauge invariant and have important factorisation properties in the collinear and soft limits that can help us isolate the divergent behaviour of a Feynman amplitude.

Let us take an example to further what we mean. Consider the matrix-element for the tree level process $q\bar{q} \rightarrow gg$. The diagrams and their amplitudes, involved at this level of the calculation, are the ones shown in fig.(5.1). Each amplitude has been written in

$$\left(T^a T^b\right)_{ij} \mathcal{A}_1 \qquad \left(T^a T^b\right)_{ji} \mathcal{A}_2 \qquad i\,(T^c)_{ij}\,f^{abc}\,\mathcal{A}_3$$
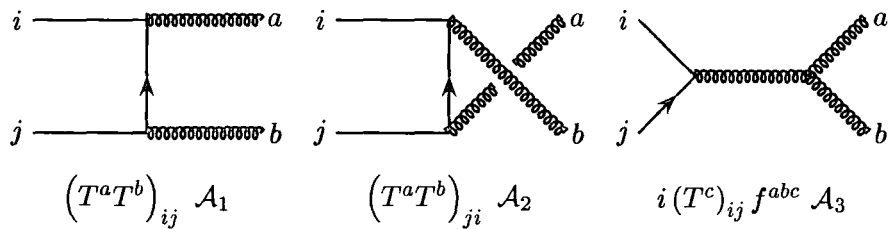
Figure 5.1: Tree-level diagrams for $q\bar{q} \rightarrow gg$

terms of a colour factor and a kinematical piece $\mathcal{A}_i$, $i = 1, 2, 3$.

Using eq.(1.4), the amplitude of the third diagram can also be written as a combination of terms, each term contributing to the first two. Then the total tree-level amplitude is
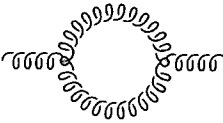
$$\mathcal{A}_{tot} = \left(T^a T^b\right)_{ij} [\mathcal{A}_1 + \mathcal{A}_3] + \left(T^b T^a\right)_{ij} [\mathcal{A}_2 - \mathcal{A}_3], \tag{5.1}$$

which is the *colour structure* for any process where these are the only coloured particles.
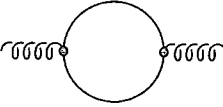
Now that we have decomposed the amplitude, we want to construct the squared matrix elements. To do this, we need a set of rules for the evaluation of colour factor products. More precisely, we need to know the Casimir colour charges of our theory and the Fierz identity which can reduce the amount of colour algebra.

5.1.1 Casimir colour charges

The diagrammatic representation of the three quadratic Casimir colour charges of SU(N) is given as follows

$$\rightarrow \quad (T^a)_{ik}(T^a)_{kj} = C_F \delta_{ij}, \tag{5.2}$$

$$\rightarrow \quad f^{acd}f^{bcd} = C_A\delta^{ab}, \tag{5.3}$$

$$\rightarrow \quad (T^a)_{ij}(T^b)_{ji} = T_R\delta^{ab}. \tag{5.4}$$

In analogy with the electric charge, these diagrams are used to interpret the Casimir factors as *colour charges*.

For this gauge group we find the following

$$C_F \quad = \quad \frac{N^2 - 1}{2N}, \tag{5.5}$$

$$C_A \quad = \quad N, \tag{5.6}$$

$$T_R \quad = \quad \frac{1}{2}, \tag{5.7}$$

the last one being a normalisation factor (a matter of choice).

5.1.2 The Fierz identity

Consider an arbitrary element of SU(N) in the adjoint representation, we can write it as a linear combination of delta functions for a fermionic line and open T matrices for the emission of gluons, i.e.

$$X_{ij} = Y\,\delta_{ij} + \sum_a Z^a T^a_{ij}, \tag{5.8}$$

where a runs over the $N^2 - 1$ generators of this gauge group. Since the generators are traceless, we can determine Y by taking the trace of this equation, so that

$$Y = \frac{\text{tr}X}{N}. \tag{5.9}$$

On the other hand, we can determine Z^a if we multiply by T^b and then take the trace on eq.(5.8)[*], as

$$
\begin{aligned}
\text{tr}\left(XT^b\right) &= \sum_a Z^a\,\text{tr}(T^aT^b) \\
&= \sum_a Z^a\,T_R\delta^{ab} \\
&= T_R Z^b,
\end{aligned}
$$

$$\Longrightarrow Z^a = \frac{\text{tr}\left(XT^a\right)}{T_R}, \tag{5.10}$$

---

[*]Recall $\text{tr}(T^a) = T^a_{ii} = 0$.

where we have used the definitions presented in eqs.(5.2) to (5.4).

The decomposition presented in eq.(5.8) can be rewritten using eqs.(5.9) and (5.10) as

$$X_{ij} = \frac{1}{N} (\text{tr}X) \; \delta_{ij} + \frac{1}{T_R} \sum_a \text{tr}\,(XT^a) \; T^a_{ij},$$

or

$$X_{ij} = \frac{1}{N} X_{kk} \; \delta_{ij} + \frac{1}{T_R} \sum_a X_{lk} T^a_{kl} \; T^a_{ij}.$$

Since this identity is valid for an arbitrary X_{ij}, we can write it as

$$X_{lk} \left(\delta_{il}\delta_{jk} - \frac{1}{N}\delta_{lk}\delta ij - \frac{1}{T_R} \sum_a T^a_{ij}T^a_{kl} \right) = 0$$

to have the following result

$$\sum_a T^a_{ij}T^a_{kl} = T_R \left(\delta_{il}\delta_{jk} - \frac{1}{N}\delta ij\delta_{kl} \right), \tag{5.11}$$

which is known as the Fierz identity. Figure (5.2) shows how this identity represents the colour flow between two quark lines and along a gluon $T^a_{ij}T^a_{kl}$, as simpler quark colour flows $\delta_{ij}, \delta_{kl}, ...$
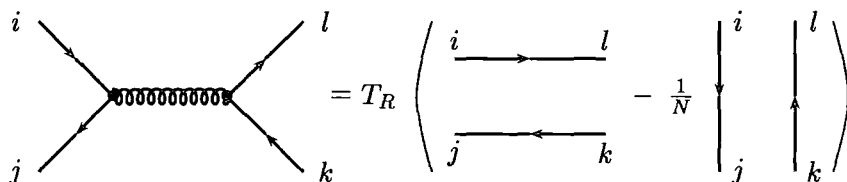
Figure 5.2: Diagrammatic representation for the Fierz identity

5.2   Factorisation of matrix elements in the singular limit

Let us extend the example of $q\bar{q} \to gg$ and use it to illustrate how the matrix elements factorise when we study their divergent behaviour. We can easily calculate $(\mathcal{A}^\dagger \mathcal{A})_{tot}$ using eq.(5.1) and the Fierz identity, as

$$|\mathcal{A}|^2_{tot} = C_F \frac{N^2}{2} \left[|\mathcal{A}_1 + \mathcal{A}_3|^2 + |\mathcal{A}_2 - \mathcal{A}_3|^2 + \mathcal{O}\left(\frac{1}{N^2}\right) \right]. \tag{5.12}$$

The first two terms on the r.h.s. of this equation are colour-less subamplitudes that represent an ordered way of emitting gluons a and b from a quark-antiquark line. There-

fore it is convenient (and commonly used) to write them as ordered subamplitudes,

$$|\mathcal{A}_1 + \mathcal{A}_3|^2 = |\mathcal{S}(q; a, b, \bar{q})|^2, \tag{5.13}$$

$$|\mathcal{A}_2 - \mathcal{A}_3|^2 = |\mathcal{S}(q; b, a, \bar{q})|^2. \tag{5.14}$$

This analysis can be easily extended to the case where we have multiple gluon emission, where the ordered subamplitudes have a special factorisation when we look into their singular limits. This is due to the fact that the emission of the partons is well ordered and forms well defined colour flows to which the soft/collinear parton can couple.

For example, in the limit where gluon b is soft [74, 75, 36] we have the QED-like factorisation into an eikonal-type singular factor and a colour ordered tree-level squared amplitude where gluon b has been removed. The amplitude for the emission of n gluons in the limit where gluon b is soft,

$$|\mathcal{S}(q; 1, \ldots, a, b, c, \ldots, n; \bar{q})|^2 \xrightarrow{E_b \to 0} \mathcal{E}(s_{ac}, s_{ab}, s_{bc}) \; |\mathcal{S}(q; 1, \ldots, a, c, \ldots, n; \bar{q})|^2 \tag{5.15}$$
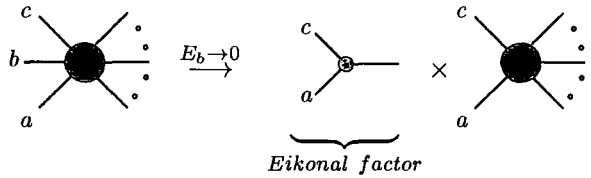
where the eikonal factor is given by,

$$\mathcal{E}(s_{ac}, s_{ab}, s_{bc}) = \frac{4 s_{ac}}{s_{ab} s_{bc}} \tag{5.16}$$

and the diagrams represent the colour ordered subamplitudes.

Similarly, in the limit where partons a and b become collinear and cluster to form a new parton c, such that $p_a + p_b = p_c$, there is a factorisation of the matrix elements [74, 75]. The factorisation is in terms of a function that is directly related to the Altarelli-Parisi splitting function and a tree-level squared-amplitude, where the partons a and b are replaced by the cluster parton c, i.e.

$$|\mathcal{S}(q; 1, \ldots, a, b, \ldots, n; \bar{q})|^2 \xrightarrow{a \| b} P_{ab \to c}(z, s_{ab}) \; |\mathcal{S}(q; 1, \ldots, c, \ldots, n; \bar{q})|^2 \tag{5.17}$$
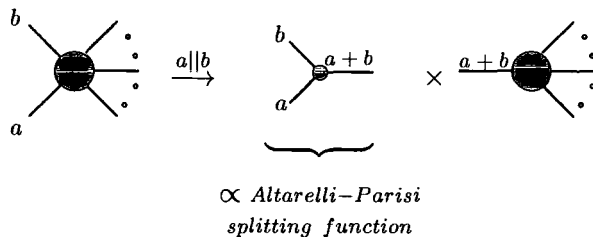
where $p_a = zp_c$ and $p_b = (1-z)p_c$ and after integrating over the azimuthal angle of the plane containing the collinear particles with respect to the rest of the hard processes, the collinear splitting function $P_{ab\to c}$ is given by

$$P_{ab\to c}(z, s_{ab}) = \frac{2}{s_{ab}} P_{ab\to c}(z). \tag{5.18}$$

The function $P_{ab\to c}(z)$ is the *Altarelli-Parisi* [76, 77, 78] splitting kernel for partons a and b with momentum fraction z, clustering to form parton c (with colour factors removed and in $D = 4 - 2\epsilon$ dimensions). These are given by

$$
\begin{aligned}
P_{qg\to q}(z) &= \frac{1 + z^2 - \epsilon(1-z)^2}{1-z} \\
P_{q\bar{q}\to g}(z) &= \frac{z^2 + (1-z)^2 - \epsilon}{1-\epsilon} \\
P_{gg\to g}(z) &= \frac{1 + z^4 + (1-z)^4}{z(1-z)}
\end{aligned}
\tag{5.19}
$$

satisfying,

$$
\begin{aligned}
P_{ab\to c}(z) &= P_{ba\to c}(1-z) \\
P_{\bar{a}\bar{b}\to\bar{c}}(z) &= P_{ab\to c}(z).
\end{aligned}
$$

Unfortunately, the squared subamplitudes corresponding to the $\mathcal{O}(\frac{1}{N^2})$ terms of eq. (5.12), do not have such a straightforward singular factorisation. Nevertheless, this example is enough to demonstrate that there is an underlying issue of utmost importance in this section. The factorisation of the matrix element

1. is *universal*, in the sense that we need only to specify the type of singular limit and the singular behaviour (at leading order in colour) will have a characteristic structure,

2. is *process independent*,

3. occurs when any parton is unresolved,

4. is always in the form of *singular term* × *finite subamplitude squared*

5.2.1   IR cancellations

In section 2.1.4 we saw how the NLO cross section for $e^+e^- \to q\bar{q}$ is finite when we sum all possible real and virtual emissions despite their individual singular behaviour. The same analysis can be performed for the NNLO calculation, only this time we will have to consider more contributions over which the cancellation of singularities has to be done.

The study of soft and collinear divergences allows for an easier analysis of the cancellation between divergent pieces at different levels in the calculation of a cross section. A lot of work has been done related to the factorisation of NLO and NNLO virtual and real emission partonic matrix elements and of the phase space integration [29, 79, 80, 81, 82, 83, 84].

Recall the general structure for the NNLO cross section for $2 \to 2$ partonic scattering provided in eq. (2.33). We can see that we will have several levels of cancellation of singularities and they have all been thoroughly studied by different people and with different approaches. It is important to have a general picture of these analyses and what they involve, since it will naturally lead to Catani's formalism, which is the one we use to verify our results.

For completeness we present some of the main results with schematic diagrams, similar to those used in the previous section, and provide some references where the details can be looked up.

Consider the partonic cross section for n-particle production at NNLO

$$
\begin{aligned}
\hat{\sigma}_{n \text{ jet}} \sim \quad & \int \left[|\langle \mathcal{M}^{(0)} | \mathcal{M}^{(0)} \rangle|^2 \right]_{n+2} d\Phi_{n+2} \\
& + \int \left[\langle \mathcal{M}^{(0)} | \mathcal{M}^{(1)} \rangle + \langle \mathcal{M}^{(1)} | \mathcal{M}^{(0)} \rangle \right]_{n+1} d\Phi_{n+1} \\
& + \int \left[\langle \mathcal{M}^{(1)} | \mathcal{M}^{(1)} \rangle + \langle \mathcal{M}^{(0)} | \mathcal{M}^{(2)} \rangle + \langle \mathcal{M}^{(2)} | \mathcal{M}^{(0)} \rangle \right]_{n} d\Phi_{n} \quad (5.20)
\end{aligned}
$$

where $[\ ]_i$ indicates the number of particles in the final state with $d\Phi_i$ the corresponding phase space and $\mathcal{M}^{(i)}$ is the i-th order scattering amplitude.

To have an idea of the different layers of cancellations between divergences, we summarise them as follows

- the cancellation between the $(n+2)$ and (n)-levels (first row in eq.(5.20), contributing to last row), when two particles are unresolved requires to take into account the cases [29, 85, 86, 87, 88] when, e.g. for isolated emissions

  - three partons are simultaneously collinear
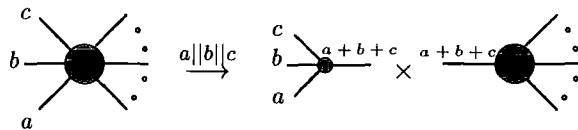
  where $p_a = w p_{a+b+c}$, $p_b = x p_{a+b+c}$ and $p_c = y p_{a+b+c}$, with $w + x + y = 1$,

– two gluons are soft
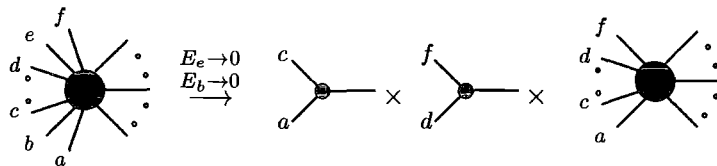
– two partons are collinear and one gluon is soft
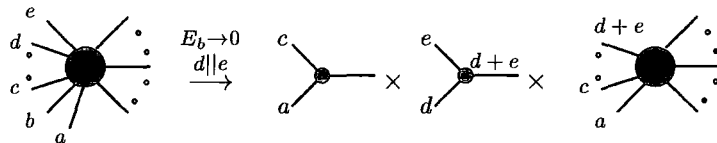
- the cancellation between the $(n + 1)$ and (n)-levels (second row in eq.(5.20), contributing to last row), when one particle is unresolved requires to take into account the cases [89, 30, 31, 82, 32, 90, 83] when, e.g. for isolated emissions

  – two partons are collinear
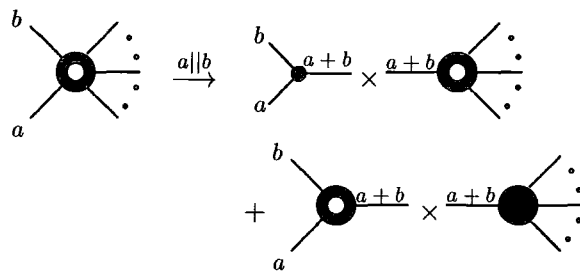
  – a gluon is soft
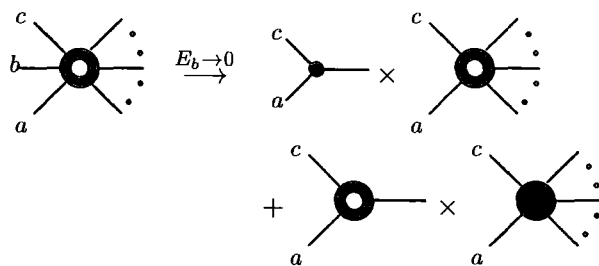
which are only examples of isolated emissions [†].

This work has provided the platform for the development of more general approaches in the prediction of the divergent behaviour of scattering amplitudes. In particular, the general (process-independent) algorithm to obtain the singular behaviour of QCD amplitudes at one- and two-loop order devised by Catani and Seymour [73, 72] provides an excellent testing ground for the divergences of our explicit two-loop calculations. Moreover, this formalism does not require the decomposition of the matrix elements into colour subamplitudes. In Chapter 6 we apply such a formalism to various partonic processes.

[†]There are also contributions from singular behaviour of partons belonging to the same colour current (colour connected singularities). See reference [29] and references therein.

The fact that we agree with the predictions stemming from Catani's formalism, is a very strong check for the divergent structure of our explicit calculation. It represents a thorough verification because typically all Feynman diagrams of the massless QCD amplitudes are infrared divergent (therefore all contribute to the structure of the singularities).

In the next sections we explore the basic results in Catani's formalism and the necessary tools required to construct the divergent structure prediction.

5.3 Colour space

Based on the fact that the singular structure of the sum of all possible real and virtual emissions cancels order by order in perturbation theory and that this structure follows a factorisation pattern that has been well studied, we can predict the infrared singularities of one- and two-loop QCD amplitudes with light-quark flavours.

By construction, we have an algorithm that allows for the amplitudes to be computed within CDR and all UV singularities removed within the $\overline{\text{MS}}$ renormalisation scheme. Together with this, the amplitudes are represented as vectors in a *colour space*. All this provides a natural environment in which the real and virtual emissions can be thought of as insertions of colour interactions between all the partons in a particular colour state amplitude. In this section we discuss this colour space and how these colour operations are defined.

Consider a general QCD amplitude with m external legs $\mathcal{M}_m$,

$$\mathcal{M}_m = \mathcal{M}_m^{c_1,...,c_m;s_1,...,s_m}(p_1,...,p_m), \tag{5.21}$$

that depends on the colours c_i, helicities s_i and momenta p_i carried by the external particles. As we have mentioned before, if the particle i is a quark (gluon), the colour indices will be $c_i = 1,\ldots,N$ $(c_i = 1,\ldots,N^2 - 1)$ and the helicities will be $s_i = 1,2$ $(s_i = 1,\ldots,D - 2)$.

In the colour + helicity-space we introduce a basis $\{|c_1,\ldots,c_m\rangle \otimes |s_1,\ldots,s_m\rangle\}$, such that our amplitude can be written as

$$\mathcal{M}_m^{c_1,...,c_m;s_1,...,s_m}(p_1,\ldots,p_m) = \left(\langle c_1,\ldots,c_m| \otimes \langle s_1,\ldots,s_m|\right)|1,\ldots,m\rangle_m, \tag{5.22}$$

so we can define the matrix element squared, summed over colours and spins, to be

$$\overline{|\mathcal{M}_m|^2} = \langle 1,\ldots,m|1,\ldots,m\rangle. \tag{5.23}$$

To study the colour structure of the amplitude within this framework (to obtain its singular behaviour), we do not need to consider the decomposition of the matrix elements into colour subamplitudes as we did before, instead we introduce the concept of *colour charges* $\mathbf{T}_i$.

We are now interested in the general case where any external parton of the amplitude radiates a gluon with colour, say, c_g. When this happens, the parton colour space increases by one parton to be able to accommodate the emitted gluon in an arbitrary emission state. This also has repercussions on the colour index of the emitter, which has to change according to the SU(N) colour algebra.

Given that the emitted gluon has colour charge c_g, we define a colour charge operator $\mathbf{T}_i$,

$$\mathbf{T}_i = T_i^{c_g}|c_g\rangle, \tag{5.24}$$

which represents the emission of such gluon from the i-th parton, acting on the colour space as

$$\langle c_1, \ldots, c_i, \ldots, c_m, c_g|\mathbf{T}_i|b_1, \ldots, b_i, \ldots, b_m\rangle = \delta_{c_1 b_1} \cdots T_{c_i b_i}^{c_g} \cdots \delta_{c_m b_m}. \tag{5.25}$$

The specific value for the T_{cb}^a matrix, is

$$T_{cb}^a = t_{cb}^a \qquad \text{if the emitter is a final} - \text{state quark or inital} - \text{state anti} - \text{quark},$$

$$T_{cb}^a = -t_{cb}^a \qquad \text{if the emitter is a final} - \text{state anti} - \text{quark or inital} - \text{state quark},$$

$$T_{cb}^a = i f_{cab} \qquad \text{if the emitter is a gluon}$$

and the colour charge algebra is simply,

$$\mathbf{T}_i \cdot \mathbf{T}_j = \begin{cases} \mathbf{T}_j \cdot \mathbf{T}_i & \text{if } i \neq j, \\ \mathbf{T}_i^2 = C_i & \text{otherwise.} \end{cases} \tag{5.26}$$

The Casimir operator C_i will be $C_i = C_F$ ($C_i = C_A$) if parton i is a quark (gluon), as given in section 5.1.1 and from colour conservation we have

$$\sum_{i=1}^m \mathbf{T}_i|1, \ldots, m\rangle = 0. \tag{5.27}$$

Using this notation, it is useful to have in mind the square of the *colour-correlated* amplitudes,

$$\begin{aligned} |\mathcal{M}_m^{i,k}|^2 &\equiv \langle 1, \ldots, m|\mathbf{T}_i \cdot \mathbf{T}_k|1, \ldots, m\rangle \\ &= \left[\mathcal{M}_m^{a_1, \ldots, b_i, \ldots, b_k, \ldots a_m}(p_1, \ldots, p_m)\right]^\dagger T_{b_i a_i}^c T_{b_k a_k}^c \mathcal{M}_m^{a_1, \ldots, a_i, \ldots, a_k, \ldots a_m}(p_1, \ldots, p_m). \end{aligned}$$

$$\tag{5.28}$$

i.e. the square of an amplitude with m external legs arising from the square of another amplitude with m partons linked with its complex-conjugated by the insertion of a gluon emission.

5.4   Singular behaviour of one-loop amplitudes

Consider the QCD amplitude $|\mathcal{M}\rangle$ in colour space with m external legs. We can perform a perturbative expansion of it as follows

$$|\mathcal{M}\rangle = \left(\frac{\alpha_s}{2\pi}\right)^n \left[|\mathcal{M}^{(0)}\rangle + \left(\frac{\alpha_s}{2\pi}\right)|\mathcal{M}^{(1)}\rangle + \left(\frac{\alpha_s}{2\pi}\right)^2 |\mathcal{M}^{(2)}\rangle + \mathcal{O}\left(\alpha_s^3\right)\right], \qquad (5.29)$$

where as before we work in the $\overline{\text{MS}}$ scheme, use CDR ($D = 4 - 2\epsilon$) and $|\mathcal{M}^{(i)}\rangle$ is the i-loop amplitude in colour space[‡].

The singularities for the one-loop amplitudes can be isolated as follows

$$|\mathcal{M}^{(1)}\rangle = \boldsymbol{I}^{(1)}(\epsilon)|\mathcal{M}^{(0)}\rangle + |\mathcal{M}^{1,fin}\rangle \qquad (5.30)$$
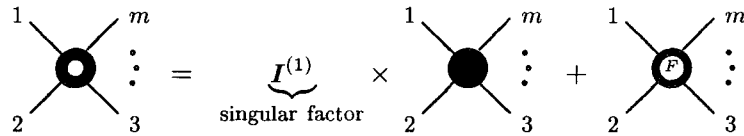
where $|\mathcal{M}^{1,fin}\rangle$ is finite when we take the $\epsilon \to 0$ limit. Note how all infrared divergences are factorised with respect to the tree-level amplitude, in agreement with our discussion of section 5.2.

The insertion operator $\boldsymbol{I}^{(1)}$ acts on the colour vector $|\mathcal{M}^{(i)}\rangle$ and contains all the singular behaviour of the loop amplitude. Its structure is given in general as

$$\boldsymbol{I}^{(1)}(\epsilon) = \frac{1}{2}\frac{e^{\epsilon\gamma}}{\Gamma(1-\epsilon)} \underbrace{\sum_i \nu_i^{sing}(\epsilon)}_{\substack{soft/collinear \\ singularities}} \underbrace{\sum_{j\neq i} \mathbf{T}_i \cdot \mathbf{T}_j \left(\frac{\mu^2\, e^{-i\lambda_{ij}\pi}}{2p_i \cdot p_j}\right)^\epsilon}_{\substack{gluon\ radiation \\ between\ two\ partons}} \qquad (5.31)$$

where $i, j = 1, \dots, m$ and p_i is the momenta for the ith external particle. Also

$$\lambda_{ij} = \begin{cases} 1 & \text{if both particles are incoming or outgoing,} \\ 0 & \text{otherwise.} \end{cases}$$

The singularities are embedded in the ν^{sing} function as poles in the dimension parameter ϵ,

$$\nu_i^{sing}(\epsilon) = \frac{1}{\epsilon^2} + \gamma_i \frac{1}{\epsilon}, \qquad (5.32)$$

[‡]n depends on the particular process we choose to study.

with

$$\gamma_q = \gamma_{\bar{q}} = \frac{3}{2}, \qquad \gamma_g = \frac{\beta_0}{C_A} \tag{5.33}$$

and β_0 given in eq. (1.42).

5.5 An example: $\gamma^* \to q\bar{q}$ one-loop singularities

We apply the Catani formalism to the example of the virtual corrections for $\gamma^* \to q\bar{q}$ at NLO we looked into in 2.1.3 and compare with our previous result.

We have from colour conservation

$$\mathbf{T}_{\bar{q}} = -\mathbf{T}_q, \tag{5.34}$$

so

$$\mathbf{T}_q \cdot \mathbf{T}_{\bar{q}} = -\mathbf{T}_q^2 = -C_F \mathbf{1} \tag{5.35}$$

and the colour charge operator is then

$$\mathbf{I}^{(1)}(\epsilon) = -C_F \frac{e^{\epsilon\gamma}}{\Gamma(1-\epsilon)} \left[\frac{1}{\epsilon^2} + \frac{3}{2\epsilon} \right] \left(-\frac{\mu^2}{s} \right)^\epsilon \mathbf{1} \tag{5.36}$$

The singular part of the one-loop amplitude is then

$$\mathcal{M}^{1,sing} = \frac{\alpha_s}{2\pi} \mathbf{I}^{(1)}(\epsilon) |\mathcal{M}^{(0)}\rangle = -C_F \frac{\alpha_s}{2\pi} \frac{e^{\epsilon\gamma}}{\Gamma(1-\epsilon)} \left[\frac{1}{\epsilon^2} + \frac{3}{2\epsilon} \right] \left(-\frac{\mu^2}{s} \right)^\epsilon \mathcal{M}^{(0)} \tag{5.37}$$

or, contracted with the tree-level amplitude, we would simply have

$$\langle \mathcal{M}^{(0)} | \mathcal{M}^{1,sing} \rangle = -C_F \frac{\alpha_s}{2\pi} \frac{e^{\epsilon\gamma}}{\Gamma(1-\epsilon)} \left[\frac{1}{\epsilon^2} + \frac{3}{2\epsilon} \right] \left(-\frac{\mu^2}{s} \right)^\epsilon \langle \mathcal{M}^{(0)} | \mathcal{M}^{(0)} \rangle \tag{5.38}$$

On the other hand, rearranging eqs. (2.3) and (2.26) and renormalising in the $\overline{\text{MS}}$ scheme (see eq.(1.40)), we can write the averaged matrix element squared for the one-loop virtual corrections as

$$\langle \mathcal{M}^{(0)} | \mathcal{M}^{V,NLO} \rangle = -C_F \frac{\alpha_s}{2\pi} \frac{e^{\epsilon\gamma}}{\Gamma(1-\epsilon)} \left[\frac{1}{\epsilon^2} + \frac{3}{2\epsilon} + 4 \right] \left(-\frac{\mu^2}{s} \right)^\epsilon \langle \mathcal{M}^{(0)} | \mathcal{M}^{(0)} \rangle, \tag{5.39}$$

where

$$\langle \mathcal{M}^{(0)} | \mathcal{M}^{V,NLO} \rangle \equiv \overline{\sum_{spin,col.} |\mathcal{M}_1^V|^2},$$

$$\langle \mathcal{M}^{(0)} | \mathcal{M}^{(0)} \rangle \equiv \overline{\sum_{spin,col.} |\mathcal{M}_0|^2}.$$

It is evident from eqs. (5.38) and (5.39), that we predict the complete singular behaviour for the one-loop matrix element, since their difference is indeed finite.

5.6   Singular behaviour of two-loop amplitudes

The divergent structure of two-loop amplitudes is given by a more complex equation, where we even have a new insertion operator and the one-loop amplitude interacts with the previous operator, i.e.

$$|\mathcal{M}^{(2)}\rangle \;=\; \boldsymbol{I}^{(1)}(\epsilon)|\mathcal{M}^{(1)}\rangle + \boldsymbol{I}^{(2)}(\epsilon)|\mathcal{M}^{(0)}\rangle + |\mathcal{M}^{2,fin}\rangle \tag{5.40}$$

Here, again we have $|\mathcal{M}^{2,fin}\rangle$ which is finite in the limit $\epsilon \to 0$. Now, the singularities are embedded in two terms. First, the double and single poles of $\boldsymbol{I}^{(1)}(\epsilon)$ are multiplying those in the one-loop amplitude $|\mathcal{M}^{(1)}\rangle$, providing poles of up to $1/\epsilon^4$. Then, the new operator $\boldsymbol{I}^{(2)}(\epsilon)$ multiplying the finite tree amplitude $|\mathcal{M}^{(0)}\rangle$, is also carrying up to $1/\epsilon^4$ poles, as can be seen in its expression

$$\begin{aligned}
\boldsymbol{I}^{(2)}(\epsilon) \;=\; & -\frac{1}{2}\boldsymbol{I}^{(1)}(\epsilon)\left(\boldsymbol{I}^{(1)}(\epsilon) + \frac{2\beta_0}{\epsilon}\right) \\
& +e^{-\epsilon\gamma}\frac{\Gamma(1-2\epsilon)}{\Gamma(1-\epsilon)}\left(\frac{\beta_0}{\epsilon} + K\right)\boldsymbol{I}^{(1)}(2\epsilon) \\
& +\mathbf{H}^{(2)},
\end{aligned} \tag{5.41}$$

with

$$K = \left(\frac{67}{18} - \frac{\pi^2}{6}\right)C_A - \frac{10}{9}T_R. \tag{5.42}$$

Here, the function $\mathbf{H}^{(2)}$ contains poles of $\mathcal{O}(\epsilon^{-1})$ and it is *not* universal. It depends on both the process we analyse and the renormalisation scheme we use. Usually, it contains characteristic constants such as $C_A, C_F, \pi, \beta_0, \beta_1$ and the Riemann zeta function evaluated at different points (ζ_2, ζ_3).

If we gather the results presented in eqs. (5.40) and (5.41), we can specify all the singularities of the two-loop amplitudes up to and including $\mathcal{O}(\epsilon^{-2})$. Furthermore, we can largely predict the $1/\epsilon$ poles that depend on generalised polylogarithms. The remaining parts, namely $\mathbf{H}^{(2)}$ and $|\mathcal{M}^{2,fin}\rangle$, can only be obtained by the *explicit* calculation of the Feynman diagrams conributing to the two-loop amplitude.

5.7 An example: unlike quark-quark scattering

Consider the scattering of unlike quarks as

$$q(p_1) + \bar{q}(p_2) \to q'(p_3) + \bar{q}'(p_4), \tag{5.43}$$
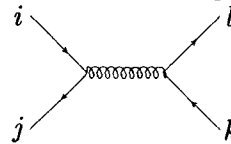
where the partons are all incoming with conserved light-like momenta,

$$p_1^\mu + p_2^\mu + p_3^\mu + p_4^\mu = 0, \qquad p_i^2 = 0.$$

And we use the associated Mandelstam variables given by

$$s = (p_1 + p_2)^2, \; t = (p_2 + p_3)^2, \; u = (p_1 + p_3)^2 = -s - t. \tag{5.44}$$

Now, to be able to isolate the singular parts of the renormalised one and two-loop amplitudes for this process, we need to construct the operator $\mathbf{I}^{(1)}$ of eq. (5.31) in colour space. For this, we need the amplitude at tree-level associated with this process

$$\equiv T_{ij}^a T_{kl}^a = \tfrac{1}{2}\left(\delta_{il}\delta_{jk} - \tfrac{1}{N}\delta_{ij}\delta_{kl}\right)$$

where we have used eq. (5.11) for the Fierz identity.

The tree-level amplitude for this diagram is then

$$|\mathcal{M}^{(0)}\rangle \propto \underbrace{\left(|=\rangle - \frac{1}{N}|\;\|\rangle\right)}_{colour \;\; space} \times \underbrace{M^{(0)}}_{kinematics} \tag{5.45}$$

where we have defined the colour vectors

$$
\begin{aligned}
|=\rangle &= \delta_{il}\delta_{jk}, \\
|\;\|\rangle &= \delta_{ij}\delta_{kl},
\end{aligned}
\tag{5.46}
$$

to represent each of the colour currents as shown in fig. (5.2) and to act as a colour basis over which the insertion operator $\mathbf{I}^{(1)}$ acts.

We can see both pictorially and using eqs. (5.31), (5.11) and eqs.(5.2)-(5.4), that the operator $\boldsymbol{I}^{(1)}$ acts on each colour state as

- $\boldsymbol{I}^{(1)}|=\rangle$

$$s - channel : \qquad = \frac{1}{2}\left(|\;\|\rangle - \frac{1}{N}|=\rangle\right)\mathcal{S} \tag{5.47}$$

$$t - channel : \qquad = \left(\frac{N^2-1}{2N}|=\rangle\right)\mathcal{T} \tag{5.48}$$

$$u - channel : \qquad = \frac{1}{2}\left(|\;\|\rangle - \frac{1}{N}|=\rangle\right)\mathcal{U} \tag{5.49}$$

⊙ $I^{(1)}|\ ||\rangle$

$$s - channel: \quad = \quad \left(\frac{N^2-1}{2N}|=\rangle\right)\mathcal{S} \tag{5.50}$$

$$t - channel: \quad = \quad \frac{1}{2}\left(|=\rangle - \frac{1}{N}|\ ||\rangle\right)\mathcal{T} \tag{5.51}$$

$$u - channel: \quad = \quad \frac{1}{2}\left(|=\rangle - \frac{1}{N}|\ ||\rangle\right)\mathcal{U} \tag{5.52}$$

which is a pictorial interpretation of the calculation of the operands $\mathbf{T}_i \cdot \mathbf{T}_j|=\rangle$ and $\mathbf{T}_i \cdot \mathbf{T}_j|\ ||\rangle$, together with the fact that each operand has an associated scale ratio,

$$\mathcal{S} = \left(-\frac{\mu^2}{s}\right)^\epsilon, \qquad \mathcal{T} = \left(-\frac{\mu^2}{t}\right)^\epsilon, \qquad \mathcal{U} = \left(-\frac{\mu^2}{u}\right)^\epsilon. \tag{5.53}$$

It is worth noting in these equations that the natural structure of the amplitudes and the insertion operand within colour states, allows these results to be presented also using matrices in the same space, so that schematically we can have the following mapping

$$\mathbf{I}^{(0)}\begin{pmatrix} M_= \\ M_{||} \end{pmatrix} = \begin{pmatrix} \mathcal{I}_{=,=} & \mathcal{I}_{=,||} \\ \mathcal{I}_{||,=} & \mathcal{I}_{||,||} \end{pmatrix}M^{(0)},$$

where $M_=, M_{||}$ are the components of the colour vector for the tree-level matrix element given in eq. (5.45).

So we can now calculate the action of this operator onto the tree-level amplitude, using eqs. (5.47) to (5.52), as

$$\begin{aligned}
I^{(1)}|\mathcal{M}^{(0)}\rangle &= \frac{e^{\epsilon\gamma}}{\Gamma(1-\epsilon)}\left(\frac{1}{\epsilon^2}+\frac{3}{2\epsilon}\right)M^{(0)} \\
&\times \left[(\mathcal{S}+\mathcal{U})|\ ||\rangle + \left(-\frac{\mathcal{S}}{N}+\frac{N^2-1}{N}\mathcal{T}-\frac{\mathcal{U}}{N}\right)|=\rangle \right. \\
&\left. -\frac{1}{N}\left(\left(\frac{N^2-1}{N}\mathcal{S}-\frac{\mathcal{T}}{N}-\frac{\mathcal{U}}{N}\right)|\ ||\rangle + (\mathcal{T}+\mathcal{U})|=\rangle\right)\right],
\end{aligned}$$

which can be rewritten to be

$$\begin{aligned}
I^{(1)}|\mathcal{M}^{(0)}\rangle &= \frac{e^{\epsilon\gamma}}{\Gamma(1-\epsilon)}\left(\frac{1}{\epsilon^2}+\frac{3}{2\epsilon}\right)M^{(0)} \\
&\times \left[\left(\frac{\mathcal{S}}{N^2}+\frac{\mathcal{T}}{N^2}+\frac{N^2+1}{N^2}\mathcal{U}\right)|\ ||\rangle \right. \\
&\left. +\left(-\frac{\mathcal{S}}{N}+\frac{N^2-2}{N}\mathcal{T}-\frac{2\mathcal{U}}{N}\right)|=\rangle\right].
\end{aligned} \tag{5.54}$$

We saw in eq. (5.30) of previous sections how the singularities of, say the one-loop amplitude, looks like

$$|\mathcal{M}^{(1)}\rangle = I^{(1)}(\epsilon)|\mathcal{M}^{(0)}\rangle + |\mathcal{M}^{1,fin}\rangle,$$

so, if we want to calculate the singularities for the one-loop amplitude (or even the two-loop amplitude) contracted with the tree-level amplitude, we will need to calculate terms like $\langle \mathcal{M}^{(0)} | \boldsymbol{I}^{(1)} | \mathcal{M}^{(0)} \rangle$ or $\langle \mathcal{M}^{(0)} | \boldsymbol{I}^{(2)} | \mathcal{M}^{(0)} \rangle$. The need for the calculation of such terms will become clear in the next Chapter. Let us assume that indeed we need these terms, then we proceed with our example and we can now calculate

$$
\begin{aligned}
\langle \mathcal{M}^{(0)} | \boldsymbol{I}^{(1)} | \mathcal{M}^{(0)} \rangle \;=\;& M^{*(0)} \left(\langle = | - \frac{1}{N} \langle \| | \right) \; \boldsymbol{I}^{(1)} | \mathcal{M}^{(0)} \rangle \\
=\;& \frac{e^{\epsilon\gamma}}{\Gamma(1-\epsilon)} \left(\frac{1}{\epsilon^2} + \frac{3}{2\epsilon} \right) M^{*(0)} M^{(0)} \\
& \times \left[\left(\frac{\mathcal{S}}{N^2} + \frac{\mathcal{T}}{N^2} + \frac{N^2+1}{N^2} \mathcal{U} \right) \left(\langle = | - \frac{1}{N} \langle \| | \right) | \, \| \rangle \right. \\
& \left. + \left(-\frac{\mathcal{S}}{N} + \frac{N^2-2}{N} \mathcal{T} - \frac{2\mathcal{U}}{N} \right) \left(\langle = | - \frac{1}{N} \langle \| | \right) | = \rangle \right]
\end{aligned}
\tag{5.55}
$$

which is a result of using simply eqs. (5.45) and (5.54).

Now, using eq. (5.46), the action of these colour states among themselves, can easily be verified as

$$
\begin{aligned}
\langle \| \, | = \rangle = \langle = | \, \| \rangle \;&=\; N, \\
\langle \| \, | \, \| \rangle = \langle = | = \rangle \;&=\; N^2,
\end{aligned}
\tag{5.56}
$$

so that we can calculate

$$
\begin{aligned}
\left(\langle = | - \frac{1}{N} \langle \| | \right) | \, \| \rangle \;&=\; 0, \\
\left(\langle = | - \frac{1}{N} \langle \| | \right) | = \rangle \;&=\; N^2 - 1.
\end{aligned}
\tag{5.57}
$$

Then using eq. (5.57), we can see that the first term on the r.h.s. of eq. (5.55) does not contribute and we are left with

$$
\begin{aligned}
\langle \mathcal{M}^{(0)} | \boldsymbol{I}^{(1)} | \mathcal{M}^{(0)} \rangle \;=\;& \frac{e^{\epsilon\gamma}}{\Gamma(1-\epsilon)} \left(\frac{1}{\epsilon^2} + \frac{3}{2\epsilon} \right) \left(N^2 - 1 \right) M^{*(0)} M^{(0)} \\
& \times \left(-\frac{\mathcal{S}}{N} + \frac{N^2-2}{N} \mathcal{T} - \frac{2\mathcal{U}}{N} \right)
\end{aligned}
\tag{5.58}
$$

where we identify the Born level matrix element

$$
\left(N^2 - 1 \right) M^{*(0)} M^{(0)} \;\rightarrow\; \langle \mathcal{M}^{(0)} | \mathcal{M}^{(0)} \rangle.
\tag{5.59}
$$

Applying the same colour algebra and following the same procedure, we can obtain other terms that make up the ingredients for the two-loop matrix element singularities,

such as

$$
\begin{aligned}
\langle \mathcal{M}^{(0)} | \boldsymbol{I}^{(1)}(\epsilon) \boldsymbol{I}^{(1)}(\epsilon) | \mathcal{M}^{(0)} \rangle = {} & \langle \mathcal{M}^{(0)} | \mathcal{M}^{(0)} \rangle \\
& \times \frac{e^{2\epsilon\gamma}}{\Gamma(1-\epsilon)^2} \left(\frac{1}{\epsilon^2} + \frac{3}{2\epsilon} \right)^2 \left[\left(\frac{N^4 - 3N^2 + 3}{N^2} \right) \mathcal{T}^2 + \left(\frac{N^2 + 3}{N^2} \right) \mathcal{U}^2 \right. \\
& \left. - 2 \left(\frac{N^2 - 2}{N^2} \right) \mathcal{ST} + 2 \left(\frac{N^2 - 3}{N^2} \right) \mathcal{UT} \right. \\
& \left. - \frac{4}{N^2} \mathcal{SU} + \frac{1}{N^2} \mathcal{S}^2 \right],
\end{aligned}
\tag{5.60}
$$

which arises from the first term on the r.h.s. of eq. (5.41) acting between the tree-level amplitude and its complex conjugated.

This example shows how we calculate these terms individually and how the insertion operator is working at the level of the colour states. In the next Chapter we present our results using the notation we have just introduced and, as was mentioned before, using matrices in colour space.

Chapter 6

Results

In Chapters 2 and 5 we looked at the structure of the infrared divergences of the loop amplitudes associated with the divergent loop-momenta integration. We saw how we can isolate the divergent behaviour so that we can have an explicit cancellation of the singularities when combining virtual and real emissions. All this can be done systematically using the Catani formalism.

In this Chapter we apply this knowledge to the calculation matrix elements for $2 \to 2$ scattering of massless partons at next-to-next-to-leading order. First, we present the general structure of the IR divergences for any of the matrix elements and in terms of general operators. We also provide the general structure for the finite pieces and introduce our notation.

Sections 6.2 through to 6.5 are dedicated to each of the partonic processes and provide the process-dependent definitions of the operators involved in the IR structure, We finish each section by providing the processes' structure of the finite piece and refer the reader to Apendix C for its expansion.

6.1   General structure of IR divergences

In this section we provide the general structure of the IR singularities [72, 73], associated to the one and two-loop matrix element for a generic $2 \to 2$ partonic scattering process.

The description presented in this section is valid for all the processes and the fact that we can present it in this way provides a very powerful check on our highly non trivial calculation.

Before the general expressions, we start with some general notation.

6.1.1   Notation

We work in conventional dimensional regularisation treating all external states in D dimensions. We renormalise in the $\overline{\text{MS}}$ scheme where the bare coupling α_0 is related to the

running coupling $\alpha_s \equiv \alpha_s(\mu^2)$ at renormalisation scale μ via

$$\alpha_0 \, S_\epsilon = \alpha_s \left[1 - \frac{\beta_0}{\epsilon} \left(\frac{\alpha_s}{2\pi} \right) + \left(\frac{\beta_0^2}{\epsilon^2} - \frac{\beta_1}{2\epsilon} \right) \left(\frac{\alpha_s}{2\pi} \right)^2 + \mathcal{O}\left(\alpha_s^3 \right) \right]. \tag{6.1}$$

In this expression

$$S_\epsilon = (4\pi)^\epsilon e^{-\epsilon\gamma}, \qquad \gamma = 0.5772\ldots = \text{Euler constant} \tag{6.2}$$

is the typical phase-space volume factor in $D = 4 - 2\epsilon$ dimensions, and β_0, β_1 are the first two coefficients of the QCD beta function for N_F (massless) quark flavours

$$\beta_0 = \frac{11C_A - 4T_R N_F}{6} \quad , \qquad \beta_1 = \frac{17C_A^2 - 10C_A T_R N_F - 6C_F T_R N_F}{6} \; . \tag{6.3}$$

For an $SU(N)$ gauge theory (N is the number of colours)

$$C_F = \left(\frac{N^2 - 1}{2N} \right), \qquad C_A = N, \qquad T_R = \frac{1}{2}. \tag{6.4}$$

6.1.2   Two-loop contribution

We can write the infrared pole structure of the two loop contributions renormalised in the $\overline{\text{MS}}$ scheme in terms of the tree and unrenormalised one-loop amplitudes, $|\mathcal{M}^{(0)}\rangle$ and $|\mathcal{M}^{(1,un)}\rangle$ respectively, as

$$\begin{aligned}
\mathcal{P}oles = 2\,\mathrm{Re}\Bigg[\quad &-\frac{1}{2}\langle\mathcal{M}^{(0)}|\boldsymbol{I}^{(1)}(\epsilon)\boldsymbol{I}^{(1)}(\epsilon)|\mathcal{M}^{(0)}\rangle - \frac{2\beta_0}{\epsilon}\,\langle\mathcal{M}^{(0)}|\boldsymbol{I}^{(1)}(\epsilon)|\mathcal{M}^{(0)}\rangle \\
&+ \langle\mathcal{M}^{(0)}|\boldsymbol{I}^{(1)}(\epsilon)|\mathcal{M}^{(1,un)}\rangle \\
&+ e^{-\epsilon\gamma}\frac{\Gamma(1-2\epsilon)}{\Gamma(1-\epsilon)}\left(\frac{\beta_0}{\epsilon}+K\right)\langle\mathcal{M}^{(0)}|\boldsymbol{I}^{(1)}(2\epsilon)|\mathcal{M}^{(0)}\rangle \\
&+ \langle\mathcal{M}^{(0)}|\boldsymbol{H}^{(2)}(\epsilon)|\mathcal{M}^{(0)}\rangle \Bigg]
\end{aligned} \tag{6.5}$$

This expression is valid for all the processes to be considered, except for the scattering of like quarks. In this case, it will become clear that we need to analyse only the interference of the s-channel graphs with the t-channel graphs. For this specific function we have the following expression for the infrared pole structure

$$\begin{aligned}
\mathcal{P}oles = 2\,\mathrm{Re}\Bigg[\quad &-\frac{1}{2}\langle\overline{\mathcal{M}}^{(0)}|\boldsymbol{I}^{(1)}(\epsilon)\boldsymbol{I}^{(1)}(\epsilon)|\mathcal{M}^{(0)}\rangle - \frac{2\beta_0}{\epsilon}\,\langle\overline{\mathcal{M}}^{(0)}|\boldsymbol{I}^{(1)}(\epsilon)|\mathcal{M}^{(0)}\rangle \\
&+ \langle\overline{\mathcal{M}}^{(0)}|\boldsymbol{I}^{(1)}(\epsilon)|\mathcal{M}^{(1,un)}\rangle \\
&+ e^{-\epsilon\gamma}\frac{\Gamma(1-2\epsilon)}{\Gamma(1-\epsilon)}\left(\frac{\beta_0}{\epsilon}+K\right)\langle\overline{\mathcal{M}}^{(0)}|\boldsymbol{I}^{(1)}(2\epsilon)|\mathcal{M}^{(0)}\rangle \\
&+ \langle\overline{\mathcal{M}}^{(0)}|\boldsymbol{H}^{(2)}(\epsilon)|\mathcal{M}^{(0)}\rangle + (s \leftrightarrow t) \Bigg],
\end{aligned} \tag{6.6}$$

The unrenormalised one-loop amplitude $|\mathcal{M}^{(1,un)}\rangle$ is what is obtained by direct Feynman diagram evaluation of the one-loop graphs. As discussed before, the matrix $\boldsymbol{I}^{(1)}(\epsilon)$ acts directly as a rotation matrix on $|\mathcal{M}^{(0)}\rangle$ and $|\mathcal{M}^{(1,un)}\rangle$ in colour space.

6.1.3   One-loop self-interference contribution

In the same spirit, we can write the infrared pole structure of the one-loop contributions renormalised in the $\overline{\text{MS}}$ scheme as

$$
\begin{aligned}
\mathcal{P}oles \;=\; 2\,\text{Re}\Bigg[&-\frac{1}{2}\langle\mathcal{M}^{(0)}|\boldsymbol{I}^{(1)\dagger}(\epsilon)\boldsymbol{I}^{(1)}(\epsilon)|\mathcal{M}^{(0)}\rangle \\
&-\frac{\beta_0}{\epsilon}\,\langle\mathcal{M}^{(0)}|\boldsymbol{I}^{(1)}(\epsilon)|\mathcal{M}^{(0)}\rangle \\
&+\langle\mathcal{M}^{(1,un)}|\boldsymbol{I}^{(1)}(\epsilon)|\mathcal{M}^{(0)}\rangle\Bigg]
\end{aligned}
\tag{6.7}
$$

which is valid for all processes except for like quark scattering. In this case, again we only need to look at the interference of the s-channel graphs with the t-channel graphs. For this specific function we have the following expression

$$
\begin{aligned}
\mathcal{P}oles \;=\; 2\,\text{Re}\Bigg[&-\frac{1}{2}\langle\overline{\mathcal{M}}^{(0)}|\boldsymbol{I}^{(1)\dagger}(\epsilon)\boldsymbol{I}^{(1)}(\epsilon)|\mathcal{M}^{(0)}\rangle \\
&-\frac{\beta_0}{\epsilon}\,\langle\overline{\mathcal{M}}^{(0)}|\boldsymbol{I}^{(1)}(\epsilon)|\mathcal{M}^{(0)}\rangle \\
&+\langle\overline{\mathcal{M}}^{(1,un)}|\boldsymbol{I}^{(1)}(\epsilon)|\mathcal{M}^{(0)}\rangle + (s\leftrightarrow t)\Bigg].
\end{aligned}
\tag{6.8}
$$

Again, $|\mathcal{M}^{(1,un)}\rangle$ is the unrenormalised one-loop amplitude, obtained by direct Feynman diagram evaluation and the matrix $\boldsymbol{I}^{(1)}(\epsilon)$ acts directly as a rotation matrix on $|\mathcal{M}^{(0)}\rangle$ and $|\mathcal{M}^{(1,un)}\rangle$ in colour space.

In this case, since we calculate the one-loop self-interference divergent piece, we have to be careful in the expansion, since the operator $I^{(1)}(\epsilon)$ also depends on the scales of the process s, t and u. On expanding this operator imaginary parts are generated, the sign of which is fixed by the small imaginary part $+i0$ assigned to each Mandelstam variable. Combinations such as $\langle\mathcal{M}^{(0)}|I^{(1)\dagger}(\epsilon)$ are obtained using the hermitian conjugate operator $I^{(1)\dagger}(\epsilon)$ where the only practical change is that the sign of the imaginary part of s, t and u are reversed.

6.1.4 Finite piece

In general the expansions of the two-loop master integrals [54, 91, 53, 10, 64, 67, 55] contain the generalised polylogarithms of Nielsen

$$S_{n,p}(x) = \frac{(-1)^{n+p-1}}{(n-1)!\,p!} \int_0^1 dt \, \frac{\log^{n-1}(t) \log^p(1-xt)}{t}, \qquad n,p \geq 1, \quad x \leq 1 \qquad (6.9)$$

where the level is $n+p$. Keeping terms up to $\mathcal{O}(\epsilon)$ corresponds to probing level 4 so that only polylogarithms with $n+p \leq 4$ occur. For $p = 1$ we find the usual polylogarithms

$$S_{n-1,1}(z) \equiv \mathrm{Li}_n(z). \qquad (6.10)$$

A basis set of 6 polylogarithms (one with $n+p = 2$, two with $n+p = 3$ and three with $n+p = 4$ is sufficient to describe a function of level 4. At level 4, we choose to eliminate the S_{22}, S_{13} and S_{12} functions using the standard polylogarithm identities [92] and retain the three Li_4 functions with arguments x and $1-x$ and $(x-1)/x$ where

$$x = -\frac{t}{s}, \qquad y = -\frac{u}{s} = 1-x, \qquad z = -\frac{u}{t} = \frac{x-1}{x}. \qquad (6.11)$$

For convenience, we also introduce the following logarithms

$$X = \log\left(\frac{-t}{s}\right), \qquad Y = \log\left(\frac{-u}{s}\right), \qquad S = \log\left(\frac{s}{\mu^2}\right), \qquad U = \log\left(\frac{-u}{\mu^2}\right), \qquad (6.12)$$

where μ is the renormalisation scale. The common choice $\mu^2 = s$, for example, corresponds to setting $S = 0$.

For each channel, we choose to present our results by grouping terms according to the power of the number of colours N and the number of light quarks N_F so that in channel c, we can have for example

$$\mathcal{F}inite_c = N^2 A_c + B_c + \frac{1}{N^2} C_c + N N_F D_c + \frac{N_F}{N} E_c + N_F^2 F_c \qquad (6.13)$$

All the expansions for the finite pieces are compiled in Appendix C and are organised for each process and for the one and two-loop contributions, separately.

6.2 Unlike quark scattering

It is the purpose of this section to provide dimensionally regularised and renormalised analytic expressions at the two-loop level for the process

$$q + \bar{q} \quad \rightarrow \quad q' + \bar{q}',$$

together with the time-reversed and crossed processes,

$$q + q' \rightarrow q + q',$$

$$q + \bar{q}' \rightarrow q + \bar{q}',$$

$$\bar{q} + \bar{q}' \rightarrow \bar{q} + \bar{q}'.$$

As it has been specified before, we use the $\overline{MS}$ renormalisation scheme and conventional dimensional regularisation (CDR) where all external particles are treated in D dimensions.

6.2.1 Notation

For calculational convenience, we treat all particles as incoming so that

$$q(p_1) + \bar{q}(p_2) + q'(p_3) + \bar{q}'(p_4) \rightarrow 0 \tag{6.14}$$

The renormalised four point amplitude in the $\overline{MS}$ scheme is thus

$$|\mathcal{M}\rangle \;=\; 4\pi\alpha_s \left[|\mathcal{M}^{(0)}\rangle + \left(\frac{\alpha_s}{2\pi}\right) |\mathcal{M}^{(1)}\rangle + \left(\frac{\alpha_s}{2\pi}\right)^2 |\mathcal{M}^{(2)}\rangle + \mathcal{O}\left(\alpha_s^3\right) \right], \tag{6.15}$$

where the $|\mathcal{M}^{(i)}\rangle$ represents the colour-space vector describing the i-loop amplitude. The dependence on both renormalisation scale μ and renormalisation scheme is implicit.

We denote the squared amplitude summed over spins and colours by,

$$\langle \mathcal{M}|\mathcal{M}\rangle = \mathcal{A}(s,t,u), \tag{6.16}$$

For the physical processes, the spin and colour averaged amplitudes are related to $\mathcal{A}$ by,

$$\overline{\sum |\mathcal{M}(q + \bar{q} \rightarrow \bar{q}' + q')|^2} \;=\; \frac{1}{4N^2}\, \mathcal{A}(s,t,u) \tag{6.17}$$

$$\overline{\sum |\mathcal{M}(q + q' \rightarrow q + q')|^2} \;=\; \frac{1}{4N^2}\, \mathcal{A}(u,t,s) \tag{6.18}$$

$$\overline{\sum |\mathcal{M}(q + \bar{q}' \rightarrow q + \bar{q}')|^2} \;=\; \frac{1}{4N^2}\, \mathcal{A}(t,s,u) \tag{6.19}$$

$$\overline{\sum |\mathcal{M}(\bar{q} + \bar{q}' \rightarrow \bar{q} + \bar{q}')|^2} \;=\; \frac{1}{4N^2}\, \mathcal{A}(u,t,s), \tag{6.20}$$

where N is the number of colours.

The summed and squared amplitude has the perturbative expansion,

$$\mathcal{A}(s,t,u) = 16\pi^2\alpha_s^2 \left(\mathcal{A}^4(s,t,u) + \left(\frac{\alpha_s}{2\pi}\right) \mathcal{A}^6(s,t,u) + \left(\frac{\alpha_s}{2\pi}\right)^2 \mathcal{A}^8(s,t,u) + \mathcal{O}\left(\alpha_s^3\right) \right). \tag{6.21}$$

In terms of the amplitudes,

$$\mathcal{A}^4(s,t,u) \;=\; \langle \mathcal{M}^{(0)}|\mathcal{M}^{(0)}\rangle \equiv 2(N^2-1)\left(\frac{t^2+u^2}{s^2}-\epsilon\right), \qquad (6.22)$$

$$\mathcal{A}^6(s,t,u) \;=\; \left(\langle \mathcal{M}^{(0)}|\mathcal{M}^{(1)}\rangle + \langle \mathcal{M}^{(1)}|\mathcal{M}^{(0)}\rangle\right), \qquad (6.23)$$

$$\mathcal{A}^8(s,t,u) \;=\; \left(\langle \mathcal{M}^{(1)}|\mathcal{M}^{(1)}\rangle + \langle \mathcal{M}^{(0)}|\mathcal{M}^{(2)}\rangle + \langle \mathcal{M}^{(2)}|\mathcal{M}^{(0)}\rangle\right). \qquad (6.24)$$

Expressions for $\mathcal{A}^6$ are given in ref.[39] using dimensional regularisation to isolate the infrared and ultraviolet singularities.

We concentrate on the next-to-next-to-leading order contribution $\mathcal{A}^8$ which consists of the interference of the two-loop and tree graphs and the self-interference of the one-loop graphs.

We give explicit formulae for the ϵ-expansion of the two-loop contribution to the next-to-next-to-leading order term $\mathcal{A}^8(s,t,u)$. To distinguish between the genuine two-loop contribution $\langle \mathcal{M}^{(0)}|\mathcal{M}^{(2)}\rangle + \langle \mathcal{M}^{(2)}|\mathcal{M}^{(0)}\rangle$ and the squared one-loop part $\langle \mathcal{M}^{(1)}|\mathcal{M}^{(1)}\rangle$, we decompose $\mathcal{A}^8$ as

$$\mathcal{A}^8 = \mathcal{A}^{8\ (2\times 0)} + \mathcal{A}^{8\ (1\times 1)}, \qquad (6.25)$$

where

$$\mathcal{A}^{8\ (2\times 0)} \;\equiv\; \langle \mathcal{M}^{(0)}|\mathcal{M}^{(2)}\rangle + \langle \mathcal{M}^{(2)}|\mathcal{M}^{(0)}\rangle,$$

$$\mathcal{A}^{8\ (1\times 1)} \;\equiv\; \langle \mathcal{M}^{(1)}|\mathcal{M}^{(1)}\rangle.$$

Section 6.2.2 deals with $\mathcal{A}^{8\ (2\times 0)}$ and section 6.2.3 with $\mathcal{A}^{8\ (1\times 1)}$.

6.2.2   Two-loop contribution

We divide the two-loop contributions into into two classes, those that multiply poles in the dimensional regularisation parameter ϵ and those that are finite as $\epsilon \to 0$,

$$\mathcal{A}^{8\ (2\times 0)}(s,t,u) = \mathcal{P}oles + \mathcal{F}inite. \qquad (6.26)$$

$\mathcal{P}oles$ contains both infrared singularities and ultraviolet divergences. The latter are removed by renormalisation, while the former must be analytically cancelled by the infrared singularities occuring in radiative processes of the same order. The structure of these infrared divergences has been provided in eq.(6.5).

6.2.2.1   Infrared pole structure

It is convenient to decompose $|\mathcal{M}^{(0)}\rangle$ and $|\mathcal{M}^{(1,un)}\rangle$ in terms of $SU(N)$ matrices in the fundamental representation, T^a, so that the tree amplitude may be written as [93, 36, 94,

95, 96, 97, 98]

$$
\begin{aligned}
|\mathcal{M}^{(0)}\rangle &= \sum_a \left(T_{ij}^a T_{kl}^a\right) \mathcal{A}_4^{\text{tree}}(1_q, 2_{\bar{q}}, 3_{q'}, 4_{\bar{q}'}) \\
&= \left(\delta_{il}\delta_{jk} - \frac{1}{N}\delta_{ij}\delta_{kl}\right) \mathcal{A}_4^{\text{tree}}(1_q, 2_{\bar{q}}, 3_{q'}, 4_{\bar{q}'})
\end{aligned} \tag{6.27}
$$

while the one-loop amplitude has the form [33, 30, 82]

$$
\begin{aligned}
|\mathcal{M}^{(1,un)}\rangle &= \left(\delta_{il}\delta_{jk} - \frac{1}{N}\delta_{ij}\delta_{kl}\right) \mathcal{A}_{4;1}^{[1]}(1_q, 2_{\bar{q}}, 3_{q'}, 4_{\bar{q}'}) \\
&\quad + (\delta_{il}\delta_{jk}) \, \mathcal{A}_{4;2}^{[1]}(1_q, 2_{\bar{q}}, 3_{q'}, 4_{\bar{q}'})
\end{aligned} \tag{6.28}
$$

To evaluate eq. (6.5) we find it convenient to express $|\mathcal{M}^{(0)}\rangle$ and $|\mathcal{M}^{(1,un)}\rangle$ as two-dimensional vectors in colour space

$$
|\mathcal{M}^{(0)}\rangle = (\mathcal{T}_1, \ \mathcal{T}_2)^T, \tag{6.29}
$$

$$
|\mathcal{M}^{(1,un)}\rangle = (\mathcal{L}_1, \ \mathcal{L}_2)^T, \tag{6.30}
$$

where ^{T} indicate the transpose vector. Here the $\mathcal{T}_i$ and $\mathcal{L}_i$ are the components of $|\mathcal{M}^{(0)}\rangle$ and $|\mathcal{M}^{(1,un)}\rangle$ in the colour space spanned by the basis

$$
\mathcal{C}_1 = \delta_{il}\delta_{jk},
$$

$$
\mathcal{C}_2 = \delta_{ij}\delta_{kl},
$$

The tree and loop amplitudes $\mathcal{T}_i$ and $\mathcal{L}_i$ are directly obtained in terms of $\mathcal{A}_4^{\text{tree}}$, $\mathcal{A}_{4;1}^{[1]}$, $\mathcal{A}_{4;3}^{[1]}$ and $\mathcal{A}_{4;1}^{[1/2]}$ by reading off from eqs. (6.27) and (6.28). As we will see, the amplitudes themselves are not required since we compute the interference of tree and loop amplitudes directly.

In the same colour basis, the infrared-singularity operator $I^{(1)}(\epsilon)$ has the form

$$
I^{(1)}(\epsilon) = -\frac{e^{\epsilon\gamma}}{\Gamma(1-\epsilon)}\frac{1}{N}\left(\frac{1}{\epsilon^2} + \frac{3}{2\epsilon}\right) \times \begin{pmatrix} A(\epsilon, s, t, u) & B(\epsilon, s, t, u) \\ B(\epsilon, t, s, u) & A(\epsilon, t, s, u) \end{pmatrix} \tag{6.31}
$$

where

$$
A(\epsilon, s, t, u) = \left[N^2 - 1\right]\left(-\frac{\mu^2}{t}\right)^\epsilon + \left(-\frac{\mu^2}{u}\right)^\epsilon - \left(-\frac{\mu^2}{s}\right)^\epsilon \tag{6.32}
$$

$$
B(\epsilon, s, t, u) = N\left[\left(-\frac{\mu^2}{t}\right)^\epsilon - \left(-\frac{\mu^2}{u}\right)^\epsilon\right] \tag{6.33}
$$

The matrix $I^{(1)}(\epsilon)$ acts directly as a rotation matrix on $|\mathcal{M}^{(0)}\rangle$ and $|\mathcal{M}^{(1,un)}\rangle$ in colour space, to give a new colour vector $|X\rangle$, equal to $I^{(1)}(\epsilon)|\mathcal{M}^{(0)}\rangle$, $I^{(1)}(\epsilon)I^{(1)}(\epsilon)|\mathcal{M}^{(0)}\rangle$ or $I^{(1)}(\epsilon)|\mathcal{M}^{(1,un)}\rangle$.

The contraction of the colour vector $|X\rangle$ with the conjugate tree amplitude obeys the rule

$$\langle \mathcal{M}^{(0)}|X\rangle = \sum_{\text{spins}} \sum_{\text{colours}} \sum_{i,j=1}^{9} \mathcal{T}_i^* X_j \mathcal{C}_i^* \mathcal{C}_j. \qquad (6.34)$$

In evaluating these contractions, we typically encounter $\sum_{\text{colours}} \mathcal{C}_i^* \mathcal{C}_j$ which is given by the ij component of the symmetric matrix $\mathcal{CC}$

$$\mathcal{CC} = \begin{pmatrix} N^2 & N \\ N & N^2 \end{pmatrix}, \qquad (6.35)$$

Similarly, we find that the interference of the tree-level amplitudes $\sum_{\text{spins}} \mathcal{T}_i^* \mathcal{T}_j$ is given by $\mathcal{TT}_{ij}$, where

$$\mathcal{TT} = 2\left(\frac{t^2 + u^2}{s^2} - \epsilon\right) \mathcal{V}^T \mathcal{V}, \qquad (6.36)$$

and the vector $\mathcal{V}$ is

$$\mathcal{V} = \left(1, -\frac{1}{N}\right), \qquad (6.37)$$

while the interference of the tree-level amplitudes with one-loop amplitudes $\sum_{\text{spins}} \mathcal{T}_i^* \mathcal{L}_j$ is given by $\mathcal{TL}_{ij}$, where

$$\mathcal{TL} = \mathcal{V}^T \mathcal{W}, \qquad (6.38)$$

and the vector $\mathcal{W}$ is

$$\mathcal{W} = \Big(\mathcal{L}_1(s,t,u), \ \mathcal{L}_2(s,t,u)\Big). \qquad (6.39)$$

Here the functions $\mathcal{L}_1$ and $\mathcal{L}_2$ are defined as

$$\begin{aligned}
\mathcal{L}_1(s,t,u) &= \frac{N^2 - 2}{2N} f(s,t,u) + \frac{1}{N} f(s,u,t) + 3\beta_0 \mathcal{T}(s,t,u) \frac{1-\epsilon}{3-2\epsilon} \text{Bub}(s) \\
&\quad + \frac{1}{2N} \frac{\mathcal{T}(s,t,u)}{\epsilon(3-2\epsilon)} \left[\left(N^2 - 1\right)\left(-6 + 7\epsilon + 2\epsilon^2\right) + 10\epsilon^2 - 4\epsilon^3\right] \text{Bub}(s) \quad (6.40) \\
\mathcal{L}_2(s,t,u) &= -\frac{1}{N}\mathcal{L}_1(s,u,t) + \frac{3}{2N^2}\left(f(s,t,u) - f(s,u,t)\right) \qquad (6.41)
\end{aligned}$$

where the function f is

$$\begin{aligned}
f(s,t,u) &= \left(\frac{4(u^2 + t^2) - 2\epsilon(3ut + 6t^2 + 5u^2) - \epsilon^2 s(7t + 5u)}{s^2}\right)\left(\frac{\text{Bub}(s) - \text{Bub}(t)}{\epsilon}\right) \\
&\quad + \frac{u(1-2\epsilon)(6t^2 + 2u^2 - 3\epsilon s^2)}{s^2}\text{Box}^6(s,t) \qquad (6.42)
\end{aligned}$$

and the tree type structure

$$\mathcal{T}(s,t,u) = 2\left(\frac{t^2 + u^2}{s^2} - \epsilon\right). \qquad (6.43)$$

These expressions are valid in all kinematic regions. However, to evaluate the pole structure in a particular region, the one-loop bubble graph Bub and the one-loop box

integral in $D = 6 - 2\epsilon$ dimensions, Box^6, must be expanded as a series in ϵ. This analytic expansion is given in Appendix B.

The function $\mathcal{H}_2$, that appears in eq. (6.5), exhibits only a single pole in ϵ and is given by

$$\mathcal{H}_2 \equiv \langle \mathcal{M}^{(0)} | \boldsymbol{H}^{(2)}(\epsilon) | \mathcal{M}^{(0)} \rangle = \frac{e^{\epsilon\gamma}}{2\,\epsilon\,\Gamma(1-\epsilon)} H^{(2)} \langle \mathcal{M}^{(0)} | \mathcal{M}^{(0)} \rangle \tag{6.44}$$

with

$$H^{(2)} = \left[\frac{1}{4}\gamma_{(1)} + 3C_F K + \frac{5}{2}\zeta_2\beta_0 C_F - \frac{28}{9}\beta_0 C_F - \left(\frac{16}{9} - 7\zeta_3 \right) C_F C_A \right] \tag{6.45}$$

and

$$\gamma_{(1)} = (-3 + 24\zeta_2 - 48\zeta_3)C_F^2 + \left(-\frac{17}{3} - \frac{88}{3}\zeta_2 + 24\zeta_3 \right) C_F C_A + \left(\frac{4}{3} + \frac{32}{3}\zeta_2 \right) C_F T_R N_F. \tag{6.46}$$

and ζ_n is the Riemann Zeta function with $\zeta_2 = \pi^2/6$ and $\zeta_3 = 1.202056\ldots$ We note that $H^{(2)}$ is renormalisation-scheme dependent and eq. (6.45) is valid in the $\overline{\text{MS}}$ scheme. We expect that in the four-quark two loop amplitude, we might obtain contributions from $\boldsymbol{H}^{(2)}$ for each of the six colour antennae.

It can be easily noted that the leading infrared singularity in Eq. (6.5) is $\mathcal{O}\left(1/\epsilon^4\right)$. It is a very stringent check on the reliability of our calculation that the pole structure obtained by computing the Feynman diagrams directly and introducing series expansions in ϵ for the scalar master integrals agrees with eq. (6.5) through to $\mathcal{O}\left(1/\epsilon\right)$. We therefore construct the finite remainder by subtracting eq. (6.5) from the full result.

6.2.2.2 Finite contributions

In this subsection, we give explicit expressions for the finite two-loop contribution to $\mathcal{A}^{8\ (2\times0)}$, $\mathcal{F}inite$ which is given by (see eq.(6.26) and eq.(6.5)

$$\mathcal{F}inite = \mathcal{A}^{8\ (2\times0)}(s,t,u) - \mathcal{P}oles \tag{6.47}$$

For high energy hadron-hadron collisions, we probe all parton-parton scattering processes simultaneously. We therefore need to be able to evaluate the finite parts in the s-, t- and u-channels corresponding to the processes,

$$q + \bar{q} \;\rightarrow\; \bar{q}' + q'$$
$$q + \bar{q}' \;\rightarrow\; q + \bar{q}'$$
$$q + q' \;\rightarrow\; q + q',$$

respectively. In principle, the analytic expressions for different channels are related by crossing symmetry. However, the Xbox has cuts in all three channels yielding complex parts in all physical regions. The analytic continuation is therefore rather involved and prone to error.

Due to this, we choose to give expressions describing $\mathcal{A}^{8\ (2\times0)}(s,t,u)$, $\mathcal{A}^{8\ (2\times0)}(t,s,u)$ and $\mathcal{A}^{8\ (2\times0)}(u,t,s)$ which are directly valid in the physical region, $s > 0$ and $u,t < 0$, and are given in terms of logarithms and polylogarithms that have no imaginary parts.

In channel c,

$$\mathcal{F}inite_c = V\left(N^2 A_c + B_c + \frac{1}{N^2}C_c + NN_F D_c + \frac{N_F}{N}E_c + N_F^2 F_c\right). \tag{6.48}$$

The values of A_c, B_c, C_c, D_c, E_c, and F_c, are presented in sections C.1.1.1 and C.1.2.1 of Appendix C.

We can check some of these results by comparing with the analytic expressions presented in ref.[71] for the QED process $e^+e^- \to \mu^+\mu^-$. Taking the QED limit correspond to setting $C_A = 0$, $C_F = 1$, $T_R = 1$ as well as setting the cubic Casimir $C_3 = (N^2-1)(N^2-2)/N^2 = 0$. This means that we can compare directly $E_s(\propto C_F T_R N_F)$ and $F_s(\propto T_R^2 N_F^2)$ but not C_s which receives contributions from both C_3 and C_F^2. We see that eqs.(C.5) and (C.6) agree with eqs.(2.38) and (2.39) of ref.[71].

6.2.3 One-loop self-interference contribution

We divide the one-loop self-interference contributions into into two classes, those that multiply poles in the dimensional regularisation parameter ϵ and those that are finite as $\epsilon \to 0$,

$$\mathcal{A}^{8\ (1\times1)}(s,t,u) = \mathcal{P}oles + \mathcal{F}inite. \tag{6.49}$$

$\mathcal{P}oles$ contains both infrared singularities and ultraviolet divergences. The latter are removed by renormalisation, while the former must be analytically cancelled by the infrared singularities occuring in radiative processes of the same order. The structure of these infrared divergences has been provided in eq.(6.7).

6.2.3.1 Infrared pole structure

Again, the pole structure of the one-loop self-interference given in eq.(6.7) involves the contraction of the colour vector $|X\rangle$ with the conjugate colour vector $\langle Y|$ obeys the rule

$$\langle Y|X\rangle = \sum_{\text{spins}} \sum_{\text{colours}} \sum_{i,j=1}^{9} Y_i^* X_j C_i^* C_j. \tag{6.50}$$

For the expansion of the pole structure coming from this contribution, eqs.(6.31) through to (6.43) are valid. This calculation is somewhat simpler than the two-loop one, nevertheless contributes at the same level.

It can be easily noted that the leading infrared singularity in eq. (6.7) is $\mathcal{O}\left(1/\epsilon^4\right)$. It is a very stringent check on the reliability of our calculation that the pole structure obtained by computing the Feynman diagrams directly and introducing series expansions in ϵ for the scalar master integrals agrees with eq. (6.7) up to and including $\mathcal{O}(1/\epsilon)$. We therefore construct the finite remainder by subtracting eq. (6.7) from the full result.

6.2.3.2   Finite contributions

The finite one-loop self-interference contribution to $\mathcal{A}^8(s,t,u)$ is defined as

$$\mathcal{F}inite(s,t,u) = \mathcal{A}^{8\,(1\times1)}(s,t,u) - \mathcal{P}oles(s,t,u), \qquad (6.51)$$

where we subtract the series expansions of both $\mathcal{A}^{8\,(1\times1)}(s,t,u)$ and $\mathcal{P}oles(s,t,u)$ and set $\epsilon \to 0$.

Then in channel c,

$$\mathcal{F}inite_c = V\left(N^2 A_c + B_c + \frac{1}{N^2}C_c + NN_F D_c + \frac{N_F}{N}E_c + N_F^2 F_c\right). \qquad (6.52)$$

The values of A_c, B_c, C_c, D_c, E_c, and F_c, are presented in sections C.1.1.2 and C.1.2.2 of Appendix C.

6.3   Like quark scattering

In this section we extend the work of section 6.2 to describe the case of identical quark scattering. We use the $\overline{\text{MS}}$ renormalisation scheme and conventional dimensional regularisation where all external particles are treated in D dimensions to provide dimensionally regularised and renormalised analytic expressions at the two-loop level for the scattering process

$$q\bar{q} \to q\bar{q},$$

together with the time-reversed and crossed processes

$$q + q \;\; \to \;\; q + q,$$
$$\bar{q} + \bar{q} \;\; \to \;\; \bar{q} + \bar{q}.$$

As in the unlike quark case, we present analytic expressions for the infrared pole structure, as well as explicit formulae for the finite remainder decomposed according to powers of the number of colours N and the number of light-quark flavours N_F.

6.3.1 Notation

For calculational convenience, we treat all particles as incoming so that

$$q(p_1) + \bar{q}(p_2) + q(p_3) + \bar{q}(p_4) \to 0. \tag{6.53}$$

The renormalised four point amplitude in the $\overline{\text{MS}}$ scheme is thus

$$
|\mathcal{M}\rangle = 4\pi\alpha_s \left[\left(|\mathcal{M}^{(0)}\rangle - |\overline{\mathcal{M}}^{(0)}\rangle \right) + \left(\frac{\alpha_s}{2\pi} \right) \left(|\mathcal{M}^{(1)}\rangle - |\overline{\mathcal{M}}^{(1)}\rangle \right) \right.
$$
$$
\left. + \left(\frac{\alpha_s}{2\pi} \right)^2 \left(|\mathcal{M}^{(2)}\rangle - |\overline{\mathcal{M}}^{(2)}\rangle \right) + \mathcal{O}\left(\alpha_s^3 \right) \right], \tag{6.54}
$$

where the $|\mathcal{M}^{(i)}\rangle$ represents the colour-space vector describing the i-loop amplitude for the s-channel graphs, and the t-channel contribution $|\overline{\mathcal{M}}^{(i)}\rangle$ is obtained by exchanging the roles of particles 2 and 4:

$$|\overline{\mathcal{M}}^{(i)}\rangle = |\mathcal{M}^{(i)}\rangle(2 \leftrightarrow 4). \tag{6.55}$$

The dependence on both renormalisation scale μ and renormalisation scheme is implicit.

We denote the squared amplitude summed over spins and colours by

$$
\begin{aligned}
\langle \mathcal{M} | \mathcal{M} \rangle &= \sum |\mathcal{M}(q + \bar{q} \to \bar{q} + q)|^2 \\
&= \mathcal{A}(s,t,u) + \mathcal{A}(t,s,u) + \mathcal{B}(s,t,u),
\end{aligned} \tag{6.56}
$$

The squared matrix elements for the $qq \to qq$ process are obtained by exchanging s and u

$$\sum |\mathcal{M}(q + q \to q + q)|^2 = \mathcal{A}(u,t,s) + \mathcal{A}(t,u,s) + \mathcal{B}(u,t,s). \tag{6.57}$$

The function $\mathcal{A}$ is related to the squared matrix elements for unlike quark scattering

$$\mathcal{A}(s,t,u) = \sum |\mathcal{M}(q + \bar{q} \to \bar{q}' + q')|^2 \tag{6.58}$$

$$\mathcal{A}(t,s,u) = \sum |\mathcal{M}(q + \bar{q}' \to \bar{q}' + q)|^2 \tag{6.59}$$

while $\mathcal{B}(s,t,u)$ represents the interference between s-channel and t-channel graphs that is only present for identical quark scattering.

The function $\mathcal{A}$ can be expanded perturbatively to yield

$$\mathcal{A}(s,t,u) = 16\pi^2\alpha_s^2 \left[\mathcal{A}^4(s,t,u) + \left(\frac{\alpha_s}{2\pi}\right)\mathcal{A}^6(s,t,u) + \left(\frac{\alpha_s}{2\pi}\right)^2 \mathcal{A}^8(s,t,u) + \mathcal{O}\left(\alpha_s^3\right)\right],$$

$$(6.60)$$

where

$$\mathcal{A}^4(s,t,u) = \langle\mathcal{M}^{(0)}|\mathcal{M}^{(0)}\rangle \equiv 2(N^2-1)\left(\frac{t^2+u^2}{s^2} - \epsilon\right), \qquad (6.61)$$

$$\mathcal{A}^6(s,t,u) = \left(\langle\mathcal{M}^{(0)}|\mathcal{M}^{(1)}\rangle + \langle\mathcal{M}^{(1)}|\mathcal{M}^{(0)}\rangle\right), \qquad (6.62)$$

$$\mathcal{A}^8(s,t,u) = \left(\langle\mathcal{M}^{(1)}|\mathcal{M}^{(1)}\rangle + \langle\mathcal{M}^{(0)}|\mathcal{M}^{(2)}\rangle + \langle\mathcal{M}^{(2)}|\mathcal{M}^{(0)}\rangle\right). \qquad (6.63)$$

Expressions for $\mathcal{A}^6$ are given in ref. [39] using dimensional regularisation to isolate the infrared and ultraviolet singularities. Analytical formulae for the two-loop contribution to $\mathcal{A}^8$, $\langle\mathcal{M}^{(0)}|\mathcal{M}^{(2)}\rangle + \langle\mathcal{M}^{(2)}|\mathcal{M}^{(0)}\rangle$, are given in ref. [40].

Similarly, the expansion of $\mathcal{B}$ can be written

$$\mathcal{B}(s,t,u) = 16\pi^2\alpha_s^2 \left[\mathcal{B}^4(s,t,u) + \left(\frac{\alpha_s}{2\pi}\right)\mathcal{B}^6(s,t,u) + \left(\frac{\alpha_s}{2\pi}\right)^2 \mathcal{B}^8(s,t,u) + \mathcal{O}\left(\alpha_s^3\right)\right],$$

$$(6.64)$$

where, in terms of the amplitudes, we have

$$\mathcal{B}^4(s,t,u) = -\left(\langle\overline{\mathcal{M}}^{(0)}|\mathcal{M}^{(0)}\rangle + \langle\mathcal{M}^{(0)}|\overline{\mathcal{M}}^{(0)}\rangle\right)$$
$$\equiv -4\left(\frac{N^2-1}{N}\right)(1-\epsilon)\left(\frac{u^2}{st} + \epsilon\right), \qquad (6.65)$$

$$\mathcal{B}^6(s,t,u) = -\left(\langle\overline{\mathcal{M}}^{(1)}|\mathcal{M}^{(0)}\rangle + \langle\mathcal{M}^{(0)}|\overline{\mathcal{M}}^{(1)}\rangle + \langle\overline{\mathcal{M}}^{(0)}|\mathcal{M}^{(1)}\rangle + \langle\mathcal{M}^{(1)}|\overline{\mathcal{M}}^{(0)}\rangle\right)$$

$$(6.66)$$

$$\mathcal{B}^8(s,t,u) = -\left(\langle\overline{\mathcal{M}}^{(1)}|\mathcal{M}^{(1)}\rangle + \langle\mathcal{M}^{(1)}|\overline{\mathcal{M}}^{(1)}\rangle\right.$$
$$\left. + \langle\overline{\mathcal{M}}^{(0)}|\mathcal{M}^{(2)}\rangle + \langle\mathcal{M}^{(2)}|\overline{\mathcal{M}}^{(0)}\rangle + \langle\mathcal{M}^{(0)}|\overline{\mathcal{M}}^{(2)}\rangle + \langle\overline{\mathcal{M}}^{(2)}|\mathcal{M}^{(0)}\rangle\right). $$

$$(6.67)$$

As before, expressions for $\mathcal{B}^6$ which are valid in conventional dimensional regularisation are given in ref. [39]. Here, in order to complete the calculation of the two-loop contribution to quark-quark scattering, we concentrate on the next-to-next-to-leading order contribution $\mathcal{B}^8$ which contains both the interference of the two-loop with tree graphs and the one-loop self-interference.

We provide explicit formulae for the ϵ-expansion of the two-loop contribution to the next-to-next-to-leading order term $\mathcal{B}^8(s,t,u)$. To distinguish between the genuine two-

loop contribution and the squared one-loop part, we decompose $\mathcal{B}^8$ as

$$\mathcal{B}^8 = \mathcal{B}^{8\ (2\times0)} + \mathcal{B}^{8\ (1\times1)}, \tag{6.68}$$

where

$$\mathcal{B}^{8\ (2\times0)} \equiv -\left(\langle\overline{\mathcal{M}}^{(0)}|\mathcal{M}^{(2)}\rangle + \langle\mathcal{M}^{(2)}|\overline{\mathcal{M}}^{(0)}\rangle + \langle\mathcal{M}^{(0)}|\overline{\mathcal{M}}^{(2)}\rangle + \langle\overline{\mathcal{M}}^{(2)}|\mathcal{M}^{(0)}\rangle\right)$$

$$\mathcal{B}^{8\ (1\times1)} \equiv -\left(\langle\overline{\mathcal{M}}^{(1)}|\mathcal{M}^{(1)}\rangle + \langle\mathcal{M}^{(1)}|\overline{\mathcal{M}}^{(1)}\rangle\right)$$

The former is discussed in section 6.3.2, while the latter in section 6.3.3.

6.3.2   Two-loop contribution

As before, we divide the two-loop contributions into two classes: those that multiply poles in the dimensional regularisation parameter ϵ and those that are finite as $\epsilon \to 0$

$$\mathcal{B}^{8\ (2\times0)}(s,t,u) = \mathcal{P}oles + \mathcal{F}inite. \tag{6.69}$$

$\mathcal{P}oles$ contains infrared singularities that will be analytically canceled by the infrared singularities occurring in radiative processes of the same order (ultraviolet divergences are removed by renormalisation). The structure of these infrared divergences has been provided in eq.(6.6).

6.3.2.1   Infrared pole structure

It is convenient to decompose $|\mathcal{M}^{(0)}\rangle$ and $|\mathcal{M}^{(1,un)}\rangle$ in terms of $SU(N)$ matrices in the fundamental representation, T^a, so that the tree amplitude may be written as [93, 36, 94, 95, 96, 97, 98]

$$\begin{aligned}|\mathcal{M}^{(0)}\rangle &= \sum_a \left(T_{ij}^a T_{kl}^a\right) \mathcal{A}_4^{\text{tree}}(1_q, 2_{\bar{q}}, 3_{q'}, 4_{\bar{q}'}) \\ &= \left(\delta_{il}\delta_{jk} - \frac{1}{N}\delta_{ij}\delta_{kl}\right) \mathcal{A}_4^{\text{tree}}(1_q, 2_{\bar{q}}, 3_{q'}, 4_{\bar{q}'})\end{aligned} \tag{6.70}$$

and

$$\begin{aligned}|\overline{\mathcal{M}}^{(0)}\rangle &= \sum_a \left(T_{il}^a T_{jk}^a\right) \bar{\mathcal{A}}_4^{\text{tree}}(1_q, 2_q, 3_{q'}, 4_{q'}) \\ &= \left(\delta_{ij}\delta_{kl} - \frac{1}{N}\delta_{il}\delta_{jk}\right) \bar{\mathcal{A}}_4^{\text{tree}}(1_q, 2_q, 3_{q'}, 4_{q'})\end{aligned} \tag{6.71}$$

while the one-loop amplitude has the form [33, 30, 82]

$$\begin{aligned}|\mathcal{M}^{(1,un)}\rangle &= \left(\delta_{il}\delta_{jk} - \frac{1}{N}\delta_{ij}\delta_{kl}\right) \mathcal{A}_{4;1}^{[1]}(1_q, 2_{\bar{q}}, 3_{q'}, 4_{\bar{q}'}) \\ &\quad + (\delta_{il}\delta_{jk}) \mathcal{A}_{4;2}^{[1]}(1_q, 2_{\bar{q}}, 3_{q'}, 4_{\bar{q}'})\end{aligned} \tag{6.72}$$

To evaluate Eq. (6.6) we find it convenient to express $|\mathcal{M}^{(0)}\rangle$ and $|\mathcal{M}^{(1,un)}\rangle$ as two-dimensional vectors in colour space

$$|\mathcal{M}^{(0)}\rangle = (\mathcal{T}_1, \mathcal{T}_2)^T, \tag{6.73}$$

$$|\mathcal{M}^{(1,un)}\rangle = (\mathcal{L}_1, \mathcal{L}_2)^T, \tag{6.74}$$

where T indicates the transpose vector. Here the $\mathcal{T}_i$ and $\mathcal{L}_i$ are the components of $|\mathcal{M}^{(0)}\rangle$ and $|\mathcal{M}^{(1,un)}\rangle$ in the colour space spanned by the basis

$$\mathcal{C}_1 = \delta_{il}\delta_{jk},$$

$$\mathcal{C}_2 = \delta_{ij}\delta_{kl},$$

whereas

$$|\overline{\mathcal{M}}^{(0)}\rangle = (\bar{\mathcal{T}}_1, \bar{\mathcal{T}}_2)^T \tag{6.75}$$

is spanned by the basis

$$\mathcal{C}_1 = \delta_{ij}\delta_{kl},$$

$$\mathcal{C}_2 = \delta_{il}\delta_{jk}.$$

The tree and loop amplitudes $\mathcal{T}_i$ and $\mathcal{L}_i$ are directly obtained in terms of $\mathcal{A}_4^{\text{tree}}$, $\mathcal{A}_{4;1}^{[1]}$, $\mathcal{A}_{4;3}^{[1]}$ and $\mathcal{A}_{4;1}^{[1/2]}$ by reading off from eqs. (6.70) and (6.72). As we will see, the amplitudes themselves are not required since we compute the interference of tree and loop amplitudes directly.

In the same colour basis, the infrared-singularity operator $\boldsymbol{I}^{(1)}(\epsilon)$ has the form

$$\boldsymbol{I}^{(1)}(\epsilon) = -\frac{e^{\epsilon\gamma}}{\Gamma(1-\epsilon)}\frac{1}{N}\left(\frac{1}{\epsilon^2}+\frac{3}{2\epsilon}\right) \times \left(\begin{array}{cc} A(\epsilon,s,t,u) & B(\epsilon,s,t,u) \\ B(\epsilon,t,s,u) & A(\epsilon,t,s,u) \end{array} \right) \tag{6.76}$$

where

$$A(\epsilon,s,t,u) = \left[N^2-1\right]\left(-\frac{\mu^2}{t}\right)^\epsilon + \left(-\frac{\mu^2}{u}\right)^\epsilon - \left(-\frac{\mu^2}{s}\right)^\epsilon \tag{6.77}$$

$$B(\epsilon,s,t,u) = N\left[\left(-\frac{\mu^2}{t}\right)^\epsilon - \left(-\frac{\mu^2}{u}\right)^\epsilon\right] \tag{6.78}$$

The matrix $\boldsymbol{I}^{(1)}(\epsilon)$ acts directly as a rotation matrix on $|\mathcal{M}^{(0)}\rangle$ and $|\mathcal{M}^{(1,un)}\rangle$ in colour space, to give a new colour vector $|X\rangle$, equal to $\boldsymbol{I}^{(1)}(\epsilon)|\mathcal{M}^{(0)}\rangle$, $\boldsymbol{I}^{(1)}(\epsilon)\boldsymbol{I}^{(1)}(\epsilon)|\mathcal{M}^{(0)}\rangle$ or $\boldsymbol{I}^{(1)}(\epsilon)|\mathcal{M}^{(1,un)}\rangle$.

Similar to the unlike quark scattering case, the contraction of the colour vector $|X\rangle$ with the conjugate tree amplitude obeys the rule

$$\langle\overline{\mathcal{M}}^{(0)}|X\rangle = \sum_{\text{spins}} \sum_{\text{colours}} \sum_{i,j=1}^{2} \bar{\mathcal{T}}_i^* X_j \mathcal{C}_i^* \mathcal{C}_j. \tag{6.79}$$

In evaluating these contractions, we typically encounter $\sum_{\text{colours}} \mathcal{C}_i^* \mathcal{C}_j$ which is given by the ij component of the symmetric matrix $\mathcal{CC}$

$$\mathcal{CC} = \begin{pmatrix} N & N^2 \\ N^2 & N \end{pmatrix}, \tag{6.80}$$

Similarly, we find that the interference of the tree-level amplitudes $\sum_{\text{spins}} \bar{\mathcal{T}}_i^* \mathcal{T}_j$ is given by $\mathcal{TT}_{ij}$, where

$$\mathcal{TT} = 2(1-e)\left(\frac{u^2}{st} + \epsilon\right) \mathcal{V}^T \mathcal{V}, \tag{6.81}$$

and the vector $\mathcal{V}$ is

$$\mathcal{V} = \left(1, -\frac{1}{N}\right), \tag{6.82}$$

while the interference of the tree-level amplitudes with one-loop amplitudes $\sum_{\text{spins}} \bar{\mathcal{T}}_i^* \mathcal{L}_j$ is given by $\mathcal{TL}_{ij}$, where

$$\mathcal{TL} = \mathcal{V}^T \mathcal{W}, \tag{6.83}$$

and the vector $\mathcal{W}$ is

$$\mathcal{W} = \Big(\mathcal{L}_1(s,t,u), \ \mathcal{L}_2(s,t,u)\Big). \tag{6.84}$$

The functions $\mathcal{L}_1$ and $\mathcal{L}_2$ are defined as

$$\begin{aligned}
\mathcal{L}_1(s,t,u) &= \frac{N^2-2}{2N} f_1(s,t,u) + \frac{1}{N} f_2(s,t,u) + 3\beta_0 \mathcal{T}(s,t,u)\frac{1-\epsilon}{3-2\epsilon}\text{Bub}(s) \\
&+ \frac{1}{2N}\frac{\mathcal{T}(s,t,u)}{\epsilon(3-2\epsilon)}\left[\left(N^2-1\right)\left(-6+7\epsilon+2\epsilon^2\right)+10\epsilon^2-4\epsilon^3\right]\text{Bub}(s) \quad (6.85)
\end{aligned}$$

$$\mathcal{L}_2(s,t,u) = -\frac{1}{N}\mathcal{L}_1(s,t,u) + \frac{N^2-1}{2N^2}\left(f_1(s,t,u)-f_2(s,t,u)\right) \tag{6.86}$$

where the functions f_1 and f_2 are

$$\begin{aligned}
f_1(s,t,u) &= \frac{2u}{st}(1-2\epsilon)\left[u^2+t^2-2\epsilon\left(t^2+s^2\right)+\epsilon^2 s^2\right]\text{Box}^6(s,t) \\
&+ \frac{2}{st}\left[2u^2-\epsilon\left(5s^2+6t^2+9st\right)+\left(2s^2+4t^2+st\right)\epsilon^2\right. \\
&\qquad\qquad \left.+\left(s^2+3st\right)\epsilon^3-st\epsilon^4\right]\left[\frac{\text{Bub}(s)-\text{Bub}(t)}{\epsilon}\right], \quad (6.87)
\end{aligned}$$

$$\begin{aligned}
f_2(s,t,u) &= \frac{2}{s}(1-2\epsilon)\left[2u^2-\epsilon\left(t^2+s^2+u^2\right)+3\epsilon^2 s^2+s^2\epsilon^3\right]\text{Box}^6(s,u) \\
&+ \frac{2}{st}\left[2u^2-\epsilon\left(6s^2+6t^2+10st\right)+\left(3s^2+4t^2+3st\right)\epsilon^2\right. \\
&\qquad\qquad \left.+\left(s^2+2st\right)\epsilon^3-st\epsilon^4\right]\left[\frac{\text{Bub}(s)-\text{Bub}(u)}{\epsilon}\right]. \quad (6.88)
\end{aligned}$$

and the tree type structure

$$\mathcal{T}(s,t,u) = 2(1-e)\left(\frac{u^2}{st}+\epsilon\right) \tag{6.89}$$

These expressions are valid in all kinematic regions. However, to evaluate the pole structure in a particular region, the one-loop bubble graph Bub and the one-loop box integral in $D = 6 - 2\epsilon$ dimensions, Box^6, must be expanded as a series in ϵ. This analytic expansion is given in Appendix B.

The function $\mathcal{H}_2$, that appears in eq. (6.6), exhibits only a single pole in ϵ and is given by

$$\mathcal{H}_2 \equiv \langle \mathcal{M}^{(0)} | \boldsymbol{H}^{(2)}(\epsilon) | \mathcal{M}^{(0)} \rangle = \frac{e^{\epsilon \gamma}}{2\,\epsilon\,\Gamma(1 - \epsilon)} H^{(2)} \langle \mathcal{M}^{(0)} | \mathcal{M}^{(0)} \rangle \qquad (6.90)$$

with

$$H^{(2)} = \left[\frac{1}{4}\gamma_{(1)} + 3C_F K + \frac{5}{2}\zeta_2\beta_0 C_F - \frac{28}{9}\beta_0 C_F - \left(\frac{16}{9} - 7\zeta_3 \right) C_F C_A \right] \qquad (6.91)$$

and

$$\gamma_{(1)} = (-3 + 24\zeta_2 - 48\zeta_3)C_F^2 + \left(-\frac{17}{3} - \frac{88}{3}\zeta_2 + 24\zeta_3 \right) C_F C_A + \left(\frac{4}{3} + \frac{32}{3}\zeta_2 \right) C_F T_R N_F. \qquad (6.92)$$

We note that $H^{(2)}$ is renormalisation-scheme dependent and eq. (6.91) is valid in the $\overline{\text{MS}}$ scheme. We expect that in the four-quark two loop amplitude, we might obtain contributions from $\boldsymbol{H}^{(2)}$ for each of the six colour antennae.

It can be easily noted that the leading infrared singularity in eq. (6.6) is $\mathcal{O}\left(1/\epsilon^4\right)$. It is a very stringent check on the reliability of our calculation that the pole structure obtained by computing the Feynman diagrams directly and introducing series expansions in ϵ for the scalar master integrals agrees with eq. (6.6) through to $\mathcal{O}\left(1/\epsilon\right)$. We therefore construct the finite remainder by subtracting Eq. (6.6) from the full result.

6.3.2.2 Finite contributions

In this subsection, we give explicit expressions for the finite two-loop contribution to $\mathcal{B}^{8\ (2 \times 0)}$, $\mathcal{F}inite$ which is given by (see eq.(6.69) and eq.(6.6)

$$\mathcal{F}inite = \mathcal{B}^{8\ (2 \times 0)}(s, t, u) - \mathcal{P}oles \qquad (6.93)$$

The identical-quark processes probed in high-energy hadron-hadron collisions are the mixed s- and t-channel process

$$q + \bar{q} \to \bar{q} + q,$$

controlled by $\mathcal{B}(s, t, u)$ (as well as the distinct quark matrix elements $\mathcal{A}(s, t, u)$ and $\mathcal{A}(t, s, u)$ as indicated in eq. (6.57)), and the mixed t- and u-channel processes

$$q + q \ \to \ q + q,$$
$$\bar{q} + \bar{q} \ \to \ \bar{q} + \bar{q},$$

which are determined by the $\mathcal{B}(t, s, u)$. We need to be able to evaluate the finite parts for each of these processes. Of course, the analytic expressions for different channels are related by crossing symmetry. However, the master crossed boxes have cuts in all three channels yielding complex parts in all physical regions. The analytic continuation is therefore rather involved and prone to error. We therefore choose to give expressions describing $\mathcal{B}^8(s, t, u)$ and $\mathcal{B}^8(t, s, u)$ which are directly valid in the physical region $s > 0$ and $u, t < 0$, and are given in terms of logarithms and polylogarithms that have no imaginary parts.

In channel c

$$\mathcal{F}inite_c = \left(\frac{N^2 - 1}{N}\right)\left(N^2 A_c + B_c + \frac{1}{N^2}C_c + NN_F D_c + \frac{N_F}{N}E_c + N_F^2 F_c\right). \qquad (6.94)$$

Here $c = st$ (ut) to denote the mixed s- and t-channel (u- and t-channel) processes respectively. The values of A_c, B_c, C_c, D_c, E_c, and F_c, are presented in sections C.2.1.1 and C.2.2.1 of Appendix C.

6.3.3 One-loop self-interference contribution

We divide the one-loop self-interference contributions into into two classes, those that multiply poles in the dimensional regularisation parameter ϵ and those that are finite as $\epsilon \to 0$,

$$\mathcal{B}^{8\ (1\times1)}(s, t, u) = \mathcal{P}oles + \mathcal{F}inite. \qquad (6.95)$$

$\mathcal{P}oles$ contains both infrared singularities and ultraviolet divergences. The latter are removed by renormalisation, while the former must be analytically cancelled by the infrared singularities occuring in radiative processes of the same order. The structure of these infrared divergences has been provided in eq.(6.8).

6.3.3.1 Infrared pole structure

Again, the pole structure of the one-loop self-interference given in eq.(6.8) involves the contraction of the colour vector $|X\rangle$ with the conjugate colour vector $\langle Y|$ obeys the rule

$$\langle Y|X\rangle = \sum_{\text{spins}} \sum_{\text{colours}} \sum_{i,j=1}^{9} Y_i^* X_j C_i^* C_j. \qquad (6.96)$$

For the expansion of the pole structure coming from this contribution, eqs.(6.76) through to (6.89) are valid. This calculation is somewhat simpler than the two-loop one, nevertheless it contributes at the same level.

6.3.3.2   Finite contributions

The finite one-loop self-interference contribution to $\mathcal{B}^8(s,t,u)$ is defined as

$$\mathcal{F}inite(s,t,u) = \mathcal{B}^{8\,(1\times1)}(s,t,u) - \mathcal{P}oles(s,t,u), \qquad (6.97)$$

where we subtract the series expansions of both $\mathcal{B}^{8\,(1\times1)}(s,t,u)$ and $\mathcal{P}oles(s,t,u)$ and set $\epsilon \to 0$.

Then in channel c,

$$\mathcal{F}inite_c = \frac{V}{N}\left(N^2 A_c + B_c + \frac{1}{N^2}C_c + N N_F D_c + \frac{N_F}{N}E_c + N_F^2 F_c\right). \qquad (6.98)$$

The values of A_c, B_c, C_c, D_c, E_c, and F_c, are presented in sections C.2.1.2 and C.2.2.2 of Appendix C.

6.4   Quark-gluon scattering

In this section, we address the $\mathcal{O}\left(\alpha_s^4\right)$ one- and two-loop corrections to the QCD process

$$q + \bar{q} \to g + g, \qquad (6.99)$$

together with the time-reversed and crossed processes

$$q + g \;\; \to \;\; q + g, \qquad (6.100)$$

$$g + \bar{q} \;\; \to \;\; g + \bar{q}, \qquad (6.101)$$

$$g + g \;\; \to \;\; q + \bar{q}. \qquad (6.102)$$

As is in the previous sections, we use the $\overline{\text{MS}}$ renormalisation scheme to remove the ultraviolet singularities and conventional dimensional regularisation, where all external particles are treated in D dimensions. We provide expressions for both the interference of tree-level and two-loop graphs as well as the self-interference of one-loop amplitudes.

Also in this section, we give explicit analytic expressions valid for each of the processes of eqs. (6.99)–(6.102) in terms of logarithms and polylogarithms that are real in the physical domain.

6.4.1   Notation

For calculational purposes, the process we consider is

$$q(p_1) + \bar{q}(p_2) + g(p_3) + g(p_4) \to 0, \qquad (6.103)$$

The renormalised four point amplitude in the $\overline{\text{MS}}$ scheme is thus

$$|\mathcal{M}\rangle \;=\; 4\pi\alpha_s\left[|\mathcal{M}^{(0)}\rangle + \left(\frac{\alpha_s}{2\pi}\right)|\mathcal{M}^{(1)}\rangle + \left(\frac{\alpha_s}{2\pi}\right)^2|\mathcal{M}^{(2)}\rangle + \mathcal{O}\left(\alpha_s^3\right)\right],$$

(6.104)

where the $|\mathcal{M}^{(i)}\rangle$ represents the colour-space vector describing the i-loop amplitude. The dependence on both renormalisation scale μ and renormalisation scheme is implicit.

We denote the squared amplitude summed over spins and colours by

$$\langle\mathcal{M}|\mathcal{M}\rangle = \sum |\mathcal{M}(q + \bar{q} \to g + g)|^2 = \mathcal{C}(s,t,u).$$

(6.105)

which is symmetric under the exchange of t and u.

The squared matrix elements for the crossed processes are obtained by exchanging the Mandelstam variables and introducing a minus sign for each quark change between initial and final states

$$\sum |\mathcal{M}(g + g \to q + \bar{q})|^2 \;=\; \mathcal{C}(s,t,u),$$

(6.106)

$$\sum |\mathcal{M}(q + g \to q + g)|^2 \;=\; -\mathcal{C}(u,t,s),$$

(6.107)

$$\sum |\mathcal{M}(g + \bar{q} \to g + \bar{q})|^2 \;=\; -\mathcal{C}(u,t,s).$$

(6.108)

The function $\mathcal{C}$ can be expanded perturbatively to yield

$$\mathcal{C}(s,t,u) \;=\; 16\pi^2\alpha_s^2\left[\mathcal{C}^4(s,t,u) + \left(\frac{\alpha_s}{2\pi}\right)\mathcal{C}^6(s,t,u) + \left(\frac{\alpha_s}{2\pi}\right)^2\mathcal{C}^8(s,t,u) + \mathcal{O}\left(\alpha_s^3\right)\right],$$

(6.109)

where

$$\mathcal{C}^4(s,t,u) \;=\; \langle\mathcal{M}^{(0)}|\mathcal{M}^{(0)}\rangle =$$
$$=\; 2\frac{N^2-1}{N}(1-\epsilon)\left(\frac{N^2-1}{ut} - 2\frac{N^2}{s^2}\right)\left(t^2 + u^2 - \epsilon s^2\right),$$

(6.110)

$$\mathcal{C}^6(s,t,u) \;=\; \left(\langle\mathcal{M}^{(0)}|\mathcal{M}^{(1)}\rangle + \langle\mathcal{M}^{(1)}|\mathcal{M}^{(0)}\rangle\right),$$

(6.111)

$$\mathcal{C}^8(s,t,u) \;=\; \left(\langle\mathcal{M}^{(1)}|\mathcal{M}^{(1)}\rangle + \langle\mathcal{M}^{(0)}|\mathcal{M}^{(2)}\rangle + \langle\mathcal{M}^{(2)}|\mathcal{M}^{(0)}\rangle\right).$$

(6.112)

Expressions for $\mathcal{C}^6$ are given in ref. [39] using dimensional regularisation to isolate the infrared and ultraviolet singularities.

In the following sections, we present expressions for the infrared singular and finite contributions to $\mathcal{C}^8$ and the crossed processes. For convenience, we divide $\mathcal{C}^8(s,t,u)$ into two pieces

- the pure two-loop contributions

$$\mathcal{C}^{8\,(2\times0)}(s,t,u) = \langle\mathcal{M}^{(0)}|\mathcal{M}^{(2)}\rangle + \langle\mathcal{M}^{(2)}|\mathcal{M}^{(0)}\rangle, \tag{6.113}$$

described in sec. 6.4.2 and

- the self-interference of the one-loop amplitude

$$\mathcal{C}^{8\,(1\times1)}(s,t,u) = \langle\mathcal{M}^{(1)}|\mathcal{M}^{(1)}\rangle, \tag{6.114}$$

described in sec. 6.4.3.

For simplicity the arbitrary vectors for the axial gauge we use in this process are $n_3^\mu = p_4^\mu$ and $n_4^\mu = p_3^\mu$.

6.4.2 Two-loop contribution

We further decompose the two-loop contributions as a sum of two terms

$$\mathcal{C}^{8\,(2\times0)}(s,t,u) = \mathcal{P}oles(s,t,u) + \mathcal{F}inite(s,t,u). \tag{6.115}$$

$\mathcal{P}oles$ contains infrared singularities that will be analytically canceled by the infrared singularities occurring in radiative processes of the same order (ultraviolet divergences are removed by renormalisation), which is given by eq. (6.5). $\mathcal{F}inite$ is the remainder which is finite as $\epsilon \to 0$.

6.4.2.1   Infrared pole structure

It is convenient to decompose $|\mathcal{M}^{(0)}\rangle$ and $|\mathcal{M}^{(1,un)}\rangle$ in terms of $SU(N)$ matrices in the fundamental representation, T^a, so that the tree amplitude may be written as [93, 36, 94, 95, 96, 97, 98]

$$|\mathcal{M}^{(0)}\rangle = \sum_{P(4)} (T^{a_3}T^{a_4})_{ij}\, \mathcal{A}_4^{\text{tree}}(1_q, 2_{\bar{q}}, 3, 4), \tag{6.116}$$

while the one-loop amplitude has the form [33, 30, 82]

$$\begin{aligned}
|\mathcal{M}^{(1,un)}\rangle &= N \sum_{P(4)} (T^{a_3}T^{a_4})_{ij}\, \mathcal{A}_{4;1}^{[1]}(1_q, 2_{\bar{q}}, 3, 4) \\
&+ \text{Tr}\,(T^{a_3}T^{a_4})\, \delta_{ij} \mathcal{A}_{4;3}^{[1]}(1_q, 2_{\bar{q}}, 3, 4) \\
&+ N_F \left[\sum_{P(4)} (T^{a_3}T^{a_4}) - \frac{2}{N}\text{Tr}\,(T^{a_3}T^{a_4})\, \delta_{ij}\right] \mathcal{A}_{4;4}^{[1/2]}(1_q, 2_{\bar{q}}, 3, 4). \tag{6.117}
\end{aligned}$$

In these expressions $\sum_{P(4)}$ runs over the 2 permutations of indices of gluons 3 and 4 as it is further detailed in eq. (6.120). We note that the tree subamplitudes are further

related by cyclic and reflection properties as well as by the dual Ward identity [36, 94, 81] and more general identities [88, 99], while the subleading-colour loop amplitudes $\mathcal{A}_{4;3}^{[1]}$ are related to the leading-colour amplitudes $\mathcal{A}_{4;1}^{[1]}$ [33, 30, 82]. Some of these relationships are made explicit using an alternative basis in terms of $SU(N)$ matrices in the adjoint representation [87].

To evaluate eq. (6.5) we find it convenient to express $|\mathcal{M}^{(0)}\rangle$ and $|\mathcal{M}^{(1,un)}\rangle$ as three-dimensional vectors in colour space

$$|\mathcal{M}^{(0)}\rangle = (\mathcal{T}_1,\ 0,\ \mathcal{T}_2)^T\,, \tag{6.118}$$

$$|\mathcal{M}^{(1,un)}\rangle = (\mathcal{L}_1,\ \mathcal{L}_2,\ \mathcal{L}_3)^T\,, \tag{6.119}$$

where ^{T} indicate the transpose vector. Here the $\mathcal{T}_i$ and $\mathcal{L}_i$ are the components of $|\mathcal{M}^{(0)}\rangle$ and $|\mathcal{M}^{(1,un)}\rangle$ in the colour space spanned by the (non-orthogonal) basis

$$
\begin{aligned}
\mathcal{C}_1 &= (T^{a_3}T^{a_4})_{ij}\,, \\
\mathcal{C}_2 &= (T^{a_4}T^{a_3})_{ij}\,, \\
\mathcal{C}_3 &= \mathrm{Tr}\,(T^{a_3}T^{a_4})\,\delta_{ij},
\end{aligned} \tag{6.120}
$$

The tree and loop amplitudes $\mathcal{T}_i$ and $\mathcal{L}_i$ are directly obtained in terms of $\mathcal{A}_4^{\mathrm{tree}}$, $\mathcal{A}_{4;1}^{[1]}$, $\mathcal{A}_{4;3}^{[1]}$ and $\mathcal{A}_{4;1}^{[1/2]}$ by reading off from Eqs. (6.116) and (6.117). As we will see, the amplitudes themselves are not required since we compute the interference of tree and loop amplitudes directly.

In the same colour basis, the infrared-singularity operator $\boldsymbol{I}^{(1)}(\epsilon)$ has the form

$$\boldsymbol{I}^{(1)}(\epsilon) = \frac{e^{\epsilon\gamma}}{\Gamma(1-\epsilon)} \quad \times \quad \begin{pmatrix} \boldsymbol{A}(\epsilon,s,t,u) & \boldsymbol{D}(\epsilon,s,t,u) & 0 \\ \boldsymbol{B}(\epsilon,s,t,u) & \boldsymbol{C}(\epsilon,s) & \boldsymbol{B}(\epsilon,s,u,t) \\ 0 & \boldsymbol{D}(\epsilon,s,u,t) & \boldsymbol{A}(\epsilon,s,u,t) \end{pmatrix} \tag{6.121}$$

where

$$
\begin{aligned}
\boldsymbol{A}(\epsilon,s,t,u) &= -\left(\frac{1}{\epsilon^2}+\frac{3}{2\epsilon}\right)\left[N\left(-\frac{\mu^2}{u}\right)^{\epsilon}+C_F\left(-\frac{\mu^2}{s}\right)^{\epsilon}\right] \\
&\quad + N\left(\frac{\beta_0}{2N\epsilon}-\frac{3}{4\epsilon}\right)\left[\left(-\frac{\mu^2}{s}\right)^{\epsilon}+\left(-\frac{\mu^2}{u}\right)^{\epsilon}\right]
\end{aligned} \tag{6.122}
$$

$$\boldsymbol{B}(\epsilon,s,t,u) = \left(\frac{1}{\epsilon^2}+\frac{3}{4\epsilon}+\frac{\beta_0}{2N\epsilon}\right)\left[\left(-\frac{\mu^2}{t}\right)^{\epsilon}-\left(-\frac{\mu^2}{s}\right)^{\epsilon}\right] \tag{6.123}$$

$$\boldsymbol{C}(\epsilon,s) = -\left[\left(\frac{1}{\epsilon^2}+\frac{3}{2\epsilon}\right)C_F+\left(\frac{1}{\epsilon^2}+\frac{\beta_0}{N\epsilon}\right)N\right]\left(-\frac{\mu^2}{s}\right)^{\epsilon} \tag{6.124}$$

$$\boldsymbol{D}(\epsilon,s,t,u) = \left(\frac{1}{\epsilon^2}+\frac{3}{4\epsilon}+\frac{\beta_0}{2N\epsilon}\right)\left[\left(-\frac{\mu^2}{t}\right)^{\epsilon}-\left(-\frac{\mu^2}{u}\right)^{\epsilon}\right] \tag{6.125}$$

The matrix $I^{(1)}(\epsilon)$ acts directly as a rotation matrix on $|\mathcal{M}^{(0)}\rangle$ and $|\mathcal{M}^{(1,un)}\rangle$ in colour space, to give a new colour vector $|X\rangle$, equal to $I^{(1)}(\epsilon)|\mathcal{M}^{(0)}\rangle$, $I^{(1)}(\epsilon)I^{(1)}(\epsilon)|\mathcal{M}^{(0)}\rangle$ or $I^{(1)}(\epsilon)|\mathcal{M}^{(1,un)}\rangle$.

The contraction of the colour vector $|X\rangle$ with the conjugate tree amplitude obeys the rule

$$\langle \mathcal{M}^{(0)}|X\rangle = \sum_{\text{spins}} \sum_{\text{colours}} \sum_{i,j=1}^{9} \mathcal{T}_i^* X_j \, \mathcal{C}_i^* \, \mathcal{C}_j. \tag{6.126}$$

In evaluating these contractions, we typically encounter $\sum_{\text{colours}} \mathcal{C}_i^* \mathcal{C}_j$ which is given by the ij component of the symmetric matrix $\mathcal{CC}$

$$\mathcal{CC} = \frac{V}{4N} \begin{pmatrix} V & N & -1 \\ N & N^2 & N \\ -1 & N & V \end{pmatrix}, \tag{6.127}$$

Similarly, we find that the interference of the tree-level amplitudes $\sum_{\text{spins}} \mathcal{T}_i^* \mathcal{T}_j$ is given by $\mathcal{TT}_{ij}$, where

$$\mathcal{TT} = \frac{8(1-\epsilon)(t^2 + u^2 - \epsilon s^2)}{s^2 tu} \mathcal{V}^T \mathcal{V}, \tag{6.128}$$

and the vector $\mathcal{V}$ is

$$\mathcal{V} = (t, \ 0, \ u), \tag{6.129}$$

while the interference of the tree-level amplitudes with one-loop amplitudes $\sum_{\text{spins}} \mathcal{T}_i^* \mathcal{L}_j$ is given by $\mathcal{TL}_{ij}$, where

$$\mathcal{TL} = \mathcal{V}^T \mathcal{W}, \tag{6.130}$$

and the vector $\mathcal{W}$ is

$$\mathcal{W} = \Big(\mathcal{L}_1(s,t,u), \ \mathcal{L}_2, \ \mathcal{L}_1(s,u,t) \Big), \tag{6.131}$$

where

$$\mathcal{L}_2 = \ell_2(s,t,u) + \ell_2(s,u,t) \tag{6.132}$$

and

$$\begin{aligned} \mathcal{L}_1(s,t,u) &= \frac{N^2+1}{N} f_2(s,t,u) - \frac{1}{Nu} f_1(s,u,t) + f_3(s,t,u) \\ &\quad - 3\beta_0 \frac{(1-\epsilon)}{3-2\epsilon} \frac{1}{u} \mathcal{T}(s,t,u) \, \text{Bub}(s) \\ &\quad - \epsilon(1-2\epsilon) \left[\frac{N}{\epsilon^2} \text{Bub}(u) + \frac{N}{2} \left(\frac{1}{\epsilon^2} - \frac{2\beta_0}{N\epsilon} + \frac{3}{2\epsilon} \right) \text{Bub}(s) \right. \\ &\quad \left. - \frac{1}{2N} \left(\frac{1}{\epsilon^2} + \frac{3}{2\epsilon} \right) \text{Bub}(s) \right] \frac{1}{u} \mathcal{T}(s,t,u) \end{aligned} \tag{6.133}$$

$$\begin{aligned} \ell_2(s,t,u) &= 4(1-2\epsilon)\frac{1}{tu} \left[t^2 + u^2 + \left(ut - 2t^2 - 2u^2 \right)\epsilon + \left(t^2 + u^2 + 3ut \right)\epsilon^2 \right] \text{Box}^6(t,u) \\ &\quad + \left(\frac{1}{\epsilon} - 2 \right) [\text{Bub}(t) - \text{Bub}(s)] \frac{1}{u} \mathcal{T}(s,t,u) + \frac{1}{t} f_1(s,t,u). \end{aligned} \tag{6.134}$$

The infrared-finite functions f_1, f_2 and f_3 are

$$
\begin{aligned}
f_1(s,t,u) &= 4(1-2\epsilon)\frac{1}{s^2}\Big[u\left(2u^2+5t^2+3tu\right)+\epsilon\left(3t^3-4u^3-3tu^2\right)\\
&\quad -\epsilon^2 s\left(4t^2+2u^2+5tu\right)+s^2 t\epsilon^3\Big]\mathrm{Box}^6(s,t) \qquad (6.135)
\end{aligned}
$$

$$
\begin{aligned}
f_2(s,t,u) &= 4(1-2\epsilon)\frac{1}{s^2 u}\Big[(t-u)\left(t^2+2u^2+tu\right)+\epsilon\left(-2t^3+ut^2+4tu^2+5u^3\right)\\
&\quad -s^3\epsilon^2\Big]\mathrm{Box}^6(s,u) \qquad (6.136)
\end{aligned}
$$

$$
\begin{aligned}
f_3(s,t,u) &= -2(1-\epsilon)\frac{1}{su}\Big\{\frac{V}{N}\Big[2s-t-\epsilon(2s-3u)-3s\epsilon^2\Big]\\
&\quad +4N(u-u\epsilon+s\epsilon^2)\Big\}\,[\mathrm{Bub}(u)-\mathrm{Bub}(s)]\\
&\quad +\frac{2}{s^2 u(1-\epsilon)(3-2\epsilon)}\Big\{-N\Big[18u^2+15t^2-3t(s-t)\\
&\quad -\epsilon\left(78u^2-36t(s-t)+st\right)+\epsilon^2\left(80u^2+10s(s-t)-69st\right)\Big]\\
&\quad -\frac{1}{N}\Big[-24u^2+3tu-21t^2+\epsilon\left(85u^2-43t(s-t)+3st\right)\\
&\quad -\epsilon^2\left(112u^2+6s(s-t)-109st\right)\Big]+\beta_0\Big[20s^2-40tu\\
&\quad -2\epsilon\left(38s^2-3us-62tu\right)+4\epsilon^2\left(27s^2-26tu\right)\Big]\Big\}\,\epsilon\mathrm{Bub}(s)+\mathcal{O}(\epsilon^3)
\end{aligned}
$$

$$(6.137)$$

and the tree type structure

$$
\mathcal{T}(s,t,u) = 8(1-\epsilon)\frac{t^2+u^2-\epsilon s^2}{s^2} \qquad (6.138)
$$

These expressions are valid in all kinematic regions. However, to evaluate the pole structure in a particular region, the one-loop bubble graph Bub and the one-loop box integral in $D = 6-2\epsilon$ dimensions, Box^6, must be expanded as a series in ϵ. This analytic expansion is given in Appendix B.

The function $\mathcal{H}_2$, that appears in Eq. (6.5), exhibits only a single pole in ϵ and is given by

$$
\mathcal{H}_2 \equiv \langle\mathcal{M}^{(0)}|\boldsymbol{H}^{(2)}(\epsilon)|\mathcal{M}^{(0)}\rangle = \frac{e^{\epsilon\gamma}}{4\,\epsilon\,\Gamma(1-\epsilon)}H^{(2)}\langle\mathcal{M}^{(0)}|\mathcal{M}^{(0)}\rangle \qquad (6.139)
$$

where the constant $H^{(2)}$ is

$$
\begin{aligned}
H^{(2)} &= \left(\zeta_3+\frac{5}{6}+\frac{11}{72}\pi^2\right)C_A^2 + \left(13\,\zeta_3+\frac{245}{108}-\frac{23}{24}\pi^2\right)C_A\,C_F+\frac{10}{27}N_F^2\\
&\quad +\left(-\frac{\pi^2}{36}-\frac{58}{27}\right)C_A\,N_F + \left(\frac{\pi^2}{12}+\frac{29}{54}\right)N_F\,C_F+\left(-\frac{3}{4}+\pi^2-12\,\zeta_3\right)C_F^2,
\end{aligned}
$$

$$(6.140)$$

We note that $H^{(2)}$ is renormalisation-scheme dependent and eq. (6.140) is valid in the $\overline{\mathrm{MS}}$ scheme. We also note that eq. (6.140) differs from the corresponding expressions found in

the singularity structure of two-loop quark-quark scattering in all but the C_F^2 coefficient. This is due to the presence of infrared emissions from gluons which modify the terms involving either C_A or N_F.

It can be easily noted that the leading infrared singularity in Eq. (6.5) is $\mathcal{O}\left(1/\epsilon^4\right)$. It is a very stringent check on the reliability of our calculation that the pole structure obtained by computing the Feynman diagrams directly and introducing series expansions in ϵ for the scalar master integrals agrees with eq. (6.5) through to $\mathcal{O}\left(1/\epsilon\right)$. We therefore construct the finite remainder by subtracting eq. (6.5) from the full result.

6.4.2.2 Finite contributions

In this subsection, we give explicit expressions for the finite two-loop contribution to $\mathcal{C}^{8\ (2\times0)}$, $\mathcal{F}inite$ which is given by (see eq.(6.115) and eq.(6.5))

$$\mathcal{F}inite = \mathcal{C}^{8\ (2\times0)}(s,t,u) - \mathcal{P}oles \tag{6.141}$$

In hadronic collisions, all parton scattering processes (eqs. (6.99)–(6.102)) contribute simultaneously. We therefore need to evaluate $\mathcal{F}inite(s,t,u)$ for the $q\bar{q} \to gg$ and $gg \to q\bar{q}$ process (which we denote as the s-channel since, although the tree-level process contains graphs in all three channels, the squared tree matrix elements are proportional to $1/s^2$) and $\mathcal{F}inite(u,t,s)$ for the QCD Compton processes $qg \to qg$ and $g\bar{q} \to g\bar{q}$ (which we label as the u-channel).

Of course, the analytic expressions for the various processes are related by crossing symmetry. However, the master crossed boxes have cuts in all three channels yielding complex parts in all physical regions. The analytic continuation is therefore rather involved and prone to error. We therefore choose to give expressions describing $\mathcal{C}^8(s,t,u)$ and $\mathcal{C}^8(u,t,s)$ which are directly valid in the physical region $s > 0$ and $u,t < 0$, and are given in terms of logarithms and polylogarithms that have no imaginary parts.

In the generic c-channel we write

$$
\begin{aligned}
\mathcal{F}inite_c(s,t,u) \;=\; V\Bigg(& N^3 A_c + N B_c + \frac{1}{N}C_c + \frac{1}{N^3}D_c + N_F N^2 E_c \\
& + N_F F_c + \frac{N_F}{N^2}G_c + N_F^2 N H_c + \frac{N_F^2}{N}I_c \Bigg)
\end{aligned}
\tag{6.142}
$$

The values of A_c, B_c, C_c, D_c, E_c, F_c, G_c, H_c and I_c are presented in sections C.3.1.1 and C.3.2.1 of Appendix C.

6.4.3 One-loop self-interference contribution

We divide the one-loop self-interference contributions into into two classes, those that multiply poles in the dimensional regularisation parameter ϵ and those that are finite as $\epsilon \to 0$,

$$\mathcal{C}^{8\ (1\times1)}(s,t,u) = \mathcal{P}oles + \mathcal{F}inite. \qquad (6.143)$$

$\mathcal{P}oles$ contains both infrared singularities and ultraviolet divergences. The latter are removed by renormalisation, while the former must be analytically cancelled by the infrared singularities occuring in radiative processes of the same order. The structure of these infrared divergences has been provided in eq.(6.7).

6.4.3.1 Infrared pole structure

Again, the pole structure of the one-loop self-interference given in eq.(6.7) involves the contraction of the colour vector $|X\rangle$ with the conjugate colour vector $\langle Y|$ obeys the rule

$$\langle Y|X\rangle = \sum_{\text{spins}} \sum_{\text{colours}} \sum_{i,j=1}^{9} Y_i^* X_j C_i^* C_j. \qquad (6.144)$$

For the expansion of the pole structure coming from this contribution, eqs.(6.121) through to (6.138) are valid. This calculation is somewhat simpler than the two-loop one, nevertheless it contributes at the same level.

It can be easily noted that the leading infrared singularity in eq. (6.7) is $\mathcal{O}\left(1/\epsilon^4\right)$. It is a very stringent check on the reliability of our calculation that the pole structure obtained by computing the Feynman diagrams directly and introducing series expansions in ϵ for the scalar master integrals agrees with eq. (6.7) up to and including $\mathcal{O}\left(1/\epsilon\right)$. We therefore construct the finite remainder by subtracting eq. (6.7) from the full result.

6.4.3.2 Finite contributions

The finite one-loop self-interference contribution to $\mathcal{C}^8(s,t,u)$ is defined as

$$\mathcal{F}inite(s,t,u) = \mathcal{C}^{8\ (1\times1)}(s,t,u) - \mathcal{P}oles(s,t,u), \qquad (6.145)$$

where we subtract the series expansions of both $\mathcal{C}^{8\,(1\times1)}(s,t,u)$ and $\mathcal{P}oles(s,t,u)$ and set $\epsilon \to 0$.

Then in channel c,

$$\mathcal{F}inite_c(s,t,u) = V\left(N^3 A_c + N B_c + \frac{1}{N} C_c + \frac{1}{N^3} D_c + N_F N^2 E_c \right.$$
$$\left. + N_F F_c + \frac{N_F}{N^2} G_c + N_F^2 N H_c + \frac{N_F^2}{N} I_c \right) \qquad (6.146)$$

The values of A_c, B_c, C_c, D_c, E_c, F_c, G_c, H_c and I_c are presented in sections C.3.1.2 and C.3.2.2 of Appendix C.

6.5 Gluon-gluon scattering

It is the goal of this section to provide analytic expressions for the $\mathcal{O}\left(\alpha_s^4\right)$ two-loop and one-loop corrections to gluon-gluon scattering

$$g + g \rightarrow g + g. \tag{6.147}$$

6.5.1 Notation

For calculational purposes, the process we consider is

$$g(p_1) + g(p_2) + g(p_3) + g(p_4) \rightarrow 0, \tag{6.148}$$

where the gluons are all incoming with light-like momenta. The gluons also carry colour indexes, a_i, in the adjoint representation.

We denote the squared amplitude summed over spins and colours by

$$\langle \mathcal{M}|\mathcal{M} \rangle = \sum |\mathcal{M}(g + g \rightarrow g + g)|^2 = \mathcal{D}(s,t,u). \tag{6.149}$$

which is symmetric under the exchange of s, t and u. The function $\mathcal{D}$ can be expanded perturbatively to yield

$$\mathcal{D}(s,t,u) \;=\; 16\pi^2\alpha_s^2 \left[\mathcal{D}^4(s,t,u) + \left(\frac{\alpha_s}{2\pi}\right) \mathcal{D}^6(s,t,u) + \left(\frac{\alpha_s}{2\pi}\right)^2 \mathcal{D}^8(s,t,u) + \mathcal{O}\left(\alpha_s^3\right) \right], \tag{6.150}$$

where

$$
\begin{aligned}
\mathcal{D}^4(s,t,u) &= \langle \mathcal{M}^{(0)}|\mathcal{M}^{(0)} \rangle \\
&= 16\, VN^2(1-\epsilon)^2 \left(3 - \frac{ut}{s^2} - \frac{us}{t^2} - \frac{st}{u^2} \right), \tag{6.151}
\end{aligned}
$$

$$\mathcal{D}^6(s,t,u) = \left(\langle \mathcal{M}^{(0)}|\mathcal{M}^{(1)} \rangle + \langle \mathcal{M}^{(1)}|\mathcal{M}^{(0)} \rangle \right), \tag{6.152}$$

$$\mathcal{D}^8(s,t,u) = \left(\langle \mathcal{M}^{(1)}|\mathcal{M}^{(1)} \rangle + \langle \mathcal{M}^{(0)}|\mathcal{M}^{(2)} \rangle + \langle \mathcal{M}^{(2)}|\mathcal{M}^{(0)} \rangle \right). \tag{6.153}$$

Expressions for $\mathcal{D}^6$ are given in ref. [39] using dimensional regularisation to isolate the infrared and ultraviolet singularities.

In the following sections, we present expressions for the infrared singular and finite two-loop contributions to $\mathcal{D}^8$

$$\mathcal{D}^{8\,(2\times 0)}(s,t,u) = \langle \mathcal{M}^{(0)}|\mathcal{M}^{(2)} \rangle + \langle \mathcal{M}^{(2)}|\mathcal{M}^{(0)} \rangle. \tag{6.154}$$

and the self-interference of the one-loop amplitudes

$$\mathcal{D}^{8\,(1\times1)}(s,t,u) = \langle \mathcal{M}^{(1)} | \mathcal{M}^{(1)} \rangle. \tag{6.155}$$

For simplicity the arbitrary vectors for the axial gauge we use in this process are $n_1^\mu = p_2^\mu$, $n_2^\mu = p_1^\mu$, $n_3^\mu = p_4^\mu$ and $n_4^\mu = p_3^\mu$.

6.5.2 Two-loop contribution

We further decompose the two-loop contributions as a sum of two terms

$$\mathcal{D}^{8\,(2\times0)}(s,t,u) = \mathcal{P}oles(s,t,u) + \mathcal{F}inite(s,t,u). \tag{6.156}$$

$\mathcal{P}oles$ contains infrared singularities that will be analytically canceled by those occurring in radiative processes of the same order (ultraviolet divergences are removed by renormalisation) and is given by eq. (6.5). $\mathcal{F}inite$ is the remainder which is finite as $\epsilon \to 0$.

6.5.2.1 Infrared pole structure

It is convenient to decompose $|\mathcal{M}^{(0)}\rangle$ and $|\mathcal{M}^{(1,un)}\rangle$ in terms of $SU(N)$ matrices in the fundamental representation, T^a, so that the tree amplitude may be written as [93, 36, 94, 95, 96, 97, 98]

$$|\mathcal{M}^{(0)}\rangle = \sum_{P(2,3,4)} \mathrm{Tr}\,(T^{a_1} T^{a_2} T^{a_3} T^{a_4})\, \mathcal{A}_4^{\mathrm{tree}}(1,2,3,4), \tag{6.157}$$

while the one-loop amplitude has the form [33, 30, 82]

$$\begin{aligned}
|\mathcal{M}^{(1,un)}\rangle &= N \sum_{P(2,3,4)} \mathrm{Tr}\,(T^{a_1} T^{a_2} T^{a_3} T^{a_4})\, \mathcal{A}_{4;1}^{[1]}(1,2,3,4) \\
&+ \sum_{Q(2,3,4)} \mathrm{Tr}\,(T^{a_1} T^{a_2})\,\mathrm{Tr}\,(T^{a_3} T^{a_4})\, \mathcal{A}_{4;3}^{[1]}(1,2,3,4) \\
&+ N_F \sum_{P(2,3,4)} \mathrm{Tr}\,(T^{a_1} T^{a_2} T^{a_3} T^{a_4})\, \mathcal{A}_{4;1}^{[1/2]}(1,2,3,4).
\end{aligned} \tag{6.158}$$

In these expressions $\sum_{P(2,3,4)}$ runs over the 6 permutations of indices of gluons 2, 3 and 4 while $\sum_{Q(2,3,4)}$ includes the three choices of pairs of indices, as it is further detailed in eq. (6.161). We note that the tree subamplitudes are further related by cyclic and reflection properties as well as by the dual Ward identity [36, 94, 81] and more general identities [88, 99], while the subleading-colour loop amplitudes $\mathcal{A}_{4;3}^{[1]}$ are related to the leading-colour amplitudes $\mathcal{A}_{4;1}^{[1]}$ [33, 30, 82]. Some of these relationships are made explicit using an alternative basis in terms of $SU(N)$ matrices in the adjoint representation [87].

To evaluate eq. (6.5) we find it convenient to express $|\mathcal{M}^{(0)}\rangle$ and $|\mathcal{M}^{(1,un)}\rangle$ as nine-dimensional vectors in colour space

$$|\mathcal{M}^{(0)}\rangle = (\mathcal{T}_1,\ \mathcal{T}_2,\ \mathcal{T}_3,\ \mathcal{T}_4,\ \mathcal{T}_5,\ \mathcal{T}_6,\ 0,\ 0,\ 0)^T, \qquad (6.159)$$

$$|\mathcal{M}^{(1,un)}\rangle = (\mathcal{L}_1,\ \mathcal{L}_2,\ \mathcal{L}_3,\ \mathcal{L}_4,\ \mathcal{L}_5,\ \mathcal{L}_6,\ \mathcal{L}_7,\ \mathcal{L}_8,\ \mathcal{L}_9)^T, \qquad (6.160)$$

where T indicate the transpose vector. Here the $\mathcal{T}_i$ and $\mathcal{L}_i$ are the components of $|\mathcal{M}^{(0)}\rangle$ and $|\mathcal{M}^{(1,un)}\rangle$ in the colour space spanned by the (non-orthogonal) basis

$$
\begin{aligned}
\mathcal{C}_1 &= \text{Tr}\left(T^{a_1}T^{a_2}T^{a_3}T^{a_4}\right), \\[4pt]
\mathcal{C}_2 &= \text{Tr}\left(T^{a_1}T^{a_2}T^{a_4}T^{a_3}\right), \\[4pt]
\mathcal{C}_3 &= \text{Tr}\left(T^{a_1}T^{a_4}T^{a_2}T^{a_3}\right), \\[4pt]
\mathcal{C}_4 &= \text{Tr}\left(T^{a_1}T^{a_3}T^{a_2}T^{a_4}\right), \\[4pt]
\mathcal{C}_5 &= \text{Tr}\left(T^{a_1}T^{a_3}T^{a_4}T^{a_2}\right), \\[4pt]
\mathcal{C}_6 &= \text{Tr}\left(T^{a_1}T^{a_4}T^{a_3}T^{a_2}\right), \\[4pt]
\mathcal{C}_7 &= \text{Tr}\left(T^{a_1}T^{a_2}\right)\text{Tr}\left(T^{a_3}T^{a_4}\right), \\[4pt]
\mathcal{C}_8 &= \text{Tr}\left(T^{a_1}T^{a_3}\right)\text{Tr}\left(T^{a_2}T^{a_4}\right), \\[4pt]
\mathcal{C}_9 &= \text{Tr}\left(T^{a_1}T^{a_4}\right)\text{Tr}\left(T^{a_2}T^{a_3}\right).
\end{aligned}
\qquad (6.161)
$$

The tree and loop amplitudes $\mathcal{T}_i$ and $\mathcal{L}_i$ are directly obtained in terms of $\mathcal{A}_4^{\text{tree}}$, $\mathcal{A}_{4;1}^{[1]}$, $\mathcal{A}_{4;3}^{[1]}$ and $\mathcal{A}_{4;1}^{[1/2]}$ by reading off from eqs. (6.157) and (6.158). As we will see, the amplitudes themselves are not required since we compute the interference of tree and loop amplitudes directly.

In the same colour basis, the infrared-singularity operator $\boldsymbol{I}^{(1)}(\epsilon)$ has the form

$$
\boldsymbol{I}^{(1)}(\epsilon) = -\frac{e^{\epsilon\gamma}}{\Gamma(1-\epsilon)}\left(\frac{1}{\epsilon^2}+\frac{\beta_0}{N\epsilon}\right)
$$

$$
\times
\begin{pmatrix}
N(\text{S}+\text{T}) & 0 & 0 & 0 & 0 & 0 & (\text{T}-\text{U}) & 0 & (\text{S}-\text{U}) \\
0 & N(\text{S}+\text{U}) & 0 & 0 & 0 & 0 & (\text{U}-\text{T}) & (\text{S}-\text{T}) & 0 \\
0 & 0 & N(\text{T}+\text{U}) & 0 & 0 & 0 & 0 & (\text{T}-\text{S}) & (\text{U}-\text{S}) \\
0 & 0 & 0 & N(\text{T}+\text{U}) & 0 & 0 & 0 & (\text{T}-\text{S}) & (\text{U}-\text{S}) \\
0 & 0 & 0 & 0 & N(\text{S}+\text{U}) & 0 & (\text{U}-\text{T}) & (\text{S}-\text{T}) & 0 \\
0 & 0 & 0 & 0 & 0 & N(\text{S}+\text{T}) & (\text{T}-\text{U}) & 0 & (\text{S}-\text{U}) \\
(\text{S}-\text{U}) & (\text{S}-\text{T}) & 0 & 0 & (\text{S}-\text{T}) & (\text{S}-\text{U}) & 2N\text{S} & 0 & 0 \\
0 & (\text{U}-\text{T}) & (\text{U}-\text{S}) & (\text{U}-\text{S}) & (\text{U}-\text{T}) & 0 & 0 & 2N\text{U} & 0 \\
(\text{T}-\text{U}) & 0 & (\text{T}-\text{S}) & (\text{T}-\text{S}) & 0 & (\text{T}-\text{U}) & 0 & 0 & 2N\text{T}
\end{pmatrix}
$$

$$(6.16$$

where

$$S = \left(-\frac{\mu^2}{s}\right)^\epsilon, \qquad T = \left(-\frac{\mu^2}{t}\right)^\epsilon, \qquad U = \left(-\frac{\mu^2}{u}\right)^\epsilon. \qquad (6.163)$$

The matrix $I^{(1)}(\epsilon)$ acts directly as a rotation matrix on $|\mathcal{M}^{(0)}\rangle$ and $|\mathcal{M}^{(1,un)}\rangle$ in colour space, to give a new colour vector $|X\rangle$, equal to $I^{(1)}(\epsilon)|\mathcal{M}^{(0)}\rangle$, $I^{(1)}(\epsilon)I^{(1)}(\epsilon)|\mathcal{M}^{(0)}\rangle$ or $I^{(1)}(\epsilon)|\mathcal{M}^{(1,un)}\rangle$.

The contraction of the colour vector $|X\rangle$ with the conjugate tree amplitude obeys the rule

$$\langle\mathcal{M}^{(0)}|X\rangle = \sum_{\text{spins}} \sum_{\text{colours}} \sum_{i,j=1}^{9} \mathcal{T}_i^* X_j \, \mathcal{C}_i^* \, \mathcal{C}_j. \qquad (6.164)$$

In evaluating these contractions, we typically encounter $\sum_{\text{colours}} \mathcal{C}_i^* \, \mathcal{C}_j$ which is given by the ij component of the symmetric matrix $\mathcal{CC}$

$$\mathcal{CC} = \frac{V}{16N^2} \begin{pmatrix} C_1 & C_2 & C_2 & C_2 & C_2 & C_3 & NV & -N & NV \\ C_2 & C_1 & C_2 & C_2 & C_3 & C_2 & NV & NV & -N \\ C_2 & C_2 & C_1 & C_3 & C_2 & C_2 & -N & NV & NV \\ C_2 & C_2 & C_3 & C_1 & C_2 & C_2 & -N & NV & NV \\ C_2 & C_3 & C_2 & C_2 & C_1 & C_2 & NV & NV & -N \\ C_3 & C_2 & C_2 & C_2 & C_2 & C_1 & NV & -N & NV \\ NV & NV & -N & -N & NV & NV & N^2V & N^2 & N^2 \\ -N & NV & NV & NV & NV & -N & N^2 & N^2V & N^2 \\ NV & -N & NV & NV & -N & NV & N^2 & N^2 & N^2V \end{pmatrix}, \qquad (6.165)$$

with

$$C_1 = N^4 - 3N^2 + 3, \qquad C_2 = 3 - N^2, \qquad C_3 = 3 + N^2. \qquad (6.166)$$

Similarly, we find that the interference of the tree-level amplitudes $\sum_{\text{spins}} \mathcal{T}_i^* \mathcal{T}_j$ is given by $\mathcal{TT}_{ij}$, where

$$\mathcal{TT} = \frac{64(1-\epsilon)^2(t^2 + ut + u^2)^2}{s^2 t^2 u^2} \, \mathcal{V}^T \mathcal{V}, \qquad (6.167)$$

and the vector $\mathcal{V}$ is

$$\mathcal{V} = (u, \ t, \ s, \ s, \ t, \ u, \ 0, \ 0, \ 0), \qquad (6.168)$$

while the interference of the tree-level amplitudes with one-loop amplitudes $\sum_{\text{spins}} \mathcal{T}_i^* \mathcal{L}_j$ is given by $\mathcal{TL}_{ij}$, where

$$\mathcal{TL} = \mathcal{V}^T \mathcal{W}, \qquad (6.169)$$

and the vector $\mathcal{W}$ is

$$\mathcal{W} = \Big(\mathcal{F}(s,t), \ \mathcal{F}(s,u), \ \mathcal{F}(u,t), \ \mathcal{F}(u,t), \ \mathcal{F}(s,u), \ \mathcal{F}(s,t), \ \mathcal{G}, \ \mathcal{G}, \ \mathcal{G}\Big). \qquad (6.170)$$

Here the function $\mathcal{F}(s,t)$ is symmetric under the exchange of s and t, while $\mathcal{G}$ is symmetric under the exchange of any two Mandelstam invariants, so that

$$\mathcal{F}(s,t) \;=\; f_1(s,t,u) + f_1(t,s,u), \tag{6.171}$$

$$\mathcal{G} \;=\; f_2(s,t,u) + f_2(s,u,t) + f_2(t,s,u) + f_2(t,u,s) + f_2(u,s,t) + f_2(u,t,s). \tag{6.172}$$

Here f_1 and f_2 are given in terms of the one-loop box integral in $D = 6 - 2\epsilon$ dimensions and the one-loop bubble graph in $D = 4 - 2\epsilon$,

$$
\begin{aligned}
f_1(s,t,u) \;=\; & \frac{16N(1-2\epsilon)}{s^2 t^2}\left[2(1-\epsilon)^2\left(s^4 + s^3 t + s t^3 + t^4\right) + 3(1-5\epsilon)s^2 t^2\right]\mathrm{Box}^6(s,t) \\
& + \frac{8N_F(1-2\epsilon)}{st}\left[(1-\epsilon)^2\left(s^2 + t^2\right) + \epsilon(1+3\epsilon)st\right]\mathrm{Box}^6(s,t) \\
& - \frac{16N(1-\epsilon)}{s^2 t^2 u \epsilon(3-2\epsilon)}\Bigg[\left(12 - 22\epsilon + 12\epsilon^2 + 2\epsilon^3\right)s^4 + \left(24 - 58\epsilon + 50\epsilon^2 - 6\epsilon^3 - 2\epsilon^4\right)s^3 t \\
& \qquad + \left(36 - 99\epsilon + 93\epsilon^2 - 24\epsilon^3 - 2\epsilon^4\right)s^2 t^2 + (1-\epsilon)\left(24 - 50\epsilon + 23\epsilon^2\right)st^3 \\
& \qquad + 4(1-\epsilon)(1-2\epsilon)(3-2\epsilon)t^4\Bigg]\mathrm{Bub}(t) \\
& + \frac{16N_F}{st^2 u(3-2\epsilon)}\Bigg[\left(4 - 12\epsilon + 16\epsilon^2 - 4\epsilon^3\right)s^3 + \left(3 - 10\epsilon + 23\epsilon^2 - 8\epsilon^3\right)s^2 t \\
& \qquad + \left(6 - 15\epsilon + 21\epsilon^2 - 8\epsilon^3\right)st^2 + (1-\epsilon)\left(5 - 6\epsilon + 2\epsilon^2\right)t^3\Bigg]\mathrm{Bub}(t), \tag{6.173}
\end{aligned}
$$

$$
\begin{aligned}
f_2(s,t,u) \;=\; & \frac{32(1-2\epsilon)}{u^2}\left[-4(1-\epsilon)^2 st + 3(1-5\epsilon)u^2\right]\mathrm{Box}^6(u,t) \\
& + \frac{32(1-\epsilon)}{\epsilon s u^2}\Big[4(1-2\epsilon)(1-\epsilon)t^2 + (8-17\epsilon)(1-\epsilon)ut \\
& \qquad + \left(6 - 20\epsilon + 15\epsilon^2 + \epsilon^3\right)u^2\Big]\mathrm{Bub}(s). \tag{6.174}
\end{aligned}
$$

Series expansions around $\epsilon = 0$ for the one-loop integrals are given in Appendix B.

Finally, the last term of eq. (6.5) that involves $\boldsymbol{H}^{(2)}(\epsilon)$ produces only a single pole in ϵ and is given by

$$\langle\mathcal{M}^{(0)}|\boldsymbol{H}^{(2)}(\epsilon)|\mathcal{M}^{(0)}\rangle = \frac{e^{\epsilon\gamma}}{4\,\epsilon\,\Gamma(1-\epsilon)}H^{(2)}\langle\mathcal{M}^{(0)}|\mathcal{M}^{(0)}\rangle \tag{6.175}$$

where the constant $H^{(2)}$ is

$$H^{(2)} = \left(2\zeta_3 + \frac{5}{3} + \frac{11}{36}\pi^2\right)N^2 + \frac{20}{27}N_F^2 + \left(-\frac{\pi^2}{18} - \frac{89}{27}\right)NN_F - \frac{N_F}{N}, \tag{6.176}$$

We note that $H^{(2)}$ is renormalisation-scheme dependent and eq. (6.176) is valid in the $\overline{\mathrm{MS}}$ scheme. We also note that eq. (6.176) differs from the corresponding expressions found in the singularity structure of two-loop quark-quark and quark-gluon scattering. This is due to double emissions from the gluons. In fact, $H^{(2)}$ for quark-gluon scattering is

the average of the $H^{(2)}$ for gluon-gluon scattering and quark-quark scattering, as may be expected by counting the number of different types of radiating partons.

It can be easily noted that the leading infrared singularity in eq. (6.5) is $\mathcal{O}\left(1/\epsilon^4\right)$. It is a very stringent check on the reliability of our calculation that the pole structure obtained by computing the Feynman diagrams directly and introducing series expansions in ϵ for the scalar master integrals agrees with eq. (6.5) through to $\mathcal{O}\left(1/\epsilon\right)$. We therefore construct the finite remainder by subtracting eq. (6.5) from the full result.

6.5.2.2 Finite contributions

The finite two-loop contribution to $\mathcal{D}^8(s,t,u)$ is defined as

$$\mathcal{F}inite(s,t,u) = \mathcal{D}^{8\,(2\times 0)}(s,t,u) - \mathcal{P}oles(s,t,u), \tag{6.177}$$

where we subtract the series expansions of both $\mathcal{D}^{8\,(2\times0)}(s,t,u)$ and $\mathcal{P}oles(s,t,u)$ and set $\epsilon \to 0$.

Then

$$Finite(s,t,u) = V\left(N^4 A + N^2 B + N^3 N_F C + N N_F D + N^2 N_F^2 E + N_F^2 F\right), \tag{6.178}$$

and the values of A, B, C, D, E and F are presented in section C.4.1 of Appendix C.

6.5.3 One-loop self-interference contribution

We divide the one-loop self-interference contributions into into two classes, those that multiply poles in the dimensional regularisation parameter ϵ and those that are finite as $\epsilon \to 0$,

$$\mathcal{D}^{8\,(1\times1)}(s,t,u) = \mathcal{P}oles + \mathcal{F}inite. \tag{6.179}$$

$\mathcal{P}oles$ contains both infrared singularities and ultraviolet divergences. The latter are removed by renormalisation, while the former must be analytically cancelled by the infrared singularities occuring in radiative processes of the same order. The structure of these infrared divergences has been provided in eq.(6.7).

6.5.3.1 Infrared pole structure

The contraction of the colour vector $|X\rangle$ with the conjugate colour vector $\langle Y|$ obeys the rule

$$\langle Y|X\rangle = \sum_{\text{spins}} \sum_{\text{colours}} \sum_{i,j=1}^{9} Y_i^* X_j C_i^* C_j. \tag{6.180}$$

In evaluating these contractions, we typically encounter $\sum_{\text{colours}} C_i^* C_j$ which is given by eq.(6.165).

For the expansion of the pole structure coming from this contribution, eqs.(6.162) through to (6.174) are valid. This calculation is somewhat simpler than the two-loop one, but it is nevertheless contributing at the same level.

It can be easily noted that the leading infrared singularity in eq. (6.7) is $\mathcal{O}\left(1/\epsilon^4\right)$. It is a very stringent check on the reliability of our calculation that the pole structure obtained by computing the Feynman diagrams directly and introducing series expansions in ϵ for the scalar master integrals agrees with eq. (6.7) up to and including $\mathcal{O}\left(1/\epsilon\right)$. We therefore construct the finite remainder by subtracting eq. (6.7) from the full result.

6.5.3.2 Finite contributions

The finite two-loop contribution to $\mathcal{D}^8(s,t,u)$ is defined as

$$\mathcal{F}inite(s,t,u) = \mathcal{D}^{8\,(1\times1)}(s,t,u) - \mathcal{P}oles(s,t,u), \tag{6.181}$$

where we subtract the series expansions of both $\mathcal{D}^{8\,(1\times1)}(s,t,u)$ and $\mathcal{P}oles(s,t,u)$ and set $\epsilon \to 0$.

Then

$$Finite(s,t,u) = V\left(N^4 A + N^2 B + N^3 N_F C + N N_F D + N^2 N_F^2 E + N_F^2 F + \frac{N_F^2}{N^2} G\right), \tag{6.182}$$

and the values of A, B, C, D, E, F and G are presented in section C.4.2 of Appendix C.

Chapter 7 | *Conclusions*

7.1 Summary

The main driving force of this thesis has been to accomplish the calculation of all two-loop matrix elements for massless partonic $2 \to 2$ scattering processes. This is one of the major tasks required for the construction of numerical programs that will enable next-to-next-to leading order QCD estimates of jet production at hadron colliders. This calculation is expected to increase the quality of the theoretical predictions to a level that matches that of the improved experimental accuracy expected in forthcoming runs at the Tevatron and LHC.

To achieve the calculation of matrix elements at this level of accuracy is highly non trivial and it becomes clear that it is necessary to construct an algorithm to calculate hundreds of one- and two-loop integrals with a tensor structure.

In order to create such algorithm, we first need to study how these integrals arise within perturbative QCD and what is their characteristic structure and analytic behaviour. So, in Chapter 1 we discussed their direct relation to the Feynman diagrams contributing to the matrix elements at this order and their divergent behaviour in $D = 4$ dimensions. We saw (section 1.4) how Convensional Dimensional Regularisation (CDR) is used to expose these divergences as poles in the small non-integer parameter $\epsilon = 0$, when we continue the dimension as $D = 4 \to D = 4 - 2\epsilon$.

The singularities of Feynman integrals arise in two different momentum limits, the ultraviolet or high momentum limit (UV singularities) and the infrared or low momentum limit (IR singularities). The former type of singularities can be consistently absorbed at each order in perturbation series using a redefinition of the parameters and fields of the theory (section 1.5). This procedure is called renormalisation and it is not uniquely defined, so that any fixed order perturbative calculation result will depend on the prescription used for the absorption of the UV singularities. In all our calculations we have chosen to renormalise in the $\overline{\text{MS}}$ scheme.

Our calculations involve massless particles, so for some loop-configurations their prop-

agators vanish and give rise to IR singularities. In Chapter 2 we use the example of electron-positron annihilation into hadrons as a didactic aid to show how these divergences arise and cancel at next-to-leading order (section 2.1). This naturally leads to the more general discussion on cancellation of IR divergences for appropriately defined infrared safe observables (section 2.2). To put our calculation of NNLO matrix elements in context, we establish the link between these and the total hadronic cross section using factorisation (section 2.3) and provide some ideas as to the areas where such a calculation has an impact (section 2.4).

We then progress to Chapter 3, where we provide an overview on various methods used in the calculation of loop integrals. We start with the classification of the integrals by their topology and give a general representation for both the planar and the non-planar topologies (section 3.1). Then, we revise the different techniques for solving loop integrals explicitly, such as Mellin-Barnes and Negative Dimensions, with a preamble on the parametric forms used to represent the integrals in a suitable manner prior to their integration (section 3.2). The second half of this Chapter is dedicated to the exploration of a simple loop integration mechanism through systems of equations (section 3.3). This is the backbone of the algorithm with which we perform our calculations because it produces an environment in which loop integrals can be treated in a general and automated way. Some simple examples provide an insight on how these reduction equations work in practise. We conclude the Chapter with a discussion on how we could deal with tensor structure in Feynman integrals by replacing them with extra dimensions and extra powers in the propagators. It turns out that this only complicates the problem of solving tensorial integrals so we need to provide a better solution, which leads to the discussion of the next Chapter (section 3.4).

Given that the two-loop matrix element calculation involves a large number of scalar and tensor integrals, the need arises for an algorithm that can deal with them systematically. Furthermore, the algorithm must be able to reduce an arbitrary integral in terms of the ones we can calculate using the techniques given in the previous Chapter. This is precisely what our program for calculating matrix elements does and the characteristic elements we build into it are discussed in Chapter 4. We use the Integration by Parts (IBP) and Lorentz Invariance (LI) identities to find relations between a generic integral and the more basic (and already calculated) master integrals (section 4.1). Then we make an automatic implementation of this algorithm by generating all the identities spanning the range of tensors and powers of propagators we require and solve the system of equa-

tions using a computer program (section 4.2). A particular choice of double box master integrals, makes for a further improvement to the reduction algorithm (section 4.3). Near the end of the Chapter we discuss the solution of the new set of double box master integrals in terms of the previous one and close with the description of the general algorithm we use for the explicit matrix element calculations (section 4.4).

An independent check on the singular structure of the results is presented in the last Chapter, via the Catani formalism. This is briefly discussed in Chapter 5 and to illustrate the importance and limitations of this formalism we give a couple of examples. Chapter 6 contains the $\mathcal{O}(\alpha_s^4)$ one- and two-loop matrix elements for massless partonic $2 \rightarrow 2$ scattering. The fact that the singular structure of our results agrees with the predictions stemming from Catani's formalism is a very strong check of our explicit calculation where we made extensive use of the reduction algorithm previously discussed. This is an important verification due to the fact that typically all of the Feynman diagrams contribute to the divergent behaviour.

The results presented in this last Chapter [40, 41, 42, 43, 44, 45] provide the matrix elements needed for the NNLO contribution to inclusive jet production at hadron colliders. This moves us one step closer in the process of achieving an improved theoretical description of the high energy jet phenomena in the experimental runs to come.

7.2   Outlook

The algorithm we use to calculate NNLO matrix elements is, in principle, suitable for multi-loop calculations with integrals that have a rich tensor structure as well as extra powers on the propagators. In practice, there is a limitation due to computer resources such as memory and CPU time, directly linked to the large systems of equations we need to solve for such integrals. The number of terms in each equation grows even more if we want to consider the case with, say a massive external leg for $Z^* \rightarrow 3$ *jets*. Both the manipulation and solution of the system of equations in this case, is a major stumbling block in the path to obtain analytic matrix elements.

However, recent developments in the implementation of reduction algorithms that take different approaches to this problem and use different platforms and languages, may prove to be the solution for such important calculations. Tarasov [100], Gehrmann and Remiddi [63], and Laporta [101, 102] have provided various schemes for the automation of reduction algorithms.

Not only can the general reduction algorithm be improved, but also the numerical or analytic calculation of the master integrals. Binoth and Heinrich [58], for example, have proposed an algorithm for the isolation and removal of the poles given a Feynman representation of a loop integral and to proceed afterwards with the numerical evaluation of the finite integral. Gehrmann and Remiddi [67, 68, 69, 103] presented a method based on the analytic solution, in terms of generalised harmonic polylogarithms, of differential equations satisfied by the master integrals. Furthermore, Tarasov [100] and Laporta [102, 101], have set out to calculate master integrals using difference equations that arise from IBP identities, providing an algorithm that can also be automated.

These improvements will enable us to go further in the calculation of matrix elements which are vital ingredients for the NNLO predictions for jet cross sections in hadron collisions. However, they are insufficient to make physical predictions. A major task, still to be established for semi-inclusive jet cross sections, is a systematic procedure for analytically cancelling the IR divergences between the tree-level $2 \to 4$, the one-loop $2 \to 3$ and the $2 \to 2$ processes. Recent progress in determining the singular limits of matrix elements [29, 79, 104, 80, 88, 105, 106, 83, 86, 107, 84, 82] together with the analytic cancellation of these singularities in the case of $e^+e^- \to photon + jet$ at NLO [108], suggest that the technical problems for $2 \to 2$ scattering processes are not far from being solved.

We should note that a further complication is due to initial state radiation, since the factorisation of the collinear singularities from the incoming partons requires the evolution of the parton density functions to be known to an accuracy that matches the one from the hard scattering matrix element. This requires the knowledge of the three-loop splitting functions and in this field there are several recent results that should be noted here [22, 21, 23, 24, 27, 26, 25, 28].

Much work remains to be done, but looking at the latest results in different areas within the context of higher order corrections to jet cross sections, seems that NNLO numerical estimates of these may become available in the next couple of years. The theoretical uncertainties at this order will be smaller than the already existing NLO estimates thereby enabling improved descriptions of high energy QCD phenomena.

Appendix A

Integration over

phase-space

In this Appendix we present the D-dimensional integration over phase-space for the production of 2 and 3 particles.

A.1 2 particles in the final state

Consider the Lorentz invariant phase space factor given (in the centre of mass frame) by

$$\int d\Phi_2 = \frac{(2\pi)^D}{2^2[(2\pi)^{D-1}]^2} \int \int \frac{d\vec{p_1}}{E_1} \frac{d\vec{p_2}}{E_2} \, \delta^{(D-1)}(\vec{p_1} + \vec{p_2}) \, \delta^{(1)}(E_{tot} - E_1 - E_2), \qquad (A.1)$$

where

$$
\begin{aligned}
\vec{p_i} &\quad : \quad \text{momentum vector in } D - 1 \text{ dimensions,} \\
E_{tot} &\quad : \quad \text{incoming total energy in the CM frame } E_{tot} = \sqrt{s}, \\
(2\pi)^D &\quad : \quad \text{normalisation for each delta function,} \\
2^2[(2\pi)^{D-1}]^2 &\quad : \quad \text{for each momentum vector (normalisation} \\
&\qquad\quad \text{of volume element).}
\end{aligned}
$$

We use the delta function for the momenta to eliminate the integral over $\vec{p_2}$ to write

$$\int d\Phi_2 = \frac{1}{2^2(2\pi)^{D-2}} \int d\Omega_{D-1} \int \frac{dp_1 p_1^{D-2}}{E_1 E_2} \, \delta^{(1)}(E_{tot} - E_1 - E_2). \qquad (A.2)$$

Here, we used D-dimensional polar coordinates to express the remaining differential over the vectorial momentum as

$$d\vec{p_i} = dp_i p_i^{D-2} d\Omega_{D-1} \quad \text{with} \quad |\vec{p_i}| = p_i. \qquad (A.3)$$

Now, to eliminate the delta function for the total energy, we need to change the differential over the momentum to a differential over the energy. This is easily done (recall $E_1^2 = p_1^2$ and $E_1 = E_2$ because of momentum delta function), so eq.(A.2) becomes

$$\int d\Phi_2 = \frac{1}{2^2(2\pi)^{D-2}} \int d\Omega_{D-1} \int dE_1 E_1^{D-4} \, \delta^{(1)}(E_{tot} - 2E_1). \qquad (A.4)$$

We know that $E_1 = \sqrt{s}/2$, so after using the last delta function we can complete the integration over the energy as

$$\int d\Phi_2 = \frac{1}{2^3(2\pi)^{D-2}} \left(\frac{\sqrt{s}}{2}\right)^{D-4} \int d\Omega_{D-1}.$$ (A.5)

Finally, we use eq. (1.27) to substitute for the $(D-1)$-dimensional area of a unit sphere, to have

$$\Phi_2 = \frac{s^{\frac{D-4}{2}}}{2^{2D-4}\,\pi^{\frac{D-3}{2}}\,\Gamma\left(\frac{D-1}{2}\right)},$$ (A.6)

which in $D=4$ reduces to

$$\Phi_2 = \frac{1}{8\pi}.$$ (A.7)

A.2   3 particles in the final state

Consider the Lorentz invariant phase space factor given by

$$\int d\Phi_3 = \frac{(2\pi)^D}{2^3[(2\pi)^{D-1}]^3} \int\int\int \frac{d\vec{p_1}}{E_1}\frac{d\vec{p_2}}{E_2}\frac{d\vec{p_3}}{E_3}\,\delta^{(D-1)}\left(\vec{p_1}+\vec{p_2}+\vec{p_3}\right)$$
$$\times\delta^{(1)}\left(E_{tot}-E_1-E_2-E_3\right),$$ (A.8)

where

$$\vec{p_i} \quad : \quad \text{momentum vector in } D-1 \text{ dimensions,}$$

$$E_{tot} \quad : \quad \text{incoming total energy in the CM frame } E_{tot} = \sqrt{s},$$

$$(2\pi)^D \quad : \quad \text{normalisation for each delta function,}$$

$$2^3[(2\pi)^{D-1}]^3 \quad : \quad \text{for each momentum vector (normalisation}$$
$$\text{of volume element).}$$

We use the delta function for the momenta to eliminate the integral over $\vec{p_3}$ to write

$$\int d\Phi_3 = \frac{1}{2^3(2\pi)^{2D-3}} \int\int d_1\Theta_{D-2}\,d_2\Theta_{D-2}$$
$$\times \int\int \frac{dp_1\,dp_2\,p_1^{D-2}\,p_2^{D-2}}{E_1 E_2 E_3}\,\delta^{(1)}\left(E_{tot}-E_1-E_2-E_3\right).$$ (A.9)

Here, we used D-dimensional polar coordinates to express the remaining differentials over the vectorial momenta $\vec{p_1}$ and $\vec{p_2}$ as

$$d\vec{p_i} = dp_i p_i^{D-2} d_i\Theta_{D-2} \quad \text{with } |\vec{p_i}| = p_i.$$ (A.10)

In eq.(A.9) and using fig.(A.1), we can rewrite the integral over the two differentials of angle as
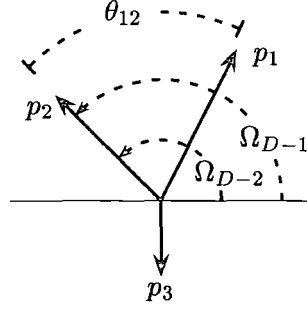
Figure A.1: Schematic representation of the relation amongst the angles for a three particle phase space. The angle for the third momenta is specified in terms of the other angles by conservation of momenta.

$$d_1\Theta_{D-2} \, d_2\Theta_{D-2} = \underbrace{d\Omega_{D-1}}_{\substack{\text{solid angle} \\ \text{for } \vec{p_1}}} \underbrace{(\sin\theta_{12})^{D-3} \, d\theta_{12}}_{\substack{\text{angle between} \\ \vec{p_1} \text{ and } \vec{p_2}}} \underbrace{d\Omega_{D-2}}_{\substack{\text{solid angle} \\ \text{for } \vec{p_2}}} \qquad (A.11)$$

Then, eq.(A.9) becomes

$$\int d\Phi_3 \;=\; \frac{1}{2^3 (2\pi)^{2D-3}} \int d\Omega_{D-1} \int d\Omega_{D-2} \;\; \delta^{(1)} \left(E_{tot} - E_1 - E_2 - E_3 \right)$$

$$\times \; \int \int \frac{dp_1 \, dp_2 \, p_1^{D-2} \, p_2^{D-2}}{E_1 E_2 E_3} \; (\sin\theta_{12})^{D-3} \, d\theta_{12}. \qquad (A.12)$$

Now, to eliminate the delta function for the total energy, we need to change the differential over the momenta and the angle, to a differential over the energy. This is easily done if we consider the following

- the usual relation $E_i dE_i = p_i dp_i$,

- from the Law of Cosines and conservation of energy, we have

$$E_3^2 \;=\; \vec{p_1}^2 + \vec{p_2}^2 + 2p_1 \, p_2 \, \cos\theta_{12}$$

$$\Rightarrow d\left(\cos\theta_{12}\right) \;=\; \frac{E_3}{p_1 p_2} dE_3, \qquad (A.13)$$

- can rewrite the integral over the angle, using eq.(A.13), as

$$(\sin\theta_{12})^{D-3} \, d\theta_{12} \;=\; -\,(\sin\theta_{12})^{D-4} \, d\left(\cos\theta_{12}\right)$$

$$\Rightarrow \; (\sin\theta_{12})^{D-3} \, d\theta_{12} \;=\; -\frac{E_3}{p_1 p_2} \, (\sin\theta_{12})^{D-4} \, dE_3, \qquad (A.14)$$

so that now eq.(A.12) looks like

$$\int d\Phi_3 = \frac{1}{2^3(2\pi)^{2D-3}} \int d\Omega_{D-1} \int d\Omega_{D-2} \int \int (E_1 E_2 \sin \theta_{12})^{D-4} \, dE_1 dE_2$$

$$\times \underbrace{\int dE_3 \, \delta^{(1)} \left(E_{tot} - E_1 - E_2 - E_3 \right)}_{\substack{\text{integrate out} \\ \Rightarrow \text{cons. of energy}}}. \tag{A.15}$$

With the aid of the kinematics analysis done in section 2.1.2, we can change the integration over energy into integration over energy fractions. We need only algebraic manipulations that can be summarised as follows

1. change of variables

$$E_i = \frac{\sqrt{s}}{2} x_i \tag{A.16}$$

$$\Rightarrow dE_i = \frac{\sqrt{s}}{2} dx_i \tag{A.17}$$

2. change cosine relations to ratios of x_i's

$$1 - \cos \theta_{12} = \frac{2(1 - x_3)}{x_1 x_2}$$

$$1 + \cos \theta_{12} = 2 \left(1 - \frac{1 - x_3}{x_1 x_2} \right)$$

$$\Rightarrow \sin^2 \theta_{12} = 4 \frac{1 - x_3}{x_1^2 x_2^2} [x_1 x_2 - (1 - x_3)] \tag{A.18}$$

3. have to consider relation amongst energy fractions $1 - x_3 = x_1 + x_2 - 1$, so

$$\sin \theta_{12} = \frac{2}{x_1 x_2} [(1 - x_1)(1 - x_2)(1 - x_3)]^{1/2}. \tag{A.19}$$

We introduce this information into eq.(A.15), to have

$$\int d\Phi_3 = \frac{2^{D-4} \, s^{D-3}}{2^{2D-3}(2\pi)^{2D-3}} \int d\Omega_{D-1} \int d\Omega_{D-2} \int \int [(1 - x_1)(1 - x_2)(1 - x_3)]^{\frac{D-4}{2}} \, dx_1 \, dx_2. \tag{A.20}$$

Finally, we use eq. (1.27) to substitute for the $(D-1)-$ and $(D-2)$-dimensional area of the unit spheres, to have

$$\int d\Phi_3 = \frac{s^{D-3}}{2^{3D-4}\pi^{\frac{2D-3}{2}}} \frac{1}{\Gamma\left(\frac{D-1}{2}\right) \Gamma\left(\frac{D-2}{2}\right)} \int \int [(1 - x_1)(1 - x_2)(1 - x_3)]^{\frac{D-4}{2}} \, dx_1 \, dx_2, \tag{A.21}$$

with $1 - x_3 = x_1 + x_2 - 1$. The integration region is $0 \le x_1, x_2 \le 1$ with $x_1 + x_2 + x_3 = 2$.

Appendix B | *Master Integrals*

In general the expansions of the master integrals contain the generalised polylogarithms of Nielsen

$$S_{n,p}(x) = \frac{(-1)^{n+p-1}}{(n-1)!\,p!} \int_0^1 dt\, \frac{\log^{n-1}(t)\log^p(1-xt)}{t}, \qquad n,p \geq 1, \quad x \leq 1$$

where the level is $n+p$. Keeping terms up to $\mathcal{O}(\epsilon)$ corresponds to probing level 4 so that only polylogarithms with $n+p \leq 4$ occur. For $p = 1$ we find the usual polylogarithms

$$S_{n-1,1}(z) \equiv \text{Li}_n(z).$$

A basis set of 6 polylogarithms (one with $n+p = 2$, two with $n+p = 3$ and three with $n+p = 4$ is sufficient to describe a function of level 4. At level 4, we choose to eliminate the S_{22}, S_{13} and S_{12} functions using the standard polylogarithm identities [92] and retain the three Li_4 functions with arguments x and $1-x$ and $(x-1)/x$ where

$$x = -\frac{t}{s}, \qquad y = -\frac{u}{s} = 1 - x, \qquad z = -\frac{u}{t} = \frac{x-1}{x}.$$

For convenience, we also introduce the following logarithms

$$X = \log\left(\frac{-t}{s}\right), \qquad Y = \log\left(\frac{-u}{s}\right), \qquad S = \log\left(\frac{s}{\mu^2}\right), \qquad U = \log\left(\frac{-u}{\mu^2}\right),$$

where μ is the renormalisation scale. The common choice $\mu^2 = s$, for example, corresponds to setting $S = 0$.

For relations between polylogarithms of different arguments and other identities see ref.[109] and references therein.

B.1   One-loop master integrals

In this appendix, we list the expansions for the one-loop box integrals in $D = 6 - 2\epsilon$. We remain in the physical region $s > 0$, $u, t < 0$, and write coefficients in terms of logarithms and polylogarithms that are real in this domain. More precisely, we use the notation presented at the beginning of this section to define the arguments of the logarithms and polylogarithms.
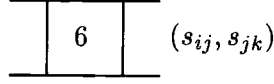
Figure B.1: Symbol for the Box^6 topology

We find that the box integrals have the expansion

$$
\begin{aligned}
\text{Box}^6(u,t) \;=\; & \frac{e^{\epsilon\gamma}\Gamma\left(1+\epsilon\right)\Gamma\left(1-\epsilon\right)^2}{2s\Gamma\left(1-2\epsilon\right)\left(1-2\epsilon\right)}\left(\frac{\mu^2}{s}\right)^\epsilon\left\{\frac{1}{2}\left[(X-Y)^2+\pi^2\right]\right. \\
& +2\epsilon\left[\text{Li}_3(x)-X\text{Li}_2(x)-\frac{1}{3}X^3-\frac{\pi^2}{2}X\right] \\
& -2\epsilon^2\left[\text{Li}_4(x)+Y\text{Li}_3(x)-\frac{1}{2}X^2\text{Li}_2(x)-\frac{1}{8}X^4-\frac{1}{6}X^3Y+\frac{1}{4}X^2Y^2\right. \\
& \left.\left.-\frac{\pi^2}{4}X^2-\frac{\pi^2}{3}XY-\frac{\pi^4}{45}\right]+(u\leftrightarrow t)\right\}+\mathcal{O}\left(\epsilon^3\right),
\end{aligned}
\tag{B.1}
$$

and

$$
\begin{aligned}
\text{Box}^6(s,t) \;=\; & \frac{e^{\epsilon\gamma}\Gamma(1+\epsilon)\Gamma(1-\epsilon)^2}{2u\Gamma(1-2\epsilon)(1-2\epsilon)}\left(-\frac{\mu^2}{u}\right)^\epsilon\left\{\left(X^2+2i\pi X\right)\right. \\
& +\epsilon\left[\left(-2\text{Li}_3(x)+2X\text{Li}_2(x)-\frac{2}{3}X^3+2YX^2-\pi^2X+2\zeta_3\right)\right. \\
& \left.+i\pi\left(2\text{Li}_2(x)+4YX-X^2-\frac{\pi^2}{3}\right)\right] \\
& +\epsilon^2\left[\left(2\text{Li}_4(z)+2\text{Li}_4(y)-2Y\text{Li}_3(x)-2X\text{Li}_3(y)+(2XY-X^2-\pi^2)\text{Li}_2(x)\right.\right. \\
& \left.+\frac{1}{3}X^4-\frac{5}{3}X^3Y+\frac{3}{2}X^2Y^2+\frac{2}{3}\pi^2X^2-2\pi^2XY+2Y\zeta_3+\frac{1}{6}\pi^4\right) \\
& +i\pi\left(-2\text{Li}_3(x)-2\text{Li}_3(y)+2Y\text{Li}_2(x)+\frac{1}{3}X^3-2X^2Y+3XY^2\right. \\
& \left.\left.\left.-\frac{\pi^2}{3}Y+2\zeta_3\right)\right]\right\}+\mathcal{O}\left(\epsilon^3\right).
\end{aligned}
\tag{B.2}
$$

Box$^6(s,u)$ is obtained from eq.(B.2) by exchanging u and t.

Finally, the one-loop bubble integral in $D = 4 - 2\epsilon$ dimensions is given by
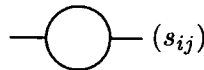
Figure B.2: Symbol for the BUB topology

$$
\text{Bub}(s) = \frac{e^{\epsilon\gamma}\Gamma\left(1+\epsilon\right)\Gamma\left(1-\epsilon\right)^2}{\Gamma\left(2-2\epsilon\right)\epsilon}\left(-\frac{\mu^2}{s}\right)^\epsilon.
\tag{B.3}
$$

B.2   Two-loop master integrals

In our calculation there are 10 master integrals for the two-loop planar and non-planar topologies. Here we list the expansion in $\epsilon = 2 - D/2$ for each of them, following the notation we introduced at the beginning of this appendix.

B.2.1   The SUNC topology
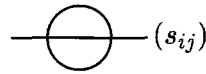
Figure B.3: Symbol for the SUNC topology

$$
\begin{aligned}
\mathrm{SUNC}(s) &= \Gamma(1+\epsilon)^2\, s^{-2\epsilon+1} \left\{ -\frac{1}{4\epsilon} - \frac{1}{2}i\pi - \frac{13}{8} + \left[\frac{7}{2}\zeta(2) - \frac{13}{4}i\pi - \frac{115}{16} \right]\epsilon \right. \\
&\quad + \left[\frac{5}{2}\zeta(3) + \frac{1}{2}i\pi^3 + \frac{91}{4}\zeta(2) - \frac{115}{8}i\pi - \frac{865}{32} \right]\epsilon^2 \\
&\quad \left. + \left[-\frac{109}{4}\zeta(4) + \left(\frac{65}{4} + 5i\pi \right)\zeta(3) + \frac{13}{4}i\pi^3 + \frac{805}{8}\zeta(2) - \frac{865}{16}i\pi - \frac{5971}{64} \right]\epsilon^3 \right\} \\
\mathrm{SUNC}(u) &= \Gamma(1+\epsilon)^2\, (-u)^{-2\epsilon+1} \left\{ -\frac{1}{4\epsilon} - \frac{13}{8} + \left[\frac{1}{2}\zeta(2) - \frac{115}{16} \right]\epsilon \right. \\
&\quad \left. + \left[\frac{5}{2}\zeta(3) + \frac{13}{4}\zeta(2) - \frac{865}{32} \right]\epsilon^2 + \left[\frac{11}{4}\zeta(4) + \frac{65}{4}\zeta(3) + \frac{115}{8}\zeta(2) - \frac{5971}{64} \right]\epsilon^3 \right\} \\
\mathrm{SUNC}(t) &= \left[\mathrm{SUNC}(u) \right]_{u=t}
\end{aligned}
$$

$$\text{(B.4)}$$

B.2.2   The TRI topology

Figure B.4: Symbol for the TRI topology

$$
\begin{aligned}
\mathrm{TRI}(s) &= \Gamma(1+\epsilon)^2\, s^{-2\epsilon} \left\{ \frac{1}{2\epsilon^2} + \frac{1}{\epsilon}\left[i\pi + \frac{5}{2} \right] - 6\zeta(2) + 5i\pi + \frac{19}{2} \right. \\
&\quad + \left[-4\zeta(3) - \frac{2}{3}i\pi^3 - 30\zeta(2) + 19i\pi + \frac{65}{2} \right]\epsilon
\end{aligned}
$$

$$+ \left[24\zeta(4) - 4\left(5 + 2i\pi\right)\zeta(3) - \frac{10}{3}i\pi^3 - 114\zeta(2) + 65i\pi + \frac{211}{2} \right]\epsilon^2 \Bigg\}$$

$$\mathrm{TRI}(u) = \Gamma(1+\epsilon)^2 \left(-u\right)^{-2\epsilon} \left\{ \frac{1}{2\epsilon^2} + \frac{5}{2\epsilon} + \frac{19}{2} + \left[-4\zeta(3) + \frac{65}{2} \right]\epsilon \right.$$

$$\left. + \left[-6\zeta(4) - 20\zeta(3) + \frac{211}{2} \right]\epsilon^2 \right\}$$

$$\mathrm{TRI}(t) = \left[\mathrm{TRI}(u) \right]_{u=t}$$

$$(\mathrm{B.5})$$

B.2.3 The GLASS topology

Figure B.5: Symbol for the GLASS topology

$$\mathrm{GLASS}(s) = \Gamma(1+\epsilon)^2 \, s^{-2\epsilon} \left\{ \frac{1}{\epsilon^2} + \frac{2}{\epsilon}\left[2 + i\pi \right] + 8i\pi - 14\zeta(2) + 12 \right.$$

$$+ \left[-4\zeta(3) - 2i\pi^3 - 56\zeta(2) + 24i\pi + 32 \right]\epsilon$$

$$\left. + \left[118\zeta(4) - 8\left(2 + i\pi\right)\zeta(3) - 8i\pi^3 - 168\zeta(2) + 64i\pi + 80 \right]\epsilon^2 \right\}$$

$$\mathrm{GLASS}(u) = \Gamma(1+\epsilon)^2 \left(-u\right)^{-2\epsilon} \left\{ \frac{1}{\epsilon^2} + \frac{4}{\epsilon} - \frac{1}{3}\left(\pi - 6\right)\left(\pi + 6\right) \right.$$

$$\left. + \left[-4\zeta(3) - 8\zeta(2) + 32 \right]\epsilon + \left[-2\zeta(4) - 16\zeta(3) - 24\zeta(2) + 80 \right]\epsilon^2 \right\}$$

$$\mathrm{GLASS}(t) = \left[\mathrm{GLASS}(u) \right]_{u=t}$$

$$(\mathrm{B.6})$$

B.2.4 The XTRI topology

Figure B.6: Symbol for the XTRI topology

$$
\begin{aligned}
\mathrm{XTRI}(s) &= \Gamma(1+\epsilon)^2 \, s^{-2(1+\epsilon)} \left\{ \frac{1}{\epsilon^4} + \frac{2i\pi}{\epsilon^3} - \frac{19\zeta(2)}{\epsilon^2} + \frac{1}{\epsilon}\left[-27\zeta(3) - \frac{11}{3}i\pi^3 \right] \right. \\
&\qquad \left. + \frac{483}{2}\zeta(4) - 54i\pi\zeta(3) \right\} \\
\mathrm{XTRI}(u) &= \Gamma(1+\epsilon)^2 \, (-u)^{-2(1+\epsilon)} \left\{ \frac{1}{\epsilon^4} - \frac{7\zeta(2)}{\epsilon^2} - \frac{27\zeta(3)}{e} - \frac{57}{2}\zeta(4) \right\} \\
\mathrm{XTRI}(t) &= \left[\mathrm{XTRI}(u) \right]_{u=t}
\end{aligned}
$$

$$(\mathrm{B.7})$$

B.2.5 The CBOX topology

$$(s_{ij}, s_{jk})$$
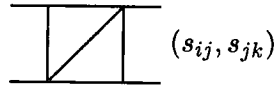
Figure B.7: Symbol for the CBOX topology

$$
\begin{aligned}
\mathrm{CBOX}(s,t) &= \frac{\Gamma(1+\epsilon)^2 \, s^{-2\epsilon}}{s+t} \left\{ \frac{1}{\epsilon^2}\left[\frac{1}{2}X^2 + i\pi X \right] + \frac{1}{\epsilon}\left[-2\mathrm{Li}_3(x) + 2\left(X + i\pi\right)\mathrm{Li}_2(x) \right. \right. \\
&\quad \left. -\frac{2}{3}X^3 + (Y - i\pi)\,X^2 + 2\left(-3\zeta(2) + iY\pi\right)X - \frac{1}{3}i\pi^3 + 2\zeta(3) \right] - 4\mathrm{S}_{2,2}(x) + 4\mathrm{Li}_4(x) \\
&\quad +4\left(X + i\pi\right)\mathrm{S}_{1,2}(x) - 4\left(Y + i\pi\right)\mathrm{Li}_3(x) + 2\left(-6\zeta(2) + 2YX + 2iY\pi - X^2\right)\mathrm{Li}_2(x) \\
&\quad +\frac{1}{2}X^4 + \frac{2}{3}\left(i\pi - 2Y\right)X^3 + \left(Y^2 - 2iY\pi + 5\zeta(2)\right)X^2 + (-4\zeta(3) - 12Y\zeta(2) \\
&\quad \left. -\frac{1}{3}i\pi^3 + 2iY^2\pi\right)X + 2\left(2\zeta(3) - \frac{1}{3}i\pi^3\right)Y + 27\zeta(4) \right\} \\
\mathrm{CBOX}(u,t) &= \frac{\Gamma(1+\epsilon)^2 \, (-u)^{-2\epsilon}}{u+t} \left\{ \frac{1}{\epsilon^2}\left[\frac{1}{2}X^2 - YX + \frac{1}{2}Y^2 + 3\zeta(2) \right] + \frac{1}{\epsilon}\left[-2\mathrm{Li}_3(z) \right. \right. \\
&\quad \left. +2(Y - X)\mathrm{Li}_2(z) - \frac{4}{3}X^3 + 3YX^2 - 2(Y^2 + 3\zeta(2))X + 2\zeta(3) + \frac{1}{3}Y^3 \right] - 4\mathrm{S}_{2,2}(z) \\
&\quad +4\mathrm{Li}_4(z) + 4(Y - X)\mathrm{S}_{1,2}(z) - 4(Y - 2X)\mathrm{Li}_3(z) + 2(3X^2 - 4YX + Y^2)\mathrm{Li}_2(z) \\
&\quad +\frac{11}{6}X^4 - \frac{14}{3}YX^3 + (4Y^2 + 5\zeta(2))X^2 - 2(\frac{2}{3}Y^3 + 2\zeta(3) - Y\zeta(2))X \\
&\quad \left. -Y^2\zeta(2) + \frac{1}{6}Y^4 - 3\zeta(4) \right\} \\
\mathrm{CBOX}(t,u) &= \left[\mathrm{CBOX}(u,t) \right]_{u=t,t=u}
\end{aligned}
$$

$$(\mathrm{B.8})$$

B.2.6 The ABOX topology

(s_{ij}, s_{jk})

Figure B.8: Symbol for the ABOX topology

$$
\begin{aligned}
\text{ABOX}(s,t) \;=\;& \Gamma(1+\epsilon)^2 \, s^{-(1+2\epsilon)} \left\{ \frac{1}{\epsilon^3} + \frac{1}{\epsilon^2}\left[i\pi - X + 2 \right] + \frac{1}{\epsilon}\left[\frac{1}{2}X^2 - (2+i\pi)X \right.\right. \\
& \left. -7\zeta(2) + 4 + 2i\pi \right] + \text{Li}_3(x) + (X+i\pi)\,\text{Li}_2(x) + \left(1 - \frac{1}{2}Y + i\pi \right)X^2 \\
& + (-iY\pi - 2i\pi + 7\zeta(2) - 4)\,X + 8 - \frac{1}{2}i\pi^3 + 4i\pi - 14\zeta(2) - 10\zeta(3) \\
& + \left[\text{S}_{2,2}(x) - 2\text{Li}_4(x) - (X+i\pi)\,\text{S}_{1,2}(x) + (2 + 2i\pi + Y)\,\text{Li}_3(x) \right. \\
& + \left(X^2 - (Y+2)X - iY\pi + \frac{1}{6}\pi(-12i + 5\pi) \right)\text{Li}_2(x) \\
& - \frac{1}{6}X^4 + \frac{2}{3}(Y - i\pi)X^3 + \left(-\frac{1}{4}Y^2 + (i\pi - 1)Y + 2i\pi - 6\zeta(2) + 2 \right)X^2 \\
& + \left(-\frac{1}{2}iY^2\pi + \frac{1}{6}\pi(-12i + 5\pi)Y + \frac{1}{3}i\pi^3 - 8 + 14\zeta(2) + 11\zeta(3) - 4i\pi \right)X \\
& \left.\left. + \left(-\zeta(3) + \frac{1}{6}i\pi^3 \right)Y - (20 + 9i\pi)\zeta(3) + 16 + \frac{31}{4}\zeta(4) - 28\zeta(2) + 8i\pi - i\pi^3 \right]\epsilon \right\} \\[6pt]
\text{ABOX}(u,t) \;=\;& \Gamma(1+\epsilon)^2 \, (-u)^{-(1+2\epsilon)} \left\{ \frac{1}{\epsilon^3} + \frac{1}{\epsilon^2}\left[2 + Y - X \right] \right. \\
& + \frac{1}{\epsilon}\left[\frac{1}{2}X^2 - (Y+2)X + 4 + 2Y - 4\zeta(2) + \frac{1}{2}Y^2 \right] \\
& + \text{Li}_3(z) + \text{Li}_2(z)(X - Y) + \frac{1}{3}X^3 + \left(1 - \frac{1}{2}Y \right)X^2 + (7\zeta(2) - 2Y - 4)\,X \\
& + \frac{1}{6}Y^3 + Y^2 + 4\left(1 - \zeta(2) \right)Y - 10\zeta(3) - 8\zeta(2) + 8 + \left[\text{S}_{2,2}(z) + (X - Y)\text{S}_{1,2}(z) \right. \\
& + (Y - 2X + 2)\,\text{Li}_3(z) + \left(-2X^2 + (3Y+2)X - 2Y + \zeta(2) - Y^2 \right)\text{Li}_2(z) \\
& - \frac{17}{24}X^4 + \left(\frac{11}{6}Y + \frac{2}{3} \right)X^3 + \left(-\frac{3}{2}Y^2 - Y - \frac{11}{2}\zeta(2) + 2 \right)X^2 \\
& + \left(\frac{1}{3}Y^3 + (\pi - 2)(\pi + 2)Y + 11\zeta(3) - 8 + 14\zeta(2) \right)X + \frac{1}{24}Y^4 + \frac{1}{3}Y^3 \\
& \left.\left. + 2(1 - \zeta(2))Y^2 + (-10\zeta(3) - 8\zeta(2) + 8)\,Y + 16 - 3\zeta(4) - 16\zeta(2) - 20\zeta(3) \right]\epsilon \right\} \\[6pt]
\text{ABOX}(t,u) \;=\;& \left[\text{ABOX}(u,t) \right]_{u=t, t=u}
\end{aligned}
$$

$$\text{(B.9)}$$

B.2.7   The PBOX1 topology
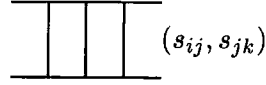
Figure B.9: Symbol for the PBOX1 topology

$$
\begin{aligned}
\mathrm{PBOX1}(s,t) \;=\; & \frac{\Gamma(1+\epsilon)^2\, s^{-2\epsilon}}{s^2 t}\left\{ \frac{4}{\epsilon^4} + \frac{1}{\epsilon^3}\left[-5X + 3i\pi \right] + \frac{1}{\epsilon^2}\left[2X^2 - 6i\pi X - 19\zeta(2) \right] \right. \\
& + \frac{1}{\epsilon}\left[4\mathrm{Li}_3(x) - 4(X+i\pi)\mathrm{Li}_2(x) + \frac{2}{3}X^3 + 2(3i\pi - Y)X^2 + (-4iY\pi + 38\zeta(2))X \right. \\
& \left. - 19\zeta(3) \right] + 4\mathrm{S}_{2,2}(x) - 44\mathrm{Li}_4(x) - 4(X+i\pi)\mathrm{S}_{1,2}(x) + 4(6X + 8i\pi + Y)\mathrm{Li}_3(x) \\
& - 2(X^2 + 2(Y+3i\pi)X - 10\zeta(2) + 2iY\pi)\mathrm{Li}_2(x) - \frac{4}{3}X^4 + 4\left(\frac{2}{3}Y - i\pi\right)X^3 \\
& + (-38\zeta(2) + 4iY\pi - Y^2)X^2 + (20Y\zeta(2) + 26\zeta(3) - 2iY^2\pi)X \\
& \left. + \left(-4\zeta(3) + \frac{2}{3}i\pi^3\right)Y - \frac{93}{2}\zeta(4) - 12i\zeta(3)\pi \right\}
\end{aligned}
$$

$$
\begin{aligned}
\mathrm{PBOX1}(u,t) \;=\; & \frac{\Gamma(1+\epsilon)^2\,(-u)^{-2\epsilon}}{u^2 t}\left\{ \frac{4}{\epsilon^4} + \frac{5}{\epsilon^3}\left[Y - X \right] + \frac{1}{\epsilon^2}\left[2X^2 - 4YX + 2Y^2 \right. \right. \\
& \left. - 19\zeta(2) \right] + \frac{1}{\epsilon}\left[4\mathrm{Li}_3(z) + 4(X - Y)\mathrm{Li}_2(z) + 2X^3 - 4YX^2 + 2(19\zeta(2) + Y^2)X \right. \\
& \left. - 26Y\zeta(2) - 19\zeta(3) \right] + 4\mathrm{S}_{2,2}(z) + 36\mathrm{Li}_4(z) + 4(X-Y)\mathrm{S}_{1,2}(z) + 4(4X - 5Y)\mathrm{Li}_3(z) \\
& + 2(-X^2 + Y^2 + 20\zeta(2))\mathrm{Li}_2(z) - 3X^4 + 8YX^3 - (7Y^2 + 18\zeta(2))X^2 \\
& \left. + 2(8Y\zeta(2) + Y^3 + 13\zeta(3))X - 22Y\zeta(3) - 4Y^2\zeta(2) + \frac{247}{2}\zeta(4) \right\}
\end{aligned}
$$

$$
\mathrm{PBOX1}(t,u) \;=\; \left[\mathrm{PBOX1}(u,t) \right]_{u=t,t=u}
$$

<div align="right">(B.10)</div>

B.2.8   The PBOX2 topology
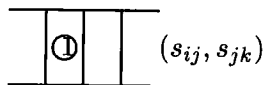
Figure B.10: Symbol for the PBOX2 topology

$$
\mathrm{PBOX2}(s,t) \;=\; \frac{\Gamma(1+\epsilon)^2\, s^{-2\epsilon}}{s^2}\left\{ \frac{9}{4\epsilon^4} + \frac{1}{\epsilon^3}\left[\frac{5}{2}i\pi - 2X \right] - \frac{1}{\epsilon^2}\left[4i\pi X + 17\zeta(2) \right] \right.
$$

$$+\frac{1}{\epsilon}\left[8\mathrm{Li}_3(x) - 8(X + i\pi)\mathrm{Li}_2(x) + \frac{4}{3}X^3 + 4(-Y + i\pi)X^2 - 4(2iY\pi - 7\zeta(2))X\right.$$

$$\left. -16\zeta(3) - \frac{1}{3}i\pi^3\right] + 20\mathrm{S}_{2,2}(x) - 28\mathrm{Li}_4(x) - 20(X + i\pi)\mathrm{S}_{1,2}(x)$$

$$+4(5Y + 2X + 6i\pi)\mathrm{Li}_3(x) + (6X^2 - 4(i\pi + 5Y)X + 52\zeta(2) - 20iY\pi)\mathrm{Li}_2(x)$$

$$-\frac{4}{3}X^4 + \frac{8}{3}(2Y - i\pi)X^3 + (8iY\pi - 5Y^2 - 26\zeta(2))X^2 - 29\zeta(4)$$

$$+\left(52Y\zeta(2) + 28\zeta(3) + \frac{2}{3}i\pi^3 - 10iY^2\pi\right)X + 10\left(\frac{1}{3}i\pi^3 - 2\zeta(3)\right)Y - 4i\zeta(3)\pi\bigg\}$$

$$\mathrm{PBOX2}(u,t) = \frac{\Gamma(1+\epsilon)^2\,(-u)^{-2\epsilon}}{u^2}\left\{\frac{9}{4\epsilon^4} + \frac{2}{\epsilon^3}\left[Y - X\right] - \frac{14\zeta(2)}{\epsilon^2}\right.$$

$$+\frac{1}{\epsilon}\left[8\mathrm{Li}_3(z) + 8(X - Y)\mathrm{Li}_2(z) + 4X^3 - 8YX^2 + 4(Y^2 + 7\zeta(2))X - 4Y\zeta(2)\right.$$

$$\left. -16\zeta(3)\right] + 20\mathrm{S}_{2,2}(z) - 12\mathrm{Li}_4(z) + 20(X - Y)\mathrm{S}_{1,2}(z) + 4(3Y - 8X)\mathrm{Li}_3(z)$$

$$+2(-13X^2 + 16YX - 3Y^2 + 4\zeta(2))\mathrm{Li}_2(z) - 7X^4 + 16YX^3$$

$$-11(Y^2 + 2\zeta(2))X^2 + 2(-4Y\zeta(2) + Y^3 + 14\zeta(3))X - 8Y\zeta(3) + 20\zeta(4)\bigg\}$$

$$\mathrm{PBOX2}(t,u) = \left[\mathrm{PBOX2}(u,t)\right]_{u=t,t=u}$$

$$(\mathrm{B.11})$$

B.2.9 The XBOX1 topology
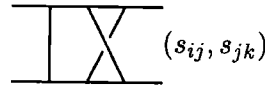
Figure B.11: Symbol for the XBOX1 topology

$$\mathrm{XBOX1}(s,t) = \frac{\Gamma(1+\epsilon)^2\,s^{-2\epsilon}}{s^2t(s+t)}\left\{-\frac{2s}{\epsilon^4} + \frac{1}{\epsilon^3}\left[\left(-t + \frac{5}{2}s\right)X + \left(t + \frac{7}{2}s\right)Y + 2i\pi s\right]\right.$$

$$+\frac{1}{\epsilon^2}\left[-sX^2 - \left(4Ys + i(2t+s)\pi + 6t\right)X - Y^2s + \left(i(2t+s)\pi + 6(s+t)\right)Y\right.$$

$$\left. -\frac{5}{2}\zeta(2)s + 6i\pi s\right] + \frac{1}{\epsilon}\left[-2s\mathrm{S}_{1,2}(x) + 2s\mathrm{Li}_3(x) - 2s\mathrm{Li}_2(x)X + \frac{1}{3}(2t - s)X^3\right.$$

$$-2(tY + i\pi s)X^2 + \left((2t + 3s)Y^2 - 2s(i\pi + 6)Y + (5s + 34t)\zeta(2)\right.$$

$$\left. -12i(s+t)\pi + 24t\right)X - \left(s + \frac{2}{3}t\right)Y^3 - 2i\pi Y^2 s - 2\left(\left(17t + \frac{29}{2}s\right)\zeta(2)\right.$$

$$
-6it\pi + 12(s+t)\Bigg)Y - 24i\pi s - \frac{31}{6}i\pi^3 s + \frac{19}{2}\zeta(3)s\Bigg] - 36(2t+s)S_{2,2}(x)
$$

$$
+2(43s+30t)\mathrm{Li}_4(x) + 2(30t-13s)S_{1,3}(x) + \Bigg(4(7s+13t)X - 2(3s-10t)Y
$$

$$
+4i(11s+3t)\pi - 24(s-t)\Bigg)S_{1,2}(x) + \Bigg(-20(3s+2t)X - 4(5t+3s)Y
$$

$$
+4i(3t-8s)\pi + 24(t+2s)\Bigg)\mathrm{Li}_3(x) + \Bigg((10t+17s)X^2 + (4(5t+3s)Y
$$

$$
-2i(-7s+6t)\pi - 24(2s+t))X + 18i\pi Ys + 60(s+2t)\zeta(2)
$$

$$
-24i(2t+s)\pi\Bigg)\mathrm{Li}_2(x) + \frac{2}{3}(s-t)X^4 + \Bigg(\frac{8}{3}(s+t)Y + \frac{2}{3}i(5s+2t)\pi + 4t\Bigg)X^3
$$

$$
+\Bigg((t-s)Y^2 - 4(3t+it\pi+3s)Y - 30\left(t+\frac{1}{6}s\right)\zeta(2) + 12i(s+t)\pi\Bigg)X^2
$$

$$
+\Bigg(-\frac{4}{3}(s+2t)Y^3 + 2(6s-it\pi)Y^2 + \Bigg(12\left(\frac{19}{3}s+5t\right)\zeta(2)
$$

$$
-24i(s+t)\pi + 48s\Bigg)Y + (-13s+38t)\zeta(3) + \frac{4}{3}i(7s+5t)\pi^3 + 84t\zeta(2)
$$

$$
+48i(s+t)\pi - 96t\Bigg)X + \frac{2}{3}(2s+t)Y^4 + \Bigg(-\frac{2}{3}i(2t-3s)\pi - 4(s+t)\Bigg)Y^3
$$

$$
+6\Bigg(\left(\frac{25}{6}s+5t\right)\zeta(2) - 2it\pi\Bigg)Y^2 + \Bigg(-(38t+33s)\zeta(3) - \frac{1}{3}i(s+20t)\pi^3
$$

$$
-84(s+t)\zeta(2) - 48it\pi + 96(s+t)\Bigg)Y - (i(12t+89s)\pi + 24t)\zeta(3)
$$

$$
+9\left(\frac{37}{4}s - \frac{67}{3}t\right)\zeta(4) + 2i(2t-s)\pi^3 + 96i\pi s\Bigg\}
$$

$$
\mathrm{XBOX1}(u,t) = \frac{\Gamma(1+\epsilon)^2\,(-u)^{-2\epsilon}}{u^2 t(u+t)}\Bigg\{-\frac{2u}{\epsilon^4} + \frac{1}{\epsilon^3}\Bigg[\left(-t+\frac{5}{2}u\right)X - 6Yu - \frac{1}{2}i(2t+7u)\pi\Bigg]
$$

$$
+\frac{1}{\epsilon^2}\Bigg[-uX^2 + 2(3Yu - 3t + 2i\pi u)X - 6Y^2u - 6u(1+i\pi)Y + \frac{31}{2}\zeta(2)u
$$

$$
-6i(u+t)\pi\Bigg] + \frac{1}{\epsilon}\Bigg[2S_{1,2}(z)u + 2i\mathrm{Li}_2(z)\pi u + \frac{2}{3}X^3 t + 2itX^2\pi + \Bigg(3Y^2u
$$

$$
+6u(2+i\pi)Y + 2\left(-\frac{31}{2}u+5t\right)\zeta(2) + 12(2t+i\pi u)\Bigg)X - 2Y^3u - 3u(4+i\pi)Y^2
$$

$$
+(54\zeta(2)u - 12i\pi u + 24u)Y + \frac{15}{2}\zeta(3)u + \frac{1}{2}i(6t+11u)\pi^3 + 24i(u+t)\pi\Bigg]
$$

$$
-2(6t+31u)S_{2,2}(z) + 12(u+2t)\mathrm{Li}_4(z) - 2S_{1,3}(z)(30t-13u)
$$

$$
+\Bigg(2(4t-27u)X + 12(4u+t)Y - 20i(2t-u)\pi - 24(t-u)\Bigg)S_{1,2}(z)
$$

$$
+\Bigg(6(5u+4t)X - 12(2t+u)Y - 4i(3t+11u)\pi + 24(u+2t)\Bigg)\mathrm{Li}_3(z)
$$

$$+\left(12(t+2u)X^2+(-6(4t+5u)Y+4i(-9u+2t)\pi+24(u+2t))X\right.$$

$$+6(u+2t)Y^2+(6i(5u+2t)\pi-24(u+2t))Y+6(-11u+2t)\zeta(2)$$

$$\left.-24i(t-u)\pi\right)\mathrm{Li}_2(z)+\frac{1}{3}\left(5t+\frac{17}{2}u\right)X^4+\left(-3(3u+2t)Y-\frac{2}{3}i(5t+13u)\pi\right.$$

$$\left.+4(3u+4t)\right)X^3+\left(9(u+t)Y^2+(3i(5u+4t)\pi-12(2u+3t))Y-2\zeta(2)u\right.$$

$$\left.-12it\pi\right)X^2+\left(-(u+4t)Y^3+6(4u+4t-it\pi)Y^2+(-12(t+4u)\zeta(2)\right.$$

$$+24i(u+t)\pi-48u)Y+3(6t-7u)\zeta(3)-2i(t+4u)\pi^3+84t\zeta(2)-48i\pi u$$

$$\left.-96t\right)X-\frac{1}{2}Y^4u-u(8+i\pi)Y^3+(33\zeta(2)+48-12i\pi)Y^2u+(5i\pi^3-96$$

$$+84\zeta(2)+48i\pi+60\zeta(3))Yu+3(5i(5u+6t)\pi-8u)\zeta(3)$$

$$\left.-\frac{933}{4}u\zeta(4)+2i(3u+t)\pi^3-96i(u+t)\pi\right\}$$

$$\mathrm{XBOX1}(t,u)\ =\ \left[\mathrm{XBOX1}(u,t)\right]_{u=t,t=u}$$

$$(\mathrm{B.12})$$

B.2.10   The XBOX2 topology
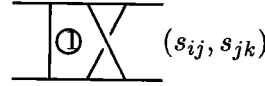
Figure B.12: Symbol for the XBOX2 topology

$$\mathrm{XBOX2}(s,t)\ =\ \frac{\Gamma(1+\epsilon)^2\ s^{-2\epsilon}}{st(s+t)}\left\{-\frac{1}{4\epsilon^4}\left[t+3s\right]+\frac{1}{\epsilon^3}\left[\left(\frac{3}{2}s-2t\right)X-2it\pi+\frac{1}{2}tY\right]\right.$$

$$+\frac{1}{\epsilon^2}\left[-\frac{1}{2}(3s+t)X^2+(-it\pi-3t+4tY)X-2tY^2+(3t+3s+it\pi)Y+\frac{5}{2}t\zeta(2)\right.$$

$$\left.+3i\pi s\right]+\frac{1}{\epsilon}\left[-4t\mathrm{S}_{1,2}(x)+(t+3s)\mathrm{Li}_3(x)+(-(3s+t)X+3i(t-s)\pi)\mathrm{Li}_2(x)\right.$$

$$+(2t+s)X^3+\left(-\frac{1}{2}(7t+3s)Y+2it\pi\right)X^2+\left(-tY^2-(i(t+3s)\pi+6s)Y\right.$$

$$\left.+29t\zeta(2)-6i(s+t)\pi+12t\right)X+\frac{7}{3}tY^3+2it\pi Y^2-(12s+12t+5t\zeta(2)-6it\pi)\,Y$$

$$\left.+\left(\frac{11}{2}t+3s\right)\zeta(3)-12i\pi s+\frac{25}{6}it\pi^3\right]+9(s-5t)\mathrm{S}_{2,2}(x)-2(3s+16t)\mathrm{Li}_4(x)$$

$$+98t\mathrm{S}_{1,3}(x)+\left((15t-9s)X+38tY-i(53t+9s)\pi-12(s-t)\right)\mathrm{S}_{1,2}(x)$$

$$+\left(20Xt + (9s+t)Y + 2i(34t+3s)\pi + 12(t+2s)\right)\mathrm{Li}_3(x) + \left((-4t+3s)X^2\right.$$

$$-((9s+t)Y + 24s + 26it\pi + 12t)X - 3i(3s+13t)\pi Y + 3(7s+13t)\zeta(2)$$

$$\left.-12i(2t+s)\pi\right)\mathrm{Li}_2(x) - \frac{1}{2}\left(s+\frac{11}{3}t\right)X^4 + 2((s+t)Y - it\pi + t)X^3$$

$$+\left(-\frac{1}{4}(9s+t)Y^2 - (i(t-3s)\pi + 6(s+t))Y - 25t\zeta(2) + 6i(s+t)\pi\right)X^2$$

$$+\left(-\frac{4}{3}tY^3 + \left(-\frac{1}{2}i(13t+9s)\pi + 6s\right)Y^2 + \left(\frac{1}{2}\left(7s+\frac{5}{3}t\right)\pi^2 - 12i(s+t)\pi + 24s\right)Y\right.$$

$$\left.+(45t-6s)\zeta(3) - \frac{8}{3}it\pi^3 + 42t\zeta(2) + 24i(s+t)\pi - 48t\right)X - \frac{5}{3}Y^4 t$$

$$-\left(\frac{10}{3}it\pi + 2(s+t)\right)Y^3 + (-6it\pi + 5t\zeta(2))Y^2 + \left(-(9s+38t)\zeta(3)\right.$$

$$\left.-\frac{1}{6}i(-9s+17t)\pi^3 - 42(s+t)\zeta(2) - 24it\pi + 48(s+t)\right)Y + (-12t+71it\pi)\zeta(3)$$

$$+9\left(-19t+\frac{7}{12}s\right)\zeta(4) + i(-s+2t)\pi^3 + 48i\pi s\Bigg\}$$

$$\mathrm{XBOX2}(u,t) \;=\; \frac{\Gamma(1+\epsilon)^2\,(-u)^{-2\epsilon}}{ut(u+t)}\left\{-\frac{1}{4\epsilon^4}\Big[3u+t\Big] + \frac{1}{\epsilon^3}\left[\left(-2t+\frac{3}{2}u\right)X\right.\right.$$

$$\left.+\frac{3}{2}(t-u)Y - \frac{1}{2}it\pi\right] + \frac{1}{\epsilon^2}\left[-\frac{1}{2}(t+3u)X^2 + (3(u-t)Y - 3t - 4it\pi)X\right.$$

$$\left.+\frac{3}{2}(t-u)Y^2 - 3Yu + \frac{5}{2}t\zeta(2) - 3i(u+t)\pi\right] + \frac{1}{\epsilon}\left[4tS_{1,2}(z) + 3(u-t)\mathrm{Li}_3(z)\right.$$

$$+\left(3(u-t)X - 3(u-t)Y + 4it\pi\right)\mathrm{Li}_2(z) + \left(2u+\frac{5}{3}t\right)X^3$$

$$+\left(-\frac{3}{2}(3u+t)Y + 5it\pi\right)X^2 + \left(3(u-t)Y^2 + 6(-2it\pi + u)Y\right.$$

$$\left.+41t\zeta(2) + 6(2t+i\pi u)\right)X - \frac{1}{2}(u-t)Y^3 - 6Y^2u + \left(9(u-t)\zeta(2)\right.$$

$$\left.-6u(i\pi - 2)\right)Y + \left(\frac{3}{2}t + 3u\right)\zeta(3) + \frac{3}{2}it\pi^3 + 12i(u+t)\pi\right]$$

$$+(9u+53t)S_{2,2}(z) + 12(2t-u)\mathrm{Li}_4(z) - 98S_{1,3}(z)t$$

$$+\left((83t+9u)X - 9(u+5t)Y - 60it\pi + 12(u-t)\right)S_{1,2}(z)$$

$$+\left(-18(u+t)X + 3(3u-7t)Y + 14it\pi + 12(2t+u)\right)\mathrm{Li}_3(z)$$

$$+\left(-6(2u+5t)X^2 + (3(5u+7t)Y + 44it\pi + 12(2t+u))X - 3(u-3t)Y^2\right.$$

$$\left.-6(it\pi + 4t + 2u)Y + 3(15t-u)\zeta(2) - 12i(t-u)\pi\right)\mathrm{Li}_2(z)$$

$$-\frac{1}{8}\left(23u + \frac{127}{3}t\right)X^4 + \left(\frac{1}{2}(13u + 25t)Y + \frac{25}{3}it\pi + 2(3u + 4t)\right)X^3$$

$$+\left(-\frac{3}{2}(4t + 3u)Y^2 - 6(2u + 3t + it\pi)Y - \frac{3}{2}\left(\frac{29}{3}t + u\right)\zeta(2) - 6it\pi\right)X^2$$

$$+\left((u - 3t)Y^3 + 3(4u + 4t - 3it\pi)Y^2 + (6(8t - 3u)\zeta(2) + 12i(u + t)\pi - 24u)Y\right.$$

$$+3(-2u + 5t)\zeta(3) + 9it\pi^3 + 42t\zeta(2) - 24(2t + i\pi u)\bigg)X + \frac{1}{8}(t - u)Y^4 - 4Y^3u$$

$$+\left(6(u - t)\zeta(2) + 6u(4 - i\pi)\right)Y^2 + \left(15(u - t)\zeta(3) + 24i\pi u - 48u + 42\zeta(2)u\right)Y$$

$$+(-12u + 45it\pi)\zeta(3) - \frac{15}{2}\left(u - \frac{11}{10}t\right)\zeta(4) + i(3u + t)\pi^3 - 48i(u + t)\pi\bigg\}$$

$$\mathrm{XBOX2}(t, u) = \left[\mathrm{XBOX2}(u, t)\right]_{u=t, t=u}$$

$$(\mathrm{B.13})$$

Appendix C | *Finite Contributions*

In this appendix we present, for each partonic process, the expressions for the colour expansion coefficients of the finite pieces for the relevant physical channels indicated in Chapter 6. We use the notation introduced in Appendix B.

C.1 Unlike quark scattering

C.1.1 The s-channel process $q\bar{q} \to \bar{q}'q'$

C.1.1.1 Two-loop contribution

$$
\begin{aligned}
A_s = {} & \left(4 \operatorname{Li}_4(x) + \left(-\frac{22}{3} - 4X \right) \operatorname{Li}_3(x) + \left(\frac{22}{3} X + 2 X^2 - \frac{4}{3} \pi^2 \right) \operatorname{Li}_2(x) + 22 X S \right. \\
& + \frac{197}{18} \zeta_3 + \frac{113}{360} \pi^4 + \frac{1}{3} X^4 + \frac{170}{9} X^2 - \frac{49}{9} X^3 - \frac{7}{3} \pi^2 - \frac{316}{27} X - \frac{5}{3} X^2 \pi^2 + \frac{11}{3} X^2 Y \\
& - \frac{4}{3} \pi^2 X Y - \frac{155}{36} \pi^2 X - \frac{2777}{108} S + \frac{2}{3} X^3 Y - 14 \zeta_3 S + \frac{11}{12} \pi^2 S - \frac{22}{3} X^2 S + \frac{23213}{1296} \\
& \left. - 2 X \zeta_3 + \frac{121}{9} S^2 \right) \left[\frac{t^2 + u^2}{s^2} \right] \\
& + \left(-6 \operatorname{Li}_4(y) + 12 \operatorname{Li}_4(x) - 6 \operatorname{Li}_4(z) + 6 \operatorname{Li}_3(y) X + \left(-7 - 4X \right) \operatorname{Li}_3(x) \right. \\
& + \left(\pi^2 + 7X + X^2 \right) \operatorname{Li}_2(x) - \frac{7}{60} \pi^4 - \frac{64}{9} X + \frac{47}{18} \pi^2 + \pi^2 X Y - \frac{11}{3} X^2 S + \frac{34}{9} X^2 \\
& \left. - 2 X \zeta_3 - \frac{26}{9} \pi^2 X + X^3 Y - \frac{3}{2} X^2 \pi^2 + \frac{7}{2} X^2 Y + \frac{11}{3} X S - \frac{49}{18} X^3 + 4 \zeta_3 \right) \left[\frac{t^2 - u^2}{s^2} \right] \\
& + \left(6 \operatorname{Li}_4(y) - 6 \operatorname{Li}_4(x) + 6 \operatorname{Li}_4(z) - 6 \operatorname{Li}_3(y) X - 5 \operatorname{Li}_3(x) + \left(-\pi^2 + 5X \right) \operatorname{Li}_2(x) \right. \\
& + \frac{1}{4} X^4 + \frac{64}{9} X + \frac{1}{2} X^2 \pi^2 + 6 X \zeta_3 - \frac{11}{18} \pi^2 - \frac{7}{3} \pi^2 X + \frac{5}{2} X^2 Y - \frac{11}{3} X S \\
& \left. + 8 \zeta_3 + \frac{2}{3} X^3 - \frac{8}{3} X^2 + \frac{1}{20} \pi^4 - X^3 Y - \pi^2 X Y \right) + 6 X^2 \frac{t}{u}
\end{aligned}
\tag{C.1}
$$

$$
\begin{aligned}
B_s = {} & \left(\left(12 X + \frac{44}{3} \right) \operatorname{Li}_3(x) - \frac{44}{3} \operatorname{Li}_3(y) - \frac{617}{18} X^2 + 4 X \zeta_3 - \frac{443}{18} \zeta_3 + \frac{125}{9} X^3 - \frac{55}{36} \pi^2 \right. \\
& + \frac{79}{360} \pi^4 - \frac{8}{3} \pi^2 X Y - \frac{16}{27} X - 12 \operatorname{Li}_4(x) - \frac{632}{27} Y - X^4 - \frac{31}{3} X^2 Y + \frac{155}{18} \pi^2 X
\end{aligned}
$$

$$+6\,X^2\,\pi^2 + \left(4\,\pi^2 - 6\,X^2 - \frac{44}{3}\,X - \frac{44}{3}\,Y\right)\mathrm{Li}_2(x) - 2\,X^3\,Y + \frac{1}{12}\,\pi^2\,S - 44\,X\,S$$

$$+2\,\zeta_3\,S + \frac{44}{3}\,X^2\,S - \frac{1502}{27}\,S + \frac{30659}{324} - 4\,Y\,\zeta_3 - \frac{4}{3}\,Y^2\,\pi^2 + X^2\,Y^2 + 44\,Y\,S$$

$$-\frac{44}{3}\,Y^2\,S + \frac{1}{2}\,Y^4 + 9\,X\,Y - \frac{71}{9}\,Y^3 - \frac{31}{3}\,X\,Y^2 - \frac{37}{6}\,Y\,\pi^2 + \frac{599}{18}\,Y^2\right)\left[\frac{t^2 + u^2}{s^2}\right]$$

$$+\left(-24\,\mathrm{Li}_4(y) - \frac{37}{18}\,X^2 - 18\,\zeta_3 + \frac{131}{18}\,X^3 - \frac{88}{9}\,\pi^2 - \frac{1}{10}\,\pi^4 - \frac{2}{3}\,\pi^2\,X\,Y + \frac{74}{9}\,X\right.$$

$$+6\,\mathrm{Li}_4(x) + \frac{128}{9}\,Y - \frac{17}{12}\,X^4 - \frac{15}{2}\,X^2\,Y + \frac{89}{18}\,\pi^2\,X + \frac{13}{6}\,X^2\,\pi^2 + 2\,X^3\,Y - X^2\,Y^2$$

$$+\left(8\,X\,Y - 3\,X^2 - \frac{8}{3}\,\pi^2 - 11\,X + 16\,Y\right)\mathrm{Li}_2(x) - \frac{22}{3}\,X\,S + \frac{22}{3}\,X^2\,S - 16\,\mathrm{Li}_4(z)$$

$$+\left(11 - 24\,Y + 8\,X\right)\mathrm{Li}_3(x) + \left(4\,Y + 16\right)\mathrm{Li}_3(y) + \frac{2}{3}\,X\,Y^3 + 12\,Y\,\zeta_3 + \frac{7}{6}\,Y^2\,\pi^2$$

$$-\frac{22}{3}\,Y\,S + \frac{22}{3}\,Y^2\,S - \frac{1}{3}\,Y^4 + \frac{34}{9}\,Y^3 + 10\,X\,Y^2 + \frac{59}{18}\,Y\,\pi^2 - \frac{181}{18}\,Y^2\right)\left[\frac{t^2 - u^2}{s^2}\right]$$

$$+\left(\left(9 - 12\,Y\right)\mathrm{Li}_3(x) + \left(4\,\pi^2 - 12\,Y - 9\,X\right)\mathrm{Li}_2(x) - 24\,\mathrm{Li}_4(y) + \frac{59}{6}\,X^2\right.$$

$$-12\,X\,\zeta_3 + 10\,\zeta_3 - \frac{5}{3}\,X^3 - \frac{4}{3}\,\pi^2 - \frac{17}{30}\,\pi^4 + 4\,\pi^2\,X\,Y - \frac{74}{9}\,X + 24\,\mathrm{Li}_4(x) + \frac{128}{9}\,Y$$

$$-X^4 - 4\,X^2\,Y + \frac{25}{6}\,\pi^2\,X - 2\,X^2\,\pi^2 + 4\,X^3\,Y + \frac{22}{3}\,X\,S + 12\left(X - 1\right)\mathrm{Li}_3(y)$$

$$+12\,Y\,\zeta_3 - 3\,X^2\,Y^2 - \frac{22}{3}\,Y\,S + X\,Y + \frac{1}{2}\,Y^3 - \frac{11}{2}\,X\,Y^2 - \frac{5}{2}\,Y\,\pi^2 - \frac{23}{6}\,Y^2 - 24\,\mathrm{Li}_4(z)\right)$$

$$-14\,X^2\,\frac{t}{u} + 10\,Y^2\,\frac{u}{t} \tag{C.2}$$

$$C_s = \left(32\,\mathrm{Li}_4(y) - \frac{5}{2}\,X^2 - 15\,\zeta_3 - 9\,X^3 + \frac{29}{12}\,\pi^2 - \frac{49}{30}\,\pi^4 + \frac{44}{3}\,\pi^2\,X\,Y + 48\,X + 16\,\mathrm{Li}_4(x)\right.$$

$$-48\,Y + \frac{5}{6}\,X^4 + 9\,X^2\,Y - \frac{22}{3}\,X^2\,\pi^2 - 16\,\mathrm{Li}_3(x)\,X + \frac{8}{3}\,X^3\,Y - \pi^2\,S + 12\,\zeta_3\,S$$

$$+\left(8\,X^2 - 16\,Y^2 + \frac{16}{3}\,\pi^2\right)\mathrm{Li}_2(x) + \frac{3}{4}\,S + \frac{511}{16} - 32\,\mathrm{Li}_3(y)\,Y - \frac{32}{3}\,X\,Y^3 - 2\,Y^2\,\pi^2$$

$$-3\,X^2\,Y^2 + \frac{1}{6}\,Y^4 - 27\,X\,Y - 9\,Y^3 + 9\,X\,Y^2 + \frac{59}{2}\,Y^2\right)\left[\frac{t^2 + u^2}{s^2}\right]$$

$$+\left(24\,\mathrm{Li}_4(y) - \frac{27}{2}\,X^2 + 16\,X\,\zeta_3 + 8\,\zeta_3 - \frac{16}{3}\,X^3 - \frac{8}{3}\,\pi^2 + \frac{1}{15}\,\pi^4 + 2\,\pi^2\,X\,Y + 12\,X\right.$$

$$-48\,\mathrm{Li}_4(x) + 12\,Y + \frac{8}{3}\,X^4 + 2\,X^2\,Y + \frac{11}{6}\,\pi^2\,X + \frac{1}{6}\,X^2\,\pi^2 - 6\,X^3\,Y$$

$$+\left(36\,Y + 8 - 4\,X\right)\mathrm{Li}_3(x) + \left(-36\,X + 20\,Y - 4\right)\mathrm{Li}_3(y)$$

$$+4\left(2\,Y^2 + X^2 - 2\,X - Y - 6\,X\,Y + 2\,\pi^2\right)\mathrm{Li}_2(x) + 6\,X\,Y^3 - 32\,Y\,\zeta_3 - \frac{1}{6}\,Y^2\,\pi^2$$

$$
-6\,X^2\,Y^2 - \frac{1}{3}\,Y^4 + \frac{14}{3}\,Y^3 - 8\,X\,Y^2 + \frac{3}{2}\,Y\,\pi^2 + \frac{3}{2}\,Y^2 + 48\,\mathrm{Li}_4(z)\Bigg)\left[\frac{t^2-u^2}{s^2}\right]
$$

$$
+\Bigg(8\,\mathrm{Li}_3(y) + 4\,\mathrm{Li}_3(x) + \Big(8\,Y - 4\,X\Big)\,\mathrm{Li}_2(x) - \frac{19}{6}\,Y\,\pi^2 - 12\,X + \frac{3}{2}\,Y^2 + \frac{7}{2}\,Y^3
$$

$$
+\frac{5}{6}\,\pi^2\,X - \frac{7}{2}\,X^2\,Y - \frac{21}{2}\,X^2 + 2\,\pi^2 + \frac{5}{2}\,X\,Y^2 + \frac{3}{2}\,X^3 - 3\,X\,Y + 12\,Y - 24\,\zeta_3\Bigg)
$$

$$
+6\,X^2\,\frac{t}{u} + 6\,Y^2\,\frac{u}{t}
\tag{C.3}
$$

$$
\begin{aligned}
D_s \;=\; &\Bigg(\frac{46}{3}\,S + \frac{37}{18}\,\pi^2\,X - \frac{2}{3}\,X^2\,Y - \frac{4}{3}\,\mathrm{Li}_2(x)\,X + \frac{4}{3}\,\mathrm{Li}_3(x) + \frac{4}{9}\,X^3 - \frac{29}{9}\,X^2 + \frac{41}{18}\,\pi^2 \\
&-\frac{1}{6}\,\pi^2\,S - \frac{455}{27} - \frac{44}{9}\,S^2 - 4\,X\,S + \frac{4}{3}\,X^2\,S + \frac{124}{27}\,X - \frac{49}{9}\,\zeta_3\Bigg)\left[\frac{t^2+u^2}{s^2}\right] \\
&+\Bigg(\frac{8}{9}\,\pi^2\,X + \frac{2}{9}\,X^3 - \frac{13}{9}\,X^2 - \frac{4}{9}\,\pi^2 - \frac{2}{3}\,X\,S + \frac{2}{3}\,X^2\,S + \frac{16}{9}\,X\Bigg)\left[\frac{t^2-u^2}{s^2}\right] \\
&+\Bigg(-\frac{1}{3}\,X^2 + \frac{4}{9}\,\pi^2 - \frac{16}{9}\,X + \frac{2}{3}\,X\,S\Bigg)
\end{aligned}
\tag{C.4}
$$

$$
\begin{aligned}
E_s \;=\; &\Bigg(\frac{8}{3}\,\mathrm{Li}_3(y) - \frac{8}{3}\,\mathrm{Li}_3(x) + \frac{8}{3}\Big(Y + X\Big)\,\mathrm{Li}_2(x) + \frac{236}{27}\,S - \frac{37}{9}\,\pi^2\,X + \frac{4}{3}\,X^2\,Y - \frac{248}{27}\,X \\
&-\frac{1370}{81} + \frac{4}{3}\,X\,Y^2 - \frac{8}{9}\,X^3 + \frac{58}{9}\,X^2 - \frac{7}{18}\,\pi^2 + \frac{1}{6}\,\pi^2\,S + \frac{8}{3}\,Y^2\,S + \frac{11}{3}\,Y\,\pi^2 + 8\,X\,S \\
&-\frac{8}{3}\,X^2\,S - \frac{58}{9}\,Y^2 - 8\,Y\,S - \frac{35}{9}\,\zeta_3 + \frac{8}{9}\,Y^3 + \frac{248}{27}\,Y\Bigg)\left[\frac{t^2+u^2}{s^2}\right] \\
&+\Bigg(-\frac{32}{9}\,X + \frac{16}{9}\,\pi^2 + \frac{26}{9}\,Y^2 - \frac{16}{9}\,\pi^2\,X - \frac{4}{9}\,Y^3 - \frac{32}{9}\,Y - \frac{4}{9}\,X^3 + \frac{4}{3}\,X\,S - \frac{4}{3}\,X^2\,S \\
&-\frac{4}{3}\,Y^2\,S + \frac{4}{3}\,Y\,S + \frac{26}{9}\,X^2 - \frac{16}{9}\,Y\,\pi^2\Bigg)\left[\frac{t^2-u^2}{s^2}\right] \\
&+\frac{2}{9}\Big(X - Y\Big)\Big(3\,X + 16 - 6\,S + 3\,Y\Big)
\end{aligned}
\tag{C.5}
$$

$$
F_s \;=\; -\frac{4}{81}\Big(3\,S - 5 + 3\,\pi\Big)\Big(-3\,S + 5 + 3\,\pi\Big)\left[\frac{t^2+u^2}{s^2}\right]
\tag{C.6}
$$

C.1.1.2   One-loop self-interference contribution

$$
\begin{aligned}
A_s \;=\; &\Bigg(\frac{4}{3}\,X\,\pi^2 - 3\,X^3 + \frac{2}{9}\,\pi^2 + 11\,X\,S - \frac{11}{3}\,X^2\,S - \frac{13}{3}\,X + \frac{121}{18}\,S^2 \\
&+\frac{107}{18}\,X^2 + \frac{169}{162} - \frac{143}{27}\,S + 2\,X^2\,\pi^2 + \frac{1}{2}\,X^4\Bigg)\left[\frac{t^2+u^2}{s^2}\right] \\
&+\Bigg(-\frac{13}{18}\,X + \frac{1}{2}\,X^4 - \frac{1}{3}\,\pi^2 - \frac{1}{3}\,X\,\pi^2 + \frac{20}{9}\,X^2
\end{aligned}
$$

$$+ \frac{11}{6} X S - 2 X^3 + 2 X^2 \pi^2 - \frac{11}{6} X^2 S \Bigg) \left[\frac{t^2 - u^2}{s^2} \right]$$

$$+ \left(\frac{1}{2} X^2 \pi^2 + \frac{1}{8} X^4 + \frac{5}{6} \pi^2 - X^2 + \frac{13}{18} X - \frac{11}{6} X S \right)$$

$$- \frac{1}{4} X \left(- 4 \pi^2 + X^3 - 2 X^2 + 4 X \pi^2 \right) \frac{t}{u} + \frac{1}{8} X^2 \left(4 \pi^2 + X^2 \right) \frac{t^2}{u^2} \quad \text{(C.7)}$$

$$B_s = \left(\frac{133}{18} Y^2 - \frac{26}{3} Y - \frac{8}{3} X \pi^2 - 6 X^2 \pi^2 + 9 X^3 - \frac{3}{2} X^4 + \frac{104}{9} - \frac{46}{3} X - \frac{22}{3} Y^2 S \right.$$

$$+ 22 Y S + \frac{22}{3} X^2 S - 22 X S + 4 Y X \pi^2 - 3 Y^2 X + 9 Y X + Y^2 X^2 - \frac{151}{18} X^2$$

$$+ 2 Y^2 \pi^2 - 3 Y^3 + \frac{1}{2} Y^4 - \frac{88}{3} S + \frac{8}{3} Y \pi^2 - 3 Y X^2 \Bigg) \left[\frac{t^2 + u^2}{s^2} \right]$$

$$+ \left(- \frac{53}{18} Y^2 + \frac{13}{9} Y + \frac{8}{3} X \pi^2 - 6 X^2 \pi^2 + 6 X^3 - \frac{3}{2} X^4 + \frac{4}{3} \pi^2 - \frac{23}{9} X \right.$$

$$+ \frac{11}{3} Y^2 S - \frac{11}{3} Y S + \frac{11}{3} X^2 S - \frac{11}{3} X S + Y^2 X - \frac{35}{18} X^2 - 2 Y^2 \pi^2 + 2 Y^3$$

$$- \frac{1}{2} Y^4 - \frac{4}{3} Y \pi^2 - Y X^2 \Bigg) \left[\frac{t^2 - u^2}{s^2} \right]$$

$$+ \left(\frac{1}{2} Y^2 X - 3 Y X - \frac{11}{3} Y S - Y^2 + \frac{13}{9} Y + X \pi^2 - \frac{3}{2} X^2 \pi^2 - \frac{3}{8} X^4 - \pi^2 \right.$$

$$+ \frac{11}{3} X S + \frac{23}{9} X + 3 X^2 + \frac{1}{2} Y^2 \pi^2 + \frac{1}{2} Y X^2 + Y \pi^2 + \frac{1}{8} Y^4 \Bigg)$$

$$- \frac{3}{8} X^2 \left(4 \pi^2 + X^2 \right) \frac{t^2}{u^2} + \frac{1}{8} Y^2 \left(Y^2 + 4 \pi^2 \right) \frac{u^2}{t^2}$$

$$+ \frac{3}{4} X \left(- 4 \pi^2 + X^3 - 2 X^2 + 4 X \pi^2 \right) \frac{t}{u}$$

$$- \frac{1}{4} Y \left(- 4 \pi^2 + 4 Y \pi^2 - 2 Y^2 + Y^3 \right) \frac{u}{t} \quad \text{(C.8)}$$

$$C_s = \left(\frac{59}{2} Y^2 - 48 Y + 6 X^2 \pi^2 - 9 X^3 + \frac{3}{2} X^4 + 48 X + 32 - 12 Y X \pi^2 + 9 Y^2 X \right.$$

$$- 27 Y X - 3 Y^2 X^2 - \frac{5}{2} X^2 + 6 Y^2 \pi^2 - 9 Y^3 + \frac{3}{2} Y^4 + 9 Y X^2 \Bigg) \left[\frac{t^2 + u^2}{s^2} \right]$$

$$+ \left(6 Y^3 - 3 Y^2 X - 6 Y^2 \pi^2 + 8 X - \frac{25}{2} Y^2 - \frac{3}{2} Y^4 + 3 Y X^2 - 6 X \pi^2 \right.$$

$$+ 6 X^2 \pi^2 + 8 Y - 6 X^3 - \frac{7}{2} X^2 + 6 Y \pi^2 + \frac{3}{2} X^4 \Bigg) \left[\frac{t^2 - u^2}{s^2} \right]$$

$$+ \left(- 8 X - 3 Y \pi^2 - \frac{3}{2} Y^2 X + 9 Y X - 3 X^2 + \frac{3}{2} Y^2 \pi^2 - 3 Y^2 \right.$$

$$+ 8 Y - 3 X \pi^2 + \frac{3}{2} X^2 \pi^2 - \frac{3}{2} Y X^2 + \frac{3}{8} X^4 + 3 \pi^2 + \frac{3}{8} Y^4 \Bigg)$$

$$+\frac{3}{8}X^2\left(4\pi^2+X^2\right)\frac{t^2}{u^2}+\frac{3}{8}Y^2\left(Y^2+4\pi^2\right)\frac{u^2}{t^2}$$

$$-\frac{3}{4}X\left(-4\pi^2+X^3-2X^2+4X\pi^2\right)\frac{t}{u}$$

$$-\frac{3}{4}Y\left(-4\pi^2+4Y\pi^2-2Y^2+Y^3\right)\frac{u}{t} \tag{C.9}$$

$$
\begin{aligned}
D_s \ = \ & \left(-\frac{4}{3}X\pi^2-\frac{4}{9}\pi^2+\frac{10}{3}X+\frac{2}{3}X^2S-2XS-\frac{22}{9}S^2-\frac{10}{9}X^2\right.\\
& \left.-\frac{130}{81}+\frac{136}{27}S\right)\left[\frac{t^2+u^2}{s^2}\right]\\
& +\left(-\frac{2}{3}X\pi^2+\frac{1}{3}\pi^2+\frac{5}{9}X+\frac{1}{3}X^2S-\frac{1}{3}XS-\frac{5}{9}X^2\right)\left[\frac{t^2-u^2}{s^2}\right]\\
& +\left(\frac{1}{3}XS-\frac{5}{9}X-\frac{1}{3}\pi^2\right)
\end{aligned} \tag{C.10}
$$

$$
\begin{aligned}
E_s \ = \ & \left(-\frac{20}{9}Y^2+\frac{20}{3}Y+\frac{8}{3}X\pi^2-\frac{20}{3}X+4XS-\frac{80}{9}+\frac{4}{3}Y^2S\right.\\
& \left.-4YS+\frac{20}{9}X^2+\frac{16}{3}S-\frac{8}{3}Y\pi^2-\frac{4}{3}X^2S\right)\left[\frac{t^2+u^2}{s^2}\right]\\
& +\left(\frac{10}{9}Y^2-\frac{10}{9}Y+\frac{4}{3}X\pi^2-\frac{4}{3}\pi^2-\frac{10}{9}X+\frac{2}{3}XS-\frac{2}{3}Y^2S\right.\\
& \left.+\frac{2}{3}YS+\frac{10}{9}X^2+\frac{4}{3}Y\pi^2-\frac{2}{3}X^2S\right)\left[\frac{t^2-u^2}{s^2}\right]\\
& -\frac{2}{9}\left(3S-5\right)\left(X-Y\right)
\end{aligned} \tag{C.11}
$$

$$F_s \ = \ \left(\frac{50}{81}-\frac{20}{27}S+\frac{2}{9}\pi^2+\frac{2}{9}S^2\right)\left[\frac{t^2+u^2}{s^2}\right] \tag{C.12}$$

C.1.2 The u-channel process $q\bar{q}' \to q\bar{q}'$

C.1.2.1 Two-loop contribution

$$
\begin{aligned}
A_u \ = \ & \left(\left(\frac{22}{3}+4X-4Y\right)\mathrm{Li}_3(x)+\left(\frac{22}{3}+4X-4Y\right)\mathrm{Li}_3(y)+\left(-\frac{2}{3}\pi^2-\frac{22}{3}X-2Y^2\right.\right.\\
& \left.-2X^2+4YX+\frac{22}{3}Y\right)\mathrm{Li}_2(x)-\frac{77}{12}\pi^2U+\frac{44}{3}YXU-\frac{4}{3}XY\pi^2-\frac{10}{3}XY^3\\
& +Y^2\pi^2+6Y\zeta_3+4X^2Y^2-6X\zeta_3+\frac{121}{9}U^2-9XY^2-\frac{22}{3}Y^2U-\frac{215}{36}X\pi^2\\
& -14\zeta_3U-\frac{22}{3}X^2U+22XU+\frac{23213}{1296}-\frac{2777}{108}U-4\,\mathrm{Li}_4(z)+\frac{1}{6}X^4-\frac{49}{9}X^3
\end{aligned}
$$

$$+\frac{38}{9}Y^3 + \frac{1}{2}Y^4 + \frac{38}{3}X^2Y + \frac{65}{18}\zeta_3 + \frac{170}{9}X^2 + \frac{170}{9}Y^2 + \frac{316}{27}Y - 22YU$$

$$+8\pi^2 + \frac{17}{72}\pi^4 - \frac{316}{27}X - \frac{4}{3}X^3Y - \frac{340}{9}YX + \frac{13}{12}Y\pi^2\Bigg)\left[\frac{t^2+s^2}{u^2}\right]$$

$$+\Bigg(\Bigg(10X + 7 - 10Y\Bigg)\mathrm{Li}_3(y) + \Bigg(4X + 7 - 4Y\Bigg)\mathrm{Li}_3(x) + \Bigg(-2\pi^2 + 7Y - X^2$$

$$-7X + 2YX - Y^2\Bigg)\mathrm{Li}_2(x) - \frac{11}{3}\pi^2U + \frac{22}{3}YXU - \frac{5}{3}XY\pi^2 - \frac{1}{2}\pi^2X^2$$

$$+6\,\mathrm{Li}_4(x) - \frac{5}{3}XY^3 - \frac{5}{6}Y^2\pi^2 + 6Y\zeta_3 + \frac{3}{2}X^2Y^2 - 6X\zeta_3 - \frac{7}{6}XY^2$$

$$-\frac{11}{3}Y^2U - \frac{67}{18}X\pi^2 - \frac{11}{3}X^2U + \frac{11}{3}XU - 12\,\mathrm{Li}_4(z) - \frac{1}{4}X^4 - \frac{49}{18}X^3$$

$$+\frac{14}{9}Y^3 - \frac{1}{12}Y^4 + 6\,\mathrm{Li}_4(y) + \frac{14}{3}X^2Y - 3\zeta_3 + \frac{34}{9}X^2 + \frac{34}{9}Y^2 + \frac{64}{9}Y$$

$$-\frac{11}{3}YU + \frac{49}{18}\pi^2 - \frac{7}{60}\pi^4 - \frac{64}{9}X + X^3Y - \frac{68}{9}YX - \frac{17}{18}Y\pi^2\Bigg)\left[\frac{t^2-s^2}{u^2}\right]$$

$$+\Bigg(\Bigg(-5X + 5Y + \pi^2\Bigg)\mathrm{Li}_2(x) + \Bigg(6Y - 6X + 5\Bigg)\mathrm{Li}_3(y) + XY\pi^2 + \frac{1}{2}\pi^2X^2$$

$$-6\,\mathrm{Li}_4(x) + Y^2\pi^2 - 6Y\zeta_3 + 6X\zeta_3 + 5\,\mathrm{Li}_3(x) + 7XY^2 - \frac{1}{3}X\pi^2 - \frac{11}{3}XU$$

$$+6\,\mathrm{Li}_4(z) + \frac{1}{4}X^4 + \frac{2}{3}X^3 - \frac{3}{2}Y^3 + \frac{1}{4}Y^4 - 6\,\mathrm{Li}_4(y) - \frac{9}{2}X^2Y + 3\zeta_3 - \frac{8}{3}X^2$$

$$-\frac{8}{3}Y^2 - \frac{64}{9}Y + \frac{11}{3}YU + \frac{7}{18}\pi^2 + \frac{11}{60}\pi^4 + \frac{64}{9}X - X^3Y + \frac{16}{3}YX - 3Y\pi^2\Bigg)$$

$$+\Bigg(6X^2 + 6\pi^2 - 12YX + 6Y^2\Bigg)\frac{t}{s} \tag{C.13}$$

$$B_u = \Bigg(\Bigg(2\pi^2 - \frac{88}{3}Y + 6Y^2 + 6X^2 - 12YX + \frac{44}{3}X\Bigg)\mathrm{Li}_2(x) + \frac{59}{4}\pi^2U - \frac{88}{3}YXU$$

$$+\frac{14}{3}XY\pi^2 + \pi^2X^2 + 8XY^3 - 5Y^2\pi^2 - 12Y\zeta_3 - 11X^2Y^2 + 16X\zeta_3$$

$$+\frac{32}{3}XY^2 + \frac{269}{18}X\pi^2 + 2\zeta_3U + \frac{44}{3}X^2U - 44XU + \frac{30659}{324} - \frac{1502}{27}U$$

$$+12\,\mathrm{Li}_4(z) - \frac{1}{2}X^4 + \frac{125}{9}X^3 - \frac{94}{3}X^2Y - \frac{179}{18}\zeta_3 - \frac{617}{18}X^2 + 8Y^2 + 24Y$$

$$-\frac{965}{36}\pi^2 - \frac{437}{360}\pi^4 - \frac{16}{27}X + 4X^3Y + \frac{536}{9}YX - \frac{130}{9}Y\pi^2$$

$$+\Bigg(12Y - \frac{44}{3} - 12X\Bigg)\mathrm{Li}_3(x) + \Bigg(-12X + 12Y - \frac{88}{3}\Bigg)\mathrm{Li}_3(y)\Bigg)\left[\frac{t^2+s^2}{u^2}\right]$$

$$+\Bigg(\Bigg(-8X + 5 - 20Y\Bigg)\mathrm{Li}_3(y) + \Bigg(-8X - 11 - 16Y\Bigg)\mathrm{Li}_3(x)$$

$$+\Bigg(-\frac{7}{3}\pi^2 + 5Y + 3X^2 + 11X + 2YX - 5Y^2\Bigg)\mathrm{Li}_2(x) + \frac{22}{3}\pi^2U - \frac{44}{3}YXU$$

$$+\frac{17}{3}XY\pi^2 - \frac{3}{2}\pi^2X^2 + 16\,\mathrm{Li}_4(x) - \frac{11}{3}XY^3 + \frac{3}{2}Y^2\pi^2 + 4Y\zeta_3 - \frac{15}{2}X^2Y^2$$

$$+8X\zeta_3 + \frac{101}{6}XY^2 + \frac{44}{3}Y^2U + \frac{73}{9}X\pi^2 + \frac{22}{3}X^2U - \frac{22}{3}XU - 6\,\mathrm{Li}_4(z)$$

$$-X^4 + \frac{131}{18}X^3 - \frac{59}{9}Y^3 + \frac{1}{6}Y^4 + 24\,\mathrm{Li}_4(y) - \frac{43}{3}X^2Y - 7\zeta_3 - \frac{37}{18}X^2 - \frac{109}{9}Y^2$$

$$-\frac{202}{9}Y + \frac{44}{3}YU + \frac{17}{6}\pi^2 - \frac{61}{45}\pi^4 + \frac{74}{9}X + \frac{14}{3}X^3Y + \frac{37}{9}YX + \frac{59}{18}Y\pi^2\Bigg)\left[\frac{t^2 - s^2}{u^2}\right]$$

$$+\left(\left(-12Y - 9\right)\mathrm{Li}_3(x) + \left(-4\pi^2 + 9X - 21Y\right)\mathrm{Li}_2(x) + 24\,\mathrm{Li}_4(x)\right.$$

$$+\left(-21 - 24Y + 12X\right)\mathrm{Li}_3(y) - 2\pi^2X^2 - 2XY^3 - 3Y^2\pi^2 + 12Y\zeta_3 - 3X^2Y^2$$

$$-12X\zeta_3 - \frac{37}{2}XY^2 + \frac{1}{6}X\pi^2 + \frac{22}{3}XU - 24\,\mathrm{Li}_4(z) - X^4 - \frac{5}{3}X^3 - \frac{1}{3}Y^3$$

$$+24\,\mathrm{Li}_4(y) + 9X^2Y + 19\zeta_3 + \frac{59}{6}X^2 + 7Y^2 - 6Y + \frac{19}{2}\pi^2 - \frac{11}{10}\pi^4$$

$$-\frac{74}{9}X + 4X^3Y - \frac{62}{3}YX + \frac{65}{6}Y\pi^2\Bigg)$$

$$+\left(28YX - 14\pi^2 - 14X^2 - 14Y^2\right)\frac{t}{s} + 10Y^2\frac{s}{t} \tag{C.14}$$

$$C_u \;=\; \left(\left(-\frac{40}{3}\pi^2 + 8Y^2 - 8X^2 + 16YX\right)\mathrm{Li}_2(x) + \left(-16Y + 16X\right)\mathrm{Li}_3(x)\right.$$

$$+\left(16Y + 16X\right)\mathrm{Li}_3(y) - \pi^2U - 6XY\pi^2 - \frac{11}{3}\pi^2X^2 + \frac{16}{3}XY^3 - \frac{22}{3}Y^2\pi^2$$

$$+16Y\zeta_3 + 10X^2Y^2 - 16X\zeta_3 - 9X\pi^2 + 12\zeta_3U + \frac{511}{16} + \frac{3}{4}U - 16\,\mathrm{Li}_4(z)$$

$$+\frac{1}{6}X^4 - 9X^3 - 32\,\mathrm{Li}_4(y) + 18X^2Y - 15\zeta_3 - \frac{5}{2}X^2 - \frac{325}{12}\pi^2 + \frac{18}{5}\pi^4 + 48X$$

$$-\frac{10}{3}X^3Y + 32YX - 18Y\pi^2\Bigg)\left[\frac{t^2 + s^2}{u^2}\right]$$

$$+\left(\left(-12Y + 12\pi^2 + 8X + 12Y^2 - 4X^2 - 16YX\right)\mathrm{Li}_2(x) - XY\pi^2\right.$$

$$+\left(4X + 32Y - 8\right)\mathrm{Li}_3(x) + \frac{25}{6}\pi^2X^2 + \left(-12 + 48Y - 32X\right)\mathrm{Li}_3(y)$$

$$-48\,\mathrm{Li}_4(x) + \frac{20}{3}XY^3 + \frac{10}{3}Y^2\pi^2 - 16Y\zeta_3 + 4X^2Y^2 + 12X\zeta_3 - 20XY^2 - \frac{27}{2}X^2$$

$$-\frac{13}{6}X\pi^2 + 48\,\mathrm{Li}_4(z) + \frac{8}{3}X^4 - \frac{16}{3}X^3 + \frac{4}{3}Y^3 + \frac{2}{3}Y^4 - 24\,\mathrm{Li}_4(y) + 14X^2Y + 16\zeta_3$$

$$-12Y^2 - 24Y - \frac{97}{6}\pi^2 + \frac{21}{10}\pi^4 + 12X - \frac{38}{3}X^3Y + 27YX + \frac{40}{3}Y\pi^2\Bigg)\left[\frac{t^2 - s^2}{u^2}\right]$$

$$+\left(-4\,\mathrm{Li}_3(x) + 4\,\mathrm{Li}_3(y) + \left(4X + 4Y\right)\mathrm{Li}_2(x) + \frac{16}{3}Y\pi^2 - 12Y^2 + \frac{7}{3}X\pi^2\right.$$

$$+\frac{3}{2}X^3 - \frac{23}{2}\pi^2 - \frac{21}{2}X^2 - X^2Y - 20\zeta_3 - 12X + 24YX\Bigg)$$

$$+\left(6X^2 + 6\pi^2 - 12YX + 6Y^2\right)\frac{t}{s} + 6Y^2\frac{s}{t} \tag{C.15}$$

$$
\begin{aligned}
D_u = & \left(-\frac{4}{3}\,\mathrm{Li}_3(x) - \frac{4}{3}\,\mathrm{Li}_3(y) + \left(\frac{4}{3}\,X - \frac{4}{3}\,Y\right)\mathrm{Li}_2(x) + \frac{1}{6}\,Y\,\pi^2 + \frac{13}{18}\,X\,\pi^2 + \frac{58}{9}\,Y\,X \right. \\
& + \frac{4}{9}\,X^3 + \frac{7}{6}\,\pi^2\,U - \frac{8}{3}\,Y\,X\,U + \frac{4}{3}\,X^2\,U - 4\,X\,U + 4\,Y\,U + \frac{4}{3}\,Y^2\,U - \frac{44}{9}\,U^2 + \frac{46}{3}\,U \\
& \left. -\frac{455}{27} - \frac{124}{27}\,Y + \frac{124}{27}\,X - \frac{2}{3}\,X^2\,Y - \frac{29}{9}\,Y^2 - \frac{11}{6}\,\pi^2 - \frac{2}{9}\,Y^3 - \frac{29}{9}\,X^2 - \frac{37}{9}\,\zeta_3 \right)\left[\frac{t^2 + s^2}{u^2}\right. \\
& + \left(-\frac{16}{9}\,Y + \frac{16}{9}\,X - \frac{2}{3}\,X^2\,Y + \frac{2}{3}\,X\,Y^2 + \frac{2}{3}\,\pi^2\,U - \frac{2}{9}\,Y\,\pi^2 + \frac{26}{9}\,Y\,X + \frac{2}{9}\,X\,\pi^2 \right. \\
& + \frac{2}{9}\,X^3 - \frac{13}{9}\,Y^2 - \frac{13}{9}\,X^2 - \frac{11}{9}\,\pi^2 - \frac{2}{9}\,Y^3 + \frac{2}{3}\,X^2\,U - \frac{2}{3}\,X\,U + \frac{2}{3}\,Y^2\,U \\
& \left. + \frac{2}{3}\,Y\,U - \frac{4}{3}\,Y\,X\,U \right)\left[\frac{t^2 - s^2}{u^2}\right] \\
& + \left(\frac{16}{9}\,Y - \frac{16}{9}\,X + \frac{2}{3}\,Y\,X - \frac{1}{3}\,Y^2 - \frac{1}{3}\,X^2 - \frac{5}{9}\,\pi^2 - \frac{2}{3}\,Y\,U + \frac{2}{3}\,X\,U \right) \quad\text{(C.1}
\end{aligned}
$$

$$
\begin{aligned}
E_u = & \left(\frac{8}{3}\,\mathrm{Li}_3(x) + \frac{16}{3}\,\mathrm{Li}_3(y) + \left(\frac{16}{3}\,Y - \frac{8}{3}\,X\right)\mathrm{Li}_2(x) + \frac{58}{9}\,X^2 + \frac{109}{18}\,\pi^2 - \frac{59}{9}\,\zeta_3 \right. \\
& - \frac{248}{27}\,X + \frac{16}{3}\,Y\,X\,U + \frac{4}{3}\,X^2\,Y + \frac{4}{3}\,X\,Y^2 - \frac{13}{9}\,X\,\pi^2 - \frac{5}{2}\,\pi^2\,U + \frac{4}{9}\,Y\,\pi^2 \\
& \left. - \frac{116}{9}\,Y\,X - \frac{8}{3}\,X^2\,U - \frac{8}{9}\,X^3 + \frac{236}{27}\,U - \frac{1370}{81} + 8\,X\,U \right)\left[\frac{t^2 + s^2}{u^2}\right] \\
& + \left(\frac{64}{9}\,Y - \frac{32}{9}\,X + \frac{4}{3}\,X^2\,Y - \frac{4}{3}\,X\,Y^2 - \frac{4}{3}\,\pi^2\,U - \frac{4}{9}\,Y\,\pi^2 - \frac{52}{9}\,Y\,X \right. \\
& - \frac{4}{9}\,X\,\pi^2 - \frac{4}{9}\,X^3 + \frac{52}{9}\,Y^2 + \frac{26}{9}\,X^2 + 2\,\pi^2 + \frac{8}{9}\,Y^3 - \frac{4}{3}\,X^2\,U + \frac{4}{3}\,X\,U \\
& \left. - \frac{8}{3}\,Y^2\,U - \frac{8}{3}\,Y\,U + \frac{8}{3}\,Y\,X\,U \right)\left[\frac{t^2 - s^2}{u^2}\right] \\
& + \left(\frac{32}{9}\,X - \frac{4}{3}\,Y\,X - \frac{4}{3}\,X\,U + \frac{2}{3}\,\pi^2 + \frac{2}{3}\,X^2 \right) \quad\text{(C.17)}
\end{aligned}
$$

$$
F_u = \frac{4}{81}\left(3\,U - 5\right)^2\left[\frac{t^2 + s^2}{u^2}\right] \quad\text{(C.18)}
$$

C.1.2.2 One-loop self-interference contribution

$$
\begin{aligned}
A_u = & \frac{1}{162}\left(-9\,X^2 + 18\,X\,Y + 27\,X - 27\,Y - 9\,Y^2 - 9\,\pi^2 + 33\,U - 13 \right)^2\left[\frac{t^2 + s^2}{u^2}\right] \\
& - \frac{1}{18}\left(\pi^2 - X + Y + X^2 + Y^2 - 2\,X\,Y \right)\left(-9\,X^2 + 18\,X\,Y + 27\,X - 27\,Y \right. \\
& \left. -9\,Y^2 - 9\,\pi^2 + 33\,U - 13 \right)\left[\frac{t^2 - s^2}{u^2}\right] \\
& + \left(-\frac{13}{18}\,Y + \frac{11}{6}\,Y\,U + \frac{1}{8}\,\pi^4 + \frac{1}{8}\,X^4 + \frac{1}{8}\,Y^4 - X^2 - \frac{1}{2}\,Y^3\,X + \frac{1}{4}\,Y^2\,\pi^2 + \frac{1}{4}\,X^2\,\pi^2 \right.
\end{aligned}
$$

$$
+2\,X\,Y - \frac{1}{2}\,Y\,X^3 + \frac{3}{4}\,Y^2\,X^2 - \frac{11}{6}\,X\,U - Y^2 - \frac{1}{2}\,Y\,X\,\pi^2 + \frac{13}{18}\,X\Bigg)
$$

$$
-\frac{1}{4}\left(X^2 - 2\,X\,Y + Y^2 + \pi^2\right)\left(X^2 - 2\,X + \pi^2 - 2\,X\,Y + 2\,Y + Y^2\right)\frac{t}{s}
$$

$$
+\frac{1}{8}\left(X^2 - 2\,X\,Y + Y^2 + \pi^2\right)^2 \frac{t^2}{s^2} \tag{C.19}
$$

$$
B_u = \Bigg(-24\,Y\,X^2 + 9\,X\,\pi^2 + 4\,Y^3\,X - 3\,X^2\,\pi^2 + \frac{70}{9}\,X\,Y + 18\,Y^2\,X + 6\,Y\,X^3
$$

$$
-8\,Y^2\,X^2 + \frac{104}{9} + \frac{22}{3}\,\pi^2\,U - 22\,X\,U + \frac{22}{3}\,X^2\,U - \frac{44}{3}\,X\,Y\,U + 24\,Y - \frac{3}{2}\,\pi^4
$$

$$
-\frac{3}{2}\,X^4 + \frac{173}{18}\,\pi^2 - \frac{151}{18}\,X^2 + 9\,X^3 + 8\,Y^2 - \frac{46}{3}\,X - \frac{88}{3}\,U + 6\,Y\,X\,\pi^2\Bigg)\left[\frac{t^2 + s^2}{u^2}\right]
$$

$$
+\Bigg(6\,X^3 - 8\,Y^3 - 17\,Y\,X^2 + 6\,X\,\pi^2 + 17\,Y^2\,X + \frac{11}{3}\,X^2\,U + \frac{22}{3}\,Y^2\,U - 9\,Y\,\pi^2
$$

$$
-\frac{22}{3}\,X\,Y\,U + 6\,Y\,X\,\pi^2 + \frac{19}{18}\,\pi^2 + \frac{11}{3}\,\pi^2\,U - \frac{3}{2}\,\pi^4 + \frac{35}{9}\,X\,Y - \frac{23}{9}\,X - \frac{35}{18}\,X^2
$$

$$
+\frac{10}{9}\,Y - \frac{44}{9}\,Y^2 - \frac{3}{2}\,X^4 - 2\,Y^4 + \frac{22}{3}\,Y\,U + 6\,Y^3\,X - 5\,Y^2\,\pi^2 - 3\,X^2\,\pi^2
$$

$$
+6\,Y\,X^3 - 9\,Y^2\,X^2 - \frac{11}{3}\,X\,U\Bigg)\left[\frac{t^2 - s^2}{u^2}\right]
$$

$$
+\Bigg(-\frac{1}{4}\,Y^2\,\pi^2 - Y^2 - \frac{3}{4}\,X^2\,\pi^2 - \frac{3}{8}\,X^4 + \frac{3}{2}\,Y^2\,X + \frac{3}{2}\,Y\,X^3 + 3\,X^2 - \frac{9}{4}\,Y^2\,X^2
$$

$$
-Y^3 - \frac{1}{4}\,Y^4 - \pi^2 - 3\,X\,Y + \frac{11}{3}\,X\,U - \frac{1}{2}\,Y\,X^2 - \frac{1}{2}\,Y\,\pi^2 - 4\,Y + \frac{3}{2}\,Y^3\,X - \frac{3}{8}\,\pi^4
$$

$$
+\frac{23}{9}\,X + \frac{3}{2}\,Y\,X\,\pi^2\Bigg)
$$

$$
-\frac{3}{8}\left(X^2 - 2\,X\,Y + Y^2 + \pi^2\right)^2 \frac{t^2}{s^2} + \frac{1}{8}\,Y^2\left(4\,\pi^2 + Y^2\right)\frac{s^2}{t^2}
$$

$$
+\frac{3}{4}\left(X^2 - 2\,X\,Y + Y^2 + \pi^2\right)\left(X^2 - 2\,X + \pi^2 - 2\,X\,Y + 2\,Y + Y^2\right)\frac{t}{s}
$$

$$
-\frac{1}{4}\,Y\left(2\,Y^2 + Y^3 + 4\,\pi^2 + 4\,Y\,\pi^2\right)\frac{s}{t} \tag{C.20}
$$

$$
C_u = \Bigg(18\,Y\,X^2 + 18\,Y\,\pi^2 - 9\,X\,\pi^2 + 6\,Y^2\,\pi^2 + 3\,X^2\,\pi^2 + 32\,X\,Y - 6\,Y\,X^3 + 6\,Y^2\,X^2
$$

$$
+\frac{3}{2}\,\pi^4 + \frac{3}{2}\,X^4 - \frac{5}{2}\,\pi^2 - \frac{5}{2}\,X^2 - 9\,X^3 + 48\,X - 6\,Y\,X\,\pi^2 + 32\Bigg)\left[\frac{t^2 + s^2}{u^2}\right]
$$

$$
+\Bigg(15\,Y\,X^2 - 9\,Y\,\pi^2 - 6\,X\,\pi^2 - 6\,Y^3\,X - 3\,Y^2\,\pi^2 + 3\,X^2\,\pi^2 + 7\,X\,Y - 15\,Y^2\,X
$$

$$
-6\,Y\,X^3 + 9\,Y^2\,X^2 - 16\,Y + \frac{3}{2}\,\pi^4 + \frac{3}{2}\,X^4 - \frac{25}{2}\,\pi^2 - \frac{7}{2}\,X^2 - 6\,X^3
$$

$$
-16\,Y^2 + 8\,X - 6\,Y\,X\,\pi^2\Bigg)\left[\frac{t^2 - s^2}{u^2}\right]
$$

$$+\left(\frac{3}{8}\,\pi^4 + \frac{3}{8}\,X^4 + 3\,Y^3 + \frac{3}{4}\,Y^4 + \frac{3}{2}\,Y\,X^2 + \frac{3}{2}\,Y\,\pi^2 - \frac{3}{2}\,Y^3\,X + \frac{9}{4}\,Y^2\,\pi^2 + \frac{3}{4}\,X^2\,\pi^2\right.$$

$$\left. -3\,X\,Y - \frac{9}{2}\,Y^2\,X - \frac{3}{2}\,Y\,X^3 + \frac{9}{4}\,Y^2\,X^2 - 3\,\pi^2 - 3\,X^2 - \frac{3}{2}\,Y\,X\,\pi^2 - 8\,X + 3\,Y^2\right)$$

$$+\frac{3}{8}\left(X^2 - 2\,X\,Y + Y^2 + \pi^2\right)^2\frac{t^2}{s^2} + \frac{3}{8}\,Y^2\left(4\,\pi^2 + Y^2\right)\frac{s^2}{t^2}$$

$$-\frac{3}{4}\left(X^2 - 2\,X\,Y + Y^2 + \pi^2\right)\left(X^2 - 2\,X + \pi^2 - 2\,X\,Y + 2\,Y + Y^2\right)\frac{t}{s}$$

$$-\frac{3}{4}\,Y\left(2\,Y^2 + Y^3 + 4\,\pi^2 + 4\,Y\,\pi^2\right)\frac{s}{t} \tag{C.21}$$

$$\begin{aligned}
D_u &= -\frac{2}{81}\left(3\,U - 5\right)\left(-9\,X^2 + 18\,X\,Y + 27\,X - 27\,Y - 9\,Y^2\right.\\
&\qquad\left. -9\,\pi^2 + 33\,U - 13\right)\left[\frac{t^2 + s^2}{u^2}\right]\\
&\quad +\frac{1}{9}\left(\pi^2 - X + Y + X^2 + Y^2 - 2\,X\,Y\right)\left(3\,U - 5\right)\left[\frac{t^2 - s^2}{u^2}\right]\\
&\quad +\frac{1}{9}\left(3\,U - 5\right)\left(X - Y\right) \tag{C.22}
\end{aligned}$$

$$\begin{aligned}
E_u &= -\frac{4}{9}\left(3\,U - 5\right)\left(\pi^2 - 3\,X + X^2 - 2\,X\,Y - 4\right)\left[\frac{t^2 + s^2}{u^2}\right]\\
&\quad -\frac{2}{9}\,X\left(3\,U - 5\right)\\
&\quad -\frac{2}{9}\left(\pi^2 - X + 2\,Y + X^2 + 2\,Y^2 - 2\,X\,Y\right)\left(3\,U - 5\right)\left[\frac{t^2 - s^2}{u^2}\right] \tag{C.23}
\end{aligned}$$

$$F_u = \frac{2}{81}\left(3\,U - 5\right)^2\left[\frac{t^2 + s^2}{u^2}\right] \tag{C.24}$$

C.2 Like quark scattering

C.2.1 The mixed st-channel process $q\bar{q} \to \bar{q}q$

C.2.1.1 Two-loop contribution

$$\begin{aligned}
A_{st} &= \left(4\,\mathrm{Li}_4(z) + 4\,\mathrm{Li}_4(x) + 4\,\mathrm{Li}_4(y) + \left(-8\,X + 8\,Y - \frac{118}{3}\right)\mathrm{Li}_3(x) - 4\left(X + 6\right)\mathrm{Li}_3(y)\right.\\
&\quad +\left(4\,X^2 + \left(-8\,Y + \frac{118}{3}\right)X + \frac{14}{3}\,\pi^2 - 24\,Y\right)\mathrm{Li}_2(x) - \frac{1}{2}\,X^4 + \left(\frac{10}{3}\,Y + \frac{113}{18}\right)X^3\\
&\quad +\left(-\frac{5}{2}\,\pi^2 - \frac{16}{3} - 6\,Y^2 + \frac{13}{6}\,Y + \frac{22}{3}\,S\right)X^2 + \left(\left(-\frac{74}{9} - \frac{44}{3}\,S + \frac{20}{3}\,\pi^2\right)Y\right.
\end{aligned}$$

$$+ \frac{2}{3} Y^3 - 12 Y^2 + \frac{1513}{108} - \frac{44}{9} S + 20 \zeta_3 + \frac{115}{9} \pi^2 \bigg) X - \frac{1}{3} Y^4 + \frac{44}{9} Y^3$$

$$+ \bigg(- \frac{169}{9} + \frac{44}{3} S + \frac{1}{3} \pi^2 \bigg) Y^2 + \bigg(- 44 S - 4 \zeta_3 + \frac{632}{27} + \frac{299}{18} \pi^2 \bigg) Y + \frac{2777}{54} S$$

$$- \frac{23213}{648} - \frac{242}{9} S^2 - \frac{1}{3} \pi^2 + \frac{11}{2} \pi^2 S - \frac{131}{9} \zeta_3 + 28 \zeta_3 S - \frac{59}{60} \pi^4 \bigg) \frac{t}{s}$$

$$+ \bigg(4 \operatorname{Li}_4(z) - 4 \operatorname{Li}_4(x) + 4 \operatorname{Li}_4(y) + \bigg(- 4 X + 8 Y - \frac{46}{3} \bigg) \operatorname{Li}_3(x) - 4 \bigg(X - 6 \bigg) \operatorname{Li}_3(y)$$

$$+ \bigg(4 X^2 + \bigg(- 8 Y + \frac{46}{3} \bigg) X + \frac{10}{3} \pi^2 + 24 Y \bigg) \operatorname{Li}_2(x) - \frac{1}{3} X^4 + \bigg(\frac{10}{3} Y + \frac{28}{9} \bigg) X^3$$

$$+ \bigg(- \frac{11}{6} \pi^2 - \frac{31}{3} - 6 Y^2 + \frac{13}{6} Y + \frac{22}{3} S \bigg) X^2 + \bigg(\bigg(\frac{16}{9} - \frac{44}{3} S + \frac{20}{3} \pi^2 \bigg) Y$$

$$+ \frac{2}{3} Y^3 + 12 Y^2 + \frac{1513}{108} - \frac{44}{9} S + 16 \zeta_3 + \frac{28}{9} \pi^2 \bigg) X - \frac{1}{3} Y^4 + \frac{44}{9} Y^3$$

$$+ \bigg(- \frac{169}{9} + \frac{44}{3} S + \frac{1}{3} \pi^2 \bigg) Y^2 + \bigg(- 44 S - 4 \zeta_3 + \frac{632}{27} + \frac{155}{18} \pi^2 \bigg) Y + \frac{2777}{54} S$$

$$- \frac{23213}{648} - \frac{242}{9} S^2 - \frac{16}{3} \pi^2 + \frac{11}{2} \pi^2 S - \frac{347}{9} \zeta_3 + 28 \zeta_3 S - \frac{121}{180} \pi^4 \bigg) \frac{s}{t}$$

$$+ \bigg(- 56 \operatorname{Li}_4(z) - 56 \operatorname{Li}_4(y) + \bigg(24 X - 40 Y - \frac{152}{3} \bigg) \operatorname{Li}_3(x) + 8 \operatorname{Li}_3(y) X$$

$$+ \bigg(4 X^2 + \bigg(- 8 Y + \frac{152}{3} \bigg) X + 4 \pi^2 \bigg) \operatorname{Li}_2(x) - \frac{8}{3} X^4 + \bigg(16 Y + \frac{74}{9} \bigg) X^3$$

$$+ \bigg(- \frac{10}{3} \pi^2 - \frac{35}{3} - 20 Y^2 + \frac{16}{3} Y + \frac{44}{3} S \bigg) X^2 + \bigg(\bigg(- \frac{88}{3} S + \frac{50}{9} + \frac{52}{3} \pi^2 \bigg) Y$$

$$+ \frac{4}{3} Y^3 - \frac{88}{9} S + \frac{1513}{54} + \frac{116}{9} \pi^2 \bigg) X - \frac{2}{3} Y^4 + \frac{88}{9} Y^3 + \bigg(- \frac{446}{9} + \frac{2}{3} \pi^2 + \frac{88}{3} S \bigg) Y^2$$

$$+ \bigg(- 88 S + \frac{1264}{27} + \frac{227}{9} \pi^2 + 48 \zeta_3 \bigg) Y + \frac{2777}{27} S - \frac{23213}{324} - \frac{484}{9} S^2 + 56 \zeta_3 S$$

$$- \frac{35}{3} \pi^2 - \frac{514}{9} \zeta_3 + 11 \pi^2 S - \frac{89}{90} \pi^4 \bigg)$$

$$+ \bigg(6 \pi^2 + 6 X^2 + 6 Y^2 - 12 X Y \bigg) \frac{t^2}{s^2} + 6 Y^2 \frac{s^2}{t^2} \tag{C.25}$$

$$B_{st} = \bigg(- 16 \operatorname{Li}_4(z) + 6 \operatorname{Li}_4(x) - 16 \operatorname{Li}_4(y) + \bigg(- 24 Y - 12 + 16 X \bigg) \operatorname{Li}_3(x) + 16 \operatorname{Li}_3(y) X$$

$$+ \bigg(- 11 X^2 + \bigg(24 Y + 12 \bigg) X - 12 \pi^2 \bigg) \operatorname{Li}_2(x) - \frac{1}{2} X^4 - X^3 + \bigg(7 Y - \frac{11}{3} S - \frac{1}{3} \pi^2$$

$$+ \frac{545}{18} + 7 Y^2 \bigg) X^2 + \bigg(2 Y^3 - 27 Y^2 + \bigg(- 10 \pi^2 + \frac{70}{9} - \frac{44}{3} S \bigg) Y + \frac{88}{3} S - 20 \zeta_3$$

$$+ \frac{154}{27} - \frac{41}{18} \pi^2 \bigg) X - Y^4 + \frac{206}{9} Y^3 + \bigg(\frac{44}{3} S + 5 \pi^2 - \frac{484}{9} \bigg) Y^2 + \bigg(\frac{1928}{27} - 44 S$$

$$
\begin{aligned}
&\left. +28\,\zeta_3 + \frac{257}{18}\,\pi^2\right)Y + \frac{3004}{27}\,S - \frac{30659}{162} + \frac{34}{9}\,\pi^2 + \frac{43}{6}\,\pi^2\,S + \frac{581}{9}\,\zeta_3 - 4\,\zeta_3\,S - \frac{11}{36}\,\pi^4\right) \\
&+ \left(-16\,\mathrm{Li}_4(z) - 6\,\mathrm{Li}_4(x) - 16\,\mathrm{Li}_4(y) + \left(-24\,Y - 12 + 24\,X\right)\mathrm{Li}_3(x) + 16\,\mathrm{Li}_3(y)\,X \right. \\
&+ \left(-13\,X^2 + \left(24\,Y + 12\right)X - 12\,\pi^2\right)\mathrm{Li}_2(x) - \frac{7}{12}\,X^4 - \frac{14}{9}\,X^3 + \left(7\,Y - \frac{11}{3}\,S - \frac{1}{3}\right)\gamma \\
&- \frac{19}{18} + 7\,Y^2\right)X^2 + \left(2\,Y^3 - 27\,Y^2 + \left(-10\,\pi^2 + \frac{502}{9} - \frac{44}{3}\,S\right)Y + \frac{44}{3}\,S - 28\,\zeta_3 + \frac{92\Z}{27} \right. \\
&- \frac{11}{6}\,\pi^2\right)X - Y^4 + \frac{206}{9}\,Y^3 + \left(\frac{44}{3}\,S + 5\,\pi^2 - \frac{484}{9}\right)Y^2 + \left(\frac{1928}{27} - 44\,S + 28\,\zeta_3 \right. \\
&+ \frac{257}{18}\,\pi^2\right)Y + \frac{3004}{27}\,S - \frac{30659}{162} - \frac{248}{9}\,\pi^2 + \frac{43}{6}\,\pi^2\,S + \frac{581}{9}\,\zeta_3 - 4\,\zeta_3\,S - \frac{31}{180}\,\pi^4\right)\frac{s}{t} \\
&+ \left(\left(-32\,Y + 16\,X - 20\right)\mathrm{Li}_3(x) + \left(-16\,X^2 + \left(32\,Y + 20\right)X - 16\,\pi^2\right)\mathrm{Li}_2(x) \right. \\
&+ \frac{1}{6}\,X^4 + \left(-\frac{8}{3}\,Y + \frac{13}{9}\right)X^3 + \left(-\frac{2}{3}\,\pi^2 - 7 + 6\,Y^2 + 12\,Y\right)X^2 + \left(4\,Y^3 - 54\,Y^2 \right. \\
&+ \left(-12\,\pi^2 + \frac{716}{9} - \frac{88}{3}\,S\right)Y + 44\,S - 24\,\zeta_3 + \frac{1076}{27} + \frac{29}{9}\,\pi^2\right)X - 2\,Y^4 + \frac{412}{9}\,Y^3 \\
&+ \left(10\,\pi^2 - \frac{1112}{9} + \frac{88}{3}\,S\right)Y^2 + \left(40\,\zeta_3 + \frac{3856}{27} + \frac{257}{9}\,\pi^2 - 88\,S\right)Y + \frac{6008}{27}\,S \\
&- \frac{30659}{81} - \frac{286}{9}\,\pi^2 + \frac{43}{3}\,\pi^2\,S + \frac{1126}{9}\,\zeta_3 - \frac{163}{90}\,\pi^4 - 8\,\zeta_3\,S\right) \\
&+ \left(8\,X^2 - 16\,X\,Y + 8\,\pi^2 + 8\,Y^2\right)\frac{t^2}{s^2} + 8\,Y^2\,\frac{s^2}{t^2}
\end{aligned}
\tag{C.26}
$$

$$
\begin{aligned}
C_{st} = &\left(-4\,\mathrm{Li}_4(z) + 10\,\mathrm{Li}_4(x) - 4\,\mathrm{Li}_4(y) + \left(-8\,Y + 2\right)\mathrm{Li}_3(x) + 4\,\mathrm{Li}_3(y)\,X \right. \\
&+ \left(-3\,X^2 + \left(8\,Y - 2\right)X - \frac{10}{3}\,\pi^2\right)\mathrm{Li}_2(x) - \frac{1}{3}\,X^4 + \left(-\frac{2}{3}\,Y + 3\right)X^3 \\
&+ \left(3\,Y^2 - \frac{3}{2}\,Y + \frac{15}{2} + \frac{13}{6}\,\pi^2\right)X^2 + \left(-9\,Y^2 + \left(16 - \frac{14}{3}\,\pi^2\right)Y - \frac{147}{4} + \frac{7}{3}\,\pi^2 \right. \\
&\left. -12\,\zeta_3\right)X + 6\,Y^3 + \left(\frac{8}{3}\,\pi^2 - 21\right)Y^2 + \left(48 + 8\,\zeta_3 + \frac{7}{3}\,\pi^2\right)Y - \frac{3}{2}\,S - \frac{511}{8} \\
&+ 2\,\pi^2\,S + 38\,\zeta_3 - 24\,\zeta_3\,S - \frac{7}{15}\,\pi^4 - \frac{16}{3}\,\pi^2\right)\frac{t}{s} \\
&+ \left(-4\,\mathrm{Li}_4(z) - 10\,\mathrm{Li}_4(x) - 4\,\mathrm{Li}_4(y) + \left(-8\,Y + 2 + 12\,X\right)\mathrm{Li}_3(x) + 4\,\mathrm{Li}_3(y)\,X \right. \\
&+ \left(-5\,X^2 + \left(8\,Y - 2\right)X - \frac{14}{3}\,\pi^2\right)\mathrm{Li}_2(x) - \frac{1}{4}\,X^4 + \left(-\frac{2}{3}\,Y + \frac{5}{6}\right)X^3 \\
&+ \left(3\,Y^2 - \frac{3}{2}\,Y + \frac{5}{2} + \frac{17}{6}\,\pi^2\right)X^2 + \left(-9\,Y^2 + \left(26 - \frac{14}{3}\,\pi^2\right)Y - \frac{51}{4} + \frac{22}{3}\,\pi^2 \right.
\end{aligned}
$$

$$
\begin{aligned}
&\left(-24\,\zeta_3\right)X + 6\,Y^3 + \left(\frac{8}{3}\,\pi^2 - 21\right)Y^2 + \left(48 + 8\,\zeta_3 + \frac{7}{3}\,\pi^2\right)Y - \frac{3}{2}\,S - \frac{511}{8} \\
&+2\,\pi^2\,S + 38\,\zeta_3 - 24\,\zeta_3\,S - \frac{1}{45}\,\pi^4 - \frac{31}{3}\,\pi^2\bigg)\frac{s}{t} \\
&+\bigg(8\,\mathrm{Li}_4(z) + 8\,\mathrm{Li}_4(y) + \left(-8\,Y + 12\right)\mathrm{Li}_3(x) - 8\,\mathrm{Li}_3(y)\,X + \left(\left(8\,Y - 12\right)X + \right. \\
&-4\,X^2 - 4\,\pi^2\bigg)\mathrm{Li}_2(x) + \frac{1}{2}\,X^4 + \left(-\frac{8}{3}\,Y + 3\right)X^3 + \left(2\,Y^2 - 4\,Y - 8 + \frac{8}{3}\,\pi^2\right)X^2 \\
&+\left(-18\,Y^2 + \left(46 - \frac{16}{3}\,\pi^2\right)Y - \frac{99}{2} + \frac{20}{3}\,\pi^2 - 24\,\zeta_3\right)X + 12\,Y^3 \\
&+\left(\frac{16}{3}\,\pi^2 - 46\right)Y^2 + \left(96 + 8\,\zeta_3 + \frac{14}{3}\,\pi^2\right)Y - 3\,S - \frac{511}{4} + 4\,\pi^2\,S + 68\,\zeta_3 \\
&-48\,\zeta_3\,S - \frac{52}{45}\,\pi^4 - \frac{53}{3}\,\pi^2\bigg) \\
&+\left(2\,\pi^2 - 4\,X\,Y + 2\,X^2 + 2\,Y^2\right)\frac{t^2}{s^2} + 2\,Y^2\,\frac{s^2}{t^2}
\end{aligned}
\tag{C.27}
$$

$$
\begin{aligned}
D_{st} = &\left(\frac{4}{3}\,\mathrm{Li}_3(x) - \frac{4}{3}\,\mathrm{Li}_2(x)\,X - \frac{10}{9}\,X^3 + \left(\frac{37}{9} + \frac{4}{3}\,Y - \frac{4}{3}\,S\right)X^2 + \left(\left(\frac{8}{3}\,S - \frac{22}{9}\right)Y\right.\right. \\
&+\frac{52}{9}\,S - \frac{290}{27} - \frac{10}{9}\,\pi^2\bigg)X - \frac{8}{9}\,Y^3 + \left(-\frac{8}{3}\,S + \frac{58}{9}\right)Y^2 + \left(-\frac{248}{27} - \frac{25}{9}\,\pi^2 + 8\,S\right)Y \\
&-\frac{92}{3}\,S + \frac{910}{27} + \frac{88}{9}\,S^2 - \frac{4}{9}\,\pi^2 - \pi^2\,S + \frac{86}{9}\,\zeta_3\bigg)\frac{t}{s} + \left(\frac{4}{3}\,\mathrm{Li}_3(x) - \frac{4}{3}\,\mathrm{Li}_2(x)\,X - \frac{10}{9}\,X^3\right. \\
&+\left(\frac{37}{9} + \frac{4}{3}\,Y - \frac{4}{3}\,S\right)X^2 + \left(\left(\frac{8}{3}\,S - \frac{22}{9}\right)Y + \frac{52}{9}\,S - \frac{290}{27} - \frac{10}{9}\,\pi^2\right)X - \frac{8}{9}\,Y^3 \\
&+\left(-\frac{8}{3}\,S + \frac{58}{9}\right)Y^2 + \left(-\frac{248}{27} - \frac{25}{9}\,\pi^2 + 8\,S\right)Y - \frac{92}{3}\,S + \frac{910}{27} + \frac{88}{9}\,S^2 - \frac{4}{9}\,\pi^2 \\
&-\pi^2\,S + \frac{86}{9}\,\zeta_3\bigg)\frac{s}{t} + \left(\frac{8}{3}\,\mathrm{Li}_3(x) - \frac{8}{3}\,\mathrm{Li}_2(x)\,X - \frac{20}{9}\,X^3 + \left(-\frac{8}{3}\,S + \frac{74}{9} + \frac{8}{3}\,Y\right)X^2\right. \\
&+\left(\left(\frac{16}{3}\,S - \frac{44}{9}\right)Y - \frac{580}{27} + \frac{104}{9}\,S - \frac{20}{9}\,\pi^2\right)X - \frac{16}{9}\,Y^3 + \left(-\frac{16}{3}\,S + \frac{116}{9}\right)Y^2 \\
&+\left(16\,S - \frac{496}{27} - \frac{50}{9}\,\pi^2\right)Y - \frac{184}{3}\,S + \frac{176}{9}\,S^2 - \frac{8}{9}\,\pi^2 + \frac{172}{9}\,\zeta_3 + \frac{1820}{27} - 2\,\pi^2\,S\bigg)
\end{aligned}
\tag{C.28}
$$

$$
\begin{aligned}
E_{st} = &\left(4\,\mathrm{Li}_3(x) - 4\,\mathrm{Li}_2(x)\,X + \left(-\frac{31}{9} + \frac{2}{3}\,S\right)X^2 + \left(\left(\frac{8}{3}\,S - \frac{22}{9}\right)Y + \frac{7}{9}\,\pi^2 - \frac{16}{3}\,S\right.\right. \\
&-\frac{16}{27}\bigg)X - \frac{8}{9}\,Y^3 + \left(-\frac{8}{3}\,S + \frac{58}{9}\right)Y^2 + \left(-\frac{248}{27} - \frac{25}{9}\,\pi^2 + 8\,S\right)Y + \frac{32}{9}\,\pi^2 \\
&+\frac{58}{9}\,\zeta_3 - \frac{5}{3}\,\pi^2\,S - \frac{472}{27}\,S + \frac{2740}{81}\bigg)\frac{t}{s}
\end{aligned}
$$

$$+\left(4\operatorname{Li}_3(x)-4\operatorname{Li}_2(x)\,X+\frac{2}{9}\,X^3+\left(-\frac{19}{9}+\frac{2}{3}\,S\right)X^2+\left(\left(\frac{8}{3}\,S-\frac{22}{9}\right)Y-\frac{208}{27}\right.\right.$$

$$\left.-\frac{8}{3}\,S+\frac{1}{3}\,\pi^2\right)X-\frac{8}{9}\,Y^3+\left(-\frac{8}{3}\,S+\frac{58}{9}\right)Y^2+\left(-\frac{248}{27}-\frac{25}{9}\,\pi^2+8\,S\right)Y-\frac{472}{27}\,S$$

$$\left.+\frac{2740}{81}+\frac{44}{9}\,\pi^2+\frac{58}{9}\,\zeta_3-\frac{5}{3}\,\pi^2\,S\right)\frac{s}{t}$$

$$+\left(8\operatorname{Li}_3(x)-8\operatorname{Li}_2(x)\,X-\frac{4}{9}\,X^3-2\,X^2+\left(\left(\frac{16}{3}\,S-\frac{44}{9}\right)Y-8\,S-\frac{2}{9}\,\pi^2-\frac{224}{27}\right)X\right.$$

$$-\frac{16}{9}\,Y^3+\left(-\frac{16}{3}\,S+\frac{116}{9}\right)Y^2+\left(16\,S-\frac{496}{27}-\frac{50}{9}\,\pi^2\right)Y+\frac{5480}{81}+\frac{116}{9}\,\zeta_3$$

$$\left.+\frac{76}{9}\,\pi^2-\frac{944}{27}\,S-\frac{10}{3}\,\pi^2\,S\right)\tag{C.29}$$

$$F_{st}\;=\;\left(-\frac{4}{9}\,X^2+\left(-\frac{8}{9}\,S+\frac{40}{27}\right)X-\frac{200}{81}+\frac{80}{27}\,S+\frac{4}{9}\,\pi^2-\frac{8}{9}\,S^2\right)\frac{t}{s}$$

$$+\left(-\frac{4}{9}\,X^2+\left(-\frac{8}{9}\,S+\frac{40}{27}\right)X-\frac{200}{81}+\frac{80}{27}\,S+\frac{4}{9}\,\pi^2-\frac{8}{9}\,S^2\right)\frac{s}{t}$$

$$+\left(-\frac{8}{9}\,X^2+\left(-\frac{16}{9}\,S+\frac{80}{27}\right)X-\frac{400}{81}+\frac{160}{27}\,S+\frac{8}{9}\,\pi^2-\frac{16}{9}\,S^2\right)\tag{C.30}$$

C.2.1.2 One-loop self-interference contribution

$$A_{st}\;=\;\left(-\frac{44}{3}\,X\,Y\,S-\frac{242}{9}\,S^2-\frac{338}{81}-\frac{8}{9}\,\pi^2+\frac{572}{27}\,S+\frac{22}{3}\,\pi^2\,S-10\,\pi^2\,Y-4\,\pi^2\,X\,Y\right.$$

$$+\frac{52}{27}\,X-\frac{3}{8}\,X^4-\frac{52}{9}\,Y^2-\frac{8}{9}\,X^2+2\,X^3+\frac{52}{3}\,Y-2\,Y^2\,X^2-4\,Y\,X^2+\frac{3}{2}\,X^2\,\pi^2$$

$$\left.-\frac{146}{9}\,Y\,X+2\,Y\,X^3+11\,\pi^2\,X+\frac{22}{3}\,Y^2\,X-44\,Y\,S-\frac{44}{9}\,X\,S+\frac{44}{3}\,Y^2\,S+\frac{22}{3}\,X^2\,S\right)$$

$$+\left(-\frac{26}{9}\,Y^2+\frac{22}{3}\,Y^2\,S-\frac{22}{3}\,X\,Y\,S-\frac{46}{9}\,Y\,X-4\,\pi^2\,X\,Y+\frac{1}{2}\,Y\,X^2+\frac{8}{3}\,Y^2\,X\right.$$

$$-\frac{3}{2}\,Y^2\,X^2+\frac{14}{9}\,\pi^2+\frac{11}{3}\,\pi^2\,S+\frac{26}{27}\,X-\frac{22}{9}\,X\,S+Y\,X^3+7\,\pi^2\,X-\frac{169}{81}+\frac{286}{27}\,S$$

$$\left.-\frac{121}{9}\,S^2+\frac{26}{3}\,Y-22\,Y\,S+\frac{3}{2}\,X^2\,\pi^2-6\,\pi^2\,Y-\frac{13}{9}\,X^2+\frac{11}{3}\,X^2\,S\right)\frac{s}{t}$$

$$+\left(-\frac{22}{3}\,X\,Y\,S-\frac{121}{9}\,S^2-\frac{13}{9}\,\pi^2-\frac{169}{81}+\frac{286}{27}\,S+\frac{11}{3}\,\pi^2\,S-4\,\pi^2\,Y-2\,\pi^2\,X\,Y\right.$$

$$+\frac{26}{27}\,X-\frac{1}{2}\,X^4-\frac{26}{9}\,Y^2+\frac{14}{9}\,X^2+\frac{1}{2}\,X^3+\frac{26}{3}\,Y-\frac{3}{2}\,Y^2\,X^2-\frac{3}{2}\,Y\,X^2+X^2\,\pi^2$$

$$\left.-\frac{100}{9}\,Y\,X+2\,Y\,X^3+7\,\pi^2\,X+\frac{14}{3}\,Y^2\,X-22\,Y\,S-\frac{22}{9}\,X\,S+\frac{22}{3}\,Y^2\,S+\frac{11}{3}\,X^2\,S\right)\frac{t}{s}$$

$$-\frac{1}{8}\,X\left(4\,\pi^2\,X-4\,X^2-8\,\pi^2+X^3\right)\frac{t^2}{u^2}-\frac{1}{8}\,X\left(4\,\pi^2\,X+X^3+4\,X^2+8\,\pi^2\right)\frac{s^2}{u^2}$$

$$\tag{C.31}$$

$$B_{st} = \left(-\frac{44}{3} X Y S - \frac{158}{9} \pi^2 + \frac{352}{3} S + \frac{22}{3} \pi^2 S + 38 \pi^2 Y + 8 \pi^2 X Y + 2 X + \frac{11}{8} X^4 \right.$$

$$-\frac{826}{9} Y^2 - \frac{44}{3} X^2 - \frac{23}{3} X^3 + \frac{340}{3} Y - 2 Y^2 X^2 - \frac{416}{9} + 26 Y X^2 - \frac{1}{2} X^2 \pi^2$$

$$+\frac{628}{9} Y X - 4 Y X^3 - \frac{44}{3} \pi^2 X - \frac{140}{3} Y^2 X - 44 Y S + 22 X S + \frac{44}{3} Y^2 S$$

$$\left. -6 \pi^2 Y^2 + 12 Y^3 X + 36 Y^3 - 6 Y^4 \right)$$

$$+\left(-\frac{22}{3} X Y S - \frac{94}{9} \pi^2 + \frac{176}{3} S + \frac{11}{3} \pi^2 S + 21 \pi^2 Y + 8 \pi^2 X Y + \frac{22}{9} X + \frac{1}{2} X^4 \right.$$

$$-\frac{413}{9} Y^2 - \frac{107}{18} X^2 - \frac{7}{3} X^3 + \frac{170}{3} Y - \frac{208}{9} + 8 Y X^2 - X^2 \pi^2 + \frac{260}{9} Y X - 2 Y X^3$$

$$-\frac{23}{3} \pi^2 X - \frac{64}{3} Y^2 X - 22 Y S + \frac{22}{3} X S + \frac{22}{3} Y^2 S - \frac{11}{6} X^2 S - 3 \pi^2 Y^2$$

$$\left. +6 Y^3 X + 18 Y^3 - 3 Y^4 \right) \frac{s}{t}$$

$$+\left(-\frac{22}{3} X Y S - \frac{73}{9} \pi^2 + \frac{176}{3} S + \frac{11}{3} \pi^2 S + 17 \pi^2 Y + 4 \pi^2 X Y - \frac{4}{9} X + \frac{3}{2} X^4 \right.$$

$$-\frac{413}{9} Y^2 - \frac{149}{18} X^2 - \frac{25}{6} X^3 + \frac{170}{3} Y - \frac{208}{9} + 12 Y X^2 + \frac{368}{9} Y X - 4 Y X^3$$

$$-\frac{28}{3} \pi^2 X - \frac{76}{3} Y^2 X - 22 Y S + \frac{44}{3} X S + \frac{22}{3} Y^2 S - \frac{11}{6} X^2 S - 3 \pi^2 Y^2 + 6 Y^3 X$$

$$\left. +18 Y^3 - 3 Y^4 \right) \frac{t}{s}$$

$$+\frac{1}{8} X \left(4 \pi^2 X - 4 X^2 - 8 \pi^2 + X^3 \right) \frac{t^2}{u^2} + \frac{1}{8} X \left(4 \pi^2 X + X^3 + 4 X^2 + 8 \pi^2 \right) \frac{s^2}{u^2}$$

$$\tag{C.32}$$

$$C_{st} = \left(-128 + \frac{3}{8} X^4 - 18 \pi^2 - \frac{3}{2} X^2 \pi^2 - 2 X^3 - 11 \pi^2 X - 2 Y X^3 - 50 Y^2 - 2 X^2 \right.$$

$$+12 Y^3 + 96 Y - 48 X + 4 Y^3 X - 2 Y^4 + 4 \pi^2 X Y - 2 \pi^2 Y^2 + 50 Y X + 10 Y X^2$$

$$\left. +16 \pi^2 Y - 18 Y^2 X \right)$$

$$+\left(6 Y^3 - Y X^3 - 64 - 11 \pi^2 + 22 Y X - 25 Y^2 + 4 X^2 - Y^4 - 7 \pi^2 X - \pi^2 Y^2 - 16 X \right.$$

$$\left. -\frac{3}{2} X^2 \pi^2 - 8 Y^2 X + 48 Y + 2 Y^3 X + 4 \pi^2 X Y + \frac{5}{2} Y X^2 + 9 \pi^2 Y + \frac{1}{2} Y^2 X^2 \right) \frac{s}{t}$$

$$+\left(-8 \pi^2 - 64 - X^2 \pi^2 - 10 Y^2 X - 2 Y X^3 - \frac{1}{2} X^3 - 25 Y^2 - 7 \pi^2 X - Y^4 - \pi^2 Y^2 \right.$$

$$+2 \pi^2 X Y + 28 Y X + \frac{1}{2} X^4 + 7 \pi^2 Y + \frac{9}{2} Y X^2 + 48 Y + 2 Y^3 X + 6 Y^3 + X^2$$

$$\left. -32 X + \frac{1}{2} Y^2 X^2 \right) \frac{t}{s}$$

$$+\frac{1}{8} X \left(4 \pi^2 X - 4 X^2 - 8 \pi^2 + X^3 \right) \frac{t^2}{u^2} + \frac{1}{8} X \left(4 \pi^2 X + X^3 + 4 X^2 + 8 \pi^2 \right) \frac{s^2}{u^2}$$

$$(C.33)$$

$$
\begin{aligned}
D_{st} = & \left(\frac{520}{81} - \frac{92}{27} X + \frac{88}{9} S^2 - \frac{4}{3} \pi^2 S + 8 Y S - \frac{4}{3} X^2 S + \frac{8}{3} X Y S + \frac{52}{9} X S + \frac{20}{9} \pi^2 \right. \\
& \left. + \frac{40}{9} Y^2 + \frac{20}{9} X^2 - \frac{4}{3} Y^2 X - \frac{40}{3} Y - \frac{8}{3} Y^2 S - \frac{544}{27} S - \frac{4}{9} Y X \right) \\
& + \left(\frac{4}{3} X Y S - \frac{2}{9} Y X + \frac{20}{9} Y^2 - \frac{4}{3} Y^2 S + \frac{26}{9} X S - \frac{46}{27} X + \frac{10}{9} \pi^2 - \frac{2}{3} \pi^2 S \right. \\
& \left. - \frac{2}{3} Y^2 X - \frac{272}{27} S + \frac{44}{9} S^2 + \frac{260}{81} - \frac{20}{3} Y + 4 Y S + \frac{10}{9} X^2 - \frac{2}{3} X^2 S \right) \frac{s}{t} \\
& + \left(\frac{4}{3} X Y S - \frac{2}{9} Y X + \frac{20}{9} Y^2 - \frac{4}{3} Y^2 S + \frac{26}{9} X S - \frac{46}{27} X + \frac{10}{9} \pi^2 - \frac{2}{3} \pi^2 S \right. \\
& \left. - \frac{2}{3} Y^2 X - \frac{272}{27} S + \frac{44}{9} S^2 + \frac{260}{81} - \frac{20}{3} Y + 4 Y S + \frac{10}{9} X^2 - \frac{2}{3} X^2 S \right) \frac{t}{s}
\end{aligned}
$$

$$(C.34)$$

$$
\begin{aligned}
E_{st} = & \left(\frac{320}{9} - 4 X + \frac{2}{3} X^3 - \frac{64}{3} S - \frac{8}{3} Y^2 S - \frac{4}{3} \pi^2 X - 4 X S + 8 Y S + \frac{8}{3} X Y S \right. \\
& \left. - \frac{10}{3} X^2 - \frac{10}{9} \pi^2 + \frac{40}{9} Y^2 - \frac{40}{3} Y - \frac{4}{3} \pi^2 S - \frac{4}{3} Y^2 X - \frac{4}{9} Y X \right) \\
& + \left(\frac{20}{9} Y^2 - \frac{4}{3} Y^2 S + \frac{1}{3} X^3 - \frac{4}{3} X S - \frac{28}{9} X - \frac{20}{3} Y + 4 Y S - \frac{8}{9} \pi^2 - \frac{2}{3} \pi^2 S \right. \\
& \left. + \frac{160}{9} - \frac{32}{3} S - \frac{4}{3} \pi^2 X - \frac{2}{3} Y^2 X + \frac{1}{3} X^2 S - \frac{17}{9} X^2 + \frac{4}{3} X Y S - \frac{2}{9} Y X \right) \frac{s}{t} \\
& + \left(\frac{4}{3} X Y S - \frac{2}{9} Y X - \frac{2}{3} \pi^2 X + \frac{20}{9} Y^2 - \frac{4}{3} Y^2 S - \frac{8}{9} X - \frac{8}{3} X S - \frac{2}{3} Y^2 X \right. \\
& \left. + \frac{2}{3} X^3 + \frac{160}{9} - \frac{32}{3} S + \frac{1}{3} X^2 S - \frac{23}{9} X^2 - \frac{2}{9} \pi^2 - \frac{2}{3} \pi^2 S - \frac{20}{3} Y + 4 Y S \right) \frac{t}{s}
\end{aligned}
$$

$$(C.35)$$

$$
\begin{aligned}
F_{st} = & -\frac{8}{81} \left(-5 + 3 S \right) \left(3 S + 3 X - 5 \right) \\
& -\frac{4}{81} \left(-5 + 3 S \right) \left(3 S + 3 X - 5 \right) \frac{s}{t} \\
& -\frac{4}{81} \left(-5 + 3 S \right) \left(3 S + 3 X - 5 \right) \frac{t}{s}
\end{aligned}
$$

$$(C.36)$$

C.2.2 The mixed ut-channel process $qq \to qq$

C.2.2.1 Two-loop contribution

$$
A_{ut} = \left(-4 \operatorname{Li}_4(y) - 4 \operatorname{Li}_4(x) - 4 \operatorname{Li}_4(z) + \left(4 X + \frac{46}{3} + 4 Y \right) \operatorname{Li}_3(y) + \left(8 X + \frac{118}{3} \right) \operatorname{Li}_3(x) \right.
$$

$$+\left(-\frac{2}{3}\,\pi^2-\frac{118}{3}\,X-4\,X^2+4\,Y^2+\frac{46}{3}\,Y\right)\mathrm{Li}_2(x)-\frac{5}{6}\,X^4+\left(\frac{113}{18}-\frac{2}{3}\,Y\right)X^3$$

$$+\left(-21\,Y+\frac{22}{3}\,U+2\,Y^2+\frac{5}{6}\,\pi^2-\frac{16}{3}\right)X^2+\left(2\,Y^3+\frac{67}{6}\,Y^2+\left(-5\,\pi^2+\frac{170}{9}\right)Y\right.$$

$$+12\,\zeta_3-\frac{44}{9}\,U+\frac{1513}{108}-\frac{61}{18}\,\pi^2\right)X-\frac{1}{2}\,Y^4-\frac{38}{9}\,Y^3+\left(\frac{22}{3}\,U+\frac{1}{6}\,\pi^2-\frac{97}{3}\right)Y^2$$

$$+\left(-\frac{449}{12}+\frac{13}{18}\,\pi^2+\frac{440}{9}\,U-16\,\zeta_3\right)Y-\frac{242}{9}\,U^2+\frac{2777}{54}\,U+\frac{29}{20}\,\pi^4+28\,\zeta_3\,U$$

$$-\frac{485}{9}\,\zeta_3+\frac{73}{9}\,\pi^2-\frac{11}{6}\,\pi^2\,U-\frac{23213}{648}\right)\frac{t}{u}$$

$$+\left(-4\,\mathrm{Li}_4(y)-4\,\mathrm{Li}_4(x)+4\,\mathrm{Li}_4(z)+\left(\frac{118}{3}+8\,Y\right)\mathrm{Li}_3(y)+\left(4\,X+\frac{46}{3}+4\,Y\right)\mathrm{Li}_3(x)\right.$$

$$+\left(\frac{2}{3}\,\pi^2-\frac{46}{3}\,X-4\,X^2+4\,Y^2+\frac{118}{3}\,Y\right)\mathrm{Li}_2(x)-\frac{1}{3}\,X^4+\left(\frac{28}{9}-\frac{8}{3}\,Y\right)X^3$$

$$+\left(-\frac{23}{2}\,Y+\frac{22}{3}\,U+3\,Y^2+\frac{7}{6}\,\pi^2-\frac{31}{3}\right)X^2+\left(\frac{8}{3}\,Y^3+\frac{77}{3}\,Y^2\right.$$

$$+\left(-5\,\pi^2+\frac{170}{9}\right)Y+12\,\zeta_3-\frac{44}{9}\,U+\frac{1513}{108}+\frac{13}{9}\,\pi^2\right)X-\frac{2}{3}\,Y^4-\frac{19}{18}\,Y^3$$

$$+\left(\frac{22}{3}\,U+\frac{1}{2}\,\pi^2-\frac{82}{3}\right)Y^2+\left(-\frac{449}{12}-\frac{73}{9}\,\pi^2+\frac{440}{9}\,U-16\,\zeta_3\right)Y-\frac{242}{9}\,U^2$$

$$+\frac{2777}{54}\,U+\frac{17}{12}\,\pi^4+28\,\zeta_3\,U-\frac{485}{9}\,\zeta_3+\frac{73}{9}\,\pi^2-\frac{11}{6}\,\pi^2\,U-\frac{23213}{648}\right)\frac{u}{t}$$

$$+\left(56\,\mathrm{Li}_4(y)+56\,\mathrm{Li}_4(x)+\left(-16\,X+\frac{152}{3}-24\,Y\right)\mathrm{Li}_3(y)\right.$$

$$+\left(-24\,X-16\,Y+\frac{152}{3}\right)\mathrm{Li}_3(x)+\left(-\frac{152}{3}\,X-4\,X^2+4\,Y^2+\frac{152}{3}\,Y\right)\mathrm{Li}_2(x)$$

$$-\frac{1}{3}\,X^4+\left(\frac{74}{9}-\frac{16}{3}\,Y\right)X^3+\left(-30\,Y+\frac{44}{3}\,U-2\,Y^2-\frac{2}{3}\,\pi^2-\frac{35}{3}\right)X^2$$

$$+\left(-\frac{4}{3}\,Y^3+\frac{106}{3}\,Y^2+\left(-\frac{4}{3}\,\pi^2+\frac{160}{9}\right)Y+24\,\zeta_3-\frac{88}{9}\,U+\frac{1513}{54}-\frac{22}{9}\,\pi^2\right)X$$

$$-\frac{1}{3}\,Y^4-\frac{58}{9}\,Y^3+\left(\frac{44}{3}\,U-\frac{4}{3}\,\pi^2-\frac{167}{3}\right)Y^2+\left(-\frac{449}{6}-\frac{65}{9}\,\pi^2+\frac{880}{9}\,U-32\,\zeta_3\right)Y$$

$$-\frac{484}{9}\,U^2+\frac{2777}{27}\,U-\frac{133}{90}\,\pi^4+56\,\zeta_3\,U-\frac{970}{9}\,\zeta_3+\frac{236}{9}\,\pi^2-\frac{11}{3}\,\pi^2\,U-\frac{23213}{324}\right)$$

$$+6\,X^2\,\frac{t^2}{u^2}+6\,Y^2\,\frac{u^2}{t^2} \tag{C.37}$$

$$B_{ut}\;=\;\left(16\,\mathrm{Li}_4(y)+16\,\mathrm{Li}_4(x)-6\,\mathrm{Li}_4(z)+12\left(1-2\,Y\right)\mathrm{Li}_3(y)+\left(-16\,X-8\,Y+12\right)\mathrm{Li}_3(x)\right.$$

$$+\left(11\,X^2+\left(2\,Y-12\right)X+12\,Y-\pi^2-13\,Y^2\right)\mathrm{Li}_2(x)-\frac{1}{12}\,X^4+\left(-1+3\,Y\right)X^3$$

$$+\left(-4\,Y+\frac{545}{18}-\frac{11}{3}\,U+\frac{15}{2}\,\pi^2\right)X^2+\left(-\frac{32}{3}\,Y^3-16\,Y^2+\left(-\pi^2+22\,U-\frac{205}{3}\right)\right.$$

$$+\frac{154}{27}+\frac{88}{3}\,U-4\,\zeta_3+\frac{337}{18}\,\pi^2\bigg)\,X+\frac{1}{12}\,Y^4+\frac{19}{9}\,Y^3+\left(\frac{29}{3}\,\pi^2-\frac{11}{3}\,U-\frac{283}{18}\right)Y^2$$

$$+\left(\frac{80}{3}\,\pi^2+\frac{44}{3}\,U-\frac{694}{9}\right)Y-\frac{79}{30}\,\pi^4-\frac{30659}{162}-\frac{67}{6}\,\pi^2\,U+\frac{113}{2}\,\pi^2+\frac{3004}{27}\,U-4\,\zeta_3\,U$$

$$\left.+\frac{473}{9}\,\zeta_3\right)\frac{t}{u}$$

$$+\left(16\,\mathrm{Li}_4(y)+16\,\mathrm{Li}_4(x)+6\,\mathrm{Li}_4(z)+\left(12-8\,X-16\,Y\right)\mathrm{Li}_3(y)+12\left(-2\,X+1\right)\mathrm{Li}_3\right.$$

$$+\left(13\,X^2+\left(-12-2\,Y\right)X-11\,Y^2+\pi^2+12\,Y\right)\mathrm{Li}_2(x)+\frac{1}{3}\,X^4+\left(-\frac{14}{9}+\frac{4}{3}\,Y\right)$$

$$+\left(-\frac{19}{18}-\frac{11}{3}\,U+8\,\pi^2-\frac{7}{3}\,Y-\frac{1}{2}\,Y^2\right)X^2+\left(-9\,Y^3-\frac{53}{3}\,Y^2\right.$$

$$+\left(-\frac{161}{3}+22\,U-\frac{2}{3}\,\pi^2\right)Y-4\,\zeta_3+\frac{44}{3}\,U+\frac{35}{2}\,\pi^2+\frac{922}{27}\bigg)\,X+\frac{1}{6}\,Y^4+\frac{8}{3}\,Y^3$$

$$+\left(\frac{17}{18}-\frac{11}{3}\,U+\frac{59}{6}\,\pi^2\right)Y^2+\left(\frac{251}{9}\,\pi^2+\frac{88}{3}\,U-\frac{950}{9}\right)Y-\frac{30659}{162}-\frac{67}{6}\,\pi^2\,U$$

$$+\frac{113}{2}\,\pi^2+\frac{3004}{27}\,U-4\,\zeta_3\,U-\frac{161}{60}\,\pi^4+\frac{473}{9}\,\zeta_3\bigg)\frac{u}{t}$$

$$+\left(\left(-16\,Y-16\,X+20\right)\mathrm{Li}_3(y)+\left(-16\,Y-16\,X+20\right)\mathrm{Li}_3(x)\right.$$

$$+\left(20\,Y-16\,Y^2-20\,X+16\,X^2\right)\mathrm{Li}_2(x)+\frac{1}{6}\,X^4+\left(\frac{13}{9}+2\,Y\right)X^3$$

$$+\left(\frac{49}{3}\,\pi^2-7-Y^2-\frac{49}{3}\,Y\right)X^2+\left(-14\,Y^3-\frac{77}{3}\,Y^2+\left(-\frac{590}{9}+\frac{88}{3}\,U-2\,\pi^2\right)Y\right.$$

$$-8\,\zeta_3+\frac{368}{9}\,\pi^2+44\,U+\frac{1076}{27}\bigg)\,X+\frac{1}{6}\,Y^4+\frac{13}{9}\,Y^3+\left(19\,\pi^2-51\right)Y^2$$

$$+\left(-\frac{548}{3}+\frac{473}{9}\,\pi^2+44\,U\right)Y-\frac{134}{45}\,\pi^4-\frac{30659}{81}-15\,\pi^2\,U+\frac{6008}{27}\,U-8\,\zeta_3\,U$$

$$\left.+\frac{763}{9}\,\pi^2+\frac{946}{9}\,\zeta_3\right)+8\,X^2\,\frac{t^2}{u^2}+8\,Y^2\,\frac{u^2}{t^2}\tag{C.3}$$

$$C_{ut}=\left(4\,\mathrm{Li}_4(y)+4\,\mathrm{Li}_4(x)-10\,\mathrm{Li}_4(z)+\left(-2+4\,X-12\,Y\right)\mathrm{Li}_3(y)-2\left(1+4\,Y\right)\mathrm{Li}_3(x)\right.$$

$$+\left(3\,X^2+\left(2\,Y+2\right)X-5\,Y^2-2\,Y-\frac{5}{3}\,\pi^2\right)\mathrm{Li}_2(x)-\frac{7}{12}\,X^4+\left(3+\frac{11}{3}\,Y\right)X^3$$

$$+\left(\frac{8}{3}\,\pi^2-2\,Y^2+\frac{15}{2}-\frac{15}{2}\,Y\right)X^2+\left(-\frac{10}{3}\,Y^3-3\,Y^2+\left(-31-\frac{4}{3}\,\pi^2\right)Y-12\,\zeta_3\right.$$

$$+\frac{31}{3}\,\pi^2-\frac{147}{4}\bigg)\,X-\frac{1}{12}\,Y^4+\frac{5}{6}\,Y^3+\left(\frac{5}{2}+\frac{7}{2}\,\pi^2\right)Y^2+\left(12\,\zeta_3-\frac{45}{4}+\frac{43}{6}\,\pi^2\right)Y$$

$$-\frac{511}{8} - \frac{3}{2} U + \frac{109}{6} \pi^2 - \frac{181}{180} \pi^4 + 40 \zeta_3 + 2 \pi^2 U - 24 \zeta_3 U \Bigg) \frac{t}{u}$$

$$+ \Bigg(4 \operatorname{Li}_4(y) + 4 \operatorname{Li}_4(x) + 10 \operatorname{Li}_4(z) - 2 \Big(1 + 4 X \Big) \operatorname{Li}_3(y) + \Big(4 Y - 12 X - 2 \Big) \operatorname{Li}_3(x)$$

$$+ \Bigg(5 X^2 + \Big(- 2 Y + 2 \Big) X + \frac{5}{3} \pi^2 - 3 Y^2 - 2 Y \Bigg) \operatorname{Li}_2(x) + \frac{1}{3} X^4 + \frac{5}{6} X^3$$

$$+ \Bigg(- Y + \frac{7}{2} \pi^2 + \frac{5}{2} - \frac{3}{2} Y^2 \Bigg) X^2 + \Bigg(- Y^3 - \frac{19}{2} Y^2 + \Big(- \pi^2 - 31 \Big) Y - 12 \zeta_3 - \frac{51}{4}$$

$$+ \frac{53}{6} \pi^2 \Bigg) X - \frac{1}{6} Y^4 + 3 Y^3 + \Big(\frac{15}{2} + 4 \pi^2 \Big) Y^2 + \Big(12 \zeta_3 + \frac{26}{3} \pi^2 - \frac{141}{4} \Big) Y - \frac{511}{8}$$

$$+ 2 \pi^2 U + \frac{109}{6} \pi^2 + 40 \zeta_3 - \frac{3}{2} U - \frac{49}{45} \pi^4 - 24 \zeta_3 U \Bigg) \frac{u}{t}$$

$$+ \Bigg(- 8 \operatorname{Li}_4(y) - 8 \operatorname{Li}_4(x) + \Big(- 12 - 8 X \Big) \operatorname{Li}_3(y) + \Big(- 8 Y - 12 \Big) \operatorname{Li}_3(x)$$

$$+ \Bigg(- 12 Y - 4 Y^2 + 12 X + 4 X^2 \Bigg) \operatorname{Li}_2(x) + \frac{1}{6} X^4 + \Big(3 + \frac{2}{3} Y \Big) X^3$$

$$+ \Big(7 \pi^2 - Y^2 - 8 - 5 Y \Big) X^2 + \Bigg(- \frac{10}{3} Y^3 - 17 Y^2 + \Big(- 30 - \frac{10}{3} \pi^2 \Big) Y - 24 \zeta_3$$

$$+ \frac{59}{3} \pi^2 - \frac{99}{2} \Bigg) X + \frac{1}{6} Y^4 + 3 Y^3 + \Big(- 8 + \frac{23}{3} \pi^2 \Big) Y^2 + \Big(24 \zeta_3 - \frac{93}{2} + \frac{53}{3} \pi^2 \Big) Y$$

$$- \frac{511}{4} - 3 U + \frac{61}{3} \pi^2 - \frac{29}{30} \pi^4 + 80 \zeta_3 + 4 \pi^2 U - 48 \zeta_3 U \Bigg) + 2 X^2 \frac{t^2}{u^2} + 2 Y^2 \frac{u^2}{t^2}$$

$$\text{(C.39)}$$

$$D_{ut} \;=\; \Bigg(- \frac{4}{3} \operatorname{Li}_3(y) - \frac{4}{3} \operatorname{Li}_3(x) + \Big(- \frac{4}{3} Y + \frac{4}{3} X \Big) \operatorname{Li}_2(x) - \frac{10}{9} X^3 + \Big(2 Y + \frac{37}{9} - \frac{4}{3} U \Big) X^2$$

$$+ \Bigg(- \frac{2}{3} Y^2 - \frac{52}{9} Y - \frac{4}{9} \pi^2 - \frac{290}{27} + \frac{52}{9} U \Bigg) X + \frac{2}{9} Y^3 + \Big(- \frac{4}{3} U + \frac{73}{9} \Big) Y^2$$

$$+ \Bigg(\frac{538}{27} - \frac{5}{9} \pi^2 - \frac{124}{9} U \Bigg) Y + \frac{910}{27} + \frac{98}{9} \zeta_3 - \frac{92}{3} U + \frac{88}{9} U^2 - \frac{25}{9} \pi^2 + \frac{1}{3} \pi^2 U \Bigg) \frac{t}{u}$$

$$+ \Bigg(- \frac{4}{3} \operatorname{Li}_3(y) - \frac{4}{3} \operatorname{Li}_3(x) + \Big(- \frac{4}{3} Y + \frac{4}{3} X \Big) \operatorname{Li}_2(x) - \frac{10}{9} X^3 + \Big(2 Y + \frac{37}{9} - \frac{4}{3} U \Big) X^2$$

$$+ \Bigg(- \frac{2}{3} Y^2 - \frac{52}{9} Y - \frac{4}{9} \pi^2 - \frac{290}{27} + \frac{52}{9} U \Bigg) X + \frac{2}{9} Y^3 + \Big(- \frac{4}{3} U + \frac{73}{9} \Big) Y^2$$

$$+ \Bigg(\frac{538}{27} - \frac{5}{9} \pi^2 - \frac{124}{9} U \Bigg) Y + \frac{910}{27} + \frac{98}{9} \zeta_3 - \frac{92}{3} U + \frac{88}{9} U^2 - \frac{25}{9} \pi^2 + \frac{1}{3} \pi^2 U \Bigg) \frac{u}{t}$$

$$+ \Bigg(- \frac{8}{3} \operatorname{Li}_3(y) - \frac{8}{3} \operatorname{Li}_3(x) + \Big(- \frac{8}{3} Y + \frac{8}{3} X \Big) \operatorname{Li}_2(x) - \frac{20}{9} X^3 + \Big(4 Y + \frac{74}{9} - \frac{8}{3} U \Big) X^2$$

$$+ \Bigg(- \frac{4}{3} Y^2 - \frac{104}{9} Y - \frac{8}{9} \pi^2 - \frac{580}{27} + \frac{104}{9} U \Bigg) X + \frac{4}{9} Y^3 + \Big(- \frac{8}{3} U + \frac{146}{9} \Big) Y^2$$

$$+ \left(\frac{1076}{27} - \frac{10}{9} \pi^2 - \frac{248}{9} U \right) Y + \frac{1820}{27} + \frac{196}{9} \zeta_3 - \frac{184}{3} U + \frac{176}{9} U^2 - \frac{50}{9} \pi^2 + \frac{2}{3} \pi^2 U \Bigg)$$

$$\text{(C.40)}$$

$$\begin{aligned}
E_{ut} &= \Bigg(-4\,\mathrm{Li}_3(y) - 4\,\mathrm{Li}_3(x) + \left(4\,X - 4\,Y \right) \mathrm{Li}_2(x) + \left(\frac{2}{3}\,U - \frac{31}{9} \right) X^2 \\
&\quad + \left(\left(\frac{28}{3} - 4\,U \right) Y - \frac{16}{3}\,U + \frac{7}{9}\,\pi^2 - \frac{16}{27} \right) X - \frac{4}{9}\,Y^3 + \left(\frac{2}{3}\,U + \frac{5}{9} \right) Y^2 \\
&\quad + \left(-\frac{8}{3}\,U + \frac{88}{9} \right) Y - \frac{472}{27}\,U + \frac{2740}{81} + \frac{5}{3}\,\pi^2 U + \frac{94}{9}\,\zeta_3 - 5\,\pi^2 \Bigg) \frac{t}{u} \\
&\quad + \Bigg(-4\,\mathrm{Li}_3(y) - 4\,\mathrm{Li}_3(x) + 4 \left(X - Y \right) \mathrm{Li}_2(x) + \frac{2}{9}\,X^3 - \frac{472}{27}\,U + \frac{2740}{81} + \frac{5}{3}\,\pi^2 U \\
&\quad + \left(-\frac{2}{3}\,Y - \frac{19}{9} + \frac{2}{3}\,U \right) X^2 + \left(\frac{2}{3}\,Y^2 + \left(-4\,U + \frac{20}{3} \right) Y + \pi^2 - \frac{8}{3}\,U - \frac{208}{27} \right) X \\
&\quad - \frac{2}{3}\,Y^3 + \left(\frac{17}{9} + \frac{2}{3}\,U \right) Y^2 + \left(-\frac{16}{3}\,U + \frac{152}{9} - \frac{2}{9}\,\pi^2 \right) Y + \frac{94}{9}\,\zeta_3 - 5\,\pi^2 \Bigg) \frac{u}{t} \\
&\quad + \Bigg(-8\,\mathrm{Li}_3(y) - 8\,\mathrm{Li}_3(x) + 8 \left(-Y + X \right) \mathrm{Li}_2(x) - \frac{4}{9}\,X^3 + \left(-2 + \frac{4}{3}\,Y \right) X^2 \\
&\quad + \left(-\frac{4}{3}\,Y^2 + \left(-\frac{16}{3}\,U + \frac{80}{9} \right) Y - 8\,U + \frac{10}{9}\,\pi^2 - \frac{224}{27} \right) X - \frac{4}{9}\,Y^3 + 6\,Y^2 \\
&\quad + \left(\frac{80}{3} - 8\,U + \frac{4}{9}\,\pi^2 \right) Y - \frac{944}{27}\,U + \frac{188}{9}\,\zeta_3 + 2\,\pi^2 U + \frac{5480}{81} - \frac{58}{9}\,\pi^2 \Bigg) \qquad \text{(C.41)}
\end{aligned}$$

$$\begin{aligned}
F_{ut} &= \left(-\frac{4}{9}\,X^2 + \left(\frac{40}{27} + \frac{8}{9}\,Y - \frac{8}{9}\,U \right) X - \frac{4}{9}\,Y^2 + \left(\frac{8}{9}\,U - \frac{40}{27} \right) Y - \frac{8}{81} \left(3\,U - 5 \right)^2 \right) \frac{t}{u} \\
&\quad + \left(-\frac{4}{9}\,X^2 + \left(\frac{40}{27} + \frac{8}{9}\,Y - \frac{8}{9}\,U \right) X - \frac{4}{9}\,Y^2 + \left(\frac{8}{9}\,U - \frac{40}{27} \right) Y - \frac{8}{81} \left(3\,U - 5 \right)^2 \right) \frac{u}{t} \\
&\quad + \left(-\frac{8}{9}\,X^2 + \left(\frac{16}{9}\,Y - \frac{16}{9}\,U + \frac{80}{27} \right) X - \frac{8}{9}\,Y^2 + \left(\frac{16}{9}\,U - \frac{80}{27} \right) Y - \frac{16}{81} \left(3\,U - 5 \right)^2 \right)
\end{aligned}$$

$$\text{(C.42)}$$

C.2.2.2   One-loop self-interference contribution

$$\begin{aligned}
A_{ut} &= \Bigg(\frac{5}{8}\,\pi^4 - \frac{242}{9}\,U^2 - \frac{5}{2}\,Y X \pi^2 + \frac{52}{27}\,X - \frac{520}{27}\,Y - \frac{8}{9}\,X^2 - \frac{206}{9}\,Y^2 - \frac{3}{8}\,Y^4 - \frac{16}{3}\,Y^3 \\
&\quad - \frac{3}{8}\,X^4 + 2\,X^3 - \frac{44}{9}\,X U + \frac{22}{3}\,Y^2 U + \frac{16}{3}\,Y^2 X + \frac{22}{3}\,X^2 U + 18\,Y X + \frac{440}{9}\,U Y \\
&\quad - \frac{1}{2}\,X^3 Y + \frac{1}{4}\,X^2 \pi^2 + \frac{1}{4}\,Y^2 \pi^2 - \frac{1}{2}\,X Y^3 - 3\,Y \pi^2 - 2\,X^2 Y - 3\,X \pi^2 + \frac{7}{4}\,X^2 Y^2 \\
&\quad + \frac{572}{27}\,U - \frac{338}{81} \Bigg) \\
&\quad - \frac{1}{8} \left(\pi^2 + Y^2 - 2\,Y X + X^2 \right) \left(Y^2 - 4\,Y + \pi^2 - 2\,Y X + 4\,X + X^2 \right) \frac{u^2}{s^2}
\end{aligned}$$

$$+\left(-\frac{121}{9}U^2-\frac{169}{81}+\frac{286}{27}U-XY^3-\frac{11}{3}Y^3+\frac{3}{2}X^2Y^2+\frac{19}{6}Y^2X-\frac{22}{9}XU\right.$$

$$+\frac{26}{27}X-\frac{5}{2}X\pi^2+\frac{11}{3}Y^2U-\frac{112}{9}Y^2+\frac{220}{9}UY-\frac{260}{27}Y-2YX\pi^2+\frac{1}{2}X^3$$

$$\left.+8YX+\frac{11}{3}X^2U+\frac{14}{9}X^2-2Y\pi^2-\frac{1}{2}X^4+\frac{1}{2}Y^2\pi^2+\frac{1}{2}\pi^4\right)\frac{t}{u}$$

$$-\frac{1}{8}\left(\pi^2-4X+X^2+4Y-2YX+Y^2\right)\left(\pi^2+Y^2-2YX+X^2\right)\frac{t^2}{s^2}$$

$$+\left(-\frac{1}{2}Y^4+\frac{220}{9}UY-\frac{260}{27}Y-\frac{22}{9}XU+\frac{26}{27}X+\frac{1}{2}X^2\pi^2+\frac{1}{2}\pi^4-\frac{19}{6}Y^3\right.$$

$$-X^3Y+\frac{11}{3}X^2U-\frac{13}{9}X^2+\frac{3}{2}X^2Y^2-2X\pi^2-2YX\pi^2+8YX-\frac{1}{2}X^2Y$$

$$\left.-\frac{5}{2}Y\pi^2+\frac{11}{3}Y^2X-\frac{85}{9}Y^2+\frac{11}{3}Y^2U-\frac{121}{9}U^2-\frac{169}{81}+\frac{286}{27}U\right)\frac{u}{t}\qquad\text{(C.43)}$$

$$B_{ut}=\left(-\frac{5}{8}\pi^4+\frac{44}{3}YXU-\frac{460}{9}\pi^2-\frac{43}{2}YX\pi^2+2X-\frac{346}{3}Y-\frac{44}{3}X^2-\frac{110}{3}Y^2\right.$$

$$+\frac{11}{8}Y^4-\frac{23}{3}Y^3+\frac{11}{8}X^4-\frac{23}{3}X^3+22XU-\frac{53}{3}Y^2X-\frac{364}{9}YX+22UY$$

$$-\frac{416}{9}-\frac{3}{2}X^3Y+\frac{3}{4}X^2\pi^2+\frac{3}{4}Y^2\pi^2-\frac{3}{2}XY^3-\frac{22}{3}\pi^2U-\frac{79}{3}Y\pi^2-3X^2Y$$

$$\left.-\frac{101}{3}X\pi^2-\frac{23}{4}X^2Y^2+\frac{352}{3}U\right)$$

$$+\frac{1}{8}\left(\pi^2+Y^2-2YX+X^2\right)\left(Y^2-4Y+\pi^2-2YX+4X+X^2\right)\frac{u^2}{s^2}$$

$$+\left(-\frac{1}{2}\pi^4+11YXU-\frac{149}{6}\pi^2-10YX\pi^2-\frac{4}{9}X-\frac{506}{9}Y-\frac{149}{18}X^2-\frac{239}{18}Y^2\right.$$

$$+\frac{1}{2}Y^4-\frac{1}{2}Y^3+\frac{3}{2}X^4-\frac{25}{6}X^3-\frac{208}{9}+\frac{44}{3}XU-\frac{11}{6}Y^2U-\frac{83}{6}Y^2X-\frac{11}{6}X^2U$$

$$-\frac{73}{3}YX+\frac{22}{3}UY-2X^3Y+X^2\pi^2-\frac{11}{2}\pi^2U-\frac{65}{6}Y\pi^2+\frac{1}{2}X^2Y-\frac{97}{6}X\pi^2$$

$$\left.-3X^2Y^2+\frac{176}{3}U\right)\frac{t}{u}$$

$$+\frac{1}{8}\left(\pi^2-4X+X^2+4Y-2YX+Y^2\right)\left(\pi^2+Y^2-2YX+X^2\right)\frac{t^2}{s^2}$$

$$+\left(-\frac{1}{2}\pi^4+11YXU-\frac{149}{6}\pi^2-10YX\pi^2+\frac{22}{9}X-\frac{532}{9}Y-\frac{107}{18}X^2-\frac{413}{18}Y^2\right.$$

$$+\frac{3}{2}Y^4-\frac{7}{3}Y^3+\frac{1}{2}X^4-\frac{7}{3}X^3-\frac{208}{9}+\frac{22}{3}XU-\frac{11}{6}Y^2U-\frac{37}{3}Y^2X-\frac{11}{6}X^2U$$

$$-17YX+\frac{44}{3}UY+Y^2\pi^2-2XY^3-\frac{11}{2}\pi^2U-\frac{32}{3}Y\pi^2-X^2Y-\frac{49}{3}X\pi^2$$

$$\left.-3X^2Y^2+\frac{176}{3}U\right)\frac{u}{t}\qquad\text{(C.44)}$$

$$C_{ut}=\left(-48X-\frac{15}{4}X^2Y^2-2X^2-2Y^2-48Y-128-\frac{11}{2}YX\pi^2-9Y\pi^2+\frac{3}{8}Y^4\right.$$

$$-2\,Y^3 - 2\,\pi^2 - 4\,X^2\,Y - 9\,X\,\pi^2 + \frac{1}{2}\,X^3\,Y - \frac{1}{4}\,X^2\,\pi^2 - \frac{1}{4}\,Y^2\,\pi^2 + \frac{1}{2}\,X\,Y^3 - \frac{5}{8}\,\pi^4$$

$$+\frac{3}{8}\,X^4 - 4\,Y^2\,X - 46\,Y\,X - 2\,X^3\Bigg)$$

$$+\frac{1}{8}\,\left(\pi^2 + Y^2 - 2\,Y\,X + X^2\right)\left(Y^2 - 4\,Y + \pi^2 - 2\,Y\,X + 4\,X + X^2\right)\frac{u^2}{s^2}$$

$$+\Bigg(-64 + 4\,Y^2 - \frac{5}{2}\,X^2\,Y^2 - 16\,Y - \frac{5}{2}\,Y^2\,X + 3\,\pi^2 - 3\,X^2\,Y + X^2 + X\,Y^3 - \frac{1}{2}\,\pi^4$$

$$+\frac{1}{2}\,X^4 - 32\,X - \frac{1}{2}\,X^3 - 2\,Y\,X\,\pi^2 - \frac{1}{2}\,Y^2\,\pi^2 - \frac{7}{2}\,X\,\pi^2 - 4\,Y\,\pi^2 - 30\,Y\,X\Bigg)\frac{t}{u}$$

$$+\frac{1}{8}\,\left(\pi^2 - 4\,X + X^2 + 4\,Y - 2\,Y\,X + Y^2\right)\left(\pi^2 + Y^2 - 2\,Y\,X + X^2\right)\frac{t^2}{s^2}$$

$$+\Bigg(-3\,Y^2\,X - \frac{5}{2}\,X^2\,Y^2 - 32\,Y + X^3\,Y - \frac{1}{2}\,Y^3 + 4\,X^2 - 64 - 2\,Y\,X\,\pi^2 + \frac{1}{2}\,Y^4$$

$$-\frac{5}{2}\,X^2\,Y - \frac{7}{2}\,Y\,\pi^2 - 16\,X - 30\,Y\,X - \frac{1}{2}\,\pi^4 - \frac{1}{2}\,X^2\,\pi^2 + Y^2 - 4\,X\,\pi^2 + 3\,\pi^2\Bigg)\frac{u}{t}$$

$$\text{(C.45)}$$

$$D_{ut} \;=\; \Bigg(\frac{520}{81} + \frac{88}{9}\,U^2 - \frac{544}{27}\,U - \frac{4}{3}\,Y^2\,X - 4\,Y\,X + \frac{20}{9}\,X^2 - \frac{4}{3}\,X^2\,U - \frac{4}{3}\,Y^2\,U + \frac{56}{9}\,Y^2$$

$$+\frac{452}{27}\,Y - \frac{124}{9}\,U\,Y - \frac{92}{27}\,X + \frac{52}{9}\,X\,U + \frac{4}{3}\,Y^3\Bigg)$$

$$+\Bigg(\frac{10}{9}\,X^2 - \frac{2}{3}\,X^2\,U - \frac{2}{3}\,Y^2\,X - 2\,Y\,X - \frac{46}{27}\,X + \frac{26}{9}\,X\,U + \frac{2}{3}\,Y^3 - \frac{2}{3}\,Y^2\,U + \frac{28}{9}\,Y^2$$

$$+\frac{226}{27}\,Y - \frac{62}{9}\,U\,Y + \frac{44}{9}\,U^2 + \frac{260}{81} - \frac{272}{27}\,U\Bigg)\frac{t}{u}$$

$$+\Bigg(\frac{10}{9}\,X^2 - \frac{2}{3}\,X^2\,U - \frac{2}{3}\,Y^2\,X - 2\,Y\,X - \frac{46}{27}\,X + \frac{26}{9}\,X\,U + \frac{2}{3}\,Y^3 - \frac{2}{3}\,Y^2\,U + \frac{28}{9}\,Y^2$$

$$+\frac{226}{27}\,Y - \frac{62}{9}\,U\,Y + \frac{44}{9}\,U^2 + \frac{260}{81} - \frac{272}{27}\,U\Bigg)\frac{u}{t} \qquad\qquad \text{(C.46)}$$

$$E_{ut} \;=\; \Bigg(\frac{320}{9} - 2\,X^2\,Y + \frac{52}{3}\,Y - 4\,U\,Y - \frac{64}{3}\,U + \frac{2}{3}\,Y^2 - \frac{20}{9}\,\pi^2 + \frac{4}{3}\,\pi^2\,U + \frac{64}{9}\,Y\,X$$

$$-\frac{8}{3}\,Y\,X\,U + \frac{2}{3}\,X\,\pi^2 + \frac{2}{3}\,Y^2\,X + \frac{2}{3}\,X^3 - 4\,X - 4\,X\,U + \frac{2}{3}\,Y^3 - \frac{2}{3}\,Y\,\pi^2 - \frac{10}{3}\,X^2\Bigg)$$

$$+\Bigg(\frac{160}{9} - \frac{32}{3}\,U - \frac{5}{3}\,\pi^2 + \pi^2\,U - \frac{5}{9}\,Y^2 + \frac{1}{3}\,Y^2\,U - \frac{2}{3}\,Y\,\pi^2 + \frac{16}{3}\,Y\,X - 2\,Y\,X\,U + \frac{2}{3}\,X\,\pi$$

$$-2\,X^2\,Y - \frac{8}{9}\,X - \frac{8}{3}\,X\,U + \frac{1}{3}\,X^2\,U - \frac{23}{9}\,X^2 + \frac{2}{3}\,X^3 + \frac{68}{9}\,Y - \frac{4}{3}\,U\,Y + \frac{4}{3}\,Y^2\,X\Bigg)\frac{t}{u}$$

$$+\Bigg(4\,Y\,X - 2\,Y\,X\,U - \frac{5}{3}\,\pi^2 + \pi^2\,U + \frac{160}{9} - \frac{32}{3}\,U - X^2\,Y - \frac{17}{9}\,X^2 + \frac{1}{3}\,X^2\,U$$

$$-\frac{1}{3}Y\pi^2 + \frac{1}{3}Y^3 + \frac{1}{3}X^3 + \frac{1}{3}X\pi^2 + \frac{1}{3}Y^2X - \frac{4}{3}XU - \frac{28}{9}X + \frac{1}{9}Y^2 + \frac{1}{3}Y^2U$$

$$+\frac{88}{9}Y - \frac{8}{3}UY\Bigg)\frac{u}{t} \tag{C.4}$$

$$
\begin{aligned}
F_{ut} &= \frac{8}{81}\bigg(-5+3U\bigg)\bigg(-3U+3Y-3X+5\bigg) \\
&\quad +\frac{4}{81}\bigg(-5+3U\bigg)\bigg(-3U+3Y-3X+5\bigg)\frac{t}{u} \\
&\quad +\frac{4}{81}\bigg(-5+3U\bigg)\bigg(-3U+3Y-3X+5\bigg)\frac{u}{t} \tag{C.48}
\end{aligned}
$$

C.3   Quark-gluon scattering

C.3.1   The s-channel process $q\bar{q} \to gg$ and $gg \to q\bar{q}$

C.3.1.1   Two-loop contribution

$$
\begin{aligned}
A_s &= \bigg(\frac{10}{3}X\pi^2 Y + \frac{11}{72}\pi^2 S + \frac{2327}{216}S + \frac{121}{9}S^2 - 20\,\mathrm{Li}_4(z) + 20\,\mathrm{Li}_4(x) - \frac{36077}{864} \\
&\quad -\frac{5}{2}\pi^2 - \frac{109}{144}\pi^4 - \frac{5}{3}X^2\pi^2 - 5X^2Y^2 - \frac{7}{12}Y^2\pi^2 + 16Y\zeta_3 - 3Y\pi^2 \\
&\quad -\frac{1}{6}XY^3 + \frac{10}{3}X^3Y - 9\zeta_3 S - \frac{11}{3}Y^2 S + \frac{121}{9}YS - 21\,\mathrm{Li}_4(y) + \frac{1}{8}Y^4 \\
&\quad -5X^2 + \frac{505}{72}Y^2 - \frac{77}{36}Y^3 + \frac{241}{12}\zeta_3 - \frac{5}{6}X^4 - \frac{35}{6}\mathrm{Li}_3(y) + \frac{2273}{216}Y - \frac{35}{12}XY^2 \\
&\quad -20\,\mathrm{Li}_3(x)Y + \bigg(-\frac{1}{2}Y^2 + 4\pi^2 - \frac{35}{6}Y\bigg)\mathrm{Li}_2(x)\bigg)\frac{t}{u} \\
&\quad +\bigg(\bigg(\frac{5}{12} - 8X\bigg)\mathrm{Li}_3(y) + \bigg(\frac{57}{4} + 4X + 8Y\bigg)\mathrm{Li}_3(x) \\
&\quad +\bigg(Y^2 - X^2 - 4\pi^2 + \frac{5}{12}Y - \frac{57}{4}X\bigg)\mathrm{Li}_2(x) - \frac{8}{3}X\pi^2 Y - \frac{11}{36}\pi^2 S - \frac{1535}{108}S \\
&\quad -\frac{242}{9}S^2 + 16\,\mathrm{Li}_4(z) - 22\,\mathrm{Li}_4(x) + \frac{30377}{432} - 2\pi^2 + \frac{29}{72}\pi^4 + \frac{977}{144}X + \frac{40}{9}X\pi^2 \\
&\quad +4X\zeta_3 + 4X^2\pi^2 + 2X^2Y^2 + \frac{7}{6}Y^2\pi^2 + \frac{431}{72}X^3 + \frac{61}{24}Y\pi^2 + \frac{1}{3}XY^3 - \frac{8}{3}X^3Y \\
&\quad +18\zeta_3 S + \frac{22}{3}X^2 S - \frac{57}{8}X^2 Y - \frac{55}{6}XS + \frac{22}{3}Y^2 S - \frac{715}{18}YS + 18\,\mathrm{Li}_4(y) \\
&\quad -\frac{1}{4}Y^4 - \frac{793}{144}X^2 - \frac{3847}{144}Y^2 + \frac{401}{72}Y^3 - \frac{205}{6}\zeta_3 + \frac{1}{12}X^4 - \frac{3059}{432}Y + \frac{5}{24}XY^2\bigg)\frac{t^2}{s^2} \\
&\quad +\bigg(\frac{457}{144} + \frac{2}{3}Y\pi^2 + \frac{9}{2}\zeta_3 + \frac{11}{90}\pi^4 + \frac{169}{36}\pi^2 - 8Y\zeta_3 + 8\,\mathrm{Li}_3(x)Y - \frac{2417}{144}Y \\
&\quad -\frac{33}{4}\mathrm{Li}_3(y) + \frac{33}{8}X^2 Y + \frac{55}{6}YS - \frac{11}{6}S + \frac{141}{16}Y^2 + \frac{33}{4}\mathrm{Li}_2(y)Y - \frac{17}{24}X^3 + X^2Y^2\bigg)
\end{aligned}
$$

$$+\left\{t \longleftrightarrow u\right\}$$

(C.49)

$$
\begin{aligned}
B_s &= \left(\frac{16}{9} X Y - \frac{44}{3} X Y S + 3 X \pi^2 Y + \left(-\frac{71}{6} + 24 X + 2 Y\right) \mathrm{Li}_3(y)\right. \\
&\quad + \left(-\frac{1}{2} Y^2 - 11 X^2 + 20 X Y - \frac{19}{3} \pi^2 - \frac{71}{6} Y - \frac{25}{3} X\right) \mathrm{Li}_2(x) \\
&\quad + \left(\frac{25}{3} + 44 X - 70 Y\right) \mathrm{Li}_3(x) + \frac{65}{9} \pi^2 S - \frac{7543}{216} S - \frac{121}{9} S^2 - 74 \mathrm{Li}_4(z) \\
&\quad + 8 \mathrm{Li}_4(x) + \frac{164771}{2592} - \frac{1055}{72} \pi^2 + \frac{317}{180} \pi^4 - \frac{22}{27} X - \frac{551}{36} X \pi^2 - 36 X \zeta_3 \\
&\quad - \frac{16}{3} X^2 \pi^2 - \frac{9}{2} X^2 Y^2 - \frac{31}{12} Y^2 \pi^2 + 74 Y \zeta_3 - \frac{17}{2} X^3 - \frac{1}{3} Y \pi^2 + \frac{7}{6} X Y^3 + 9 X^3 Y \\
&\quad + 10 \zeta_3 S + \frac{55}{6} X^2 Y - \frac{220}{9} X S + \frac{22}{3} Y^2 S - \frac{22}{9} Y S - 79 \mathrm{Li}_4(y) - \frac{3}{8} Y^4 + \frac{655}{36} X^2 \\
&\quad \left. - \frac{125}{72} Y^2 + \frac{127}{36} Y^3 - \frac{733}{18} \zeta_3 - \frac{25}{12} X^4 - \frac{5765}{216} Y - \frac{139}{12} X Y^2\right) \frac{t}{u} \\
&\quad + \left(\left(\left(-7 Y + 16 X - \frac{71}{6}\right) \mathrm{Li}_3(x) + \frac{391}{18} X Y - \frac{4}{3} X \pi^2 Y + \left(7 \pi^2 - \frac{27}{4} X^2 - 8 X Y\right.\right.\right. \\
&\quad + \frac{45}{4} Y^2 + \frac{71}{6} Y + \frac{71}{6} X\right) \mathrm{Li}_2(x) + \left(\frac{71}{6} + 7 X + 20 Y\right) \mathrm{Li}_3(y) - \frac{1}{12} \pi^2 S + \frac{1502}{27} S \\
&\quad - 22 \mathrm{Li}_4(z) + \frac{7}{2} \mathrm{Li}_4(x) - \frac{19139}{324} + \frac{16}{9} \pi^2 - \frac{17}{60} \pi^4 + \frac{359}{36} X + \frac{103}{18} X \pi^2 + X \zeta_3 \\
&\quad + \frac{11}{4} X^2 \pi^2 - \frac{19}{4} X^2 Y^2 + \frac{7}{8} Y^2 \pi^2 - Y \zeta_3 + \frac{341}{18} X^3 - \frac{277}{36} Y \pi^2 + \frac{71}{12} X Y^3 + 3 X^3 Y \\
&\quad - 2 \zeta_3 S + \frac{11}{6} X^2 S - 24 X^2 Y + \frac{11}{6} X S - \frac{11}{6} Y^2 S - \frac{11}{6} Y S - \frac{79}{2} \mathrm{Li}_4(y) + \frac{31}{48} Y^4 \\
&\quad \left. - \frac{301}{12} X^2 - \frac{167}{36} Y^2 - \frac{101}{18} Y^3 + \frac{443}{18} \zeta_3 - \frac{33}{16} X^4 + \frac{601}{36} Y + \frac{45}{2} X Y^2\right) \frac{t^2}{s^2} \\
&\quad - X^2 \frac{t^2}{u^2} + \left(\frac{65}{2} \mathrm{Li}_4(y) + \left(-9 Y - 18 X\right) \mathrm{Li}_3(x) - \frac{299}{6} \mathrm{Li}_3(y)\right. \\
&\quad + \frac{1}{12} Y \left(21 Y + 598\right) \mathrm{Li}_2(y) + \frac{73}{4} X Y + 19 Y \zeta_3 - \frac{11}{6} S + \frac{139}{36} + \frac{14}{9} Y \\
&\quad - \frac{17}{48} Y^4 - \frac{13}{8} X^2 Y^2 + \frac{73}{18} X^3 - \frac{55}{6} Y \pi^2 - \frac{347}{36} Y^2 + \frac{118}{3} \zeta_3 - \frac{229}{240} \pi^4 \\
&\quad \left. - \frac{799}{72} \pi^2 - \frac{11}{6} X^2 S + \frac{62}{3} X^2 Y - \frac{55}{6} Y S + \frac{2}{3} X^3 Y - \frac{47}{12} Y^2 \pi^2 - \frac{5}{6} X \pi^2 Y\right) \\
&\quad + \left\{t \longleftrightarrow u\right\}
\end{aligned}
$$

(C.50)

$$
C_s = \left(2 X Y - \frac{16}{3} X \pi^2 Y + \left(4 X Y + \frac{1}{2} Y^2 - 4 X^2 - \frac{8}{3} \pi^2 - \frac{15}{2} Y + 3 X\right) \mathrm{Li}_2(x)\right.
$$

$$
+\left(-\frac{15}{2}+10\,X+4\,Y\right)\mathrm{Li}_3(y)+\left(-3+10\,X+14\,Y\right)\mathrm{Li}_3(x)-\frac{13}{24}\,\pi^2\,S
$$

$$
+\frac{5297}{216}\,S+8\,\mathrm{Li}_4(z)-20\,\mathrm{Li}_4(x)-\frac{41393}{2592}-\frac{133}{36}\,\pi^2+\frac{301}{720}\,\pi^4+\frac{59}{3}\,X+\frac{49}{18}\,X\,\pi^2
$$

$$
-6\,X\,\zeta_3+\frac{3}{2}\,X^2\,\pi^2+\frac{15}{2}\,X^2\,Y^2+\frac{3}{4}\,Y^2\,\pi^2-12\,Y\,\zeta_3-\frac{65}{18}\,X^3+\frac{55}{36}\,Y\,\pi^2-\frac{1}{6}\,X\,Y^3
$$

$$
-\frac{8}{3}\,X^3\,Y+5\,\zeta_3\,S-\frac{22}{3}\,X^2\,S-\frac{10}{3}\,X^2\,Y-\frac{11}{3}\,Y^2\,S-11\,Y\,S+\mathrm{Li}_4(y)+\frac{3}{8}\,Y^4
$$

$$
+\frac{143}{18}\,X^2-\frac{425}{72}\,Y^2-\frac{23}{36}\,Y^3+\frac{173}{36}\,\zeta_3+\frac{1}{3}\,X^4+\frac{271}{24}\,Y-\frac{101}{12}\,X\,Y^2\Bigg)\frac{t}{u}
$$

$$
+\Bigg(-\frac{11}{2}\,X\,Y+\frac{2}{3}\,X\,\pi^2\,Y+\left(-\frac{11}{4}-3\,Y\right)\mathrm{Li}_3(x)+\pi^2\,S-\frac{3}{4}\,S-6\,\mathrm{Li}_4(z)
$$

$$
+\frac{11}{2}\,\mathrm{Li}_4(x)-\frac{255}{16}+\left(\frac{1}{3}\,\pi^2+\frac{1}{4}\,X^2+\frac{1}{4}\,Y^2+\frac{11}{4}\,Y+\frac{11}{4}\,X\right)\mathrm{Li}_2(x)+\frac{1}{3}\,\pi^2
$$

$$
+\left(3\,X+\frac{11}{4}\right)\mathrm{Li}_3(y)+\frac{13}{360}\,\pi^4-\frac{21}{16}\,X-\frac{7}{6}\,X\,\pi^2-3\,X\,\zeta_3-\frac{7}{12}\,X^2\,\pi^2-\frac{3}{4}\,X^2\,Y^2
$$

$$
+\frac{1}{24}\,Y^2\,\pi^2+3\,Y\,\zeta_3-\frac{13}{24}\,X^3+\frac{17}{24}\,Y\,\pi^2+\frac{1}{4}\,X\,Y^3+X^3\,Y-12\,\zeta_3\,S+\frac{25}{8}\,X^2\,Y
$$

$$
-\frac{11}{2}\,\mathrm{Li}_4(y)-\frac{5}{48}\,Y^4+\frac{21}{16}\,X^2+\frac{67}{16}\,Y^2+\frac{13}{24}\,Y^3+15\,\zeta_3-\frac{7}{48}\,X^4+\frac{21}{16}\,Y-\frac{3}{8}\,X\,Y^2\Bigg)\frac{t^2}{s^2}
$$

$$
+X^2\,\frac{t^2}{u^2}+\Bigg(-\frac{83}{2}\,\mathrm{Li}_4(y)+\left(26\,X+15\,Y\right)\mathrm{Li}_3(x)-\frac{13}{4}\,\mathrm{Li}_3(y)+\frac{3}{2}\,\zeta_3+\frac{271}{240}\,\pi^4
$$

$$
-\frac{127}{72}\,\pi^2-\frac{1}{4}\,Y\left(21\,Y-13\right)\mathrm{Li}_2(y)+\frac{55}{18}\,Y\,\pi^2-25\,Y\,\zeta_3+\frac{3133}{144}\,Y-\frac{55}{12}\,X\,Y
$$

$$
-\frac{22}{3}\,X^2\,S+\frac{7}{4}\,Y^2\,\pi^2-\frac{7}{6}\,X\,\pi^2\,Y-\frac{22}{3}\,Y\,S+\frac{23}{16}+\frac{9}{16}\,Y^4-\frac{119}{24}\,X^2\,Y+\frac{1063}{144}\,Y^2
$$

$$
-\frac{209}{72}\,X^3-\frac{4}{3}\,X^3\,Y+\frac{23}{8}\,X^2\,Y^2\Bigg)+\Big\{t\longleftrightarrow u\Big\}
$$

$$
\tag{C.51}
$$

$$
D_s=\Bigg(-\frac{7}{3}\,X\,\pi^2\,Y+\frac{1}{2}\,\pi^2\,S-\frac{3}{8}\,S+14\,\mathrm{Li}_4(z)+\frac{5}{8}\,\pi^2-\frac{1}{90}\,\pi^4+X+\frac{10}{3}\,X\,\pi^2-\frac{187}{32}
$$

$$
+4\,X\,\zeta_3+\left(16\,Y-6\,X+8\right)\mathrm{Li}_3(x)+\frac{1}{2}\,X^2\,\pi^2+4\,X^2\,Y^2+\frac{5}{12}\,Y^2\,\pi^2-18\,Y\,\zeta_3
$$

$$
+\frac{9}{4}\,Y\,\pi^2+\frac{1}{2}\,X\,Y^3-\frac{7}{3}\,X^3\,Y-6\,\zeta_3\,S-\frac{11}{2}\,X^2\,Y+11\,\mathrm{Li}_4(y)-\frac{1}{8}\,Y^4-\frac{1}{4}\,X^2
$$

$$
+\frac{5}{8}\,Y^2-\frac{3}{4}\,Y^3+\frac{5}{2}\,\zeta_3-\frac{1}{12}\,X^4+\frac{39}{8}\,Y-\frac{3}{4}\,X\,Y^2+\left(2\,Y+2\,X-\frac{3}{2}\right)\mathrm{Li}_3(y)
$$

$$
+\left(\frac{1}{2}\,Y^2-X^2+\pi^2-\frac{3}{2}\,Y-8\,X\right)\mathrm{Li}_2(x)\Bigg)\frac{t}{u}-X^2\,\frac{t^2}{u^2}
$$

$$
+\left(\frac{3}{2}\,\pi^2-3\,X\,Y+\frac{3}{2}\,Y^2+\frac{3}{2}\,X^2-3\,X+3\,Y\right)\frac{t^2}{s^2}
$$

$$
+\Bigg(10\,\mathrm{Li}_4(y)+\left(16\,Y-4\,X\right)\mathrm{Li}_3(x)+19\,\mathrm{Li}_3(y)-Y\left(Y+19\right)\mathrm{Li}_2(y)+\frac{1}{4}
$$

$$+2\,X^2\,Y^2 + \frac{4}{3}\,Y\,\pi^2 - 2\,\zeta_3 - \frac{4}{45}\,\pi^4 + \frac{43}{12}\,\pi^2 - \frac{7}{12}\,Y^4 - 12\,Y\,\zeta_3 - \frac{15}{2}\,X^2\,Y + \frac{29}{4}\,Y$$

$$-\frac{1}{3}\,Y^2\,\pi^2 + 3\,Y^2 - \frac{7}{2}\,X\,Y - \frac{4}{3}\,X\,\pi^2\,Y - \frac{11}{6}\,X^3\Bigg) + \Big\{t \longleftrightarrow u\Big\}$$

$$\text{(C.52)}$$

$$E_s \;=\; \Bigg(-\frac{4}{3}\,X\,\pi^2\,Y + \left(-\frac{4}{3}\,\pi^2 + \frac{4}{3}\,Y\right)\mathrm{Li}_2(x) - \frac{1}{36}\,\pi^2\,S + \frac{185}{54}\,S - \frac{44}{9}\,S^2 + 8\,\mathrm{Li}_4(z)$$

$$-8\,\mathrm{Li}_4(x) + \frac{1307}{216} + \frac{77}{54}\,\pi^2 + \frac{14}{45}\,\pi^4 + \frac{2}{3}\,X^2\,\pi^2 + 2\,X^2\,Y^2 - 8\,Y\,\zeta_3 + \frac{1}{2}\,Y\,\pi^2$$

$$-\frac{4}{3}\,X^3\,Y + \frac{2}{3}\,Y^2\,S - \frac{44}{9}\,Y\,S + 8\,\mathrm{Li}_4(y) + 2\,X^2 - \frac{43}{18}\,Y^2 + \frac{7}{18}\,Y^3 - \frac{17}{6}\,\zeta_3 + \frac{1}{3}\,X^4$$

$$+\frac{4}{3}\,\mathrm{Li}_3(y) + \frac{10}{9}\,Y + \frac{2}{3}\,X\,Y^2 + 8\,\mathrm{Li}_3(x)\,Y\Bigg)\frac{t}{u}$$

$$+\Bigg(\left(\frac{4}{3} + 2\,X\right)\mathrm{Li}_3(y) + \frac{2}{3}\,X\,\pi^2\,Y + \left(\frac{2}{3}\,\pi^2 + \frac{4}{3}\,Y + 4\,X\right)\mathrm{Li}_2(x) + \frac{1}{18}\,\pi^2\,S - \frac{221}{27}\,S$$

$$+\frac{88}{9}\,S^2 - 4\,\mathrm{Li}_4(z) + 4\,\mathrm{Li}_4(x) - \frac{863}{108} + \left(-2\,Y - 4\right)\mathrm{Li}_3(x) - \frac{32}{27}\,\pi^2 - \frac{17}{180}\,\pi^4 - \frac{19}{18}\,X$$

$$-\frac{16}{9}\,X\,\pi^2 - 2\,X\,\zeta_3 - \frac{1}{3}\,X^2\,\pi^2 - \frac{1}{2}\,X^2\,Y^2 + 2\,Y\,\zeta_3 - \frac{7}{9}\,X^3 - Y\,\pi^2 + \frac{2}{3}\,X^3\,Y - \frac{4}{3}\,X^2\,S$$

$$+2\,X^2\,Y + \frac{5}{3}\,X\,S - \frac{4}{3}\,Y^2\,S + \frac{109}{9}\,Y\,S - 4\,\mathrm{Li}_4(y) + \frac{1}{9}\,X^2 + \frac{70}{9}\,Y^2 - \frac{7}{9}\,Y^3 + \frac{17}{3}\,\zeta_3$$

$$-\frac{1}{6}\,X^4 - \frac{31}{6}\,Y + \frac{2}{3}\,X\,Y^2\Bigg)\frac{t^2}{s^2}$$

$$+\Bigg(-\frac{37}{36} + \frac{2}{3}\,Y\,\pi^2 - 4\,\zeta_3 - \frac{11}{360}\,\pi^4 - \frac{49}{36}\,\pi^2 + 2\,Y\,\zeta_3 - 2\,\mathrm{Li}_3(x)\,Y + \frac{91}{18}\,Y + 4\,\mathrm{Li}_3(y)$$

$$-2\,X^2\,Y - \frac{5}{3}\,Y\,S + \frac{1}{3}\,S - 2\,Y^2 - 4\,\mathrm{Li}_2(y)\,Y - \frac{1}{4}\,X^2\,Y^2\Bigg) + \Big\{t \longleftrightarrow u\Big\}$$

$$\text{(C.53)}$$

$$F_s \;=\; \Bigg(-\frac{1}{2}\,X\,Y + \frac{8}{3}\,X\,Y\,S + \frac{8}{3}\,X\,\pi^2\,Y - \frac{11}{9}\,\pi^2\,S + \frac{7}{9}\,S + \frac{44}{9}\,S^2 - 16\,\mathrm{Li}_4(z) + 16\,\mathrm{Li}_4(x)$$

$$-\frac{3661}{324} + \left(-16\,Y + 4\right)\mathrm{Li}_3(x) + \frac{347}{108}\,\pi^2 - \frac{28}{45}\,\pi^4 - \frac{161}{18}\,X - \frac{37}{18}\,X\,\pi^2 - \frac{4}{3}\,X^2\,\pi^2$$

$$-4\,X^2\,Y^2 + 16\,Y\,\zeta_3 + \frac{2}{3}\,X^3 - \frac{1}{6}\,Y\,\pi^2 + \frac{8}{3}\,X^3\,Y - \frac{2}{3}\,X^2\,Y + \frac{62}{9}\,X\,S - \frac{4}{3}\,Y^2\,S$$

$$+\frac{26}{9}\,Y\,S - 16\,\mathrm{Li}_4(y) + \frac{29}{18}\,X^2 + \frac{35}{18}\,Y^2 - \frac{7}{9}\,Y^3 - \frac{10}{9}\,\zeta_3 - \frac{2}{3}\,X^4 + \frac{4}{3}\,\mathrm{Li}_3(y)$$

$$+\frac{23}{9}\,Y + \frac{11}{6}\,X\,Y^2 + \left(\frac{8}{3}\,\pi^2 + \frac{4}{3}\,Y - 4\,X\right)\mathrm{Li}_2(x)\Bigg)\frac{t}{u}$$

$$+\Bigg(-\frac{4}{3}\,\mathrm{Li}_3(x) + \frac{4}{3}\,\mathrm{Li}_3(y) + \left(\frac{4}{3}\,Y + \frac{4}{3}\,X\right)\mathrm{Li}_2(x) + \frac{7}{9}\,X - \frac{263}{27}\,S + \frac{25}{18}\,\pi^2$$

$$+\frac{4085}{324} + \frac{13}{18}\,Y^2 + \frac{103}{18}\,X^2 - \frac{31}{9}\,Y - \frac{73}{36}\,X^3 - \frac{58}{9}\,X\,Y - \frac{1}{9}\,\zeta_3 + \frac{25}{36}\,Y^3 - \frac{1}{6}\,\pi^2\,S$$

$$+\frac{5}{2}\,X^2\,Y - \frac{31}{18}\,Y\,\pi^2 + \frac{1}{6}\,X\,Y^2 + \frac{3}{2}\,X\,\pi^2 - \frac{1}{3}\,X^2\,S - \frac{1}{3}\,X\,S + \frac{1}{3}\,Y^2\,S + \frac{1}{3}\,Y\,S\Bigg)\frac{t^2}{s^2}$$

$$-3 X^2 \frac{t^2}{u^2} + \left(-\frac{19}{36} + \frac{1}{18} Y \pi^2 + \frac{52}{3} \zeta_3 - \frac{11}{90} \pi^4 + \frac{35}{12} \pi^2 + 8 Y \zeta_3 - 8 \operatorname{Li}_3(x) Y - \frac{50}{9} Y \right.$$

$$-\frac{52}{3} \operatorname{Li}_3(y) + \frac{47}{6} X^2 Y + \frac{5}{3} Y S + \frac{1}{3} X^2 S + \frac{1}{3} S - \frac{5}{18} Y^2 + \frac{52}{3} \operatorname{Li}_2(y) Y - \frac{11}{36} X^3$$

$$\left. -X^2 Y^2 - \frac{1}{3} X Y \right) + \left\{ t \longleftrightarrow u \right\}$$

$$(C.54)$$

$$G_s = \left(\frac{1}{2} X Y - 8 X \pi^2 Y - \frac{1}{12} \pi^2 S - \frac{227}{54} S + 48 \operatorname{Li}_4(z) - 48 \operatorname{Li}_4(x) + \frac{3401}{648} + \frac{64}{9} X \pi^2 \right.$$

$$+ \left(-8 \pi^2 + 8 X \right) \operatorname{Li}_2(x) + \left(48 Y - 8 \right) \operatorname{Li}_3(x) + \frac{19}{36} \pi^2 + \frac{28}{15} \pi^4 + \frac{101}{6} X + \frac{1}{3} X^2 Y$$

$$+ 4 X^2 \pi^2 + 12 X^2 Y^2 - 48 Y \zeta_3 + \frac{7}{9} X^3 + \frac{2}{9} Y \pi^2 - 8 X^3 Y + \frac{4}{3} X^2 S + \frac{2}{3} Y^2 S$$

$$\left. + 2 Y S + 48 \operatorname{Li}_4(y) - \frac{73}{9} X^2 + \frac{4}{9} Y^2 + \frac{7}{18} Y^3 + \frac{143}{18} \zeta_3 + 2 X^4 - \frac{11}{3} Y + \frac{1}{6} X Y^2 \right) \frac{t}{u}$$

$$+ \left(4 \operatorname{Li}_3(x) - 4 \operatorname{Li}_3(y) - 4 \left(X + Y \right) \operatorname{Li}_2(x) - 4 X Y^2 - \frac{10}{3} X \pi^2 + 8 Y - 8 X + 4 Y \pi^2 \right.$$

$$+ 9 X^2 \frac{t^2}{u^2} + \left(\frac{46}{9} Y \pi^2 - 52 \zeta_3 + \frac{11}{30} \pi^4 - \frac{107}{18} \pi^2 - 24 Y \zeta_3 + 24 \operatorname{Li}_3(x) Y + \frac{71}{9} Y + \frac{7}{9} X \right.$$

$$\left. + 52 \operatorname{Li}_3(y) - \frac{71}{3} X^2 Y + \frac{4}{3} Y S + \frac{4}{3} X^2 S + \frac{44}{9} Y^2 - 52 \operatorname{Li}_2(y) Y + 3 X^2 Y^2 - \frac{2}{3} X Y \right)$$

$$+ \left\{ t \longleftrightarrow u \right\}$$

$$(C.$$

$$H_s = \left(-\frac{8}{9} Y S - \frac{8}{9} S^2 + \frac{8}{27} \pi^2 - \frac{1}{3} Y^2 + \frac{40}{27} S + \frac{20}{27} Y \right) \frac{t^2}{s^2}$$

$$+ \left(\frac{1}{6} Y^2 - \frac{10}{27} Y + \frac{4}{9} Y S - \frac{4}{27} \pi^2 - \frac{20}{27} S + \frac{4}{9} S^2 \right) \frac{t}{u}$$

$$+ \left\{ t \longleftrightarrow u \right\}$$

$$(C.56)$$

$$I_s = \left(\frac{10}{27} Y - \frac{4}{9} Y S - \frac{1}{9} X^2 - \frac{7}{54} \pi^2 - \frac{1}{18} X Y + \frac{20}{27} S \right.$$

$$\left. -\frac{4}{9} S^2 + \frac{10}{27} X - \frac{4}{9} X S - \frac{1}{6} Y^2 \right) \frac{t}{u}$$

$$-\frac{1}{18} \left(X - Y \right) \left(Y + X \right) \frac{t^2}{s^2}$$

$$+ \left\{ t \longleftrightarrow u \right\}$$

$$(C.57)$$

C.3.1.2   One-loop self-interference contribution

$$
\begin{aligned}
A_s =\ & \left(\frac{25}{12} Y^3 + \frac{55}{12} X^3 - X^4 - \frac{133}{36} Y^2 + \frac{11}{6} X \pi^2 + \frac{11}{3} Y^2 S - \frac{19}{6} Y \pi^2 - 4 X^2 \pi^2 + \frac{11}{3} X^2 S \right. \\
& \left. - \frac{205}{12} Y - 22 S - \frac{121}{9} S^2 - \frac{715}{36} Y S - \frac{55}{12} X S - \frac{82}{9} - \frac{1}{9} \pi^2 - \frac{35}{12} X - \frac{17}{12} X^2 \right) \frac{t^2}{s^2} \\
& + \left(- \frac{5}{72} Y^2 - \frac{11}{6} Y^2 S + \frac{3}{4} X^2 + 2 X^2 \pi^2 + \frac{1}{2} X^4 + \frac{121}{18} S^2 + \frac{77}{6} S + \frac{51}{8} + \frac{11}{6} Y \pi^2 \right. \\
& \left. - \frac{5}{2} X \pi^2 - \frac{5}{4} X^3 - \frac{11}{12} Y^3 + \frac{121}{18} Y S + \frac{77}{12} Y + \frac{1}{2} Y^2 \pi^2 + \frac{157}{72} \pi^2 + \frac{1}{8} Y^4 \right) \frac{t}{u} \\
& - \frac{1}{4} X \left(4 X \pi^2 - 4 \pi^2 + X^3 - 2 X^2 \right) \frac{t^2}{u^2} + \frac{1}{8} X^2 \left(4 \pi^2 + X^2 \right) \frac{t^3}{u^3} \\
& + \left(- \frac{31}{36} + \frac{8}{3} X^2 - X^2 \pi^2 + \frac{55}{12} Y S - \frac{23}{12} \pi^2 - \frac{11}{12} S + \frac{41}{12} Y - \frac{1}{4} X^4 \right) \\
& + \left\{ t \longleftrightarrow u \right\}
\end{aligned}
$$

$$(C.58)$$

$$
\begin{aligned}
B_s =\ & \left(2 X^2 Y^2 + 4 X^3 Y + \frac{200}{9} X Y + \frac{35}{3} X Y^2 - 25 X^2 Y - 4 X Y^3 + 8 X Y \pi^2 + 24 \right. \\
& + \frac{88}{3} S + \frac{79}{12} X - \frac{224}{9} X^2 + \frac{241}{12} Y - \frac{67}{12} Y^3 + \frac{227}{12} X^3 - \frac{15}{4} X^4 - \frac{16}{3} Y^2 + \frac{7}{4} Y^4 \\
& \left. + \frac{58}{3} X \pi^2 - \frac{11}{12} Y^2 S - \frac{58}{3} Y \pi^2 - 9 X^2 \pi^2 + \frac{11}{12} X^2 S - \frac{11}{12} Y S + \frac{11}{12} X S + Y^2 \pi^2 \right) \frac{t^2}{s^2} \\
& + \left(2 X^2 Y^2 - 4 X^3 Y - \frac{118}{9} X Y - 2 X Y^2 + \frac{71}{12} X^2 Y + X Y^3 - 4 X Y \pi^2 \right. \\
& - \frac{22}{3} X Y S + \frac{809}{72} \pi^2 - \frac{121}{18} S^2 - \frac{77}{3} S - \frac{35}{3} X + \frac{59}{9} X^2 - \frac{91}{12} Y + \frac{13}{12} Y^3 - \frac{77}{12} X^3 \\
& + \frac{25}{8} X^4 + \frac{455}{72} Y^2 - \frac{3}{8} Y^4 - \frac{22}{3} X \pi^2 + \frac{11}{3} Y^2 S + \frac{31}{3} Y \pi^2 + \frac{17}{2} X^2 \pi^2 - \frac{11}{9} Y S \\
& \left. - \frac{110}{9} X S + 2 Y^2 \pi^2 + \frac{1}{2} \pi^4 - \frac{145}{8} + \frac{11}{3} \pi^2 S \right) \frac{t}{u} \\
& - \frac{1}{4} X \left(4 X \pi^2 - 4 \pi^2 + X^3 - 2 X^2 \right) \frac{t^2}{u^2} + \frac{1}{8} X^2 \left(4 \pi^2 + X^2 \right) \frac{t^3}{u^3} \\
& + \left(\frac{1}{3} - X^2 Y^2 - \frac{41}{12} X^2 - \frac{11}{12} Y^2 S - \frac{55}{12} Y S - \frac{17}{12} \pi^2 - \frac{11}{12} S - \frac{109}{12} Y + \frac{27}{2} Y \pi^2 \right. \\
& \left. - \frac{3}{2} X^4 + \frac{31}{6} Y^3 + 4 X Y \pi^2 + 4 X Y^3 - \frac{10}{3} X Y + \frac{1}{6} X^2 Y \right) \\
& + \left\{ t \longleftrightarrow u \right\}
\end{aligned}
$$

$$(C.59)$$

$$
C_s = \left(\frac{7}{12} Y^3 + \frac{1}{2} X^2 Y^2 - X Y^3 - 2 X^3 Y - \frac{11}{3} X^2 S - \frac{15}{4} X^2 - \frac{13}{2} X \pi^2 + \frac{35}{3} X \right.
$$

$$-\frac{11}{2}\,Y\,S-\frac{49}{12}\,Y-\frac{14}{3}\,X\,Y^2+2\,X\,Y-\frac{11}{6}\,X^2\,Y+\frac{145}{8}+\frac{77}{6}\,S-4\,X\,Y\,\pi^2+\frac{1}{8}\,X^4$$

$$\left.-\frac{41}{8}\,\pi^2-\frac{5}{2}\,X^2\,\pi^2-\frac{11}{6}\,Y^2\,S-\frac{55}{8}\,Y^2-\frac{43}{12}\,X^3+\frac{3}{8}\,Y^4\right)\frac{t}{u}$$

$$-\frac{1}{2}\,X\left(2\,\pi^2+X^2+4\,X\,\pi^2+X^3\right)\frac{t^2}{u^2}+\left(-16-X^2+Y-X+Y^2\right)\frac{t^2}{s^2}$$

$$+\left(\frac{3}{2}-\frac{13}{3}\,X^2-X^2\,\pi^2-\frac{11}{3}\,Y^2\,S-\frac{11}{3}\,Y\,S-\frac{3}{2}\,\pi^2+\frac{3}{2}\,Y-5\,Y\,\pi^2+\frac{1}{2}\,X^4-\frac{4}{3}\,Y^3\right.$$

$$\left.-4\,X\,Y\,\pi^2-2\,X\,Y^3-\frac{10}{3}\,X\,Y-\frac{16}{3}\,X^2\,Y\right)$$

$$-\frac{1}{8}\,X^2\left(4\,\pi^2+X^2\right)\frac{t^3}{u^3}+\left\{t\longleftrightarrow u\right\}$$

$$\text{(C.60)}$$

$$D_s\;=\;\left(-\frac{1}{2}\,Y^2\,\pi^2-\frac{1}{8}\,Y^4-2\,X\,Y\,\pi^2+3\,X^2-\frac{13}{8}\,\pi^2-\frac{1}{2}\,X^2\,Y^2-\frac{51}{8}-\frac{7}{2}\,X^2\,\pi^2\right.$$

$$\left.+\frac{21}{4}\,Y-\frac{7}{4}\,X^3-\frac{3}{2}\,Y\,\pi^2-\frac{7}{8}\,X^4-5\,X\,\pi^2+\frac{5}{8}\,Y^2-\frac{3}{4}\,X^2\,Y-\frac{3}{4}\,Y^3\right)\frac{t}{u}$$

$$-\frac{1}{2}\,X\left(2\,\pi^2+X^2+4\,X\,\pi^2+X^3\right)\frac{t^2}{u^2}-\frac{1}{8}\,X^2\left(4\,\pi^2+X^2\right)\frac{t^3}{u^3}$$

$$+\left(\frac{1}{4}-\frac{1}{2}\,X^2\,Y^2+2\,X^2-2\,X^2\,\pi^2-\frac{3}{2}\,\pi^2+\frac{7}{2}\,Y-5\,Y\,\pi^2-\frac{1}{2}\,X^4-2\,Y^3-2\,X\,Y\,\pi^2\right.$$

$$\left.-\frac{1}{2}\,X^2\,Y\right)+\left\{t\longleftrightarrow u\right\}$$

$$\text{(C.61)}$$

$$E_s\;=\;\left(-\frac{1}{3}\,Y^3-\frac{1}{3}\,X^3+\frac{65}{36}\,Y^2+\frac{2}{3}\,X\,\pi^2-\frac{2}{3}\,Y^2\,S+\frac{2}{3}\,Y\,\pi^2-\frac{2}{3}\,X^2\,S+\frac{25}{12}\,Y\right.$$

$$\left.+\frac{2}{9}+4\,S+\frac{44}{9}\,S^2+\frac{109}{18}\,Y\,S+\frac{5}{6}\,X\,S+\frac{2}{9}\,\pi^2-\frac{1}{12}\,X+\frac{5}{12}\,X^2\right)\frac{t^2}{s^2}$$

$$+\left(-\frac{11}{18}\,\pi^2-\frac{11}{18}\,Y^2+\frac{1}{3}\,Y^2\,S+\frac{1}{6}\,Y^3-\frac{22}{9}\,Y\,S-\frac{7}{6}\,Y-\frac{1}{3}\,Y\,\pi^2-\frac{22}{9}\,S^2-\frac{7}{3}\,S\right)\frac{t}{u}$$

$$+\left(\frac{1}{18}-\frac{5}{12}\,X^2-\frac{5}{6}\,Y\,S+\frac{5}{12}\,\pi^2+\frac{1}{6}\,S+\frac{1}{12}\,Y\right)+\left\{t\longleftrightarrow u\right\}$$

$$\text{(C.62)}$$

$$F_s\;=\;\left(\frac{7}{12}\,Y^3-\frac{7}{6}\,X\,Y^2+\frac{1}{6}\,Y^2\,S+\frac{1}{12}\,Y^2+\frac{5}{2}\,X^2\,Y-\frac{31}{12}\,Y+\frac{11}{6}\,Y\,\pi^2+\frac{1}{6}\,Y\,S\right.$$

$$\left.-\frac{23}{12}\,X^3-\frac{1}{12}\,X-\frac{11}{6}\,X\,\pi^2-\frac{1}{6}\,X\,S-\frac{1}{6}\,X^2\,S+\frac{157}{36}\,X^2-\frac{16}{3}\,S-\frac{40}{9}\,X\,Y\right)\frac{t^2}{s^2}$$

$$+\left(\frac{14}{3}\,S+\frac{22}{9}\,S^2-\frac{10}{9}\,X^2+\frac{1}{2}\,X\,Y^2+\frac{7}{6}\,X+\frac{31}{9}\,X\,S+\frac{1}{3}\,X\,\pi^2-\frac{2}{3}\,X^2\,Y+\frac{2}{3}\,X^3+\frac{7}{3}\,Y\right.$$

$$+\frac{31}{18}XY+\frac{4}{3}XYS-\frac{1}{3}Y^3+\frac{13}{9}YS-\frac{2}{3}\pi^2 S-\frac{31}{18}\pi^2-\frac{2}{3}Y^2 S+\frac{1}{9}Y^2-\frac{4}{3}Y\pi^2\Bigg)\frac{t}{u}$$

$$+\left(\frac{1}{6}+\frac{5}{12}X^2+\frac{1}{6}Y^2 S+\frac{5}{6}YS-\frac{1}{12}\pi^2+\frac{1}{6}S+\frac{1}{12}Y\right.$$

$$\left.-\frac{3}{2}Y\pi^2-\frac{5}{12}Y^3+\frac{1}{3}XY-\frac{1}{6}X^2 Y\right)+\left\{t\longleftrightarrow u\right\}$$

$$\text{(C.63}$$

$$G_s \;=\; \frac{1}{6}\left(3Y+2X^2-7+Y^2\right)\left(Y+2S+X\right)\frac{t}{u}$$

$$+\left(\frac{1}{3}X^2+\frac{2}{3}Y^2 S+\frac{2}{3}YS+\frac{1}{3}Y^3+\frac{1}{3}XY+\frac{1}{3}X^2 Y\right)$$

$$+\left\{t\longleftrightarrow u\right\}$$

$$\text{(C.64)}$$

$$H_s \;=\; \left(-\frac{1}{9}Y^2-\frac{4}{9}YS-\frac{1}{9}\pi^2-\frac{1}{9}-\frac{4}{9}S^2\right)\frac{t^2}{s^2}$$

$$+\left(\frac{2}{9}YS+\frac{2}{9}S^2+\frac{1}{18}\pi^2+\frac{1}{18}Y^2\right)\frac{t}{u}+\frac{1}{18}$$

$$+\left\{t\longleftrightarrow u\right\}$$

$$\text{(C.65)}$$

$$I_s \;=\; -\frac{1}{18}\left(X-Y\right)\left(Y+X\right)\frac{t^2}{s^2}$$

$$+\left(-\frac{1}{18}Y^2-\frac{2}{9}YS-\frac{2}{9}S^2+\frac{1}{9}\pi^2-\frac{1}{18}XY-\frac{2}{9}XS\right)\frac{t}{u}$$

$$+\left\{t\longleftrightarrow u\right\}$$

$$\text{(C.66)}$$

C.3.2 The u-channel process $qg\to qg$ and $g\bar{q}\to g\bar{q}$

C.3.2.1 Two-loop contribution

$$A_u \;=\; \left(-\frac{1535}{108}U+\left(-\frac{22}{3}+2Y-2X\right)\mathrm{Li}_3(x)+\left(\pi^2+X^2+\frac{22}{3}X-2XY\right)\mathrm{Li}_2(x)\right.$$

$$-\frac{44}{3}XYU+\frac{4}{3}XY\pi^2-\frac{242}{9}U^2+\frac{253}{36}\pi^2 U+2\mathrm{Li}_4(z)+\frac{30377}{432}+\frac{8}{27}Y+2\mathrm{Li}_4(y)$$

$$+\frac{35}{9}\pi^2-\frac{7}{40}\pi^4-\frac{4}{27}X+\frac{223}{36}X\pi^2-\frac{1}{3}X^2\pi^2+\frac{5}{3}X^3 Y-6Y\zeta_3-2\mathrm{Li}_3(y)X$$

$$+\frac{155}{18}\,Y\,\pi^2 - \frac{220}{9}\,X\,U + 18\,\zeta_3\,U + \frac{290}{9}\,X\,Y + \frac{44}{3}\,Y^2\,U + \frac{22}{3}\,X^2\,U + \frac{440}{9}\,Y\,U - \frac{1}{3}\,X^4$$

$$+\frac{52}{9}\,X^3 - Y^4 - \frac{82}{9}\,Y^3 - \frac{145}{9}\,X^2 - \frac{290}{9}\,Y^2 - \frac{161}{6}\,\zeta_3 - \frac{41}{3}\,X^2\,Y + \frac{41}{3}\,X\,Y^2$$

$$+4\,X\,\zeta_3 - \frac{7}{2}\,X^2\,Y^2 + \frac{5}{3}\,Y^2\,\pi^2 + 2\,X\,Y^3\bigg)\left[\frac{t^2+s^2}{u^2}\right]$$

$$+\bigg(-16\,\mathrm{Li}_4(x) + 20\,\mathrm{Li}_4(z) + \bigg(-\frac{83}{12} + 10\,Y - 2\,X\bigg)\,\mathrm{Li}_3(x)$$

$$+\bigg(-\frac{83}{6} - 10\,X + 20\,Y\bigg)\,\mathrm{Li}_3(y) + \bigg(\frac{83}{12}\,X + 4\,\pi^2 - \frac{83}{6}\,Y\bigg)\,\mathrm{Li}_2(x) - 20\,\mathrm{Li}_4(y)$$

$$+\frac{509}{48}\,\pi^2 + \frac{38}{45}\,\pi^4 + \frac{2995}{432}\,X + \frac{37}{24}\,X\,\pi^2 + \frac{4}{3}\,X^2\,\pi^2 - 3\,X^3\,Y - 10\,Y\,\zeta_3 + \frac{185}{36}\,Y\,\pi^2$$

$$+\frac{275}{18}\,X\,U - \frac{509}{24}\,X\,Y + \frac{2}{3}\,X^4 + \frac{5}{24}\,X^3 + \frac{509}{48}\,X^2 + \frac{83}{12}\,\zeta_3 + \frac{17}{6}\,X^2\,Y - \frac{39}{4}\,X\,Y^2$$

$$+4\,X\,\zeta_3 + 2\,X^2\,Y^2 + 2\,Y^2\,\pi^2 + 2\,X\,Y^3\bigg)\left[\frac{t^2-s^2}{u^2}\right]$$

$$+\bigg(\frac{2327}{216}\,U + \frac{11}{3}\,X\,Y\,U + 3\,X\,Y\,\pi^2 + \frac{121}{9}\,U^2 - \frac{121}{72}\,\pi^2\,U + \frac{1}{2}\,\mathrm{Li}_4(z) - \frac{36077}{864}$$

$$-\frac{2273}{216}\,Y + \frac{1}{2}\,\mathrm{Li}_4(y) - \frac{215}{144}\,\pi^2 - \frac{181}{720}\,\pi^4 + \frac{2273}{432}\,X - \frac{55}{36}\,X\,\pi^2 + \frac{1}{12}\,X^2\,\pi^2$$

$$+\bigg(-\frac{1}{4}\,\pi^2 - \frac{1}{4}\,X^2 - \frac{35}{12}\,X + \frac{1}{2}\,X\,Y\bigg)\,\mathrm{Li}_2(x) - \frac{1}{2}\,X^3\,Y - 6\,Y\,\zeta_3 - 10\,\mathrm{Li}_3(y)\,X$$

$$-\frac{29}{18}\,Y\,\pi^2 + \frac{121}{18}\,X\,U - 9\,\zeta_3\,U - \frac{145}{72}\,X\,Y - \frac{11}{3}\,Y^2\,U - \frac{11}{6}\,X^2\,U - \frac{121}{9}\,Y\,U$$

$$+\frac{1}{12}\,X^4 - \frac{77}{72}\,X^3 + \frac{13}{12}\,Y^4 + \frac{7}{6}\,Y^3 + \frac{145}{144}\,X^2 + \frac{145}{72}\,Y^2 + \frac{103}{6}\,\zeta_3 + \frac{7}{4}\,X^2\,Y - \frac{7}{4}\,X\,Y^2$$

$$+8\,X\,\zeta_3 - \frac{13}{8}\,X^2\,Y^2 + \frac{7}{12}\,Y^2\,\pi^2 - \frac{13}{6}\,X\,Y^3 + \bigg(-10\,Y + \frac{35}{12}\bigg)\,\mathrm{Li}_3(x)\bigg)\left[\frac{t^2+s^2}{st}\right]$$

$$+\bigg(\bigg(10\,X - \frac{35}{6} - 20\,Y\bigg)\,\mathrm{Li}_3(y) + \bigg(-\frac{35}{12} - 10\,Y\bigg)\,\mathrm{Li}_3(x) - \frac{11}{3}\,X\,Y\,U + \frac{1}{3}\,X\,Y\,\pi^2$$

$$+20\,\mathrm{Li}_4(x) - \frac{41}{2}\,\mathrm{Li}_4(z) + \bigg(-\frac{35}{6}\,Y + \frac{35}{12}\,X - \frac{15}{4}\,\pi^2 - \frac{1}{2}\,X\,Y + \frac{1}{2}\,Y^2 + \frac{1}{4}\,X^2\bigg)\,\mathrm{Li}_2(x)$$

$$+\frac{41}{2}\,\mathrm{Li}_4(y) + \frac{11}{6}\,\pi^2\,U - \frac{865}{144}\,\pi^2 - \frac{35}{36}\,\pi^4 - \frac{2273}{432}\,X + \frac{55}{36}\,X\,\pi^2 - \frac{7}{4}\,X^2\,\pi^2 + \frac{23}{6}\,X^3\,Y$$

$$+10\,Y\,\zeta_3 - \frac{7}{9}\,Y\,\pi^2 - \frac{121}{18}\,X\,U + \frac{865}{72}\,X\,Y + \frac{11}{6}\,X^2\,U - \frac{11}{12}\,X^4 + \frac{77}{72}\,X^3 - \frac{865}{144}\,X^2$$

$$+\frac{35}{12}\,\zeta_3 - \frac{7}{4}\,X^2\,Y - \frac{7}{6}\,X\,Y^2 - 8\,X\,\zeta_3 - \frac{27}{8}\,X^2\,Y^2 - \frac{10}{3}\,Y^2\,\pi^2 - X\,Y^3\bigg)\left[\frac{t^2-s^2}{st}\right]$$

$$+\bigg(-\frac{11}{3}\,U - \frac{8}{3}\,X\,Y\,\pi^2 + \frac{457}{72} + \frac{2417}{72}\,Y - \frac{19}{144}\,\pi^2 + \frac{11}{45}\,\pi^4 - \frac{2417}{144}\,X - \frac{35}{24}\,X\,\pi^2$$

$$+8\,Y\,\zeta_3 + 8\,\mathrm{Li}_3(y)\,X - \frac{33}{4}\,\mathrm{Li}_2(x)\,X - \frac{10}{3}\,Y\,\pi^2 + \frac{55}{6}\,X\,U - \frac{141}{8}\,X\,Y - \frac{55}{3}\,Y\,U$$

$$-\frac{17}{24}\,X^3 - \frac{2}{3}\,Y^4 - \frac{4}{3}\,Y^3 + \frac{141}{16}\,X^2 + \frac{141}{8}\,Y^2 + \frac{3}{4}\,\zeta_3 - 2\,X^2\,Y + 2\,X\,Y^2 - 8\,X\,\zeta_3$$

$$+2\,X^2\,Y^2 - \frac{2}{3}\,Y^2\,\pi^2 + \frac{4}{3}\,X\,Y^3 + \bigg(8\,Y + \frac{33}{4}\bigg)\,\mathrm{Li}_3(x)\bigg) \tag{C.67}$$

$$
\begin{aligned}
B_u &= \Bigg(\Bigg(\Big(-18\,X + 18\,Y\Big)\,\mathrm{Li}_3(x) + \frac{1502}{27}\,U + \Big(9\,X^2 + 9\,\pi^2 - 18\,X\,Y\Big)\,\mathrm{Li}_2(x) \\
&\quad + 4\,X\,Y\,\pi^2 - \frac{1}{12}\,\pi^2\,U + 18\,\mathrm{Li}_4(z) - \frac{19139}{324} - \frac{80}{3}\,Y + 18\,\mathrm{Li}_4(y) + \frac{311}{36}\,\pi^2 \\
&\quad - \frac{883}{360}\,\pi^4 + \frac{40}{3}\,X + \frac{20}{3}\,X\,\pi^2 + \frac{11}{3}\,X^2\,\pi^2 + X^3\,Y - 18\,Y\,\zeta_3 - 18\,\mathrm{Li}_3(y)\,X \\
&\quad + \frac{40}{3}\,Y\,\pi^2 - 2\,\zeta_3\,U + 8\,X\,Y + \frac{1}{2}\,X^4 + \frac{20}{3}\,X^3 - \frac{535}{36}\,X^2 - 8\,Y^2 + \frac{443}{18}\,\zeta_3 \\
&\quad - \frac{40}{3}\,X^2\,Y + 18\,X\,\zeta_3 - \frac{17}{2}\,X^2\,Y^2 + 4\,Y^2\,\pi^2\Bigg)\left[\frac{t^2+s^2}{u^2}\right] \\
&\quad + \Bigg(\Big(\frac{71}{3}\,Y - \frac{71}{6}\,X - \frac{5}{4}\,\pi^2 - \frac{7}{2}\,X\,Y + \frac{7}{2}\,Y^2 - \frac{9}{4}\,X^2\Big)\,\mathrm{Li}_2(x) - \frac{11}{3}\,X\,Y\,U \\
&\quad + \Big(9\,X + \frac{71}{3} - 18\,Y\Big)\,\mathrm{Li}_3(y) + \Big(\frac{71}{6} - 9\,Y + 2\,X\Big)\,\mathrm{Li}_3(x) - \frac{5}{2}\,X\,Y\,\pi^2 + 22\,\mathrm{Li}_4(x) \\
&\quad + \frac{11}{6}\,\pi^2\,U - \frac{43}{2}\,\mathrm{Li}_4(z) + \frac{43}{2}\,\mathrm{Li}_4(y) - \frac{92}{9}\,\pi^2 - \frac{119}{180}\,\pi^4 - \frac{121}{36}\,X - \frac{137}{18}\,X\,\pi^2 \\
&\quad - \frac{11}{4}\,X^2\,\pi^2 + \frac{29}{6}\,X^3\,Y + 9\,Y\,\zeta_3 - \frac{211}{9}\,Y\,\pi^2 + \frac{11}{6}\,X\,U + \frac{184}{9}\,X\,Y + \frac{11}{6}\,X^2\,U \\
&\quad - \frac{43}{24}\,X^4 + \frac{221}{18}\,X^3 - \frac{92}{9}\,X^2 - \frac{71}{6}\,\zeta_3 - \frac{39}{2}\,X^2\,Y + \frac{94}{3}\,X\,Y^2 - X\,\zeta_3 - \frac{41}{8}\,X^2\,Y^2 \\
&\quad - \frac{29}{6}\,Y^2\,\pi^2 + X\,Y^3\Bigg)\left[\frac{t^2-s^2}{u^2}\right] \\
&\quad + \Bigg(-\frac{7543}{216}\,U + \Big(\frac{21}{4}\,\pi^2 + \frac{21}{4}\,X^2 - \frac{7}{4}\,X - \frac{21}{2}\,X\,Y\Big)\,\mathrm{Li}_2(x) + \Big(\frac{7}{4} - 23\,X\Big)\,\mathrm{Li}_3(x) \\
&\quad + \frac{22}{3}\,X\,Y\,U + \frac{19}{2}\,X\,Y\,\pi^2 - \frac{121}{9}\,U^2 - \frac{34}{9}\,\pi^2\,U + \frac{71}{2}\,\mathrm{Li}_4(z) + \frac{164771}{2592} + \frac{5941}{216}\,Y \\
&\quad + \frac{71}{2}\,\mathrm{Li}_4(y) + \frac{1267}{144}\,\pi^2 - \frac{4}{3}\,\pi^4 - \frac{5941}{432}\,X - \frac{91}{72}\,X\,\pi^2 + \frac{5}{12}\,X^2\,\pi^2 - \frac{19}{3}\,X^3\,Y - 38\,Y\,\zeta_3 \\
&\quad - 46\,\mathrm{Li}_3(y)\,X - \frac{347}{36}\,Y\,\pi^2 - \frac{121}{9}\,X\,U + 10\,\zeta_3\,U - \frac{1313}{72}\,X\,Y - \frac{22}{3}\,Y^2\,U + \frac{11}{3}\,X^2\,U \\
&\quad + \frac{242}{9}\,Y\,U + \frac{43}{24}\,X^4 - \frac{179}{72}\,X^3 + \frac{23}{12}\,Y^4 - \frac{59}{18}\,Y^3 + \frac{395}{48}\,X^2 + \frac{1313}{72}\,Y^2 - \frac{1529}{36}\,\zeta_3 \\
&\quad + \frac{11}{4}\,X^2\,Y + \frac{59}{12}\,X\,Y^2 + 42\,X\,\zeta_3 - \frac{47}{8}\,X^2\,Y^2 - \frac{3}{4}\,Y^2\,\pi^2 - \frac{23}{6}\,X\,Y^3\Bigg)\left[\frac{t^2+s^2}{st}\right] \\
&\quad + \Bigg(\frac{22}{3}\,X\,Y\,U + \Big(26\,X - \frac{121}{6} - 52\,Y\Big)\,\mathrm{Li}_3(y) + \Big(-\frac{121}{12} - 26\,Y - 21\,X\Big)\,\mathrm{Li}_3(x) \\
&\quad + \frac{29}{6}\,X\,Y\,\pi^2 + \Big(-\frac{121}{6}\,Y + \frac{121}{12}\,X - \frac{95}{12}\,\pi^2 + \frac{17}{2}\,X\,Y - \frac{17}{2}\,Y^2 + \frac{23}{4}\,X^2\Big)\,\mathrm{Li}_2(x) \\
&\quad + 74\,\mathrm{Li}_4(x) - \frac{11}{3}\,\pi^2\,U - \frac{87}{2}\,\mathrm{Li}_4(z) + \frac{87}{2}\,\mathrm{Li}_4(y) + \frac{1435}{144}\,\pi^2 - \frac{319}{90}\,\pi^4 + \frac{207}{16}\,X + \frac{43}{24}\,X\,\pi^2 \\
&\quad - \frac{17}{4}\,X^2\,\pi^2 + 7\,X^3\,Y + 26\,Y\,\zeta_3 + \frac{305}{18}\,Y\,\pi^2 - 11\,X\,U - \frac{1435}{72}\,X\,Y - \frac{11}{3}\,X^2\,U - \frac{9}{8}\,X^4 \\
&\quad - \frac{433}{72}\,X^3 + \frac{1435}{144}\,X^2 + \frac{121}{12}\,\zeta_3 + \frac{163}{12}\,X^2\,Y - \frac{71}{3}\,X\,Y^2 - 34\,X\,\zeta_3 - \frac{21}{8}\,X^2\,Y^2 - \frac{10}{3}\,Y^2\,\pi \\
&\quad - \frac{25}{3}\,X\,Y^3\Bigg)\left[\frac{t^2-s^2}{st}\right]
\end{aligned}
$$

$$+\left(-\frac{11}{3}U+\left(-\frac{7}{4}\pi^2+\frac{7}{2}XY-\frac{7}{4}X^2-\frac{299}{6}X\right)\mathrm{Li}_2(x)+\frac{11}{3}XYU+\frac{139}{18}\right.$$

$$+\frac{37}{6}XY\pi^2+\left(\frac{299}{6}-27Y+18X\right)\mathrm{Li}_3(x)-\frac{11}{6}\pi^2U-\frac{65}{2}\mathrm{Li}_4(z)-\frac{28}{9}Y$$

$$-\frac{65}{2}\mathrm{Li}_4(y)+23\pi^2+\frac{119}{180}\pi^4+\frac{14}{9}X-\frac{11}{6}X\pi^2-\frac{5}{4}X^2\pi^2+\frac{37}{6}X^3Y$$

$$-11Y\zeta_3+9\mathrm{Li}_3(y)X-\frac{29}{6}Y\pi^2-\frac{55}{6}XU-\frac{155}{9}XY-\frac{11}{3}Y^2U-\frac{11}{6}X^2U$$

$$+\frac{55}{3}YU-\frac{41}{24}X^4+\frac{73}{18}X^3+\frac{23}{12}Y^4-\frac{146}{9}Y^3-\frac{347}{36}X^2+\frac{155}{9}Y^2+\frac{173}{6}\zeta_3$$

$$\left.-\frac{197}{6}X^2Y+\frac{73}{3}XY^2+X\zeta_3-\frac{27}{8}X^2Y^2+\frac{1}{4}Y^2\pi^2-\frac{23}{6}XY^3\right)-Y^2\frac{s^2}{t^2}$$

$$+\left(-\pi^2-Y^2+2XY-X^2\right)\frac{t^2}{s^2} \tag{C.6?}$$

$$C_u = \left(\pi^2U+\frac{11}{4}X^2-\frac{3}{4}U+15\zeta_3-12\zeta_3U-\frac{255}{16}-\frac{29}{12}\pi^2+\frac{11}{90}\pi^4\right)\left[\frac{t^2+s^2}{u^2}\right]$$

$$+\left(\frac{1}{6}XY\pi^2+6\mathrm{Li}_4(x)-\frac{11}{2}\mathrm{Li}_4(z)+\left(\frac{11}{4}-3Y\right)\mathrm{Li}_3(x)+\frac{11}{2}\mathrm{Li}_4(y)-\frac{23}{16}\pi^2\right.$$

$$-\frac{47}{180}\pi^4-\frac{21}{16}X+\left(\frac{11}{2}+3X-6Y\right)\mathrm{Li}_3(y)+\frac{17}{24}X\pi^2-\frac{5}{12}X^2\pi^2+\frac{1}{2}X^3Y$$

$$+3Y\zeta_3-\frac{29}{12}Y\pi^2+\frac{23}{8}XY-\frac{1}{8}X^4-\frac{13}{24}X^3-\frac{23}{16}X^2-\frac{11}{4}\zeta_3-\frac{3}{2}X^2Y$$

$$+\frac{17}{4}XY^2-3X\zeta_3-\frac{1}{8}X^2Y^2-\frac{1}{6}Y^2\pi^2-XY^3+\left(-\frac{7}{12}\pi^2-\frac{11}{4}X-\frac{1}{4}X^2\right.$$

$$\left.\left.+\frac{11}{2}Y-\frac{1}{2}Y^2+\frac{1}{2}XY\right)\mathrm{Li}_2(x)\right)\left[\frac{t^2-s^2}{u^2}\right]$$

$$+\left(\frac{5297}{216}U+\left(\frac{9}{4}\pi^2-\frac{9}{2}XY+\frac{9}{4}X^2-\frac{21}{4}X\right)\mathrm{Li}_2(x)+\left(\frac{21}{4}+19Y-7X\right)\mathrm{Li}_3(x)\right.$$

$$+11XYU-\frac{13}{3}XY\pi^2-\frac{145}{24}\pi^2U+\frac{19}{2}\mathrm{Li}_4(z)-\frac{41393}{2592}-\frac{743}{24}Y+\frac{19}{2}\mathrm{Li}_4(y)$$

$$+\frac{1487}{144}\pi^2-\frac{113}{240}\pi^4+\frac{743}{48}X-\frac{27}{8}X\pi^2+\frac{3}{4}X^2\pi^2-\frac{4}{3}X^3Y-Y\zeta_3+5\mathrm{Li}_3(y)X$$

$$+\frac{5}{2}Y\pi^2-\frac{11}{2}XU+5\zeta_3U-\frac{97}{24}XY-11Y^2U-\frac{11}{2}X^2U+11YU+\frac{7}{12}X^4$$

$$-\frac{17}{8}X^3-\frac{5}{12}Y^4+12Y^3+\frac{49}{48}X^2+\frac{97}{24}Y^2-\frac{4}{9}\zeta_3+\frac{17}{2}X^2Y-18XY^2-2X\zeta_3$$

$$\left.+\frac{21}{8}X^2Y^2+\frac{5}{12}Y^2\pi^2+\frac{5}{6}XY^3\right)\left[\frac{t^2+s^2}{st}\right]$$

$$+\left(\left(-\frac{9}{2}Y+\frac{9}{4}X+\frac{5}{12}\pi^2+\frac{1}{2}XY-\frac{1}{2}Y^2+\frac{7}{4}X^2\right)\mathrm{Li}_2(x)+\frac{11}{3}XYU-\frac{1}{3}XY\pi^2\right.$$

$$+\left(-\frac{9}{4}+5Y-3X\right)\mathrm{Li}_3(x)+\left(-5X-\frac{9}{2}+10Y\right)\mathrm{Li}_3(y)-8\mathrm{Li}_4(x)-\frac{11}{6}\pi^2U$$

$$+\frac{21}{2}\mathrm{Li}_4(z)-\frac{21}{2}\mathrm{Li}_4(y)+\frac{997}{144}\pi^2+\frac{14}{45}\pi^4+\frac{67}{16}X+\frac{19}{72}X\pi^2+\frac{3}{4}X^2\pi^2-\frac{2}{3}X^3Y$$

$$-5\,Y\,\zeta_3 + \frac{77}{12}\,Y\,\pi^2 + \frac{11}{2}\,X\,U - \frac{997}{72}\,X\,Y - \frac{11}{6}\,X^2\,U + \frac{1}{4}\,X^4 - \frac{107}{72}\,X^3 + \frac{997}{144}\,X^2$$

$$+\frac{9}{4}\,\zeta_3 + \frac{17}{3}\,X^2\,Y - \frac{95}{12}\,X\,Y^2 + 6\,X\,\zeta_3 + \frac{7}{8}\,X^2\,Y^2 + \frac{5}{6}\,Y^2\,\pi^2 + X\,Y^3\bigg)\left[\frac{t^2 - s^2}{st}\right]$$

$$+\left(\left(\frac{13}{4} + 41\,Y - 26\,X\right)\mathrm{Li}_3(x) + \left(\frac{21}{4}\,\pi^2 - \frac{21}{2}\,X\,Y + \frac{21}{4}\,X^2 - \frac{13}{4}\,X\right)\mathrm{Li}_2(x)\right.$$

$$+\frac{44}{3}\,X\,Y\,U - \frac{13}{2}\,X\,Y\,\pi^2 - \frac{22}{3}\,\pi^2\,U + \frac{83}{2}\,\mathrm{Li}_4(z) + \frac{23}{8} - \frac{3133}{72}\,Y + \frac{83}{2}\,\mathrm{Li}_4(y)$$

$$+\frac{449}{48}\,\pi^2 - \frac{203}{180}\,\pi^4 + \frac{3133}{144}\,X - \frac{299}{72}\,X\,\pi^2 + \frac{25}{12}\,X^2\,\pi^2 - \frac{47}{6}\,X^3\,Y + 9\,Y\,\zeta_3$$

$$-11\,\mathrm{Li}_3(y)\,X + \frac{41}{9}\,Y\,\pi^2 - \frac{22}{3}\,X\,U - \frac{403}{72}\,X\,Y - \frac{44}{3}\,Y^2\,U - \frac{22}{3}\,X^2\,U + \frac{44}{3}\,Y\,U$$

$$+\frac{55}{24}\,X^4 - \frac{209}{72}\,X^3 - \frac{3}{4}\,Y^4 + \frac{161}{9}\,Y^3 + \frac{1063}{144}\,X^2 + \frac{403}{72}\,Y^2 - \frac{1}{4}\,\zeta_3 + \frac{41}{3}\,X^2\,Y$$

$$-\frac{161}{6}\,X\,Y^2 + X\,\zeta_3 + \frac{41}{8}\,X^2\,Y^2 - \frac{13}{12}\,Y^2\,\pi^2 + \frac{3}{2}\,X\,Y^3\bigg) + Y^2\,\frac{s^2}{t^2}$$

$$+\left(X^2 - 2\,X\,Y + \pi^2 + Y^2\right)\frac{t^2}{s^2} \tag{C.69}$$

$$D_u \;=\; \frac{3}{2}\,X^2\left[\frac{t^2 + s^2}{u^2}\right] - 3\,X\left[\frac{t^2 - s^2}{u^2}\right]$$

$$+\left(-\frac{3}{8}\,U - \frac{5}{6}\,X\,Y\,\pi^2 + \frac{1}{2}\,\pi^2\,U - \frac{11}{2}\,\mathrm{Li}_4(z) + \left(2\,X + 7\,Y - \frac{13}{4}\right)\mathrm{Li}_3(x) - \frac{187}{32}\right.$$

$$+\left(\frac{3}{4}\,\pi^2 - \frac{3}{2}\,X\,Y + \frac{13}{4}\,X + \frac{3}{4}\,X^2\right)\mathrm{Li}_2(x) - \frac{47}{8}\,Y - \frac{11}{2}\,\mathrm{Li}_4(y) + \frac{13}{16}\,\pi^2 + \frac{7}{18}\,\pi^4$$

$$+\frac{47}{16}\,X + \frac{1}{24}\,X\,\pi^2 - \frac{5}{12}\,X^2\,\pi^2 + \frac{5}{2}\,X^3\,Y + 7\,Y\,\zeta_3 + 11\,\mathrm{Li}_3(y)\,X + \frac{7}{6}\,Y\,\pi^2 - 6\,\zeta_3\,U$$

$$-\frac{3}{8}\,X\,Y - \frac{5}{8}\,X^4 - \frac{3}{8}\,X^3 - \frac{7}{12}\,Y^4 + \frac{10}{3}\,Y^3 + \frac{3}{16}\,X^2 + \frac{3}{8}\,Y^2 + \frac{23}{4}\,\zeta_3 + \frac{7}{2}\,X^2\,Y$$

$$-5\,X\,Y^2 - 9\,X\,\zeta_3 - \frac{1}{8}\,X^2\,Y^2 + \frac{5}{12}\,Y^2\,\pi^2 + \frac{7}{6}\,X\,Y^3\bigg)\left[\frac{t^2 + s^2}{st}\right]$$

$$+\left(\left(-\frac{3}{4}\,\pi^2 + \frac{19}{4}\,X + \frac{1}{4}\,X^2 - \frac{19}{2}\,Y + \frac{1}{2}\,Y^2 - \frac{1}{2}\,X\,Y\right)\mathrm{Li}_2(x)\right.$$

$$+\left(-\frac{19}{4} + 3\,Y + 4\,X\right)\mathrm{Li}_3(x) - \frac{3}{2}\,X\,Y\,\pi^2 + \left(-\frac{19}{2} - 3\,X + 6\,Y\right)\mathrm{Li}_3(y)$$

$$-14\,\mathrm{Li}_4(x) + \frac{11}{2}\,\mathrm{Li}_4(z) - \frac{11}{2}\,\mathrm{Li}_4(y) - \frac{7}{16}\,\pi^2 + \frac{103}{180}\,\pi^4 - \frac{31}{16}\,X + \frac{7}{24}\,X\,\pi^2 + \frac{3}{4}\,X^2\,\pi^2$$

$$+\frac{1}{6}\,X^3\,Y - 3\,Y\,\zeta_3 + \frac{43}{12}\,Y\,\pi^2 + \frac{7}{8}\,X\,Y - \frac{1}{24}\,X^4 + \frac{3}{8}\,X^3 - \frac{7}{16}\,X^2 + \frac{19}{4}\,\zeta_3 + 2\,X^2\,Y$$

$$-\frac{27}{4}\,X\,Y^2 + 7\,X\,\zeta_3 + \frac{1}{8}\,X^2\,Y^2 + \frac{1}{6}\,Y^2\,\pi^2 + X\,Y^3\bigg)\left[\frac{t^2 - s^2}{st}\right]$$

$$+\left(\left(-19 + 12\,Y + 4\,X\right)\mathrm{Li}_3(x) + \left(19\,X + X^2 + \pi^2 - 2\,X\,Y\right)\mathrm{Li}_2(x) + \frac{1}{2}\right.$$

$$-2\,X\,Y\,\pi^2 - 10\,\mathrm{Li}_4(z) - \frac{29}{2}\,Y - 10\,\mathrm{Li}_4(y) + \frac{19}{6}\,\pi^2 + \frac{3}{5}\,\pi^4 + \frac{29}{4}\,X - \frac{1}{6}\,X\,\pi^2$$

$$-\frac{2}{3}X^2\pi^2 + 4X^3Y + 12Y\zeta_3 + 20\operatorname{Li}_3(y)X + \frac{7}{3}Y\pi^2 + XY - X^4 - \frac{11}{6}X^3$$

$$-Y^4 + 6Y^3 + 3X^2 - Y^2 + 15\zeta_3 + 13X^2Y - 9XY^2 - 16X\zeta_3 + \frac{1}{2}X^2Y^2$$

$$+\frac{1}{3}Y^2\pi^2 + 2XY^3\Big) - Y^2\frac{s^2}{t^2} + \Big(-\pi^2 - Y^2 + 2XY - X^2\Big)\frac{t^2}{s^2} \qquad\text{(C.70)}$$

$$
\begin{aligned}
E_u = \ & \Bigg(-\frac{23}{18}\pi^2 U - \frac{10}{9}Y\pi^2 + \frac{71}{9}Y^2 + \frac{71}{18}X^2 + \frac{10}{9}Y^3 - \frac{17}{18}X\pi^2 - \frac{7}{9}X^3 - \frac{71}{9}XY \\
& -\frac{221}{27}U - \frac{28}{9}X + \frac{13}{3}\zeta_3 + \frac{4}{3}\operatorname{Li}_3(x) + \frac{56}{9}Y - \frac{4}{3}\operatorname{Li}_2(x)X + \frac{5}{3}X^2Y - \frac{5}{3}XY^2 \\
& +\frac{62}{9}XU - \frac{124}{9}YU - \frac{8}{3}Y^2U - \frac{4}{3}X^2U - \frac{863}{108} + \frac{8}{3}XYU + \frac{88}{9}U^2 - \frac{67}{54}\pi^2\Bigg)\left[\frac{t^2 + s^2}{u^2}\right] \\
& +\Bigg(\Big(\frac{8}{3} - 2Y\Big)\operatorname{Li}_3(x) + \Big(-\frac{2}{3}\pi^2 - \frac{8}{3}X + \frac{16}{3}Y\Big)\operatorname{Li}_2(x) + \Big(2X - 4Y + \frac{16}{3}\Big)\operatorname{Li}_3(y) \\
& +4\operatorname{Li}_4(x) - 4\operatorname{Li}_4(z) + 4\operatorname{Li}_4(y) - \frac{23}{6}\pi^2 - \frac{11}{60}\pi^4 + \frac{37}{18}X - \frac{1}{2}X\pi^2 - \frac{1}{3}X^2\pi^2 \\
& +\frac{2}{3}X^3Y + 2Y\zeta_3 - \frac{20}{9}Y\pi^2 - \frac{47}{9}XU + \frac{23}{3}XY - \frac{1}{6}X^4 - \frac{23}{6}X^2 - \frac{8}{3}\zeta_3 \\
& -\frac{4}{3}X^2Y + 4XY^2 - 2X\zeta_3 - \frac{1}{2}X^2Y^2 - \frac{1}{2}Y^2\pi^2 - \frac{1}{3}XY^3\Bigg)\left[\frac{t^2 - s^2}{u^2}\right] \\
& +\Bigg(\frac{185}{54}U + \Big(4Y - \frac{2}{3}\Big)\operatorname{Li}_3(x) - \frac{2}{3}XYU - \frac{4}{3}XY\pi^2 - \frac{44}{9}U^2 + \frac{11}{36}\pi^2 U + \frac{1307}{216} \\
& -\frac{10}{9}Y + \frac{133}{108}\pi^2 + \frac{11}{90}\pi^4 + \frac{5}{9}X + \frac{5}{18}X\pi^2 + 4Y\zeta_3 + 4\operatorname{Li}_3(y)X + \frac{2}{3}\operatorname{Li}_2(x)X + \frac{13}{36}Y \\
& -\frac{22}{9}XU + \frac{7}{18}XY + \frac{2}{3}Y^2U + \frac{1}{3}X^2U + \frac{44}{9}YU + \frac{7}{36}X^3 - \frac{1}{3}Y^4 - \frac{1}{6}Y^3 - \frac{7}{36}X^2 \\
& -\frac{7}{18}Y^2 - \frac{13}{6}\zeta_3 - \frac{1}{4}X^2Y + \frac{1}{4}XY^2 - 4X\zeta_3 + X^2Y^2 - \frac{1}{3}Y^2\pi^2 + \frac{2}{3}XY^3\Bigg)\left[\frac{t^2 + s^2}{st}\right] \\
& +\Bigg(\Big(\frac{4}{3} + 8Y - 4X\Big)\operatorname{Li}_3(y) + \Big(\frac{2}{3} + 4Y\Big)\operatorname{Li}_3(x) + \Big(\frac{4}{3}\pi^2 - \frac{2}{3}X + \frac{4}{3}Y\Big)\operatorname{Li}_2(x) \\
& +\frac{2}{3}XYU - 8\operatorname{Li}_4(x) - \frac{1}{3}\pi^2 U + 8\operatorname{Li}_4(z) - 8\operatorname{Li}_4(y) + \frac{79}{36}\pi^2 + \frac{11}{30}\pi^4 - \frac{5}{9}X - \frac{5}{18}X\pi^2 \\
& +\frac{2}{3}X^2\pi^2 - \frac{4}{3}X^3Y - 4Y\zeta_3 + \frac{1}{36}Y\pi^2 + \frac{22}{9}XU - \frac{79}{18}XY - \frac{1}{3}X^2U + \frac{1}{3}X^4 - \frac{7}{36}X \\
& +\frac{79}{36}X^2 - \frac{2}{3}\zeta_3 + \frac{1}{4}X^2Y + \frac{5}{12}XY^2 + 4X\zeta_3 + X^2Y^2 + Y^2\pi^2 + \frac{2}{3}XY^3\Bigg)\left[\frac{t^2 - s^2}{st}\right] \\
& +\Bigg(\frac{2}{3}U - \frac{37}{18} + \Big(-2Y - 4\Big)\operatorname{Li}_3(x) + \frac{2}{3}XY\pi^2 - \frac{91}{9}Y - \frac{25}{18}\pi^2 - \frac{11}{180}\pi^4 + \frac{91}{18}X \\
& +\frac{2}{3}X\pi^2 - 2Y\zeta_3 - 2\operatorname{Li}_3(y)X + 4\operatorname{Li}_2(x)X + \frac{2}{3}Y\pi^2 - \frac{5}{3}XU + 4XY + \frac{10}{3}YU \\
& +\frac{1}{6}Y^4 + \frac{4}{3}Y^3 - 2X^2 - 4Y^2 - 4\zeta_3 + 2X^2Y - 2XY^2 + 2X\zeta_3 - \frac{1}{2}X^2Y^2 \\
& +\frac{1}{6}Y^2\pi^2 - \frac{1}{3}XY^3\Bigg) \qquad\qquad\qquad\qquad\qquad\qquad\qquad\qquad\qquad\text{(C.7}
\end{aligned}
$$

$$
\begin{aligned}
F_u \;=\; & \left(-\frac{1}{6}\,\pi^2 U - \frac{4}{3}\,Y\,\pi^2 + \frac{29}{9}\,X^2 - \frac{2}{3}\,X\,\pi^2 - \frac{2}{3}\,X^3 - \frac{263}{27}\,U - \frac{4}{3}\,X - \frac{1}{9}\,\zeta_3 + \frac{8}{3}\,Y \right. \\
& \left. + \frac{4}{3}\,X^2 Y + \frac{4085}{324} - \frac{11}{6}\,\pi^2 \right)\left[\frac{t^2 + s^2}{u^2}\right] \\
& + \left(\frac{4}{3}\,\mathrm{Li}_3(x) + \frac{8}{3}\,\mathrm{Li}_3(y) + \left(-\frac{4}{3}\,X + \frac{8}{3}\,Y \right)\mathrm{Li}_2(x) - \frac{1}{3}\,\pi^2 U + \frac{65}{36}\,Y\,\pi^2 + \frac{5}{2}\,X^2 \right. \\
& + \frac{5}{12}\,X\,\pi^2 - \frac{49}{36}\,X^3 - 5\,X Y + \frac{19}{9}\,X + \frac{9}{4}\,X^2 Y - \frac{4}{3}\,\zeta_3 + \frac{5}{2}\,\pi^2 - \frac{1}{3}\,X^2 U + \frac{2}{3}\,X Y U \\
& \left. - \frac{11}{12}\,X Y^2 - \frac{1}{3}\,X U \right)\left[\frac{t^2 - s^2}{u^2}\right] \\
& + \left(\frac{7}{9}\,U - \frac{4}{3}\,X Y U + \frac{8}{3}\,X Y\,\pi^2 + \frac{44}{9}\,U^2 + \frac{7}{9}\,\pi^2 U + \left(-8\,Y - \frac{8}{3} \right)\mathrm{Li}_3(x) - \frac{3661}{324} \right. \\
& + \frac{115}{18}\,Y - \frac{43}{108}\,\pi^2 - \frac{11}{45}\,\pi^4 - \frac{115}{36}\,X - 8\,Y\,\zeta_3 - 8\,\mathrm{Li}_3(y)\,X + \frac{8}{3}\,\mathrm{Li}_2(x)\,X - \frac{1}{12}\,Y\,\pi^2 \\
& + \frac{44}{9}\,X U - \frac{55}{18}\,X Y + \frac{4}{3}\,Y^2 U - \frac{2}{3}\,X^2 U - \frac{88}{9}\,Y U - \frac{1}{18}\,X^3 + \frac{2}{3}\,Y^4 - \frac{3}{2}\,Y^3 + \frac{16}{9}\,X^2 \\
& \left. + \frac{55}{18}\,Y^2 + \frac{14}{9}\,\zeta_3 + \frac{1}{4}\,X^2 Y + \frac{9}{4}\,X Y^2 + 8\,X\,\zeta_3 - 2\,X^2 Y^2 + \frac{2}{3}\,Y^2\,\pi^2 - \frac{4}{3}\,X Y^3 \right)\left[\frac{t^2 + s^2}{st}\right] \\
& + \left(\left(-\frac{4}{3} - 8\,Y \right)\mathrm{Li}_3(x) - \frac{4}{3}\,X Y U + \left(-\frac{8}{3} - 16\,Y + 8\,X \right)\mathrm{Li}_3(y) + 16\,\mathrm{Li}_4(x) \right. \\
& + \frac{2}{3}\,\pi^2 U - 16\,\mathrm{Li}_4(z) + 16\,\mathrm{Li}_4(y) - \frac{1}{6}\,\pi^2 - \frac{11}{15}\,\pi^4 - \frac{23}{4}\,X + \left(-\frac{8}{3}\,\pi^2 + \frac{4}{3}\,X - \frac{8}{3}\,Y \right)\mathrm{Li}_2(\\
& - \frac{1}{18}\,X\,\pi^2 - \frac{4}{3}\,X^2\,\pi^2 + \frac{8}{3}\,X^3 Y + 8\,Y\,\zeta_3 - \frac{41}{36}\,Y\,\pi^2 + 2\,X U + \frac{1}{3}\,X Y + \frac{2}{3}\,X^2 U - \frac{2}{3}\,X^4 \\
& + \frac{13}{18}\,X^3 - \frac{1}{6}\,X^2 + \frac{4}{3}\,\zeta_3 - \frac{19}{12}\,X^2 Y + \frac{1}{4}\,X Y^2 - 8\,X\,\zeta_3 - 2\,X^2 Y^2 - 2\,Y^2\,\pi^2 \\
& \left. - \frac{4}{3}\,X Y^3 \right)\left[\frac{t^2 - s^2}{st}\right] \\
& + \left(\frac{2}{3}\,U - \frac{19}{18} - \frac{2}{3}\,X Y U + \frac{8}{3}\,X Y\,\pi^2 + \frac{1}{3}\,\pi^2 U + \left(-8\,Y + \frac{52}{3} \right)\mathrm{Li}_3(x) + \frac{100}{9}\,Y \right. \\
& + \frac{14}{9}\,\pi^2 - \frac{11}{45}\,\pi^4 - \frac{50}{9}\,X - \frac{115}{36}\,X\,\pi^2 - 8\,Y\,\zeta_3 - 8\,\mathrm{Li}_3(y)\,X - \frac{52}{3}\,\mathrm{Li}_2(x)\,X - \frac{85}{36}\,Y\,\pi^2 \\
& + \frac{5}{3}\,X U + \frac{11}{9}\,X Y + \frac{2}{3}\,Y^2 U + \frac{1}{3}\,X^2 U - \frac{10}{3}\,Y U - \frac{11}{36}\,X^3 + \frac{2}{3}\,Y^4 - \frac{7}{2}\,Y^3 - \frac{5}{18}\,X^2 \\
& \left. - \frac{11}{9}\,Y^2 + \frac{52}{3}\,\zeta_3 - \frac{83}{12}\,X^2 Y + \frac{21}{4}\,X Y^2 + 8\,X\,\zeta_3 - 2\,X^2 Y^2 + \frac{2}{3}\,Y^2\,\pi^2 - \frac{4}{3}\,X Y^3 \right) \\
& - 3\,Y^2\,\frac{s^2}{t^2} + \left(-3\,X^2 - 3\,Y^2 - 3\,\pi^2 + 6\,X Y \right)\frac{t^2}{s^2}
\end{aligned} \tag{C.7}
$$

$$
\begin{aligned}
G_u \;=\; & \left(-4\,\mathrm{Li}_3(x) - 8\,\mathrm{Li}_3(y) + \left(-8\,Y + 4\,X \right)\mathrm{Li}_2(x) - 8\,X - 4\,X Y^2 + \frac{4}{3}\,Y\,\pi^2 + \right. \\
& \left. \frac{2}{3}\,X\,\pi^2 + 4\,\zeta_3 \right)\left[\frac{t^2 - s^2}{u^2}\right]
\end{aligned}
$$

$$+ \left(- \frac{227}{54} U - 2\, X\, Y\, U - 8\, X\, Y\, \pi^2 + \left(24\, Y + 4 \right) \operatorname{Li}_3(x) + \frac{11}{12}\, \pi^2\, U + \frac{3401}{648} \right.$$

$$- \frac{79}{6}\, Y - \frac{173}{36}\, \pi^2 + \frac{11}{15}\, \pi^4 + \frac{79}{12}\, X - \frac{1}{12}\, X\, \pi^2 + 24\, Y\, \zeta_3 + 24 \operatorname{Li}_3(y)\, X - 4 \operatorname{Li}_2(x)\, X$$

$$+ \frac{5}{3}\, Y\, \pi^2 + X\, U + \frac{43}{6}\, X\, Y + 2\, Y^2\, U + X^2\, U - 2\, Y\, U + \frac{7}{12}\, X^3 - 2\, Y^4 + Y^3 - \frac{23}{6}\, X^2$$

$$\left. - \frac{43}{6}\, Y^2 + \frac{71}{18}\, \zeta_3 - 2\, X^2\, Y - \frac{3}{2}\, X\, Y^2 - 24\, X\, \zeta_3 + 6\, X^2\, Y^2 - 2\, Y^2\, \pi^2 + 4\, X\, Y^3 \right) \left[\frac{t^2 + s}{st} \right.$$

$$+ \left(\left(8 + 48\, Y - 24\, X \right) \operatorname{Li}_3(y) + \left(8\, \pi^2 - 4\, X + 8\, Y \right) \operatorname{Li}_2(x) - \frac{2}{3}\, X\, Y\, U \right.$$

$$+ \left(24\, Y + 4 \right) \operatorname{Li}_3(x) - 48 \operatorname{Li}_4(x) + \frac{1}{3}\, \pi^2\, U + 48 \operatorname{Li}_4(z) - 48 \operatorname{Li}_4(y) - \frac{77}{18}\, \pi^2 + \frac{11}{5}\, \pi^4$$

$$+ \frac{41}{4}\, X - \frac{17}{36}\, X\, \pi^2 + 4\, X^2\, \pi^2 - 8\, X^3\, Y - 24\, Y\, \zeta_3 - 2\, Y\, \pi^2 - X\, U + \frac{77}{9}\, X\, Y + \frac{1}{3}\, X^2\, U$$

$$+ 2\, X^4 + \frac{7}{36}\, X^3 - \frac{77}{18}\, X^2 - 4\, \zeta_3 - \frac{2}{3}\, X^2\, Y + \frac{14}{3}\, X\, Y^2 + 24\, X\, \zeta_3 + 6\, X^2\, Y^2 + 6\, Y^2\, \pi^2$$

$$\left. + 4\, X\, Y^3 \right) \left[\frac{t^2 - s^2}{st} \right]$$

$$+ \left(\left(- 52 + 24\, Y \right) \operatorname{Li}_3(x) - \frac{8}{3}\, X\, Y\, U - 8\, X\, Y\, \pi^2 + \frac{4}{3}\, \pi^2\, U - \frac{142}{9}\, Y - 11\, \pi^2 + \frac{11}{15}\, \pi^4 \right.$$

$$+ \frac{71}{9}\, X + \frac{85}{9}\, X\, \pi^2 + 24\, Y\, \zeta_3 + 24 \operatorname{Li}_3(y)\, X + 52 \operatorname{Li}_2(x)\, X + \frac{64}{9}\, Y\, \pi^2 + \frac{4}{3}\, X\, U - \frac{76}{9}\, X\, Y$$

$$+ \frac{8}{3}\, Y^2\, U + \frac{4}{3}\, X^2\, U - \frac{8}{3}\, Y\, U + \frac{7}{9}\, X^3 - 2\, Y^4 + \frac{100}{9}\, Y^3 + \frac{44}{9}\, X^2 + \frac{76}{9}\, Y^2 - 52\, \zeta_3$$

$$\left. + \frac{64}{3}\, X^2\, Y - \frac{50}{3}\, X\, Y^2 - 24\, X\, \zeta_3 + 6\, X^2\, Y^2 - 2\, Y^2\, \pi^2 + 4\, X\, Y^3 \right)$$

$$+ \left(9\, \pi^2 + 9\, X^2 - 18\, X\, Y + 9\, Y^2 \right) \frac{t^2}{s^2} + 9\, Y^2\, \frac{s^2}{t^2} \tag{C.7}$$

$$H_u \;=\; \left(- \frac{1}{3}\, Y^2 + \frac{40}{27}\, U - \frac{20}{27}\, Y + \frac{8}{9}\, Y\, U - \frac{8}{9}\, U^2 + \frac{7}{54}\, \pi^2 - \frac{1}{6}\, X^2 + \frac{1}{3}\, X\, Y \right.$$

$$\left. + \frac{10}{27}\, X - \frac{4}{9}\, X\, U \right) \left[\frac{t^2 + s^2}{u^2} \right]$$

$$+ \left(\frac{1}{6}\, \pi^2 + \frac{1}{6}\, X^2 - \frac{1}{3}\, X\, Y - \frac{10}{27}\, X + \frac{4}{9}\, X\, U \right) \left[\frac{t^2 - s^2}{u^2} \right]$$

$$+ \left(- \frac{20}{27}\, U + \frac{4}{9}\, U^2 - \frac{4}{9}\, Y\, U + \frac{10}{27}\, Y + \frac{1}{6}\, Y^2 - \frac{7}{108}\, \pi^2 + \frac{2}{9}\, X\, U - \frac{5}{27}\, X \right.$$

$$\left. - \frac{1}{6}\, X\, Y + \frac{1}{12}\, X^2 \right) \left[\frac{t^2 + s^2}{st} \right]$$

$$+ \left(- \frac{1}{12}\, \pi^2 - \frac{2}{9}\, X\, U + \frac{5}{27}\, X + \frac{1}{6}\, X\, Y - \frac{1}{12}\, X^2 \right) \left[\frac{t^2 - s^2}{st} \right] \tag{C.74}$$

$$I_u \;=\; \left(- \frac{1}{18}\, X^2 - \frac{1}{18}\, \pi^2 + \frac{1}{9}\, X\, Y \right) \left[\frac{t^2 - s^2}{u^2} \right]$$

$$
+\left(-\frac{4}{9}XU+\frac{10}{27}X+\frac{8}{9}YU-\frac{20}{27}Y-\frac{1}{3}Y^2+\frac{1}{3}XY-\frac{5}{36}X^2+\frac{13}{108}\pi^2\right.
$$

$$
\left.-\frac{4}{9}U^2+\frac{20}{27}U\right)\left[\frac{t^2+s^2}{st}\right]
$$

$$
+\left(-\frac{1}{18}XY+\frac{1}{36}X^2+\frac{1}{36}\pi^2\right)\left[\frac{t^2-s^2}{st}\right] \tag{C.75}
$$

C.3.2.2 One-loop self-interference contribution

$$
A_u = \left(-10X^2Y+\frac{10}{3}X\pi^2-X^2\pi^2-3X^2Y^2+10XY^2-\frac{110}{9}XU+\frac{220}{9}YU\right.
$$

$$
+\frac{11}{3}X^2U+\frac{46}{9}XY+\frac{22}{3}Y^2U-3Y^2\pi^2-10Y\pi^2+2X^3Y-\frac{1}{2}\pi^4-\frac{82}{9}-\frac{23}{9}\pi^2
$$

$$
-\frac{121}{9}U^2-22U+2XY^3-\frac{22}{3}XYU-\frac{23}{9}X^2+20Y-\frac{46}{9}Y^2+\frac{10}{3}X^3-\frac{1}{2}X^4
$$

$$
\left.-\frac{20}{3}Y^3-Y^4+2XY\pi^2-10X+\frac{11}{3}\pi^2U\right)\left[\frac{t^2+s^2}{u^2}\right]
$$

$$
+\left(\frac{85}{12}X+2XY^3-\frac{1}{2}X^4+2X^3Y+\frac{41}{36}X^2-\frac{1}{2}\pi^4+\frac{5}{4}X^3+2XY\pi^2-X^2\pi^2\right.
$$

$$
+\frac{5}{4}X\pi^2+\frac{275}{36}XU-3X^2Y^2+Y^2\pi^2-\frac{59}{36}\pi^2+\frac{15}{4}XY^2-\frac{41}{18}XY
$$

$$
\left.-\frac{15}{4}X^2Y+\frac{5}{4}Y\pi^2\right)\left[\frac{t^2-s^2}{u^2}\right]
$$

$$
+\left(\frac{13}{4}X^2Y-\frac{13}{12}X\pi^2+\frac{5}{8}X^2\pi^2+\frac{15}{8}X^2Y^2-\frac{13}{4}XY^2+\frac{121}{36}XU-\frac{121}{18}YU\right.
$$

$$
-\frac{11}{12}X^2U-\frac{49}{72}XY-\frac{11}{6}Y^2U+\frac{15}{8}Y^2\pi^2+\frac{13}{4}Y\pi^2-\frac{5}{4}X^3Y+\frac{5}{16}\pi^4+\frac{49}{144}\pi^2
$$

$$
+\frac{121}{18}U^2+\frac{77}{6}U-\frac{5}{4}XY^3+\frac{11}{6}XYU+\frac{49}{144}X^2-\frac{77}{12}Y+\frac{49}{72}Y^2-\frac{13}{12}X^3+\frac{5}{16}X^4
$$

$$
\left.+\frac{13}{6}Y^3+\frac{5}{8}Y^4-\frac{5}{4}XY\pi^2+\frac{77}{24}X-\frac{11}{12}\pi^2U+\frac{51}{8}\right)\left[\frac{t^2+s^2}{st}\right]
$$

$$
+\left(-\frac{77}{24}X-\frac{121}{36}XU-\frac{59}{72}XY+\frac{3}{16}X^4+\frac{3}{16}\pi^4-\frac{3}{4}XY\pi^2-\frac{1}{6}X^3-\frac{3}{4}XY^3\right.
$$

$$
+\frac{11}{12}X^2U+\frac{11}{12}\pi^2U-\frac{11}{6}XYU-\frac{3}{4}X^3Y+\frac{9}{8}X^2Y^2+\frac{3}{8}X^2\pi^2-\frac{3}{8}Y^2\pi^2
$$

$$
\left.-\frac{1}{2}XY^2+\frac{1}{2}X^2Y-\frac{1}{6}X\pi^2-\frac{1}{6}Y\pi^2+\frac{229}{144}\pi^2+\frac{59}{144}X^2\right)\left[\frac{t^2-s^2}{st}\right]
$$

$$
-\frac{1}{4}Y\left(Y^3+4Y\pi^2+4\pi^2+2Y^2\right)\frac{s^2}{t^2}
$$

$$
-\frac{1}{4}\left(X^2-2XY-2X+Y^2+2Y+\pi^2\right)\left(X^2-2XY+Y^2+\pi^2\right)\frac{t^2}{s^2}
$$

$$
+\frac{1}{8}Y^2\left(Y^2+4\pi^2\right)\frac{s^3}{t^3}+\frac{1}{8}\left(X^2-2XY+Y^2+\pi^2\right)^2\frac{t^3}{s^3}
$$

$$+\frac{1}{36}\Bigg(96\,X^2 + 36\,X\,Y\,\pi^2 + 192\,Y^2 + 96\,\pi^2 + 36\,X\,Y^3 + 123\,X - 62 + 36\,X^3\,Y$$

$$-54\,X^2\,Y^2 - 66\,U + 165\,X\,U - 330\,Y\,U - 192\,X\,Y - 246\,Y - 9\,X^4 - 54\,Y^2\,\pi^2$$

$$-18\,Y^4 - 9\,\pi^4 - 18\,X^2\,\pi^2\Bigg) \tag{C.76}$$

$$B_u \;=\; \Bigg(-\frac{80}{3}\,Y + \frac{40}{3}\,X + 8\,X\,Y - X^4 - \pi^4 + 4\,X\,Y\,\pi^2 + \frac{20}{3}\,X^3 + 4\,X^3\,Y - 4\,X^2\,Y^2$$

$$-2\,X^2\,\pi^2 - 4\,Y^2\,\pi^2 - \frac{40}{3}\,X^2\,Y + \frac{20}{3}\,X\,\pi^2 - \frac{40}{3}\,Y\,\pi^2 + \frac{88}{3}\,U + 24 - \frac{136}{9}\,\pi^2$$

$$-\frac{136}{9}\,X^2 - 8\,Y^2\Bigg)\left[\frac{t^2 + s^2}{u^2}\right]$$

$$+\Bigg(-\frac{27}{4}\,X + \frac{11}{12}\,X\,U + \frac{176}{9}\,X\,Y - \frac{11}{4}\,X^4 - \frac{3}{4}\,\pi^4 + 11\,X\,Y\,\pi^2 + \frac{49}{4}\,X^3 + 3\,X\,Y^3$$

$$+\frac{11}{12}\,X^2\,U + \frac{11}{12}\,\pi^2\,U - \frac{11}{6}\,X\,Y\,U + 7\,X^3\,Y - \frac{9}{2}\,X^2\,Y^2 - \frac{7}{2}\,X^2\,\pi^2 + \frac{3}{2}\,Y^2\,\pi^2$$

$$+\frac{221}{12}\,X\,Y^2 - \frac{221}{12}\,X^2\,Y + \frac{227}{12}\,X\,\pi^2 + \frac{47}{12}\,Y\,\pi^2 + \frac{97}{9}\,\pi^2 - \frac{88}{9}\,X^2\Bigg)\left[\frac{t^2 - s^2}{u^2}\right]$$

$$+\Bigg(\frac{145}{24}\,X^2\,Y - \frac{5}{12}\,X\,\pi^2 + 4\,X^2\,\pi^2 + \frac{23}{4}\,X^2\,Y^2 - \frac{17}{8}\,X\,Y^2 - \frac{121}{18}\,X\,U + \frac{121}{9}\,Y\,U$$

$$+\frac{11}{6}\,X^2\,U + \frac{17}{72}\,X\,Y - \frac{11}{3}\,Y^2\,U + \frac{25}{4}\,Y^2\,\pi^2 + \frac{109}{24}\,Y\,\pi^2 - 4\,X^3\,Y + \frac{9}{8}\,\pi^4 - \frac{145}{8}$$

$$+\frac{47}{16}\,\pi^2 - \frac{121}{18}\,U^2 - \frac{77}{3}\,U - \frac{7}{2}\,X\,Y^3 + \frac{11}{3}\,X\,Y\,U + \frac{103}{16}\,X^2 + \frac{77}{4}\,Y - \frac{17}{72}\,Y^2$$

$$-\frac{8}{3}\,X^3 + \frac{11}{8}\,X^4 + \frac{17}{12}\,Y^3 + \frac{7}{4}\,Y^4 - \frac{11}{2}\,X\,Y\,\pi^2 - \frac{77}{8}\,X - \frac{11}{6}\,\pi^2\,U\Bigg)\left[\frac{t^2 + s^2}{st}\right]$$

$$+\Bigg(-\frac{49}{24}\,X - \frac{11}{2}\,X\,U - \frac{17}{72}\,X\,Y + \frac{7}{4}\,X^4 + \frac{1}{2}\,\pi^4 - 7\,X\,Y\,\pi^2 - \frac{15}{4}\,X^3 - 2\,X\,Y^3$$

$$-\frac{11}{6}\,X^2\,U - \frac{11}{6}\,\pi^2\,U + \frac{11}{3}\,X\,Y\,U - \frac{9}{2}\,X^3\,Y + 3\,X^2\,Y^2 + \frac{9}{4}\,X^2\,\pi^2 - Y^2\,\pi^2$$

$$-\frac{175}{24}\,X\,Y^2 + \frac{175}{24}\,X^2\,Y - \frac{19}{3}\,X\,\pi^2 + \frac{21}{8}\,Y\,\pi^2 - \frac{701}{144}\,\pi^2 + \frac{17}{144}\,X^2\Bigg)\left[\frac{t^2 - s^2}{st}\right]$$

$$-\frac{1}{4}\,Y\left(Y^3 + 4\,Y\,\pi^2 + 4\,\pi^2 + 2\,Y^2\right)\frac{s^2}{t^2}$$

$$-\frac{1}{4}\left(X^2 - 2\,X\,Y - 2\,X + Y^2 + 2\,Y + \pi^2\right)\left(X^2 - 2\,X\,Y + Y^2 + \pi^2\right)\frac{t^2}{s^2}$$

$$+\frac{1}{8}\,Y^2\left(Y^2 + 4\,\pi^2\right)\frac{s^3}{t^3} + \frac{1}{8}\left(X^2 - 2\,X\,Y + Y^2 + \pi^2\right)^2\frac{t^3}{s^3}$$

$$-\frac{1}{12}\Bigg(188\,X^2\,Y - 26\,X\,\pi^2 + 12\,X^2\,\pi^2 - 12\,X^2\,Y^2 - 192\,X\,Y^2 + 55\,X\,U$$

$$-110\,Y\,U + 11\,X^2\,U - 162\,X\,Y + 22\,Y^2\,U - 60\,Y^2\,\pi^2 + 164\,Y\,\pi^2 - 24\,X^3\,Y$$

$$-6\,\pi^4 + 41\,\pi^2 + 22\,U + 72\,X\,Y^3 - 22\,X\,Y\,U + 41\,X^2 - 218\,Y + 162\,Y^2$$

$$-62\,X^3 + 18\,X^4 + 128\,Y^3 - 36\,Y^4 + 120\,X\,Y\,\pi^2 + 109\,X + 11\,\pi^2\,U - 8\Big) \quad \text{(C.77)}$$

$$
\begin{aligned}
C_u \;=\; & -16\left[\frac{t^2+s^2}{u^2}\right] + \left(-\pi^2 - X + 2\,X\,Y - X^2\right)\left[\frac{t^2-s^2}{u^2}\right] \\[4pt]
& + \left(\frac{31}{4}\,X^2\,Y - \frac{15}{4}\,X\,\pi^2 - \frac{1}{4}\,X^2\,\pi^2 - \frac{5}{2}\,X^2\,Y^2 - \frac{57}{4}\,X\,Y^2 - \frac{11}{4}\,X\,U + \frac{11}{2}\,Y\,U \right. \\[4pt]
& \quad -\frac{11}{4}\,X^2\,U + \frac{69}{8}\,X\,Y - \frac{11}{2}\,Y^2\,U - 4\,Y^2\,\pi^2 + \frac{37}{4}\,Y\,\pi^2 + \frac{1}{2}\,X^3\,Y - \frac{1}{2}\,\pi^4 - \frac{29}{16}\,\pi^2 \\[4pt]
& \quad +\frac{77}{6}\,U + \frac{145}{8} + 4\,X\,Y^3 + \frac{11}{2}\,X\,Y\,U - \frac{85}{16}\,X^2 - \frac{91}{12}\,Y - \frac{69}{8}\,Y^2 - \frac{3}{2}\,X^3 + \frac{1}{4}\,X^4 \\[4pt]
& \quad \left. +\frac{19}{2}\,Y^3 - 2\,Y^4 + 5\,X\,Y\,\pi^2 + \frac{91}{24}\,X - \frac{11}{4}\,\pi^2\,U\right)\left[\frac{t^2+s^2}{st}\right] \\[4pt]
& + \left(\frac{63}{8}\,X + \frac{11}{4}\,X\,U - \frac{25}{8}\,X\,Y - \frac{1}{8}\,X^4 - \frac{3}{8}\,\pi^4 + \frac{1}{2}\,X\,Y\,\pi^2 - \frac{25}{12}\,X^3 + \frac{3}{2}\,X\,Y^3 \right. \\[4pt]
& \quad -\frac{11}{12}\,X^2\,U - \frac{11}{12}\,\pi^2\,U + \frac{11}{6}\,X\,Y\,U + X^3\,Y - \frac{9}{4}\,X^2\,Y^2 - \frac{1}{2}\,X^2\,\pi^2 + \frac{3}{4}\,Y^2\,\pi^2 \\[4pt]
& \quad \left. -\frac{29}{6}\,X\,Y^2 + \frac{29}{6}\,X^2\,Y - \frac{17}{6}\,X\,\pi^2 - \frac{1}{2}\,Y\,\pi^2 + \frac{7}{16}\,\pi^2 + \frac{25}{16}\,X^2\right)\left[\frac{t^2-s^2}{st}\right] \\[4pt]
& -\frac{1}{2}\,Y\left(-Y^2 - 2\,\pi^2 + Y^3 + 4\,Y\,\pi^2\right)\frac{s^2}{t^2} \\[4pt]
& -\frac{1}{2}\left(X^2 + X + \pi^2 - 2\,X\,Y - Y + Y^2\right)\left(X^2 - 2\,X\,Y + Y^2 + \pi^2\right)\frac{t^2}{s^2} \\[4pt]
& -\frac{1}{8}\,Y^2\left(Y^2 + 4\,\pi^2\right)\frac{s^3}{t^3} - \frac{1}{8}\left(X^2 - 2\,X\,Y + Y^2 + \pi^2\right)^2\frac{t^3}{s^3} \\[4pt]
& -\frac{1}{6}\left(-56\,X^2\,Y + 26\,X\,\pi^2 + 18\,X^2\,Y^2 + 120\,X\,Y^2 + 22\,X\,U - 44\,Y\,U \right. \\[4pt]
& \quad +22\,X^2\,U - 92\,X\,Y + 44\,Y^2\,U + 30\,Y^2\,\pi^2 - 68\,Y\,\pi^2 + 3\,\pi^4 + 26\,\pi^2 - 36\,X\,Y^3 \\[4pt]
& \quad -44\,X\,Y\,U + 26\,X^2 + 18\,Y + 92\,Y^2 + 8\,X^3 - 3\,X^4 - 80\,Y^3 + 18\,Y^4 - 36\,X\,Y\,\pi^2 \\[4pt]
& \quad \left. -9\,X + 22\,\pi^2\,U - 18\right) \hspace{5cm} \text{(C.78)}
\end{aligned}
$$

$$
\begin{aligned}
D_u \;=\; & \left(-\frac{21}{4}\,Y + \frac{21}{8}\,X - \frac{29}{8}\,X\,Y - \frac{1}{2}\,X^4 - \frac{1}{2}\,\pi^4 - \frac{3}{2}\,Y^4 + 2\,X\,Y\,\pi^2 - \frac{5}{4}\,X^3 \right. \\[4pt]
& \quad +\frac{13}{4}\,Y^3 + 3\,X\,Y^3 + 2\,X^3\,Y - \frac{7}{2}\,X^2\,Y^2 - X^2\,\pi^2 - \frac{7}{2}\,Y^2\,\pi^2 - \frac{39}{8}\,X\,Y^2 \\[4pt]
& \quad \left. +\frac{33}{8}\,X^2\,Y - \frac{5}{4}\,X\,\pi^2 + \frac{33}{8}\,Y\,\pi^2 + \frac{29}{16}\,\pi^2 + \frac{29}{16}\,X^2 + \frac{29}{8}\,Y^2 - \frac{51}{8}\right)\left[\frac{t^2+s^2}{st}\right] \\[4pt]
& + \left(-\frac{21}{8}\,X - \frac{19}{8}\,X\,Y - \frac{3}{8}\,X^4 - \frac{3}{8}\,\pi^4 + \frac{3}{2}\,X\,Y\,\pi^2 - \frac{1}{2}\,X^3 + \frac{3}{2}\,X\,Y^3 + \frac{3}{2}\,X^3\,Y \right. \\[4pt]
& \quad -\frac{9}{4}\,X^2\,Y^2 - \frac{3}{4}\,X^2\,\pi^2 + \frac{3}{4}\,Y^2\,\pi^2 - \frac{15}{8}\,X\,Y^2 + \frac{15}{8}\,X^2\,Y - \frac{1}{2}\,X\,\pi^2 - \frac{1}{8}\,Y\,\pi^2 \\[4pt]
& \quad \left. +\frac{9}{16}\,\pi^2 + \frac{19}{16}\,X^2\right)\left[\frac{t^2-s^2}{st}\right]
\end{aligned}
$$

$$-\frac{1}{2}Y\left(-Y^2-2\pi^2+Y^3+4Y\pi^2\right)\frac{s^2}{t^2}$$

$$-\frac{1}{2}\left(X^2+X+\pi^2-2XY-Y+Y^2\right)\left(X^2-2XY+Y^2+\pi^2\right)\frac{t^2}{s^2}$$

$$-\frac{1}{8}Y^2\left(Y^2+4\pi^2\right)\frac{s^3}{t^3}-\frac{1}{8}\left(X^2-2XY+Y^2+\pi^2\right)^2\frac{t^3}{s^3}$$

$$-\frac{1}{2}\left(-4X^2-4XY\pi^2-8Y^2-4\pi^2-8XY^3-7X-13Y\pi^2-4X^3Y\right.$$

$$+8X^2Y^2+15XY^2+4X^3-1+8XY+14Y+X^4-10Y^3+8Y^2\pi^2+4Y^4$$

$$\left.-13X^2Y+\pi^4+4X\pi^2+2X^2\pi^2\right) \tag{C.79}$$

$$\begin{aligned}
E_u = & \left(-2Y+X-\frac{62}{9}YU+\frac{31}{9}XU-\frac{20}{9}XY-\frac{1}{3}X^3+\frac{2}{3}Y^3+\frac{44}{9}U^2-\frac{2}{3}X^2U\right.\\
& -\frac{2}{3}\pi^2U+\frac{4}{3}XYU-XY^2-\frac{4}{3}Y^2U+X^2Y-\frac{1}{3}X\pi^2+Y\pi^2+4U+\frac{10}{9}\pi^2\\
& \left.+\frac{10}{9}X^2+\frac{20}{9}Y^2+\frac{2}{9}\right)\left[\frac{t^2+s^2}{u^2}\right]\\
& +\left(-\frac{13}{12}X-\frac{47}{18}XU+\frac{25}{18}XY+\frac{25}{36}\pi^2-\frac{25}{36}X^2\right)\left[\frac{t^2-s^2}{u^2}\right]\\
& +\left(\frac{7}{6}Y-\frac{7}{12}X+\frac{22}{9}YU-\frac{11}{9}XU+\frac{11}{18}XY+\frac{1}{12}X^3-\frac{1}{6}Y^3-\frac{22}{9}U^2\right.\\
& +\frac{1}{6}X^2U+\frac{1}{6}\pi^2U-\frac{1}{3}XYU+\frac{1}{4}XY^2+\frac{1}{3}Y^2U-\frac{1}{4}X^2Y+\frac{1}{12}X\pi^2-\frac{1}{4}Y\pi^2\\
& \left.-\frac{7}{3}U-\frac{11}{36}\pi^2-\frac{11}{36}X^2-\frac{11}{18}Y^2\right)\left[\frac{t^2+s^2}{st}\right]\\
& +\left(\frac{7}{12}X+\frac{11}{9}XU-\frac{11}{18}XY-\frac{1}{12}X^3-\frac{1}{6}X^2U-\frac{1}{6}\pi^2U+\frac{1}{3}XYU-\frac{1}{4}XY^2\right.\\
& \left.+\frac{1}{4}X^2Y-\frac{1}{12}X\pi^2-\frac{1}{12}Y\pi^2-\frac{11}{36}\pi^2+\frac{11}{36}X^2\right)\left[\frac{t^2-s^2}{st}\right]\\
& -\frac{1}{36}\left(-4+6Y-3X-60YU+30XU-30XY-12U+15\pi^2+15X^2+30Y^2\right)
\end{aligned} \tag{C.80}$$

$$\begin{aligned}
F_u = & \left(\frac{8}{3}Y-\frac{4}{3}X-\frac{2}{3}X^3+\frac{4}{3}X^2Y-\frac{2}{3}X\pi^2+\frac{4}{3}Y\pi^2-\frac{16}{3}U+\frac{20}{9}\pi^2\right.\\
& \left.+\frac{20}{9}X^2\right)\left[\frac{t^2+s^2}{u^2}\right]\\
& +\left(\frac{5}{4}X-\frac{1}{6}XU-\frac{77}{18}XY-\frac{5}{4}X^3-\frac{1}{6}X^2U-\frac{1}{6}\pi^2U+\frac{1}{3}XYU-\frac{23}{12}XY^2\right.\\
& \left.+\frac{23}{12}X^2Y-\frac{23}{12}X\pi^2-\frac{5}{12}Y\pi^2-\frac{77}{36}\pi^2+\frac{77}{36}X^2\right)\left[\frac{t^2-s^2}{u^2}\right]
\end{aligned}$$

$$+\left(-\frac{7}{2}Y+\frac{7}{4}X-\frac{44}{9}YU+\frac{22}{9}XU-\frac{13}{18}XY+\frac{1}{6}X^3-\frac{1}{6}Y^3+\frac{22}{9}U^2\right.$$

$$-\frac{1}{3}X^2U+\frac{1}{3}\pi^2U-\frac{2}{3}XYU+\frac{1}{4}XY^2+\frac{2}{3}Y^2U-\frac{5}{12}X^2Y+\frac{1}{6}X\pi^2$$

$$\left.-\frac{5}{12}Y\pi^2+\frac{14}{3}U-\frac{1}{2}\pi^2-\frac{1}{2}X^2+\frac{13}{18}Y^2\right)\left[\frac{t^2+s^2}{st}\right]$$

$$+\left(-\frac{7}{12}X+XU+\frac{11}{9}XY+\frac{1}{2}X^3+\frac{1}{3}X^2U+\frac{1}{3}\pi^2U-\frac{2}{3}XYU+\frac{11}{12}XY^2\right.$$

$$\left.-\frac{11}{12}X^2Y+\frac{5}{6}X\pi^2-\frac{1}{4}Y\pi^2+\frac{11}{18}\pi^2-\frac{11}{18}X^2\right)\left[\frac{t^2-s^2}{st}\right]$$

$$+\frac{1}{12}\left(4-5X^3+14Y^3+2X^2U+2\pi^2U-4XYU-21XY^2+4Y^2U\right.$$

$$+17X^2Y-2Y+X-20YU+10XU-18XY-5X\pi^2+17Y\pi^2+4U$$

$$\left.+5\pi^2+5X^2+18Y^2\right) \tag{C.81}$$

$$G_u = \left(\frac{7}{3}Y-\frac{7}{6}X-YU+\frac{1}{2}XU-XY+\frac{1}{4}X^3-Y^3+\frac{1}{2}X^2U+\frac{1}{2}\pi^2U-XYU\right.$$

$$\left.+\frac{3}{2}XY^2+Y^2U-X^2Y+\frac{1}{4}X\pi^2-Y\pi^2-\frac{7}{3}U+\frac{1}{4}\pi^2+\frac{1}{4}X^2+Y^2\right)\left[\frac{t^2+s^2}{st}\right]$$

$$+\left(-\frac{1}{2}XU+\frac{1}{2}XY+\frac{1}{12}X^3+\frac{1}{6}X^2U+\frac{1}{6}\pi^2U-\frac{1}{3}XYU+\frac{1}{3}XY^2-\frac{1}{3}X^2Y\right.$$

$$\left.+\frac{1}{12}X\pi^2+\frac{1}{4}\pi^2-\frac{1}{4}X^2\right)\left[\frac{t^2-s^2}{st}\right]$$

$$+\frac{1}{3}\left(-4Y\pi^2-4YU-4Y^3-4X^2Y-4XY-4XYU+2X^2U\right.$$

$$\left.+X^2+X\pi^2+6XY^2+X^3+4Y^2+4Y^2U+2\pi^2U+2XU+\pi^2\right) \tag{C.82}$$

$$H_u = \frac{1}{9}+\left(-\frac{1}{18}\pi^2+\frac{4}{9}YU-\frac{4}{9}U^2-\frac{1}{9}Y^2-\frac{1}{9}-\frac{1}{18}X^2+\frac{1}{9}XY-\frac{2}{9}XU\right)\left[\frac{t^2+s^2}{u^2}\right]$$

$$+\left(-\frac{1}{18}\pi^2+\frac{1}{18}X^2-\frac{1}{9}XY+\frac{2}{9}XU\right)\left[\frac{t^2-s^2}{u^2}\right]$$

$$+\left(\frac{2}{9}U^2+\frac{1}{18}Y^2+\frac{1}{36}\pi^2-\frac{2}{9}YU-\frac{1}{18}XY+\frac{1}{36}X^2+\frac{1}{9}XU\right)\left[\frac{t^2+s^2}{st}\right]$$

$$+\left(\frac{1}{36}\pi^2+\frac{1}{18}XY-\frac{1}{36}X^2-\frac{1}{9}XU\right)\left[\frac{t^2-s^2}{st}\right] \tag{C.83}$$

$$I_u = \left(\frac{1}{9}XY-\frac{1}{18}X^2+\frac{1}{18}\pi^2\right)\left[\frac{t^2-s^2}{u^2}\right]$$

$$+\left(-\frac{2}{9}XU-\frac{1}{9}Y^2-\frac{2}{9}U^2+\frac{4}{9}YU-\frac{1}{36}\pi^2+\frac{1}{9}XY-\frac{1}{36}X^2\right)\left[\frac{t^2+s^2}{st}\right]$$

$$+\left(-\frac{1}{18}\,XY+\frac{1}{36}\,X^2-\frac{1}{36}\,\pi^2\right)\left[\frac{t^2-s^2}{st}\right] \tag{C.84}$$

C.4 Gluon-gluon scattering

C.4.1 Two-loop contribution

$$
\begin{aligned}
A = & \left(\left(-48\,X-\frac{304}{3}+96\,Y\right)\mathrm{Li}_3(y)+\left(-\frac{304}{3}\,Y+\frac{64}{3}\,X-\frac{32}{3}\,\pi^2\right)\mathrm{Li}_2(x)-\frac{16}{3}\,XY\,\pi^2\right. \\
& -\frac{308}{9}\,\pi^2 S+\frac{8624}{27}\,S-256\,\mathrm{Li}_4(x)+96\,\mathrm{Li}_4(z)+\frac{968}{9}\,S^2-\frac{44372}{81}+\frac{1864}{9}\,\zeta_3+76\,X^2 \\
& +\frac{26}{3}\,X^4+4\,Y^4-96\,\mathrm{Li}_4(y)+\frac{176}{3}\,XYS+\frac{5392}{27}\,Y-\frac{176}{9}\,Y^3+\frac{200}{9}\,\pi^2+\frac{496}{45}\,\pi^4 \\
& -32\,\zeta_3 S+\frac{2350}{27}\,X-\frac{64}{3}\,X^3-\frac{50}{3}\,X\,\pi^2-\frac{88}{3}\,X^2 S-\frac{64}{3}\,X^3 Y-\frac{176}{3}\,Y^2 S+\frac{440}{3}\,XS \\
& -\frac{136}{3}\,XY-64\,Y\,\zeta_3+\frac{136}{3}\,X^2 Y-\frac{200}{3}\,XY^2+24\,X^2\,\pi^2-38\,Y\,\pi^2-48\,X\,\zeta_3 \\
& \left.+\frac{8}{3}\,XY^3+20\,X^2 Y^2+\frac{4}{3}\,Y^2\,\pi^2+\left(-\frac{64}{3}+80\,X+48\,Y\right)\mathrm{Li}_3(x)\right)\frac{t}{u} \\
& +\left(\left(-40-64\,Y+40\,X\right)\mathrm{Li}_3(x)+\left(\frac{32}{3}-40\,Y+64\,X\right)\mathrm{Li}_3(y)+8\,XY\,\pi^2-\frac{22}{9}\,\pi^2 S\right. \\
& +\left(40\,X-\frac{16}{3}\,\pi^2+\frac{32}{3}\,Y\right)\mathrm{Li}_2(x)+\frac{4312}{27}\,S+48\,\mathrm{Li}_4(x)-128\,\mathrm{Li}_4(z)+\frac{484}{9}\,S^2-\frac{22186}{81} \\
& +\frac{836}{9}\,\zeta_3-\frac{38}{9}\,X^2-\frac{17}{3}\,X^4+38\,Y^2+\frac{7}{3}\,Y^4-48\,\mathrm{Li}_4(y)+\frac{1175}{27}\,Y-\frac{32}{3}\,Y^3+\frac{62}{9}\,\pi^2 \\
& -\frac{19}{15}\,\pi^4-16\,\zeta_3 S+\frac{49}{3}\,X-\frac{124}{9}\,X^3-\frac{16}{3}\,X\,\pi^2-\frac{44}{3}\,X^2 S+28\,X^3 Y-\frac{44}{3}\,Y^2 S \\
& +\frac{308}{9}\,XS+\frac{220}{3}\,YS+20\,XY+16\,Y\,\zeta_3+20\,X^2 Y+\frac{16}{3}\,XY^2-14\,X^2\,\pi^2-\frac{67}{9}\,Y\,\pi^2 \\
& \left.-24\,X\,\zeta_3-\frac{20}{3}\,XY^3-16\,X^2 Y^2-6\,Y^2\,\pi^2\right)\frac{t^2}{s^2} \\
& +\left(-\frac{16}{3}\,XY\,\pi^2-\frac{308}{9}\,\pi^2 S+\frac{8624}{27}\,S+\frac{88}{3}\,\mathrm{Li}_3(x)+\frac{968}{9}\,S^2-\frac{44372}{81}+\frac{1408}{9}\,\zeta_3\right. \\
& +\frac{304}{9}\,X^2+2\,X^4+4\,Y^4+\frac{176}{3}\,XYS+\frac{5392}{27}\,Y-\frac{176}{9}\,Y^3-20\,\pi^2-\frac{4}{15}\,\pi^4-32\,\zeta_3 S \\
& +\frac{1616}{27}\,X-\frac{220}{9}\,X^3-\frac{77}{3}\,X\,\pi^2-\frac{88}{3}\,X^2 S-8\,X^3 Y-\frac{176}{3}\,Y^2 S+\frac{968}{9}\,XS \\
& -\frac{88}{3}\,\mathrm{Li}_2(x)\,X-16\,Y\,\zeta_3+\frac{88}{3}\,X^2 Y+\frac{8}{3}\,X^2\,\pi^2-\frac{638}{9}\,Y\,\pi^2-8\,X\,\zeta_3-8\,XY^3 \\
& \left.+12\,X^2 Y^2-\frac{20}{3}\,Y^2\,\pi^2\right)\frac{t^2}{u^2}+\left(\left(88\,Y-\frac{184}{3}\right)\mathrm{Li}_3(y)+\frac{64}{3}\,XY\,\pi^2-\frac{253}{9}\,\pi^2 S\right. \\
& +\frac{11374}{27}\,S+\frac{1210}{9}\,S^2+\frac{1334}{9}\,\zeta_3-\frac{746}{9}\,Y^2+\frac{31}{3}\,Y^4-176\,\mathrm{Li}_4(y)+44\,XYS \\
& +\frac{8579}{27}\,Y-\frac{80}{3}\,Y^3-\frac{196}{9}\,\pi^2+\frac{5}{3}\,\pi^4-40\,\zeta_3 S-\frac{220}{3}\,Y^2 S+\frac{1628}{9}\,YS+\frac{194}{3}\,XY \\
& +\frac{184}{3}\,\mathrm{Li}_2(x)\,X+\frac{104}{3}\,XY^2-\frac{428}{9}\,Y\,\pi^2-16\,X\,\zeta_3-168\,\mathrm{Li}_3(x)\,Y-\frac{40}{3}\,XY^3
\end{aligned}
$$

$$-15\,X^2\,Y^2 + 12\,Y^2\,\pi^2 - \frac{59191}{81}\Bigg) + \Big\{t \longleftrightarrow u\Big\}$$

$$(C.85)$$

$$
\begin{aligned}
B = \Bigg(&\Bigg(\Big(384\,X\,Y - 544\,\pi^2 + 896\,Y - 192\,X^2 - 448\,X\Big)\,\mathrm{Li}_2(x) - 128\,X\,Y\,\pi^2 - 576\,\mathrm{Li}_4(x)\\
&-1152\,\mathrm{Li}_4(z) - 448\,\zeta_3 - 64\,X^2 - 28\,X^4 + 384\,\mathrm{Li}_4(y) - \frac{1912}{3}\,\pi^2 + \frac{1216}{15}\,\pi^4 + 160\,X\\
&+\frac{320}{3}\,X^3 - 288\,X\,\pi^2 + 144\,X^3\,Y + \frac{1888}{3}\,X\,Y + 768\,Y\,\zeta_3 - 224\,X^2\,Y + 1024\,X\,Y^2\\
&-40\,X^2\,\pi^2 - \frac{3232}{3}\,Y\,\pi^2 - 1248\,X\,\zeta_3 - 32\,X\,Y^3 + 48\,X^2\,Y^2 - 240\,Y^2\,\pi^2\\
&+\Big(768\,X + 896 - 768\,Y\Big)\,\mathrm{Li}_3(y) + \Big(448 + 1056\,X - 768\,Y\Big)\,\mathrm{Li}_3(x)\Bigg)\frac{t}{u}\\
&+\Bigg(\Big(-176\,\pi^2 - 224\,X - 224\,Y + 96\,X^2 - 96\,Y^2\Big)\,\mathrm{Li}_2(x) - 192\,\mathrm{Li}_4(x) - 288\,\mathrm{Li}_4(z)\\
&+\Big(-144\,Y + 224 + 144\,X\Big)\,\mathrm{Li}_3(x) + \Big(144\,X - 528\,Y - 224\Big)\,\mathrm{Li}_3(y) + 32\,X\,Y\,\pi^2\\
&+\frac{848}{3}\,X^2 - 14\,X^4 - 32\,Y^2 + 10\,Y^4 + 576\,\mathrm{Li}_4(y) + 80\,Y + \frac{160}{3}\,Y^3 - 36\,\pi^2 + \frac{10}{3}\,\pi^4\\
&-80\,X - \frac{688}{3}\,X^3 - 16\,X\,\pi^2 + 128\,X^3\,Y - \frac{752}{3}\,X\,Y - 96\,Y\,\zeta_3 + 224\,X^2\,Y - 272\,X\,Y^2\\
&-64\,X^2\,\pi^2 + \frac{160}{3}\,Y\,\pi^2 + 96\,X\,\zeta_3 - 112\,X\,Y^3 - 60\,X^2\,Y^2 - 40\,Y^2\,\pi^2\Bigg)\frac{t^2}{s^2}\\
&+\Bigg(-384\,\mathrm{Li}_4(z) - 384\,\mathrm{Li}_4(y) + \Big(-384\,Y + 384\,X\Big)\,\mathrm{Li}_3(x) + 384\,\mathrm{Li}_3(y)\,X\\
&+\Big(-192\,X^2 + 384\,X\,Y - 192\,\pi^2\Big)\,\mathrm{Li}_2(x) + 352\,X^2\,Y - \frac{968}{3}\,\pi^2 - 352\,Y\,\pi^2\\
&-32\,X^3\,Y + 384\,Y\,\zeta_3 - 96\,Y^2\,\pi^2 - 96\,X\,Y\,\pi^2 + 192\,X^2\,Y^2 + 56\,\pi^4 + \frac{752}{3}\,X^2\\
&-384\,X\,\zeta_3 - 8\,X^4 - 176\,X\,\pi^2 - 80\,X^2\,\pi^2 - 176\,X^3\Bigg)\frac{t^2}{u^2}\\
&+\Bigg(-96\,\mathrm{Li}_4(y) + 144\,\mathrm{Li}_3(x)\,Y + \Big(672 + 144\,Y\Big)\,\mathrm{Li}_3(y) - 36 - 96\,Y^2\,\mathrm{Li}_2(y) - 624\,Y\,\pi^2\\
&+\frac{268}{3}\,X\,Y + \frac{128}{3}\,Y^3 - 672\,\mathrm{Li}_2(x)\,X - 48\,X\,Y^3 - 288\,X\,\zeta_3 + \frac{1256}{3}\,Y^2 - 168\,Y^2\,\pi^2\\
&+14\,Y^4 + 48\,X\,Y\,\pi^2 - 32\,X\,Y^2 - 2800\,\zeta_3 + \frac{541}{15}\,\pi^4 + 30\,X^2\,Y^2 + 80\,Y - 698\,\pi^2\Bigg)\\
&+\Big\{t \longleftrightarrow u\Big\}
\end{aligned}
$$

$$(C.86)$$

$$C = \Bigg(-\frac{2}{3}\,X\,Y\,\pi^2 - \frac{10}{9}\,\pi^2\,S - \frac{1544}{27}\,S + 224\,\mathrm{Li}_4(x) - 48\,\mathrm{Li}_4(z) - \frac{352}{9}\,S^2 - \frac{388}{9}\,\zeta_3$$

$$-\frac{70}{3}\,X^2 - \frac{31}{6}\,X^4 + 48\,\mathrm{Li}_4(y) + 4\,X\,Y\,S - \frac{1096}{27}\,Y + \frac{32}{9}\,Y^3 - \frac{356}{27}\,\pi^2 - \frac{829}{90}\,\pi^4$$

$$+\frac{938}{27}\,X - \frac{4}{3}\,X^3 - \frac{22}{3}\,X\,\pi^2 - 2\,X^2\,S + 6\,X^3\,Y + \frac{32}{3}\,Y^2\,S - \frac{124}{3}\,X\,S + \frac{148}{3}\,X\,Y$$

$$+24\,Y\,\zeta_3 - \frac{56}{3}\,X^2\,Y + \frac{202}{3}\,X\,Y^2 - \frac{55}{3}\,X^2\,\pi^2 - 16\,Y\,\pi^2 + 64\,X\,\zeta_3 - 6\,X\,Y^3$$

$$-3\,X^2\,Y^2 - 3\,Y^2\,\pi^2 + \frac{9698}{81} + \left(\frac{64}{3}\,\pi^2 + \frac{280}{3}\,Y - \frac{124}{3}\,X\right)\mathrm{Li}_2(x)$$

$$+\left(24\,X + \frac{280}{3} - 48\,Y\right)\mathrm{Li}_3(y) + \left(-24\,Y + \frac{124}{3} - 88\,X\right)\mathrm{Li}_3(x)\right)\frac{t}{u}$$

$$+\left(\left(26 - 44\,X + 56\,Y\right)\mathrm{Li}_3(x) + \left(44\,Y - \frac{62}{3} - 56\,X\right)\mathrm{Li}_3(y) - 24\,\mathrm{Li}_4(x) + 112\,\mathrm{Li}_4(z)\right.$$

$$+\left(-26\,X + \frac{32}{3}\,\pi^2 - \frac{62}{3}\,Y\right)\mathrm{Li}_2(x) - 4\,X\,Y\,\pi^2 + \frac{4}{9}\,\pi^2\,S - \frac{772}{27}\,S - \frac{176}{9}\,S^2 - \frac{8}{9}\,\zeta_3$$

$$+\frac{127}{9}\,X^2 + \frac{25}{4}\,X^4 - \frac{35}{3}\,Y^2 - \frac{19}{12}\,Y^4 + 24\,\mathrm{Li}_4(y) + \frac{469}{27}\,Y - \frac{2}{3}\,Y^3 + \frac{203}{27}\,\pi^2 + \frac{1}{5}\,\pi^4$$

$$-\frac{77}{3}\,X + \frac{46}{9}\,X^3 + \frac{17}{3}\,X\,\pi^2 + \frac{19}{3}\,X^2\,S - 26\,X^3\,Y - Y^2\,S - \frac{166}{9}\,X\,S - \frac{62}{3}\,Y\,S$$

$$-22\,X\,Y - 12\,Y\,\zeta_3 - 13\,X^2\,Y - \frac{31}{3}\,X\,Y^2 + 7\,X^2\,\pi^2 - \frac{2}{9}\,Y\,\pi^2 + 12\,X\,\zeta_3 + \frac{22}{3}\,X\,Y^3$$

$$+14\,X^2\,Y^2 + \frac{7}{3}\,Y^2\,\pi^2 + \frac{4849}{81}\right)\frac{t^2}{s^2}$$

$$+\left(-\frac{1096}{27}\,Y - \frac{224}{27}\,X - \frac{352}{9}\,X\,S + \frac{32}{9}\,Y^3 + \frac{340}{27}\,\pi^2 + \frac{56}{9}\,\pi^2\,S + \frac{16}{3}\,\mathrm{Li}_2(x)\,X\right.$$

$$+\frac{14}{3}\,X\,\pi^2 - \frac{16}{3}\,\mathrm{Li}_3(x) - \frac{1544}{27}\,S - \frac{352}{9}\,S^2 + \frac{9698}{81} + \frac{32}{3}\,Y^2\,S - \frac{16}{3}\,X^2\,Y + \frac{32}{9}\,\zeta_3$$

$$+\frac{40}{9}\,X^3 + \frac{22}{9}\,X^2 + \frac{16}{3}\,X^2\,S - \frac{32}{3}\,X\,Y\,S + \frac{116}{9}\,Y\,\pi^2\right)\frac{t^2}{u^2}$$

$$+\left(\left(-68\,Y + \frac{202}{3}\right)\mathrm{Li}_3(y) - \frac{62}{3}\,X\,Y\,\pi^2 + \frac{46}{9}\,\pi^2\,S - \frac{2632}{27}\,S - \frac{440}{9}\,S^2 + \frac{934}{9}\,\zeta_3\right.$$

$$+\frac{481}{9}\,Y^2 - \frac{71}{12}\,Y^4 + 136\,\mathrm{Li}_4(y) - 8\,X\,Y\,S - \frac{1319}{27}\,Y - \frac{26}{3}\,Y^3 + \frac{899}{27}\,\pi^2 - \frac{47}{30}\,\pi^4$$

$$+\frac{73}{3}\,Y^2\,S - \frac{538}{9}\,Y\,S - \frac{53}{3}\,X\,Y - \frac{202}{3}\,\mathrm{Li}_2(x)\,X + \frac{7}{3}\,X\,Y^2 - \frac{163}{9}\,Y\,\pi^2 + 4\,X\,\zeta_3$$

$$+120\,\mathrm{Li}_3(x)\,Y + \frac{14}{3}\,X\,Y^3 + 15\,X^2\,Y^2 - \frac{29}{3}\,Y^2\,\pi^2 + \frac{16294}{81}\right) + \left\{t \longleftrightarrow u\right\}$$

$$\tag{C.87}$$

$$D = \left(\left(-104\,X + 32\,Y - \frac{92}{3}\right)\mathrm{Li}_3(x) + \left(-32\,X + 64\,Y - \frac{184}{3}\right)\mathrm{Li}_3(y) - 6\,X\,Y\,\pi^2\right.$$

$$+\left(\frac{160}{3}\,\pi^2 - \frac{184}{3}\,Y + \frac{92}{3}\,X - 16\,X\,Y + 16\,Y^2 - 8\,X^2\right)\mathrm{Li}_2(x) + 8\,S + \frac{742}{3}\,\pi^2$$

$$+176\,\mathrm{Li}_4(x) + 48\,\mathrm{Li}_4(z) + \frac{188}{3}\,\zeta_3 + \frac{80}{3}\,X^2 - \frac{23}{6}\,X^4 - 48\,\mathrm{Li}_4(y) + 8\,Y - \frac{571}{90}\,\pi^4$$

$$-\frac{152}{3}\,X - \frac{385}{9}\,X^3 + \frac{215}{3}\,X\,\pi^2 - 10\,X^3\,Y - 260\,X\,Y - 32\,Y\,\zeta_3 + \frac{161}{3}\,X^2\,Y - \frac{110}{3}$$

$$-\frac{445}{3}\,X\,Y^2 - 17\,X^2\,\pi^2 + \frac{1727}{9}\,Y\,\pi^2 + 168\,X\,\zeta_3 + \frac{34}{3}\,X\,Y^3 + 3\,X^2\,Y^2 + \frac{13}{3}\,Y^2\,\pi^2\Big)\,\frac{t}{u}$$

$$+\Big(-\frac{4}{3}\,X\,Y\,\pi^2 + 4\,S + 24\,\mathrm{Li}_4(x) + 88\,\mathrm{Li}_4(z) + 16\,\zeta_3 - \frac{350}{3}\,X^2 + \frac{79}{12}\,X^4 + \frac{40}{3}\,Y^2$$

$$-\frac{35}{12}\,Y^4 - 24\,\mathrm{Li}_4(y) - \frac{76}{3}\,Y - \frac{385}{18}\,Y^3 + 7\,\pi^2 - \frac{11}{30}\,\pi^4 + \frac{76}{3}\,X + \frac{961}{18}\,X^3 - 10\,X\,\pi^2$$

$$-\frac{82}{3}\,X^3\,Y + \frac{310}{3}\,X\,Y + 32\,Y\,\zeta_3 - \frac{208}{3}\,X^2\,Y + \frac{158}{3}\,X\,Y^2 + \frac{13}{3}\,X^2\,\pi^2 + \frac{67}{9}\,Y\,\pi^2$$

$$-32\,X\,\zeta_3 + \frac{26}{3}\,X\,Y^3 + 19\,X^2\,Y^2 + \frac{11}{3}\,Y^2\,\pi^2 - \frac{55}{3} + \Big(-\frac{46}{3} - 52\,X + 36\,Y\Big)\,\mathrm{Li}_3(x)$$

$$+\Big(52\,Y + \frac{46}{3} - 36\,X\Big)\,\mathrm{Li}_3(y) + \Big(16\,X\,Y + \frac{46}{3}\,Y - 4\,X^2 + \frac{46}{3}\,X + \frac{44}{3}\,\pi^2 - 4\,Y^2\Big)\,\mathrm{Li}_2(x$$

$$+\Big(8\,Y - 64\,X^2\,Y - \frac{110}{3} + 8\,S - \frac{310}{3}\,X^2 + 32\,\zeta_3 + 64\,Y\,\pi^2 + \frac{352}{3}\,\pi^2 + 32\,X\,\pi^2 + 32\,X^3$$

$$+\Big(64\,\mathrm{Li}_4(y) - 108\,\mathrm{Li}_3(x)\,Y + \big(-46 - 20\,Y\big)\,\mathrm{Li}_3(y) - \frac{545}{18}\,Y^3 - \frac{83}{3}\,X\,Y + 46\,\mathrm{Li}_2(x)\,X$$

$$-\frac{203}{6} - \frac{574}{3}\,Y^2 - 10\,X\,Y^3 + 10\,S + \frac{5}{12}\,Y^4 - \frac{10}{3}\,X\,Y^2 - \frac{67}{20}\,\pi^4 - \frac{16}{3}\,X\,Y\,\pi^2 + \frac{340}{3}\,Y\,\pi^2$$

$$+104\,X\,\zeta_3 + \frac{740}{3}\,\pi^2 - \frac{21}{2}\,X^2\,Y^2 - \frac{52}{3}\,Y - 12\,Y^2\,\mathrm{Li}_2(y) + \frac{1154}{3}\,\zeta_3 - \frac{1}{3}\,Y^2\,\pi^2\Big)$$

$$+\Big\{t \longleftrightarrow u\Big\}$$

$$($$

$$E \;=\; \Big(\frac{4}{3}\,Y\,S + \frac{16}{9}\,S^2 + \frac{2}{3}\,Y^2 + \frac{20}{9}\,X\,S + \frac{4}{27}\,\pi^2 + \frac{10}{9}\,X^2 - \frac{2}{3}\,X - \frac{2}{3}\,X\,\pi^2 - \frac{2}{3}\,X^2\,S$$

$$-\frac{1}{3}\,X^3 + \frac{1}{3}\,Y^3 + \frac{2}{3}\,Y^2\,S + \frac{2}{3}\,Y + \frac{2}{3}\,Y\,\pi^2\Big)\,\frac{t^2}{s^2}$$

$$+\Big(-\frac{52}{27}\,\pi^2 + \frac{4}{3}\,\pi^2\,S + \frac{8}{3}\,X\,S + \frac{4}{3}\,X - \frac{2}{3}\,Y\,\pi^2 - \frac{2}{3}\,X\,Y^2 + \frac{2}{3}\,X\,\pi^2 + \frac{32}{9}\,S^2$$

$$-\frac{2}{3}\,X^2\,Y + \frac{4}{3}\,X^2 + \frac{4}{3}\,X^2\,S + \frac{2}{3}\,X^3 - \frac{8}{3}\,X\,Y\,S\Big)\,\frac{t}{u}$$

$$+\Big(\frac{32}{9}\,S^2 + \frac{32}{9}\,X\,S - \frac{40}{27}\,\pi^2 + \frac{16}{9}\,X^2\Big)\,\frac{t^2}{u^2}$$

$$+\Big(\frac{1}{2} - 2\,Y\,\pi^2 - Y^3 - 2\,Y^2\,S + \frac{44}{9}\,Y\,S + \frac{22}{9}\,Y^2 + 4\,S + \frac{10}{3}\,Y + \frac{40}{9}\,S^2 - \frac{44}{27}\,\pi^2\Big)$$

$$+\Big\{t \longleftrightarrow u\Big\}$$

$$(\mathrm{C.89})$$

$$F \;=\; \Big(-4\,X\,\pi^2 - \frac{8}{3}\,X^2\,Y - \frac{8}{3}\,Y\,\pi^2 + \frac{8}{3}\,X\,Y^2 + \frac{80}{3}\,X\,Y - \frac{8}{3}\,X^2 - 24\,\pi^2 + \frac{16}{3}\,X + 4\,X^3\Big)\,\frac{t}{u}$$

$$-\frac{2}{3}\left(X-Y\right)\left(3\,Y^2-2\,Y-4\,X\,Y+2\,\pi^2+3\,X^2-18\,X+4\right)\frac{t^2}{s^2}$$

$$-\frac{32}{3}\left(\pi-X\right)\left(\pi+X\right)\frac{t^2}{u^2}$$

$$+\left(-\frac{16}{3}\,Y\,\pi^2+\frac{2}{3}\,Y^3+4\,X\,Y+\frac{52}{3}\,Y^2+2\,X\,Y^2+\frac{8}{3}\,Y-\frac{64}{3}\,\pi^2\right)$$

$$+\left\{t\longleftrightarrow u\right\}$$

(C.90)

C.4.2 One-loop self-interference contribution

$$\begin{aligned}
A &= \frac{1}{2}\left(X^2-2\,X-2\,X\,Y+2\,Y+Y^2+\pi^2\right)\left(X^2-2\,X\,Y+Y^2+\pi^2\right)\frac{t^4}{s^4}\\[4pt]
&+X^2\left(4\,\pi^2+X^2\right)\frac{t^4}{u^4}+2\,X\left(4\,X\,\pi^2+X^3+2\,X^2+4\,\pi^2\right)\frac{t^3}{u^3}\\[4pt]
&+\left(\frac{2948}{27}\,S+\pi^2+\frac{9014}{81}+\pi^4+\frac{242}{9}\,S^2+20\,X^2\,Y+10\,X^2\,\pi^2-4\,X\,Y^3+2\,Y^2\,\pi^2+Y^4\right.\\[4pt]
&\quad-4\,X^3\,Y+16\,Y\,\pi^2+\frac{110}{3}\,Y\,S+\frac{154}{9}\,X\,S+6\,X^2\,Y^2-\frac{22}{3}\,X^2\,S-\frac{22}{3}\,Y^2\,S-20\,X\,Y^2+\\[4pt]
&\quad\left.-\frac{28}{9}\,Y^2-\frac{56}{3}\,X^3+\frac{721}{9}\,Y+\frac{56}{9}\,X^2+\frac{785}{27}\,X-6\,X\,Y-16\,X\,\pi^2+4\,Y^3-4\,X\,Y\,\pi^2\right)\frac{t^2}{s^2}\\[4pt]
&+\left(4\,Y^4-\frac{536}{9}\,Y^2-\frac{88}{3}\,Y^2\,S+\frac{88}{3}\,X\,Y\,S+\frac{880}{9}\,X\,Y+12\,X^3+\frac{1442}{9}\,X+\frac{220}{3}\,X\,S\right.\\[4pt]
&\quad+16\,Y^2\,\pi^2-\frac{44}{3}\,\pi^2\,S+\frac{58}{9}\,\pi^2-\frac{44}{3}\,X^2\,S-\frac{56}{9}\,X^2+\frac{4}{3}\,X^2\,Y+\frac{116}{3}\,Y\,\pi^2+16\,X^2\,\pi^2\\[4pt]
&\quad\left.+\frac{5896}{27}\,S+\frac{484}{9}\,S^2+\frac{18028}{81}+4\,X^4+\frac{88}{3}\,X\,\pi^2+\frac{40}{3}\,X\,Y^2\right)\frac{t}{u}\\[4pt]
&+\left(\frac{5896}{27}\,S+\frac{10}{9}\,\pi^2+2\,\pi^4+\frac{484}{9}\,S^2+\frac{18028}{81}+\frac{88}{3}\,X^2\,Y-\frac{44}{3}\,\pi^2\,S+24\,X^2\,\pi^2-8\,X\,Y^3\right.\\[4pt]
&\quad+12\,Y^2\,\pi^2-8\,X^3\,Y+\frac{88}{3}\,Y\,\pi^2+\frac{484}{9}\,X\,S+12\,X^2\,Y^2-\frac{44}{3}\,X^2\,S-\frac{88}{3}\,Y^2\,S-\frac{44}{3}\,X\,Y^2\\[4pt]
&\quad+7\,X^4+4\,Y^4-\frac{536}{9}\,Y^2-\frac{26}{3}\,X^3+\frac{28}{9}\,X^2+\frac{2948}{27}\,X+\frac{536}{9}\,X\,Y-\frac{8}{3}\,X\,\pi^2-8\,X\,Y\,\pi^2\\[4pt]
&\quad\left.+\frac{88}{3}\,X\,Y\,S\right)\frac{t^2}{u^2}\\[4pt]
&+\left(\frac{24533}{81}+\frac{596}{9}\,X\,Y-\frac{122}{3}\,X^2+\frac{17}{2}\,Y^4+\frac{107}{3}\,X\,\pi^2+\frac{814}{9}\,X\,S+\frac{15}{2}\,X^2\,Y^2\right.\\[4pt]
&\quad-\frac{110}{3}\,Y^2\,S+\frac{113}{18}\,\pi^2+22\,X\,Y\,S-11\,\pi^2\,S+\frac{605}{9}\,S^2-\frac{7}{3}\,X^3+\frac{5}{4}\,\pi^4+11\,X^2\,Y\\[4pt]
&\quad\left.+\frac{7667}{27}\,S-10\,X\,Y^3+29\,Y^2\,\pi^2+\frac{5309}{27}\,Y-5\,X\,Y\,\pi^2\right)+\left\{t\leftrightarrow u\right\}
\end{aligned}$$

(C

$$B = 6\left(X^2 - 2X - 2XY + 2Y + Y^2 + \pi^2\right)\left(X^2 - 2XY + Y^2 + \pi^2\right)\frac{t^4}{s^4}$$

$$+12X^2\left(4\pi^2 + X^2\right)\frac{t^4}{u^4} + 24X\left(4X\pi^2 + X^3 + 2X^2 + 4\pi^2\right)\frac{t^3}{u^3}$$

$$+\Big(-120X^3Y + 156X^2\pi^2 - 392X\pi^2 - 404XY^2 + 580X^2Y + 392Y\pi^2$$

$$+48X^2Y^2 - \frac{1184}{3}XY + 24XY^3 - 12Y^2\pi^2 - 32Y^2 + 12\pi^2 + 72X^4 - 24Y^4$$

$$+\frac{1280}{3}X^2 + 180Y^3 - 356X^3 + 12\pi^4 - 144XY\pi^2 - 112X + 112Y\Big)\frac{t^2}{s^2}$$

$$+\Big(624XY^2 - 64X^2 + 528Y\pi^2 + 144X^3Y + 792X\pi^2 + 96XY^3 + 224X$$

$$-272X^2Y + 408X^3 + \frac{2752}{3}XY + 144Y^2\pi^2 + 288XY\pi^2 - 48X^2Y^2 - 24X^4$$

$$+120X^2\pi^2 + \frac{2200}{3}\pi^2\Big)\frac{t}{u}$$

$$+\Big(352X^2Y - 32X\pi^2 + 24\pi^4 + 288X^2\pi^2 + 352Y\pi^2 - 104X^3 + 84X^4 + 96Y^2\pi^2$$

$$+\frac{1184}{3}X^2 - 96XY\pi^2 + \frac{1112}{3}\pi^2 - 96X^3Y + 96X^2Y^2\Big)\frac{t^2}{u^2}$$

$$+\Big(48 + \frac{424}{3}XY + \frac{1808}{3}X^2 + 42Y^4 + 716X\pi^2 + 66X^2Y^2 + 666\pi^2 + 32X^3$$

$$+15\pi^4 + 416X^2Y + 288Y^2\pi^2 + 112Y + 84XY\pi^2\Big) + \Big\{t \leftrightarrow u\Big\}$$

(C.92)

$$C = -\left(X^2 - 2X - 2XY + 2Y + Y^2 + \pi^2\right)\left(X^2 - 2XY + Y^2 + \pi^2\right)\frac{t^4}{s^4}$$

$$-2X^2\left(4\pi^2 + X^2\right)\frac{t^4}{u^4} - 4X\left(4X\pi^2 + X^3 + 2X^2 + 4\pi^2\right)\frac{t^3}{u^3}$$

$$+\Big(-\frac{976}{27}S - 2\pi^2 - \frac{1}{2}\pi^4 - \frac{88}{9}S^2 - 22X^2Y - 3X^2\pi^2 + 2XY^3 + Y^2\pi^2 + 2X^3Y$$

$$-\frac{32}{3}Y\pi^2 - \frac{31}{3}YS - \frac{83}{9}XS - 3X^2Y^2 + \frac{19}{6}X^2S - \frac{1}{2}Y^2S + 22XY^2 - X^4 - \frac{127}{18}Y^2$$

$$+\frac{73}{6}X^3 - \frac{242}{9}Y - \frac{185}{18}X^2 - \frac{250}{27}X + 12XY + \frac{32}{3}X\pi^2 - \frac{19}{2}Y^3 - \frac{2752}{81} + 2XY\pi^2\Big)$$

$$+\Big(-\frac{1952}{27}S - \frac{247}{9}\pi^2 + \pi^4 - \frac{176}{9}S^2 + 12X^2Y - \pi^2S - 18X^2\pi^2 - 4XY^3 - 2Y^2\pi^2$$

$$-4X^3Y - 16Y\pi^2 - \frac{62}{3}XS + 6X^2Y^2 - X^2S + \frac{16}{3}Y^2S - 11XY^2 - 4X^4 + \frac{80}{9}Y^2$$

$$-27X^3 - \frac{127}{9}X^2 - \frac{484}{9}X - \frac{148}{9}XY - \frac{149}{3}X\pi^2 - \frac{5504}{81} - 4XY\pi^2 + 2XYS\Big)\frac{t}{u}$$

$$+\left(-\frac{80}{9}XY - \frac{16}{3}XYS + \frac{80}{9}Y^2 + \frac{16}{3}Y^2S - \frac{28}{3}X^3 - 7X^4 - \frac{976}{27}X - \frac{176}{9}XS\right.$$

$$-\frac{16}{3}X^2Y - \frac{16}{3}Y\pi^2 + \frac{8}{3}XY^2 - \frac{176}{9}S^2 - \frac{5504}{81} - \frac{1952}{27}S - \frac{64}{3}X\pi^2 - 28X^2\pi^2$$

$$\left.+\frac{8}{3}\pi^2 S - \frac{40}{3}\pi^2 + \frac{8}{3}X^2 S - \frac{52}{3}X^2\right)\frac{t^2}{u^2} + \left(-\frac{9337}{81} - \frac{97}{9}XY - \frac{131}{18}X^2\right.$$

$$-4Y^4 - \frac{94}{3}X\pi^2 - \frac{269}{9}XS - \frac{3}{2}X^2Y^2 + \frac{73}{6}Y^2S - \frac{367}{18}\pi^2 - 4XYS + 2\pi^2 S$$

$$\left.-\frac{220}{9}S^2 - \frac{13}{2}X^3 - \frac{1}{4}\pi^4 - 2X^2Y - \frac{2791}{27}S + 2XY^3 - 15Y^2\pi^2 - \frac{1936}{27}Y + XY\pi^2\right)$$

$$+\left\{t \leftrightarrow u\right\}$$

(C.9

$$D = -2\left(X^2 - 2X - 2XY + 2Y + Y^2 + \pi^2\right)\left(X^2 - 2XY + Y^2 + \pi^2\right)\frac{t^4}{s^4}$$

$$-4X^2\left(4\pi^2 + X^2\right)\frac{t^4}{u^4} - 8X\left(4X\pi^2 + X^3 + 2X^2 + 4\pi^2\right)\frac{t^3}{u^3}$$

$$+\left(8X^3Y - 8X^2\pi^2 + \frac{232}{3}X\pi^2 + \frac{293}{3}XY^2 - \frac{389}{3}X^2Y - \frac{232}{3}Y\pi^2 - 6X^2Y^2\right.$$

$$+\frac{424}{3}XY + 4Y^2\pi^2 + \frac{22}{3}Y^2 - 4\pi^2 - 4X^4 + 2Y^4 - \frac{446}{3}X^2 - 43Y^3$$

$$\left.+75X^3 - \pi^4 + 4XY\pi^2 + \frac{116}{3}X - \frac{116}{3}Y\right)\frac{t^2}{s^2}$$

$$+\left(-\frac{578}{3}X\pi^2 - 4X^4 - \frac{820}{3}\pi^2 - 312XY + \frac{44}{3}X^2 - 16X^3Y - \frac{380}{3}XY^2\right.$$

$$+12X^2Y^2 + 2\pi^4 - \frac{332}{3}Y\pi^2 - 8XY^3 - 32X^2\pi^2 + \frac{188}{3}X^2Y - 102X^3 - 4Y^2\pi^2$$

$$\left.-\frac{232}{3}X - 24XY\pi^2\right)\frac{t}{u}$$

$$+\left(-\frac{400}{3}\pi^2 - 16X\pi^2 + 8X^3 - 56X^2\pi^2 - 64X^2Y - \frac{424}{3}X^2 - 64Y\pi^2 - 14X^4\right)\frac{t^2}{u^2}$$

$$+\left(-16 - \frac{148}{3}XY - 206X^2 - 4Y^4 - \frac{484}{3}X\pi^2 - \frac{721}{3}\pi^2 - \frac{35}{3}X^3 - \frac{1}{2}\pi^4\right.$$

$$\left.-85X^2Y - 4XY^3 - 26Y^2\pi^2 - \frac{116}{3}Y - 2XY\pi^2\right) + \left\{t \leftrightarrow u\right\}$$

(C.94)

$$E = \frac{1}{2}\left(X^2 - 2X - 2XY + 2Y + Y^2 + \pi^2\right)\left(X^2 - 2XY + Y^2 + \pi^2\right)\frac{t^4}{s^4}$$

$$+X^2\left(4\pi^2 + X^2\right)\frac{t^4}{u^4} + 2X\left(4X\pi^2 + X^3 + 2X^2 + 4\pi^2\right)\frac{t^3}{u^3}$$

$$+\left(\frac{236}{81} + \frac{80}{27}S + \pi^2 - \frac{1}{2}\pi^4 + \frac{8}{9}S^2 + 2X^2Y - X^2\pi^2 + 2XY^3 - Y^2\pi^2 + 2X^3Y\right.$$

$$+\frac{2}{3} Y \pi^2 + \frac{2}{3} Y S + \frac{10}{9} X S - 3 X^2 Y^2 - \frac{1}{3} X^2 S + \frac{1}{3} Y^2 S - 2 X Y^2 - \frac{1}{2} X^4 - \frac{1}{2} Y^4$$

$$+\frac{10}{3} Y^2 - X^3 + \frac{34}{9} Y + \frac{32}{9} X^2 - \frac{22}{27} X - 6 X Y - \frac{2}{3} X \pi^2 + Y^3 + 2 X Y \pi^2 \Big) \frac{t^2}{s^2}$$

$$+\Big(\frac{2}{3} X Y^2 + \frac{68}{9} X + \frac{4}{3} X S - \frac{4}{3} X^2 Y + X^4 + 6 X^3 + \frac{4}{3} Y \pi^2 + \frac{2}{3} X^2 S + \frac{20}{3} X^2$$

$$+\frac{34}{3} X \pi^2 + \frac{22}{3} \pi^2 + \frac{2}{3} \pi^2 S + 4 X^2 \pi^2 - \frac{4}{3} X Y S + \frac{16}{9} S^2 + \frac{160}{27} S + \frac{472}{81} \Big) \frac{t}{u}$$

$$+\Big(\frac{62}{9} X^2 + 2 X^4 + \frac{16}{9} S^2 + \frac{160}{27} S + \frac{472}{81} + \frac{16}{9} X S + \frac{80}{27} X + 6 X^3 + \frac{44}{9} \pi^2$$

$$+8 X^2 \pi^2 + 12 X \pi^2 \Big) \frac{t^2}{u^2}$$

$$+\Big(\frac{1049}{81} + \frac{5}{9} X Y + \frac{28}{9} X^2 + \frac{1}{2} Y^4 + \frac{14}{3} X \pi^2 + \frac{22}{9} X S + \frac{3}{4} X^2 Y^2 - Y^2 S$$

$$+\frac{37}{9} \pi^2 + \frac{20}{9} S^2 + \frac{4}{3} X^3 + \frac{1}{8} \pi^4 + \frac{254}{27} S - X Y^3 + \frac{3}{2} Y^2 \pi^2 + \frac{218}{27} Y - \frac{1}{2} X Y \pi^2 \Big)$$

$$+\Big\{t \leftrightarrow u\Big\}$$

<div align="right">(C.95)</div>

$$F = -\Big(X^2 - 2 X - 2 X Y + 2 Y + Y^2 + \pi^2\Big)\Big(X^2 - 2 X Y + Y^2 + \pi^2\Big) \frac{t^4}{s^4}$$

$$-2 X^2 \Big(4 \pi^2 + X^2\Big) \frac{t^4}{u^4} - 4 X \Big(4 X \pi^2 + X^3 + 2 X^2 + 4 \pi^2\Big) \frac{t^3}{u^3}$$

$$+\Big(-4 X^3 Y + 2 X^2 \pi^2 - \frac{4}{3} X \pi^2 - \frac{14}{3} X Y^2 + \frac{14}{3} X^2 Y + \frac{4}{3} Y \pi^2 + 6 X^2 Y^2$$

$$+\frac{4}{3} X Y - 4 X Y^3 + 2 Y^2 \pi^2 - \frac{22}{3} Y^2 - 2 \pi^2 + X^4 + Y^4 + 6 X^2 + 2 Y^3 - 2 X^3$$

$$+\pi^4 - 4 X Y \pi^2 + \frac{4}{3} X - \frac{4}{3} Y \Big) \frac{t^2}{s^2}$$

$$+\Big(\frac{80}{3} X Y - \frac{8}{3} X^2 Y - 4 X^3 + \frac{8}{3} X Y^2 - 8 X^2 \pi^2 - \frac{44}{3} X^2 - \frac{28}{3} X \pi^2 + \frac{8}{3} Y \pi^2$$

$$+16 \pi^2 - 2 X^4 - \frac{8}{3} X \Big) \frac{t}{u}$$

$$+\Big(-24 X \pi^2 - 16 X^2 \pi^2 + \frac{8}{3} \pi^2 - 12 X^3 - 4 X^4 - \frac{4}{3} X^2 \Big) \frac{t^2}{u^2}$$

$$+\Big(-8 + 2 X Y + \frac{46}{3} X^2 - Y^4 + \frac{4}{3} X \pi^2 - \frac{3}{2} X^2 Y^2 + \frac{58}{3} \pi^2 - \frac{4}{3} X^3 - \frac{1}{4} \pi^4$$

$$+2 X^2 Y + 2 X Y^3 - 3 Y^2 \pi^2 - \frac{4}{3} Y + X Y \pi^2 \Big) + \Big\{t \leftrightarrow u\Big\}$$

<div align="right">(C.96)</div>

$$
\begin{aligned}
G \;=\; & 3\left(X^2 - 2X - 2XY + 2Y + Y^2 + \pi^2\right)\left(X^2 - 2XY + Y^2 + \pi^2\right)\frac{t^4}{s^4} \\[2mm]
& + 6X^2\left(4\pi^2 + X^2\right)\frac{t^4}{u^4} + 12X\left(4X\pi^2 + X^3 + 2X^2 + 4\pi^2\right)\frac{t^3}{u^3} \\[2mm]
& - 3\left(X^2 - 2X - 2XY + 2Y + Y^2 + \pi^2\right)\left(X^2 + 2X - 2 + \pi^2 - 2XY - 2Y + Y^2\right)\frac{t^2}{s^2} \\[2mm]
& + \left(24\pi^2 + 6X^4 + 24X^2\pi^2 + 48X\pi^2 + 24X^3 + 24X + 36X^2\right)\frac{t}{u} \\[2mm]
& + \left(12X^4 + 24\pi^2 + 48X^2\pi^2 + 36X^3 + 36X^2 + 72X\pi^2\right)\frac{t^2}{u^2} \\[2mm]
& + \left(24 + 6XY + 6X^2 + 3Y^4 + 12X\pi^2 + \frac{9}{2}X^2Y^2 + 6\pi^2 + 6X^3 + \frac{3}{4}\pi^4\right. \\[2mm]
& \left. - 6XY^3 + 9Y^2\pi^2 + 12Y - 3XY\pi^2\right) + \left\{t \leftrightarrow u\right\}
\end{aligned}
$$

$$\text{(C.97)}$$

Bibliography

[1] M. E. Peskin and D. V. Schroeder, *An Introduction to quantum field theory* , Reading, USA: Addison-Wesley (1995) 842p.

[2] T. Muta, *Foundations of Quantum Chromodynamics* , World Scientific (2000) 409p.

[3] P. Pascual and R. Tarrach, *QCD: renormalisation for the practitioner* , Springer-Verlag (1984) 277p.

[4] J. C. Collins, *Renormalization* , Cambridge, UK: CUP (1989) 380p.

[5] R. K. Ellis, W. J. Stirling, and B. R. Webber, *QCD and Collider Physics* , Cambdrige, UK: CUP (1996) 435p.

[6] C. Itzykson and J. Zuber, *Quantum Field Theory* , McGraw-Hill (1980) 705p.

[7] L. H. Ryder, *Quantum Field Theory* , Cambridge, UK: CUP (1996) 487p.

[8] D. H. Perkins, *Introduction to high energy physics* , Cambridge, UK: CUP (2000) 426p.

[9] R. J. Eden, P. V. Landshoff, D. I. Olive, and J. C. Polkinghorne, *The Analytic S-Matrix* , Cambridge, UK: CUP (1966) 287p.

[10] C. Anastasiou, T. Gehrmann, C. Oleari, E. Remiddi, and J. B. Tausk, Nucl. Phys. **B580**, 577 (2000), hep-ph/0003261.

[11] S. Catani, M. H. Seymour, and Z. Trocsanyi, Phys. Rev. **D55**, 6819 (1997), hep-ph/9610553.

[12] G. Leibbrandt, Rev. Mod. Phys. **47**, 849 (1975).

[13] D. E. Soper, (2000), hep-ph/0011256.

[14] Particle Data Group, D. E. Groom *et al.*, Eur. Phys. J. **C15**, 1 (2000).

[15] L. R. Surguladze and M. A. Samuel, Rev. Mod. Phys. **68**, 259 (1996), hep-ph/9508351.

[16] T. Kinoshita, J. Math. Phys. **3**, 650 (1962).

[17] T. D. Lee and M. Nauenberg, Phys. Rev. **133**, B1549 (1964).

[18] F. Bloch and A. Nordsieck, Phys. Rev. **52**, 54 (1937).

[19] S. Bethke, Z. Kunszt, D. E. Soper, and W. J. Stirling, Nucl. Phys. **B370**, 310 (1992).

[20] J. C. Collins, D. E. Soper, and G. Sterman, ITP-SB-89-31.

[21] S. A. Larin, T. van Ritbergen, and J. A. M. Vermaseren, Nucl. Phys. **B427**, 41 (1994).

[22] S. A. Larin, P. Nogueira, T. van Ritbergen, and J. A. M. Vermaseren, Nucl. Phys. **B492**, 338 (1997), hep-ph/9605317.

[23] A. Retey and J. A. M. Vermaseren, (2000), hep-ph/0007294.

[24] J. A. Gracey, Phys. Lett. **B322**, 141 (1994), hep-ph/9401214.

[25] W. L. van Neerven and A. Vogt, Phys. Lett. **B490**, 111 (2000), hep-ph/0007362.

[26] W. L. van Neerven and A. Vogt, Nucl. Phys. **B588**, 345 (2000), hep-ph/0006154.

[27] W. L. van Neerven and A. Vogt, Nucl. Phys. **B568**, 263 (2000), hep-ph/9907472.

[28] A. D. Martin, R. G. Roberts, W. J. Stirling, and R. S. Thorne, Eur. Phys. J. **C18**, 117 (2000), hep-ph/0007099.

[29] J. M. Campbell and E. W. N. Glover, Nucl. Phys. **B527**, 264 (1998), hep-ph/9710255.

[30] Z. Bern, L. Dixon, and D. A. Kosower, Ann. Rev. Nucl. Part. Sci. **46**, 109 (1996), hep-ph/9602280.

[31] Z. Bern, L. Dixon, and D. A. Kosower, Nucl. Phys. **B437**, 259 (1995), hep-ph/9409393.

[32] Z. Bern, L. Dixon, and D. A. Kosower, Phys. Rev. Lett. **70**, 2677 (1993), hep-ph/9302280.

[33] Z. Bern and D. A. Kosower, Nucl. Phys. **B362**, 389 (1991).

[34] J. F. Gunion and J. Kalinowski, Phys. Rev. **D34**, 2119 (1986).

[35] S. J. Parke and T. R. Taylor, Nucl. Phys. **B269**, 410 (1986).

[36] F. A. Berends and W. Giele, Nucl. Phys. **B294**, 700 (1987).

[37] J. F. Gunion and Z. Kunszt, Phys. Lett. **B176**, 163 (1986).

[38] Z. Kunszt, A. Signer, and Z. Trocsanyi, Phys. Lett. **B336**, 529 (1994), hep-ph/9405386.

[39] R. K. Ellis and J. C. Sexton, Nucl. Phys. **B269**, 445 (1986).

[40] C. Anastasiou, E. W. N. Glover, C. Oleari, and M. E. Tejeda-Yeomans, Nucl. Phys. **B601**, 318 (2001), hep-ph/0010212.

[41] C. Anastasiou, E. W. N. Glover, C. Oleari, and M. E. Tejeda-Yeomans, Nucl. Phys. **B601**, 341 (2001), hep-ph/0011094.

[42] C. Anastasiou, E. W. N. Glover, C. Oleari, and M. E. Tejeda-Yeomans, Phys. Lett. **B506**, 59 (2001), hep-ph/0012007.

[43] C. Anastasiou, E. W. N. Glover, C. Oleari, and M. E. Tejeda-Yeomans, Nucl. Phys. **B605**, 486 (2001), hep-ph/0101304.

[44] E. W. N. Glover, C. Oleari, and M. E. Tejeda-Yeomans, Nucl. Phys. **B605**, 467 (2001), hep-ph/0102201.

[45] E. W. N. Glover and M. E. Tejeda-Yeomans, JHEP **05**, 010 (2001), hep-ph/0104178.

[46] E. W. N. Glover, (2001), hep-ph/0106069.

[47] S. D. Ellis, Z. Kunszt, and D. E. Soper, Phys. Rev. Lett. **69**, 3615 (1992), hep-ph/9208249.

[48] M. H. Seymour, Nucl. Phys. **B513**, 269 (1998), hep-ph/9707338.

[49] H. L. Lai *et al.*, Phys. Rev. **D55**, 1280 (1997), hep-ph/9606399.

[50] CDF, F. Abe *et al.*, Phys. Rev. Lett. **77**, 438 (1996), hep-ex/9601008.

[51] D0, N. Varelas, Contributed to 28th International Conference on High-energy Physics (ICHEP 96), Warsaw, Poland, 25-31 Jul 1996.

[52] CDF, F. Abe *et al.*, Phys. Rev. Lett. **77**, 448 (1996), hep-ex/9603003.

[53] V. A. Smirnov and O. L. Veretin, Nucl. Phys. **B566**, 469 (2000), hep-ph/9907385.

[54] V. A. Smirnov, Phys. Lett. **B460**, 397 (1999), hep-ph/9905323.

[55] C. Anastasiou, J. B. Tausk, and M. E. Tejeda-Yeomans, Nucl. Phys. Proc. Suppl. **89**, 262 (2000), hep-ph/0005328.

[56] C. Anastasiou, E. W. N. Glover, and C. Oleari, Nucl. Phys. **B565**, 445 (2000), hep-ph/9907523.

[57] C. Anastasiou, E. W. N. Glover, and C. Oleari, Nucl. Phys. **B572**, 307 (2000), hep-ph/9907494.

[58] T. Binoth and G. Heinrich, Nucl. Phys. **B585**, 741 (2000), hep-ph/0004013.

[59] C. Anastasiou, *Two-Loop integrals and QCD scattering* , Ph.D. Thesis, University of Durham (2001) 204p.

[60] G. 't Hooft and M. Veltman, Nucl. Phys. **B44**, 189 (1972).

[61] K. G. Chetyrkin and F. V. Tkachov, Nucl. Phys. **B192**, 159 (1981).

[62] F. V. Tkachov, Phys. Lett. **B100**, 65 (1981).

[63] T. Gehrmann and E. Remiddi, Nucl. Phys. **B580**, 485 (2000), hep-ph/9912329.

[64] C. Anastasiou, E. W. N. Glover, and C. Oleari, Nucl. Phys. **B575**, 416 (2000), hep-ph/9912251.

[65] S. Laporta and E. Remiddi, Phys. Lett. **B379**, 283 (1996), hep-ph/9602417.

[66] R. J. Gonsalves, Phys. Rev. **D28**, 1542 (1983).

[67] T. Gehrmann and E. Remiddi, Nucl. Phys. Proc. Suppl. **89**, 251 (2000), hep-ph/0005232.

[68] T. Gehrmann and E. Remiddi, Nucl. Phys. **B601**, 248 (2001), hep-ph/0008287.

[69] T. Gehrmann and E. Remiddi, Nucl. Phys. **B601**, 287 (2001), hep-ph/0101124.

[70] P. Nogueira, J. Comput. Phys. **105**, 279 (1993).

[71] Z. Bern, L. Dixon, and A. Ghinculov, Phys. Rev. **D63**, 053007 (2001), hep-ph/0010075.

[72] S. Catani, Phys. Lett. **B427**, 161 (1998), hep-ph/9802439.

[73] S. Catani and M. H. Seymour, Nucl. Phys. **B485**, 291 (1997), hep-ph/9605323.

[74] D. R. Yennie, S. C. Frautschi, and H. Suura, Ann. Phys. **13**, 379 (1961).

[75] A. Bassetto, M. Ciafaloni, and G. Marchesini, Phys. Rept. **100**, 201 (1983).

[76] V. N. Gribov and L. N. Lipatov, Yad. Fiz. **15**, 781 (1972).

[77] G. Altarelli and G. Parisi, Nucl. Phys. **B126**, 298 (1977).

[78] Y. L. Dokshitzer, Sov. Phys. JETP **46**, 641 (1977).

[79] S. Catani and M. Grazzini, Phys. Lett. **B446**, 143 (1999), hep-ph/9810389.

[80] V. D. Duca, A. Frizzo, and F. Maltoni, Nucl. Phys. **B568**, 211 (2000), hep-ph/9909464.

[81] F. A. Berends and W. T. Giele, Nucl. Phys. **B306**, 759 (1988).

[82] Z. Bern, L. Dixon, D. C. Dunbar, and D. A. Kosower, Nucl. Phys. **B425**, 217 (1994), hep-ph/9403226.

[83] Z. Bern, V. D. Duca, W. B. Kilgore, and C. R. Schmidt, Phys. Rev. **D60**, 116001 (1999), hep-ph/9903516.

[84] D. A. Kosower and P. Uwer, Nucl. Phys. **B563**, 477 (1999), hep-ph/9903515.

[85] M. L. Mangano and S. J. Parke, Phys. Rept. **200**, 301 (1991).

[86] S. Catani and M. Grazzini, Nucl. Phys. **B591**, 435 (2000), hep-ph/0007142.

[87] V. D. Duca, L. Dixon, and F. Maltoni, Nucl. Phys. **B571**, 51 (2000), hep-ph/9910563.

[88] F. A. Berends and W. T. Giele, Nucl. Phys. **B313**, 595 (1989).

[89] Z. Bern, L. Dixon, and D. A. Kosower, Nucl. Phys. Proc. Suppl. **51C**, 243 (1996), hep-ph/9606378.

[90] Z. Bern, V. D. Duca, W. B. Kilgore, and C. R. Schmidt, (1998), hep-ph/9903525.

[91] J. B. Tausk, Phys. Lett. **B469**, 225 (1999), hep-ph/9909506.

[92] K. S. Kolbig, J. A. Mignaco, and E. Remiddi, **10**, 38 (1970).

[93] P. Cvitanovic, P. G. Lauwers, and P. N. Scharbach, Nucl. Phys. **B186**, 165 (1981).

[94] M. Mangano, S. Parke, and Z. Xu, Nucl. Phys. **B298**, 653 (1988).

[95] D. A. Kosower, B.-H. Lee, and V. P. Nair, Phys. Lett. **B201**, 85 (1988).

[96] D. A. Kosower, Nucl. Phys. **B315**, 391 (1989).

[97] M. Mangano, Nucl. Phys. **B309**, 461 (1988).

[98] D. Zeppenfeld, Int. J. Mod. Phys. **A3**, 2175 (1988).

[99] R. Kleiss and H. Kuijf, Nucl. Phys. **B312**, 616 (1989).

[100] O. V. Tarasov, Nucl. Phys. Proc. Suppl. **89**, 237 (2000), hep-ph/0102271.

[101] S. Laporta, Phys. Lett. **B504**, 188 (2001), hep-ph/0102032.

[102] S. Laporta, Int. J. Mod. Phys. **A15**, 5087 (2000), hep-ph/0102033.

[103] T. Gehrmann and E. Remiddi, (2001), hep-ph/0101147.

[104] S. Catani and M. Grazzini, Nucl. Phys. **B570**, 287 (2000), hep-ph/9908523.

[105] S. Catani, Proceedings of the workshop on *New Techniques for Calculating Higher Order QCD Corrections*,report **ETH-TH/93-01** (1992), Zurich.

[106] Z. Bern, V. D. Duca, and C. R. Schmidt, Phys. Lett. **B445**, 168 (1998), hep-ph/9810409.

[107] D. A. Kosower, Nucl. Phys. **B552**, 319 (1999), hep-ph/9901201.

[108] A. Gehrmann-De Ridder and E. W. N. Glover, Nucl. Phys. **B517**, 269 (1998), hep-ph/9707224.

[109] A. Devoto and D. W. Duke, Riv. Nuovo Cim. **7N6**, 1 (1984).